The Role of the Tumor Suppressor, p190RhoGAP, in Apoptosis and Cytokinesis

Kirsten Ludwig
Charlottesville, Virginia

B.A. Biology, University of Virginia, 2003
M.S. Biological and Physical Sciences, University of Virginia, 2007

A Dissertation Presented to the Graduate Faculty
of the University of Virginia in Candidacy for the Degree of
Doctor of Philosophy

Department of Microbiology
University of Virginia
May, 2011

Sarah Parsons

Marty Mayo

Michael Weber

Kodi Ravichandran

Dennis Templeton

Ulrike Lorenz

ABSTRACT

p190RhoGAP (p190) is a RhoGTPase activating protein which regulates a variety of biological events by enhancing Rho-mediated hydrolysis of RhoGTP to RhoGDP. Multiple lines of evidence suggest that p190 can function as a tumor suppressor, although its mechanism of action remains unknown. p190 has also been implicated in the apoptotic process as both protein and mRNA levels are upregulated upon apoptotic initiation in rat prostate cells undergoing apoptosis. To gain insights into its mechanism of action as a tumor suppressor, an overexpression approach was taken. Previous studies revealed that overexpression of p190 in epithelial transformed cells led to a multinucleated phenotype. Chromatin condensation, a marker of apoptosis, was also frequently observed. In contrast, overexpression of p190 in non-transformed fibroblasts led to a dendrite-like phenotype, in addition to chromatin condensation.

Work presented in this dissertation revealed that the primary phenotype of p190 overexpression is apoptosis, which occurs in a caspase- and Rho-dependent manner. p190 overexpression also preferentially induced multinucleation in transformed cells and dendrite-like formation in non-transformed cells, indicating that the secondary phenotypes are determined by transformation status and may act as intermediate phenotypes in the p190-apoptotic pathway. Preliminary data revealed that the NF-κB pathway may be responsible for the differential response to p190 overexpression and that apoptosis may proceed through a JNK-Bim/Mcl-1 pathway regardless of transformation

status. Finally, we show that p190 conferred docetaxel sensitivity to breast cancer cells through its down regulation of Rho.

In addition to apoptosis, p190 regulates progression through cytokinesis. Previous work demonstrated that p190 overexpression induces multinucleation as a result of decreased RhoGTP levels at the cleavage furrow. This study demonstrates that p190 overexpression inhibited myosin II activation, which is required for completion of cytokinesis. p190 overexpression also reduced anillin localization to the cleavage furrow, and silencing of anillin prevented p190 localization to the cleavage furrow. Further studies revealed that p190 and anillin physically interact and regulate the localization of each other in a contractility-dependent manner. Together the data from this study further define the role of p190 in cytokinesis and clarify p190's role as a tumor suppressor.

TABLE OF CONTENTS

LIST OF FIGURES

Chapter 5:

Chapter 6:

LIST OF TABLES

ABBREVIATIONS:

ABL2	v-abl Abelson murine leukemia viral oncogene 2
ADP	Adenosine diphosphate
AHR	Anillin homoly region
APC	Adenomatous polyposis coli
APC/C	Anaphase promoting complex/cyclosome
Arg	Arginine
Asn	Asparagine
ATM	Ataxia telangiectasia mutated
ATP	Adenosine triphosphate
Bcl-2	B-cell lymphoma 2
BH	Bcl-2 homology
Brk	Breast tumor kinase
C3	Clostridium blotulinum enodotxin C3
CA	Constitutively active
Cdc42	Cell division cycle protein 42
Cdh1	Fizzy-related protein homolgy isoform 1
Cdk1	Cyclin dependent kinase 1
CPC	Chromosomal Passenger Complex
CR	Cysteine rich
C-terminal	Carboxyl-terminus
DAD	Diaphonous autoinhibitory domain
DAP1	4',6-Diamidino-2-phenylindole
DH	Dbl-homology
DIC	Differential interference contrast
DID	Diaphanous inhibitory domain
DISC	Death-inducing signaling complex
DLC1	Deleted in liver cancer 1
DLC1	Dyein Light Chain 1
DMEM	Dulbecco's modified eagle medium
DN	Dominant negative
Dox	Doxycycline
EB1	Microtubule-associated protein RP/EB family member 1
ECL	Enhanced chemiluminescence
Ect2	Epithelial cell transforming sequence 2
EGF	Epidermal growth factor
EGFR	Epidermal growth factor receptor

ERK	Extracellular Receptor Kinase
FADD	Fas-associated death domain
FAK	Focal Adhesion Kinase
FF	Diphenylalanine
FH	Formin homology
FL	Full length
FRET	Fluorescence resonance energy transfer
G1 phase	Gap-1 phase
G2 phase	Gap-2 phase
GADD45	Growth Arrest and DNA Damage
GAP	GTP-ase activating protein
GBD	GTP binding domain
GDI	Guanine dissociation inhibitor
GDP	Guanine diphosphate
GEF	Guanine nucleotide exchange factor
GFP	Green fluorescent protein
Gln	Glutamine
GSK-3β	Glycogen synthase kinase 3 beta
GTP	Guanine triphosphate
GTPase	GTPase activating protein
HA	Hyaluronic Acid
HRP	Horseradish peroxidase
IAP	Inhibitor of apoptosis protein
IF	Immunofluorescence
IGFR	Insulin-like Growth Factor 1
IKK	IκB kinase
IP	Immunoprecipitation
JNK	c-Jun N-terminal kinases
kDa	Kilo Dalton
LIMK	LIM domain kinase 1
LMW-PTP	Low molecular weight-protein tyrosine phosphatase
M phase	Mitosis phase
mAb	Monoclonal antibody
MAPK	Mitogen-activated protein kinases
MAPKKK	Mitogen-Activated Protein Kinase Kinase Kinase
Mcl-1	Myeloid cell leukemia
MD	Middle domain

mDia	Mammalian diaphanous
MDM2	Murine double minute
MET	MNNG HOS Transforming gene
MKK	MAP Kinase Kinase
MKLP1	Mitotic kinesin-like protein 1
MLC	Myosin light chain
MMP	Matrix metalloproteinases
MN	Multinucleation
MOMP	Major Outer Membrane Protein
MT	Microtubules
NCI	National Cancer Institute
NF-κB	Nuclear factor kappa-light-chain-enhancer of activated B cells
NLS	Nuclear localization sequence
Nox-1	NADPH oxidase
NSCLC	Non-small cell lung cancer
N-terminal	Amino-terminus
p190	p190RhoGAP
pAb	Polyclonal antibody
PAGE	Polyacrylamide gel electrophoresis
PAK	p21-activated kinase
PBS	Phosphate buffered saline
PDGF	Platelet-derived growth factor
PDK1	3-phosphoinositide dependent protein kinase-1
PEST	Proline, Glutamic acid, Serine, and Threonine
PH	Pleckstrin homology
PI3K	Phosphatidylinositol 3-kinases
PIP3	Phosphatidylinositol (3,4,5)-trisphosphate
PKA	Protein kinase A
PKC	Protein kinase C
PML	Probable transcription factor
Ptprz	Protein tyrosine phosphatase receptor type z
RACK1	Receptor for activated protein kinase C
RBD	Rho binding domain
RNAi	RNA interference
ROCK	Rho associated, coiled-coil containing protein kinase 1
ROI	Region of interference
ROS	Reactive oxygen species

S phase	Synthesis phase
SAC	Spindle-assembly checkpoint
Sam68	Src-associated in mitosis
SDS	Sodium dodecyl sufate
SEM	Standard error of the mean
Ser	Serine
SH2	Src homology domain 2
SH3	Src homology domain 3
siRNA	Small interfering RNA
SRF	Serum response factor
TBST	Tris-Buffered Saline and Tween 20
TF-II	Transcription factor I
Thr	Threonine
TNF	Tumor necrosis factor
Tox B	*Clostridium difficile* toxin
TRAIL	TNF-related apoptosis inducing ligand
TUNEL	Terminal deoxynucleotidyl transferase dUTP nick end labeling
UV	Ultraviolet
VEGF	Vascular endothelial growth factor
VEGFR	Vascular endothelial growth factor receptor
WASP	Wiskott-Aldrich syndrome protein
WB	Western blot
WCL	Whole cell lysate

ACKNOWLEDGMENTS:

First, I would like to thank Sally Parsons, whose belief in me has made this all possible. Without her support, understanding, and encouragement I would not be in graduate school at UVa and this dissertation would not exist. Her belief in my desire, drive, and ability has given me so many opportunities, and her guidance has made me the scientist I am.

My sincere thanks to my committee: Marty Mayo, Dennis Templeton, Ulrike Lorenz, Mike Weber, and Kodi Ravichandran. Their advice and guidance over the past several years has been extremely helpful and I am grateful to have had such an amazing committee. They are all amazing scientists, and I will be lucky to one day have any of their careers.

I would also like to thank my coworkers and friends who kept me sane and helped me deal with life in general. The p190 group: Ling Su, Masahito Mikawa, and Sergio Sanchez, whose input and suggestions kept me truthful and honest. I would also like to thank my old benchmate Jessica Pritchard, whose friendship got me through the day and whose advice and commiseration made this dissertation what it is. Cat Cowan-Hall who fed me and made sure that I always had contact with other humans when I secluded myself away, her friendship made life in Charlottesville feel like home. I also owe thanks to Akbar Shakoor, without his supply of food, wine, and friendship, grad school would have been a much more difficult experience.

Finally I would like to thank my family, both two- and four-legged. I would not have survived grad school without Gaea, Frodo, and Mama and the wonderful drama that

comes with them. The friendship I have with Rose and Dawson is one of the things I value most in this world. And lastly, my parents, words cannot express everything that they have given to me. Aside from the support, guidance and teaching, they also taught me that by following my dreams and working hard, life really would be ok. Everything they have accomplished in life is truly awe inspiring.

DEDICATION:

To all scientists who came before me and made this possible, in particular:
my mentor, Sally Parsons, Ph.D,
my mother, Janet Ludwig, Ph.D., and
my grandfather, Richard Carroll, M.D.

CHAPTER 1

Introduction

Chapter 1
Introduction:

To date, more than one hundred distinct types of cancers exist, many of which are comprised of multiple subtypes (Kimura et al., 1996). Tumorigenesis, or the process of tumor formation, is a multi-step process based on genetic alterations which cause the transformation of normal cells into highly malignant cells. Hanahan and Weinberg (Hanahan and Weinberg, 2000) defined "…..six essential alterations in cell physiology that collectively dictate malignant growth.". These alterations are self-sufficiency in growth signals, insensitivity to growth-inhibiting signals, evasion of apoptosis, limitless replicative potential, sustained angiogenesis, and tissue invasion and metastasis. While it is not necessary that a tumor have all six of these alterations, it is generally accepted that the presence of a single alteration cannot alone lead to malignant transformation; it is a combination of these six that proves deleterious. In other words, cancer is not due to a single mutation, but a series of progressive mutations that cooperate to promote un-inhibited cell growth. Multiple types of proteins contribute to the aforementioned processes, including kinases, transcription factors, G-protein coupled receptors, phosphatases, chaperones, and small-G proteins.

Thirty years after the identification of the first three oncogenes, Ras (Harvey, 1964), c-Src (Tal et al., 1977), and the Epidermal Growth Factor Receptor (EGFR) (Anderson et al., 1980; Vennstrom and Bishop, 1982), these proteins continue to be a major focus of cancer research. While one is a small-G protein (Ras), one is a cytosolic kinase (Src), and the third is a receptor tyrosine kinase (EGFR), all are instrumental in

many of the six previously mentioned “essential alterations in cell physiology” necessary for malignant transformation. Unfortunately modern medicine has only developed drugs to two of the three oncogenes; c-Src and EGFR, while targeting Ras has proved much more elusive. In fact, developing drugs to inhibit kinase activity is where the majority of cancer research has been focused for the last thirty years. At this date there are currently 1,309 active oncology clinical trials for kinase inhibitors, and 1,540 oncology clinical trials for monoclonal antibodies to receptor tyrosine kinase inhibitors. Conversely there are only 109 active clinical trials for gene therapy and no active clinical trials targeting either transcription factors or small-G proteins (Institute, 2011).

Rho, a member of the Ras superfamily of GTPases, functions in, apoptosis, angiogenesis, invasion, and metastasis (Karlsson et al., 2009). More importantly, multiple activators of Rho have been classified as oncogenes, while several of Rho’s negative regulators are considered tumor suppressors. Additionally, Rho and Rho family members are up-regulated in a variety of tumors and are often associated with poor prognosis. (Vega and Ridley, 2008) Given all of this, the Rho family of proteins or their effectors might be a promising new direction for cancer therapy to go.

Rho:

Rho was originally isolated from the mollusk *Aplysia californica* in 1985 (Madaule and Axel, 1985) and is the prototype for the Rho family of proteins. There are 20 members of the Rho family, grouped into 8 subfamilies: the prototypical Rho subfamily contains RhoA, RhoB, and RhoC; the Rac subfamily consists of Rac1, Rac2, Rac3, and RhoG; subfamily 3 comprises Cdc42, TC10/RhoQ, and TCL/RhoJ; the fourth

subfamily includes CHP/RhoV, WRCH1/RhoU; RhoH is alone in the fifth subfamily; subfamily 6 contains RhoBTB1 and RhoBTB2; the Rnd subfamily consists of Rnd1, Rnd2, and Rnd3; and finally the last subfamily contains RIF/RhoF and RhoD (Heasman and Ridley, 2008). Rho orthologs have been identified in protozoa, fungi, nematodes, insects, and vertebrates, by comparative genome analysis, although no ortholog has ever been found in plants (Miyoshi J., 2009).

Regulation of Rho:

Within this subfamily, Rho A, B, and C share greater than 50% overall sequence homology to each other, including the same amino acid sequence in their effector domain (amino acids 32-41). More importantly, they are all regulated in the same manner (Kaibuchi et al., 1999; Nobes and Hall, 1994). Rho GTPases are controlled by GTP binding. All GTPases act as molecular switches cycling between an active GTP-bound state and an inactive GDP-bound state (Fig. 1). In the active state, RhoGTPases bind effector molecules to activate them. The activities of the GTPases are controlled by three different molecules; guanine nucleotide exchange factors (GEFs), GTPase-activating proteins (GAPs), and guanine nucleotide dissociation inhibitors (GDIs). GEFs activate Rho by catalyzing the exchange of GDP for GTP. While Rho molecules have a high affinity for both GTP and GDP alike, their intrinsic GTPase activity is slow ($t_{1/2}$ is about 5-10 min.) (Haeusler et al., 2003; Piekny et al., 2005). For this reason, they need GAPs to stimulate their intrinsic GTPase activities and activate the switch. The role of the GDI is to block the activation of the GTPase, keeping it in the inactive GDP-bound form (Jaffe and Hall, 2005; Schmidt and Hall, 2002).

Figure 1

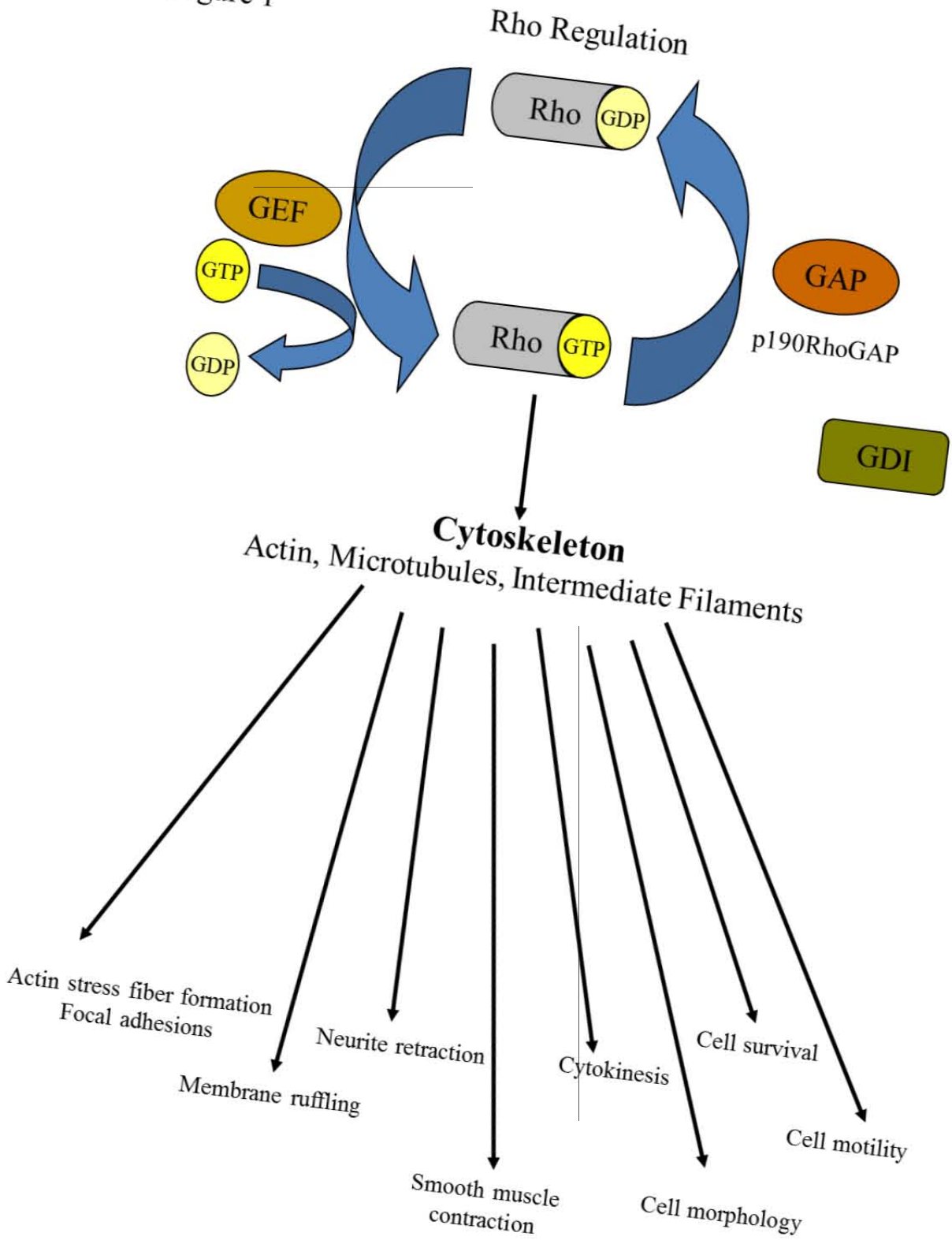
Rho Regulation
Rho
GDP
GEF
GTP
GDP
Rho
GTP
GAP
p190RhoGAP
GDI
Cytoskeleton
Actin, Microtubules, Intermediate Filaments
Actin stress fiber formation
Focal adhesions
Membrane ruffling
Neurite retraction
Smooth muscle contraction
Cytokinesis
Cell survival
Cell morphology
Cell motility

Figure 1: The Rho activation cycle

The activity of Rho is regulated by three classes of proteins: guanine nucleotide exchange factors (GEFs), GTPase-activating proteins (GAPs), and guanine nucleotide dissociation inhibitors (GDI). Rho binds GTP with the aid of GEF's, which exchange GDP with GTP, activating the protein. GAP's stimulate the intrinsic GTPase activity of Rho, promoting hydrolysis of GTP to GDP, inactivating the protein. GDI's prevent GDP release, thereby maintaining Rho in the inactive state. While active, Rho can regulate actin stress fiber and focal adhesion formation, membrane ruffling, neurite retraction, smooth muscle contraction, cytokinesis, cell morphology, motility, and survival, primarily through regulation of the cytoskeleton.

Rho molecules contain two important domains, switch 1 and switch 2. Switch 1, or the effector domain, comprises amino acids 31-42 and is involved in the activation of downstream signaling molecules. Switch 2, amino acids 63-79, undergoes a conformational change to a closed position upon GDP binding (Wittinghofer and Nassar, 1996). When GDP is exchanged for GTP, this switch moves to an open, active conformation (Bishop and Hall, 2000; Jaffe and Hall, 2005).

To date, 70 RhoGEFs have been identified in mammals (Vega and Ridley, 2008). GEFs activate Rho by stimulating the release of GDP in exchange for GTP. Catalysis is necessary, since the concentration of GDP is five times greater than GTP in the cell (Cerione and Zheng, 1996; Kaibuchi et al., 1999). The vast majority of GEFs contain a Dbl-homology (DH) domain and a Pleckstrin-homology (PH) domain tandem repeat (Cerione and Zheng, 1996). The DH domain of GEFs interact with the switch 1 region of the Rho molecule, while the PH domain is responsible for localizing the protein to the plasma membrane (Ron et al., 1991; Whitehead et al., 1995).

GAP molecules counter the action of GEFs by stimulating Rho's innate GTPase activity (Moon and Zheng, 2003). There are currently 60 known mammalian RhoGAP's (Vega and Ridley, 2008), all of which contain a related GAP homology domain, roughly 140 amino acids in length (Kaibuchi et al., 1999). GAPs interact with RhoGTPases at both switch 1 and 2, which constitute the GTP-binding core of the protein (Moon and Zheng, 2003). Every GAP contains an arginine residue proposed to interact with Gln63 of the Rho molecule. This arginine donates an electrical charge which stabilizes the Gln residue, properly orienting a water molecule for hydrolysis of the γ-phosphate (Gamblin

and Smerdon, 1998). In this way, GAPs increase Rho's ability to hydrolyze GTP and down regulate their activity.

The multiplicity of RhoGEFs and RhoGAPs suggests that the different regulators of Rho may have different biological functions. Conversely, only 3 RhoGDIs have been identified (Vega and Ridley, 2008). Active RhoGTP is prenylated at the C-terminus, which targets the protein to the cell membrane (Isomura et al., 1991; Katayama et al., 1991; Takai et al., 1995). RhoGDI masks the prenyl modification of Rho, sequestering it in the cytosol of the cell, preventing it from being activated by RhoGEFs. Moreover, RhoGDI can also extract RhoGDP from the membrane, keeping it locked in its GDP bound form (Isomura et al., 1991). In cells, Rho is primarily found as RhoGDP in complex with RhoGDI (Takai et al., 1995).

Rho protein activation is also regulated by post-translational modifications. All Rho family members contain a CAAX motif at their C-termini, which is essential for many post-translation modifications (Glomset and Farnsworth, 1994). A prenyl group, like the geranylgeranyl group, is added to the cysteine in this motif and is necessary for localization to the membrane and subsequent activation (Horiuchi et al., 1991; Katayama et al., 1991). Phosphorylation of Rho can also affect its activity. Specifically, phosphorylation at Ser188 by PKA prevents its association with the plasma membrane, enhances its affinity for RhoGDI and protects it from degradation (Ellerbroek et al., 2003; Forget et al., 2002; Lang et al., 1996; Rolli-Derkinderen et al., 2005). Furthermore, ubiquitination of Rho promotes proteosomal degradation of the protein (Ozdamar et al., 2005; Wang et al., 2003).

Finally, Rho's activity can be modulated by bacterial toxins. The C3 exoenzyme family of toxins includes the *Clostridium limosum* transferase, which ADP-riboslyates Rho at Asn 41. This ribosylation is thought to interfere with Rho's ability to interact with its downstream targets, effectively inhibiting its function (Aktories et al., 1989; Sekine et al., 1989). Other bacterial toxins which affect the activity of Rho are the *Clostridium difficile* toxins A and B. These toxins inactivate Rho by glycosylating the protein at Thr37 (Just et al., 1994; Just et al., 1995). Finally, multiple studies have found that the activities of some Rho family members can affect the activities of other Rho family members. Specifically, Rho activation is inversely correlated with the activation of Rac1 and Cdc42. This is regulated primarily through the activation of GEFs and GAPs, which are activated or inactivated by one RhoGTPase to alter the activity of another RhoGTPase (Karlsson et al., 2009; Miyoshi J., 2009; Vega and Ridley, 2008). However, the major regulation of Rho proteins continues to be through the activity of GEFs, GAPs, and GDIs.

Functions of Rho:

RhoGTPases directly and indirectly regulate a myriad of targets, including serine/threonine kinases, tyrosine kinases, lipid kinases, lipases, phosphatases, oxidases, and scaffold proteins (Jaffe and Hall, 2005). Rho functions in so many pathways that 1% of the human genome encodes proteins that either regulate or are regulated by direct interaction with members of the RhoGTPase family (Kaibuchi et al., 1999). Through its multiple targets, Rho functions in cell morphology determination (Paterson et al., 1990), smooth-muscle contraction (Hirata et al., 1992), formation of stress fibers and focal

adhesions (Nobes and Hall, 1994; Ridley and Hall, 1992), cell motility (Takai et al., 1995; Takaishi et al., 1994), cytokinesis (Kishi et al., 1993; Mabuchi et al., 1993), cell-cycle progression (Khosravi-Far et al., 1995; Olson et al., 1995; Yamamoto et al., 1993), axon guidance and extension (Jalink et al., 1994; Nishiki et al., 1990), transformation (Qiu et al., 1997; Qiu et al., 1995a; Qiu et al., 1995b), gene expression (Hill et al., 1995; Perona et al., 1993), vesicle trafficking (Caron and Hall, 1998; Komuro et al., 1996; Lamaze et al., 1996), and development (Glise and Noselli, 1997) (Miyoshi J., 2009) (Figure 1).

Rho carries out these functions through the activation of its many effector proteins, which include Rho-kinase/ROK/ROCK, myosin light chain phosphatase, citron kinase, mDia, and LIM-kinase (LIMK) (Kaibuchi et al., 1999; Van Aelst and D'Souza-Schorey, 1997). Rho can also affect gene transcription through the SRF (serum response factor)-actin sensor, which is a promoter found in many genes whose products comprise the cytoskeleton (Jaffe and Hall, 2005; Miralles et al., 2003). As Rho functions in so many essential functions, it is of no surprise that alterations in the RhoGTPase pathways have been implicated in a variety of malignancies.

Rho and Cancer:

RhoGTPases function in the acquisition by cancer cells of unlimited proliferation potential, survival and evasion of apoptosis, tissue invasion, and the establishment of metastases (Vega and Ridley, 2008). Unlike its family member Ras, no activating mutations of RhoGTPases have been reported in cancers. However, an increase in expression in hepatocellular carcinoma, bladder cancer, esophageal squamous cell

carcinoma, head and neck squamous cell carcinoma, ovarian carcinoma, gastric carcinoma, testicular carcinoma, colorectal carcinoma, non-small cell lung cancer, breast cancer, pancreatic ductal adenocarcinoma, prostate carcinoma, melanoma, oral squamous cell carcinoma, chronic myelogenous leukemia, non-Hodgkin's lymphoma, multiple myeloma, acute myeloid leukemia, hairy cell leukemia, and diffuse large-cell lymphoma is often seen (Karlsson et al., 2009). Additionally, increased expression of RhoA and activity in hepatocellular carcinoma and breast cancer correlates with poorer prognosis (Fukui et al., 2006; Karlsson et al., 2009; Li et al., 2006). Rho activation also regulates production of MMPs (Matrix Metalloproteinases), thereby affecting matrix remodeling and tumor cell invasion (Braga et al., 1999).

Rho- and Rac-transformed murine fibroblasts can develop distant metastases in the lung, spleen, lymph nodes, and other tissues when injected into immuno-compromised mice (del Peso et al., 1997; Gomez del Pulgar et al., 2005), and the overexpression of a constituently active Rho is tumorigenic in syngeneic mice (Perona et al., 1993; van Leeuwen et al., 1995). Recently, overexpression of wild type RhoA was shown to increase metastasis of ovarian cancer cells injected into the peritoneal cavity of mice, providing further evidence to the notion that overexpression of wild type RhoA is sufficient to promote tumorigenesis (Horiuchi et al., 2008). Furthermore, Rho signaling is necessary for aberrant growth promoted by several oncogenic pathways, including the EGFR (Boerner et al., 2000; Kim et al., 1998), IGFR (Sachdev et al., 2001), MET (Royal et al., 2000), RET (Barone et al., 2001), and G-protein coupled receptors (Whitehead et

al., 2001) (Gomez del Pulgar et al., 2005). RhoA, Rac1, and Cdc42, are also crucial for Ras-induced transformation (Qiu et al., 1997; Qiu et al., 1995a; Qiu et al., 1995b).

However, it is not just the RhoGTPases that are mis-regulated in cancer tissues. The upstream and downstream regulators of these pathways can also function aberrantly in malignant cells. Many RhoGEFs are well established oncogenes, including Dbl, Ost, Ect-2, and Vav-1 (Hoffman and Cerione, 2002), while RhoGAPs play roles in tumor suppression, like p190RhoGAP (Ludwig et al., 2009) and DLC-1 (Gomez del Pulgar et al., 2005). Finally, ROCK, a downstream effector of RhoA (Jordan et al., 1999), and PAK, a downstream effector of Rac1/Cdc42 (Schnelzer et al., 2000), are reported to be upregulated in some cancers. Aberrant signaling within the RhoGTPase signaling pathways is thought to be especially detrimental, because these pathways regulate many crucial biological processes, including migration, cell cycle progression and survival.

Rho and Cytokinesis:

One of the primary cellular processes regulated by Rho is cytokinesis. This is evidenced by the fact that depletion or inactivation of RhoA leads to cytokinesis failure (Drechsel et al., 1997; Jantsch-Plunger et al., 2000; Kishi et al., 1993; Piekny et al., 2005). Cytokinesis is a coordinated series of events that occurs in late mitosis. It is initiated by specification of the cleavage plane and followed by furrow assembly and ingression, midbody formation, and cell separation. These events result in the production of two daughter cells with an equal complement of chromosomes and membrane. (Glotzer, 2001; Prokopenko et al., 2000; Zeitlin and Sullivan, 2001). Cytokinesis requires the spatial and temporal control of actin and myosin which are controlled by Rho (Piekny

et al., 2005). Specifically, Rho controls cytoplasmic division through the regulation of the contractile ring, which contracts to separate the two daughter cells. The contractile ring is comprised of an actin and myosin network that forms under the surface of cells undergoing cell division (Drechsel et al., 1997; Kaibuchi et al., 1999; Kishi et al., 1993; Mabuchi et al., 1993).

RhoA localizes to the cleavage furrow formation site (Nishimura et al., 1998; Takaishi et al., 1995), and the inhibition of RhoA activity prevents cleavage furrow formation (Kishi et al., 1993; Mabuchi et al., 1993). During the later stages of mitosis, RhoGTP levels increase at the contractile ring (Kimura et al., 2000; Maddox and Burridge, 2003; Yoshizaki et al., 2004). This increase is necessary for cleavage furrow formation and function (Bement et al., 2005; Bement et al., 2006; Su et al., 2009), suggesting that increased Rho activity at the equatorial midzone during cytokinesis is required for cell division.

Rho has three main effector proteins that participate in this process: mDia, a member of the formin family, Rho-dependent kinase (ROCK), and citron kinase (Piekny et al., 2005). mDia has three isoforms, mDia1, mDia2, and mDia3, which belong to the family of Diaphanous-related formins (Goode and Eck, 2007); however, only mDia2 is believed to play a role in cytokinesis (Miki et al., 2009; Watanabe et al., 2008). Binding to active Rho relieves mDia's autoinhibition by competing with the N-terminal DID (Diaphanous inhibitory domain), preventing its association with mDia's C-terminal DAD (Diaphanous autoinhibitory domain) (Alberts, 2001) (Fig. 2A). This relief of autoinhibition exposes the core FH1 and FH2 (formin-homology) domains of mDia

Figure 2

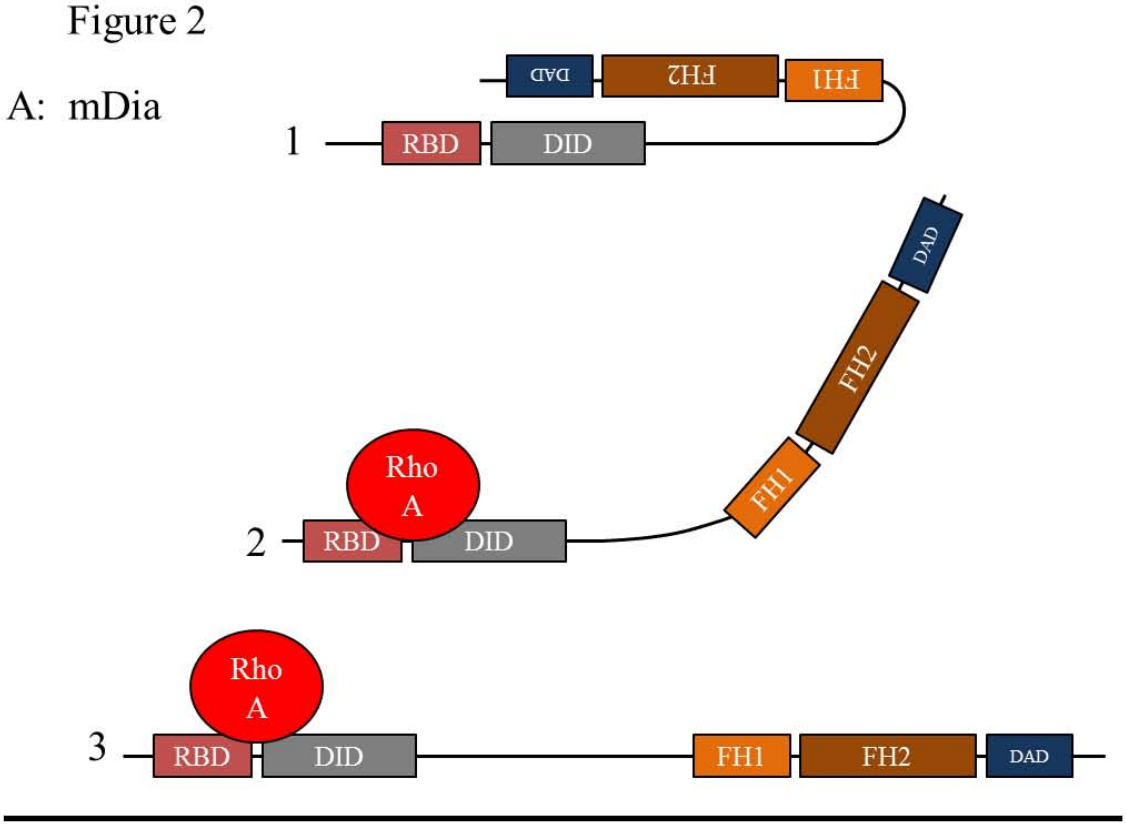
A: mDia
1
RBD
DID
FH1
FH2
DAD
2
Rho A
RBD
DID
FH1
FH2
DAD
3
Rho A
RBD
DID
FH1
FH2
DAD
B: ROCK and Citron Kinase
1
RBD
PH
CR
Kinase
2
Kinase
RBD
PH
CR
Rho A
3
Kinase
Rho A
RBD
PH
CR

Figure 2: Activation of Rho effectors

A: Activation of mDia. mDia is normally autoinhibited by the N-terminal DID binding the C-terminus. This conformation blocks the FH1 and FH2 domains in the center of the protein and prevents actin polymerization by mDia. When Rho is active, it binds the N-terminal RBD and overlaps into the DID. This prevents association between the DID and the DAD and relieves mDia's autoinhibition. DID= Diaphonous inhibitory domain, DAD=Diaphonous autoinhibitory domain, FH=Formin-homology, RBD=Rho-binding domain

B: Activation of ROCK and citron kinase. The CR domain binds and inhibits the kinase domain. Active Rho binds the RBD in the center of the protein and relieves the autoinhibition of the enzymes. This allows the kinase domain of each protein to interact with their downstream effectors. CR=Cysteine rich, PH=Pleckstrin homology domain, RBD=Rho-binding domain.

which promote actin polymerization (Otomo et al., 2005a; Piekny et al., 2005; Rose et al., 2005). Once the FH2 domain has been exposed, mDia becomes elongated and dimerizes to create a ring-like molecule that makes contact with multiple actin subunits. This event promotes the association of two actin monomers and creates a binding site for a third monomer (Otomo et al., 2005b; Shimada et al., 2004; Xu et al., 2004). The formin dimer then remains associated with the barbed end of the actin filament, capping it, while still allowing for recruitment of additional actin monomers, in this way facilitating actin polymerization (Kovar and Pollard, 2004). These actions are necessary for the formation of the contractile ring, as was evidenced when depletion of mDia led to a disruption in furrow formation and phenotypes similar to actin depletion.

In addition to its role in actin nucleation, mDia functions in the stabilization of MTs (DeWard and Alberts, 2008; Fukata et al., 2003; Narumiya et al., 2009), which is a Rho-dependent process (Cook et al., 1998; Palazzo et al., 2001). Depletion of mDia1 destabilizes MTs (Goulimari et al., 2005; Yamana et al., 2006). The mechanism by which mDia promotes MT stabilization is still not completely understood; however, it is known that mDia binds two plus end MT-tip interacting proteins, EB1 and APC. Evidence suggests that binding of these proteins at the growing end stabilizes MTs (Wen et al., 2004). A second possible mechanism has also been proposed based upon the data that the FH2 domain of mDia2 binds directly to MTs (Bartolini et al., 2008). This theory puts forth the idea that mDia binds along the length of the filament, stabilizing it, and suggests that dimerization of mDia allows bundling of MT, further promoting stabilization (Bartolini et al., 2008; DeWard and Alberts, 2008). While the mechanism of

regulation may not be completely understood, the connection and biological effect of Rho activation on MT stabilization through mDia has been well documented.

Another target of Rho, ROCK, regulates furrow ingression by activating myosin II and promoting actin filament polymerization (Riento and Ridley, 2003). Two isoforms of Rho dependent kinases (ROCK), ROCK I, and ROCK II have been described (Nakagawa et al., 1996). ROCKs are serine/threonine kinases that are autoinhibited in their native state. The N-terminus of the protein contains the kinase domain, while the C-terminus has a Pleckstrin Homology (PH) domain with an internal cysteine-rich domain. The kinase domain binds to the cysteine-rich domain within the PH-domain, maintaining the protein in an inhibited form. (Amano et al., 1999) In the center of the protein is the Rho binding domain (RBD). When Rho is bound to GTP, it binds ROCK at the RBD, resulting in release of the kinase domain and the cysteine rich domain and ultimately activation of ROCK (Alberts et al., 1998) (Fig. 2B). Activated ROCK can lead to increased polymerization of actin filaments through the activation of LIM kinases. ROCK phosphorylates LIMK1 at Thr508 (Ohashi et al., 2000) and LIMK2 at Thr505 (Sumi et al., 2001), which in turn phosphorylate and inactivate cofilin, an actin-depolymerizing protein (Agnew et al., 1995). In this way ROCK phosphorylation of LIMK prevents actin depolymerization.

Actin is only one component, albeit a major one, of the actomyosin network that provides the mechanical force responsible for contraction of the cleavage furrow. The other major member of the network is myosin II, whose activity is also regulated by ROCK. Myosin II is a hexamer containing two heavy chains, each with an ATPase

activity, two essential light chains, and two regulatory light chains (rMLC). Phosphorylation of Ser19 on the rMLC stimulates assembly of myosin II into filaments and activates the actin-dependent ATPase activity of the motor. This phosphorylation and subsequent activation of myosin II drive cleavage furrow contraction (Matsumura, 2005; Piekny et al., 2005). ROCK is one of multiple kinases that can directly phosphorylate Ser19 of rMLC resulting in its activation (Amano et al., 1996). ROCK also phosphorylates and inactivates the phosphatase responsible for dephosphorylating rMLC at Ser19, myosin light chain phosphatase, thus further promoting contraction (Kimura et al., 1996).

The final Rho target in this process is citron kinase, another serine/threonine kinase, which also phosphorylates rMLC. The structure of citron kinase is very similar to ROCK, in that it has an N-terminal kinase domain, a middle coiled-coil domain, which contains the RBD, and a C-terminal PH-domain (Madaule et al., 2000). Citron kinase phosphorylates rMLC at Ser19 and at Thr18 as well, the latter of which is thought to be critical for increasing myosin's activity (Yamashiro et al., 2003). Activity of citron kinase is required for completion of cytokinesis, as mutation or deletion of the protein results in cytokinesis failure (Di Cunto et al., 2000; Echard et al., 2004; Shandala et al., 2004). However ROCK and citron kinase do not have redundant activities in cytokinesis. Several studies suggest that ROCK plays a role in regulating the rate of contractile ring ingression, while citron kinase functions in contraction of the cleavage furrow and cytokinesis completion (Matsumura, 2005; Piekny et al., 2005). In fact, ROCK may not be required for cytokinesis, as the ROCK inhibitor, Y-27632, neither blocks initiation nor

the completion of cytokinesis, though it does slow contraction of the cleavage furrow (Kosako et al., 2000; Madaule et al., 2000).

While mDia, ROCK, and citron kinase are the most well studied targets of Rho, they are not the only effectors of Rho that affect the cell-cycle. Rho can also influence the activity of cyclin-dependent kinases (CDKs) during G1, as well as promote organization of microtubules and the actin cytoskeleton during M phase (Jaffe and Hall, 2005). As additional evidence of Rho's importance for the completion of cytokinesis, its activity has been shown to increase during the process (Bishop and Hall, 2000; Glotzer, 2001; Prokopenko et al., 2000). While it is evident that Rho is critical for cytokinesis, it is important to remember that Rho also functions in many different aspects of cellular function, including adhesion and motility.

Rho and Apoptosis:

Conversely, inactive RhoGTPases also have effects on the cell. Many groups have found that prolonged inactivation of the RhoGTPases, Rho, Rac1, or Cdc42, leads to aberrant cellular function and ultimately cell death. Treatment of cerebellar granule neurons with *Clostridium difficile* toxin (Tox B), a specific Rho family inhibitor, leads to cytochrome c release and the activation of both caspases-9 and -3. Similar outcomes were seen when dominant negative Rac1 was introduced into neurons, which led to apoptosis via a c-Jun-dependent pathway (Le et al., 2005). Transfection of dominant negative Rac1 or Cdc42 into Balb/c 3T3 murine fibroblasts resulted in p53-mediated apoptosis (Lassus et al., 2000). Moorman and colleagues specifically inhibited RhoA in EL4 T lymphoma cells with C3 toxin, resulting in 95% cell death (Moorman et al., 1996).

The final piece of evidence that control of RhoGTPase activity is necessary for cell survival comes from the fact that cell lines stably expressing RhoGAPs (resulting in inactive Rho) cannot be generated, presumably due to the deleterious effects on RhoGTP levels.

Attempts to characterize molecular pathways leading to apoptosis that are initiated by Rho inactivation have yielded many candidates, including a decrease in Akt activity (Khwaja et al., 2006; Stepan et al., 2004), a decrease in NF-κB activity (Hippenstiel et al., 2002b; Liu et al., 2004), and an increase in p53 activity (Costello et al., 2000; Li et al., 2002), among others. Taken together, these pieces of evidence underscore the idea that control of RhoGTPase activity is necessary for cell survival.

Rho and Neurite Regulation:

The three main RhoGTPase family members, RhoA, Rac1, and Cdc42 exhibit antagonistic effects on neurite regulation, with Rho promoting neurite retraction and Rac1 and Cdc42 promoting neurite outgrowth (Koh, 2006). For example constitutively active Rho induces neurite retraction in PC12 and N1E115 cells (Koh, 2006; Tigyi et al., 1996), while Rho inactivation by C3 toxin, or dominant negative Rho results in neurite outgrowth (Jalink et al., 1994; Koh, 2006; Kozma et al., 1995). Neurite outgrowth in N1E115 cells requires activation of both Rac1 and Cdc42, and expression of dominant negative forms of either protein inhibits formation of neuritic processes (Sarner et al., 2000). Interestingly, neurite extension induced by Rho inhibition can be blocked by concomitant expression of dominant negative Cdc42 (Kozma et al., 1997), thus highlighting the inter-relationship between the two proteins. Regulators of each of these

proteins can also promote or inhibit neurite extension. GEFs specific for Rac1 and Cdc42 such as Tiam1, STEF, and FIR, all promote neurite extension, as do RhoGAP's such as p190RhoGAP. In contrast, the Rho GEFs, GEF KIAA03880 and Kalirin, stimulate neurite retraction, similar to the Rac1 and Cdc42 GAP, RICS (Koh, 2006). These observations underscore the fact that RhoGTPases regulate the growth and retraction of neurite process and that members of the family function in opposing ways to do so.

Neurite outgrowth and retraction are also regulated by the interplay between actin and myosin (Georges et al., 2008; Koh, 2006; Luo, 2002). Actin dynamics are controlled primarily by two proteins: Arp2/3, which regulates its polymerization; and cofilin, which regulates its depolymerization (Luo, 2002). Arp2/3 can be activated by N-WASP, a downstream effector of Cdc42 (Miki et al., 1998; Rohatgi et al., 1999), and SCAR/WAVE, a target of Rac1 (Kim et al., 2006; Machesky et al., 1999; Miki et al., 1998). Cofillin, on the other hand, is inhibited by LIMK (Agnew et al., 1995), a known substrate of PAK (Edwards et al., 1999). PAK is one of the major effectors for both Rac1 and Cdc42 (Jaffe and Hall, 2005). Through PAK and other downstream effectors, Rac1 and Cdc42 promote, regulate, and maintain actin polymerization, a key element of neurite outgrowth. In this way activation of Rac1 and Cdc42 promote neurite extension.

Although the mechanism by which Rho induces neurite retraction is not yet completely understood, the prevailing theory is that ROCK activates rMLC to activate myosin, thereby increasing the speed of retrograde flow of actin, resulting in greater actin depolymerization (Luo, 2002). Evidence supporting this model is provided by the

finding that ROCK activation induces neurite retraction, a similar phenotype seen with increased MLC phosphorylation. Additionally, treatment with a ROCK inhibitor blocks both neurite retraction and MLC phosphorylation (Hirose et al., 1998). Finally, when Rho levels are maintained at below basal levels, an increase in the activation of Rac1 and Cdc42 is observed (Luo, 2002; Moorman et al., 1999), ultimately resulting in neurite extension. These observations support the idea that Rho inactivation induces neurite outgrowth through two mechanisms. First, Rho inactivation increases Rac1 and Cdc42 GTP levels which promote actin polymerization and neurite extension. Second, Rho inactivation reduces myosin activity through ROCK, decreasing retrograde flow of actin, further promoting neurite extension through increased actin polymerization at the neurite tip.

p190RhoGAP:

As discussed above, GTPase Activating Proteins (GAPs) stimulate the intrinsic GTPase activity of the Rho proteins leading to the inactivation of Rho (Hall, 1990; Kaibuchi et al., 1999; Takai et al., 1995). The first RhoGAP protein was described in 1991 (Diekmann et al., 1991), and since then about 60 GAP-domain containing proteins have been identified (Vega and Ridley, 2008). The RhoGAP family of proteins is defined by the presence of a GAP domain, which is comprised of approximately 150 amino acids that share a minimum of 20% sequence identity (Moon and Zheng, 2003). The GAP domain is characterized by nine α-helices and a loop structure containing an arginine finger (Gamblin and Smerdon, 1998). The arginine finger inserts into the phosphate-binding pocket of the small-G protein target to activate the intrinsic GTPase

activity (Nassar et al., 1998). Mutation of the arginine ablates this activity and results in a dominant negative GAP protein. This mutant is capable of binding its respective small-G protein but is unable to stimulate the small-G's GTPase activity (Li et al., 1997).

Structure of p190:

Among the 60 defined GAPs is a 190 kD protein termed p190RhoGAP (p190). p190 has a high affinity for Rho, although it can also regulate Rac1 and Cdc42 to a much lesser degree (Kaibuchi et al., 1999; Ridley et al., 1993; Settleman et al., 1992a). p190 regulates actin cytoskeleton dynamics by inactivating RhoA (Chang et al., 1995; Ridley et al., 1993), one demonstration of this occurred when microinjection of p190 into Swiss 3T3 cells blocked Rho-mediated actin stress fiber formation (Ridley et al., 1993).

The p190RhoGAP family is comprised of only two members, p190RhoGAP-A (p190-A) (Settleman et al., 1992b) and p190RhoGAP-B (p190-B) (Burbelo et al., 1995), each encoded by a different gene. The gene encoding p190-A localizes to human chromosome 19q13.3 (Tikoo et al., 2000), while p190-B is located at the ArhGAP5 locus on 14q12 (Burbelo et al., 1998). The two 190 kDa proteins share 50% sequence identity and function as GTPase activating proteins (GAPs) for the Rho family of small GTPases. p190-A was identified six years before p190-B, and hence many initial reports refer to the protein as simply p190RhoGAP. Unless otherwise noted, this dissertation describes attributes ascribed to p190-A and to p190, which is assumed to mean p190-A. p190-A, like p190-B, is composed of three major domains (Fig. 3) an amino (N)-terminal GTP-binding domain (GBD), a large middle domain that contains numerous protein–protein

Figure 3

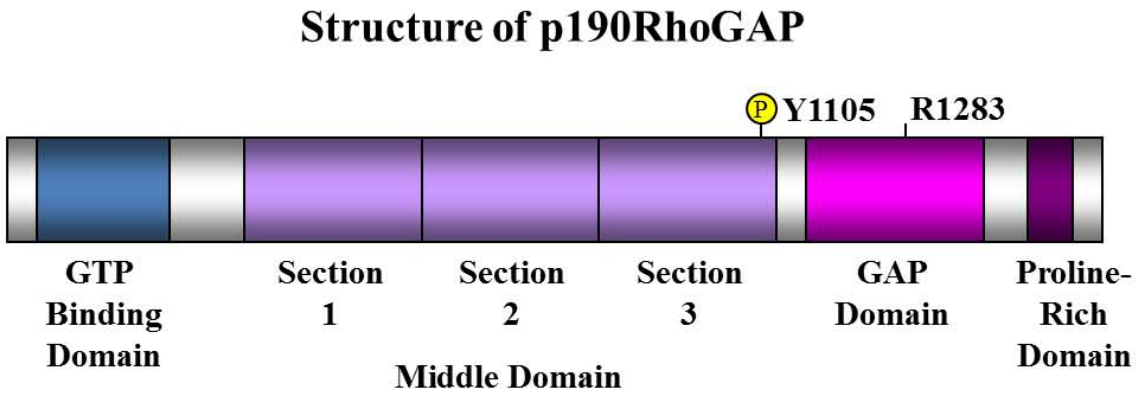
Structure of p190RhoGAP
P
Y1105
R1283
GTP Binding Domain
Section 1
Section 2
Section 3
GAP Domain
Proline-Rich Domain
Middle Domain

Figure 3: Schematic representation of p190RhoGAP

p190 is a RhoGTPase activating protein (GAP) that consists of a N-terminal GTP-binding domain (GBD), a Middle Domain, and a GAP domain. Phosphorylation at Y1105 activates the protein. The MD domain has been arbitrarily divided into 3 sections (Sec1, Sec2, and Sec3). The GAP domain is specific for Rho family members and contains the arginine finger, R1283. Adjacent to the GAP domain is a proline rich region.

interaction motifs and a single major site of tyrosine phosphorylation, Tyr 1105 (Roof et al., 1998), and a carboxyl (C)-terminal GAP domain (Riento et al., 2005). The N-terminal GBD of p190-A binds GTP in a specific and saturable manner (Foster et al., 1994; Roof et al., 2000), but to date, no binding partners specific for the GTP-bound state have been identified, nor has an intrinsic GTPase activity of the region been confirmed. Thus, the significance of GTP binding to this domain remains unclear. However, the GBD, in conjunction with the first third of the middle domain, regulates p190 degradation during the last phase of cell division (cytokinesis) (Manchinelly et al., 2010; Su et al., 2009) and contains a preponderance of ubiquitination sites, several of which are critical for this purpose. Finally, Roof *et al*. found that Src-mediated phosphorylation of the N-terminal GBD of p190 alters the protein's ability to bind GTP (Roof et al., 2000), which affects the GAP activity of p190 (Tatsis et al., 1998).

The middle domain contains several diphenylalanine (FF) motifs that bind RNA-binding proteins, including the transcription factor TF-II (Jiang et al., 2005; Mammoto et al., 2009), numerous putative Src homology 3 (SH3)-domain binding tracts, a plethora of consensus sites for phosphorylation of serines and threonines, and one dominant phospho-tyrosine site, Tyr 1105, which serves as the major binding site for p120RasGAP (Hu and Settleman, 1997; Roof et al., 1998). Phosphorylation of Tyr 1105 by Src family kinases and other tyrosine kinases results in activation of p190's RhoGAP activity and inhibition of the RasGAP activity of bound p120RasGAP (Haskell et al., 2001a; Koehler and Moran, 2001; Settleman et al., 1992a). This event co-regulates signaling through the Ras (upregulated) and Rho (down regulated) pathways. Finally, the middle domain binds

RhoE, which in turn activates the GAP activity of p190, decreasing cellular Rho-GTP levels (Fortier et al., 2008; Wennerberg et al., 2003). This pathway is functional in many cell types, but is particularly well studied in muscle, where RhoE regulates myoblast alignment prior to myotube formation.

In vitro, the C-terminal GAP domain functions in a hierarchical fashion to activate the intrinsic GTPase activity of Rho family members (Rho > Rac > Cdc42) in a reaction that converts activated, GTP-bound small GTPase to its inactive, GDP-bound state. Like many RhoGAP proteins, the active site of p190 is dependent upon the presence of an arginine finger located at Arg 1283. Mutation of this site inactivates the catalytic activity of p190 and results in a dominant-negative protein (Li et al., 1997). In intact cells, p190 preferentially targets Rho (Ridley et al., 1993), and inactivation of Rho by p190 impairs Rho-dependent cytoskeleton re-arrangements (Chang et al., 1995; Ridley et al., 1993). These processes are regulated by Rho effectors, such as ROCK, citron kinase, mDia and others (Narumiya et al., 2009; Narumiya and Yasuda, 2006).

Regulation of p190:

The activation of p190 was originally found to be dependent upon phosphorylation at Y1105 by Src (Haskell et al., 2001a; Roof et al., 1998; Settleman et al., 1992b). Since then, a variety of tyrosine kinases and other enzymes have been shown to regulate p190. Tyrosine kinases Fyn (Liang et al., 2004; Wolf et al., 2001), breast tumor kinase (Brk) (Shen et al., 2008), focal adhesion kinase (FAK) (Holinstat et al., 2006), Fgr (Continolo et al., 2005), v-abl Abelson murine leukemia viral oncogene 2 (ABL2; also called ABL-related gene (Arg) (Hernandez et al., 2004; Shimizu et al.,

2008), and the TEL-ARG oncogenic fusion protein (Palmi et al., 2006), all directly activate p190. While, v-FMS (Trouliaris et al., 1995), NADPH oxidase (Nox-1) (Shinohara et al., 2007), angiotensin II (Rattan et al., 2003; Schieffer et al., 1996), $G\alpha_{13}$ (Bartolome et al., 2008), protein kinase C (PKC) (Brandt et al., 2002), and the p110Δ isoform of phosphatidylinositol 3-kinase (PI3K) (Papakonstanti et al., 2007) indirectly increase either the tyrosine phosphorylation of p190 and/or its activation. While these are the pathways that have been implicated in p190 activation, other groups have looked farther upstream at the activation of p190. A major pathway for p190 activation occurs through engagement of various integrins, such as $\alpha_6\beta_1$ (Nakahara et al., 1998), $\alpha_4\beta_1$ (Moyano et al., 2003), $\alpha_5\beta_1$ (Bass et al., 2008; Wickstrom et al., 2003), and β_2 (Dib et al., 2001), along with soluble fibronectin, type I collagen, or laminin treatment (Svoboda et al., 1999). p190 is also activated upon cadherin engagement (Noren et al., 2003), plexin activation (Barberis et al., 2005), and filamin accumulation (Janiak et al., 2006). Furthermore, treatment with epidermal growth factor (EGF) (Chang et al., 1995; Haskell et al., 2001b), vascular endothelial growth factor (VEGF) (Singleton et al., 2008) or PDGF (Chiarugi et al., 2000a) leads to an increase in p190RhoGAP activity through phosphorylation at Y1105 by c-Src.

Phosphorylation at Y1105 promotes binding to p120RasGAP (p120), allowing for further RhoGAP activation (Bradley et al., 2006; Chang et al., 1995; Sharma, 1998). However, this binding is not required for activation, as p190 is still active even when binding to p120 is inhibited (Tsubouchi et al., 2002). Furthermore, the presence of p120RasGAP can indirectly increase the tyrosine phosphorylation status of p190,

possibly through the mitogen-activated protein kinase (MAPK) pathway (van der Geer et al., 1997). Within the structure of p190 there are two closely linked tyrosine-containing peptides surrounding Y1087 and Y1105 that can bind simultaneously to the two tandem SH2 domains of p120RasGAP upon p190 phosphorylation. This binding can lead to an increase in the accessibility of p120RasGAP's SH3 domain, and an increase in the binding of the complex's downstream targets (Hu and Settleman, 1997). Therefore, p190 often goes through two steps of activation, phosphorylation at Y1105 and binding to p120RasGAP, which further stimulates activation.

While tyrosine phosphorylation promotes activation of p190, multiple mechanisms can decrease its activity. Some serine/threonine phosphorylations can down regulate the activity of p190 (Maddox and Burridge, 2003), as evidenced by a decrease in activation upon glycogen synthase kinase-3β (GSK-3β) phosphorylation (Jiang et al., 2008). Different phospholipids have also been shown to inhibit the RhoGAP activity of p190 and increase its RacGAP activity, although the biological processes regulated by this conversion are still not known (Ligeti et al., 2004; Ligeti and Settleman, 2006). Whereas the tyrosine phosphorylation of p190 increases activation, the dephosphorylation of p190 can lead to a decrease in activity. Several different phosphatases have been implicated in the negative regulation of p190RhoGAP, including protein tyrosine phosphatase 20 (PTP20) (Shiota et al., 2003) and protein tyrosine phosphatase receptor type z (Ptprz) (Tamura et al., 2006), which have been shown to dephosphorylate Y1105. LMW-PTP (Chiarugi et al., 2000b) and protein tyrosine phosphatase PEST (PTP-PEST) (Sastry et al., 2006) have also been shown to

dephosphorylate p190-A, but details of the exact residue are not known. Interestingly, p190 activation by phosphorylation is sensitive to the redox state of the cell. Rac1 activation results in the production of reactive oxygen species (ROS), which inactivate the low molecular weight-protein tyrosine phosphatase (LMW-PTP), inhibiting p190 dephosphorylation, and increasing the activity of p190RhoGAP (Nimnual et al., 2003). In this way, Rac1 activation is thought to decrease activation of Rho.

Aside from phosphatase activity, a decrease in the activity of p190 can also be due to down regulation of one of the activation pathways of p190. For example, Thy-1 (Barker et al., 2004), Src-associated in mitosis (Sam68) (Huot et al., 2009), caveolin-1 (Grande-Garcia et al., 2007), and receptor for activated protein kinase C (RACK1) (Miller et al., 2004) all inhibit Src activation, resulting in a decrease in p190 activation. Furthermore, while most isoforms of PKC have been shown to activate p190 (Brandt et al., 2002), inhibition of PKCΔ increases activity of p190, suggesting that PKCΔ may also negatively regulate p190, at either the FF domain, or the GTPase domain (Fordjour and Harrington, 2009). Recently ROCK was found to regulate Rho activity in a positive feed back loop involving p190. Specifically, endothelin-1 treatment activates RhoA, which stimulates ROCK. ROCK, in turn phosphorylates p190 at Ser1150 resulting in a decrease in p190's activity, thus maintaining Rho activation (Mori et al., 2009). While multiple kinases and phosphatases modify p190 and alter its activation, the primary regulation of activity remains phosphorylation at Y1105.

Functions of p190:

Through Rho-dependent and independent mechanisms, p190 regulates both actin and microtubule dynamics, which modulate a variety of cellular processes, including cell–substratum interaction (Bass et al., 2008; Shiota et al., 2003) cell–cell adhesion (Playford et al., 2008; Wildenberg et al., 2006), cell spreading (Arthur and Burridge, 2001), motility and migration (Barker et al., 2004; Jiang et al., 2008; Shimizu et al., 2008), invasion (Bartolome et al., 2008; Nakahara et al., 1998), cell-fate determination and angiogenesis (Mammoto et al., 2009), vascular permeability (Holinstat et al., 2006; Mammoto et al., 2007), cell-cycle progression (Maddox and Burridge, 2003; Su et al., 2003; Su et al., 2009), death (Morrissey et al., 1999), and neuronal differentiation/development (Billuart et al., 2001; Brouns et al., 2000; Lamprecht et al., 2002; Liang et al., 2004; Sfakianos et al., 2007; Zhang and Macara, 2008). Like Rho, it too has been implicated in tumorigenesis, specifically as a tumor suppressor, given that p190 regulates cell-cycle progression, apoptosis, and invasion and migration.

p190 and Tumor Suppression:

Like many tumor suppressors, the exact mechanism by which p190 controls unregulated cell growth is still unknown. However, like its counterpart, the RhoGAP Deleted in Liver Cancer (DLC-1), mounting evidence suggests that p190 does function as a tumor suppressor. The gene for p190-A has been mapped to chromosome 19q13.3, a region that is rearranged in pancreatic, ovarian, thyroid, and brain cancers (Tikoo et al., 2000). Overexpression of p190 can inhibit PDGF-induced gliomas in a mouse model (Wolf et al., 2003), and the N- and C-terminal domains independently suppress Ras-induced transformation in NIH3T3 cells (Wang et al., 1997). In mouse models,

Morrissey *et. al.* found that p190 expression was increased in apoptotic epithelial cells following castration (Morrissey et al., 1999). Mammoto *et. al.* demonstrated that p190 inhibits angiogenesis in both mice and tissue culture by sequestering the transcription factors, TF-II and GATA2, in the cytosol and inhibiting the production of VEGFR (Mammoto et al., 2009). Finally, p190 also inhibits metastasis and invasion. A p190/Rho chimera reduced human pancreatic cancer invasion and metastasis (Kusama et al., 2006), while p190 activation inhibited invasion of melanoma cells (Molina-Ortiz et al., 2009). Taken together, these findings suggest that p190RhoGAP may be a tumor suppressor protein that functions through Rho.

p190 and Cytokinesis:

p190 levels are modulated during cell cycle progression, like many negative regulators of the cell cycle (Su et al., 2003). Since the primary target of p190 is RhoA, and the activity of Rho is known to increase during cytokinesis, we posit that p190 levels or activity should decrease during the process. If p190 cannot be decreased due to overexpression in breast cancer cells, failure to complete cytokinesis and multinucleated cells result (Su et al., 2003). To test this hypothesis levels of endogenous p190 were measured throughout the cell-cycle, and a significant decrease in p190 levels upon entry into mitosis were observed (Su et al., 2003). Further investigation revealed that p190 is degraded in a ubiquitin-dependent manner and that this down regulation is required for completion of cytokinesis. Specifically, when endogenous p190 was knocked down and a non-degradable mutant was re-introduced at endogenous levels, cytokinesis failure was seen (Manchinelly et al., 2010). Recently, a group in Japan identified an activator of the

anaphase-promoting complex (APC), Cdh1, as the protein responsible for targeting p190 for mitotic degradation (Naoe et al., 2010).

During cytokinesis active Rho localizes to the cleavage furrow (Piekny et al., 2005), where the remaining p190 that is not degraded also localizes (Su et al., 2003). FRET analysis and real time microscopy indicated that cells with appropriate amounts of p190 during cytokinesis have high levels of RhoGTP at the cleavage furrow and are able to successfully complete cytokinesis. However, upon overexpression of p190, a significant decrease in RhoGTP levels can be visualized at the cleavage furrow, ultimately resulting in failure of cytokinesis and multinucleation (Su et al., 2009). p190-induced multinucleation is dependent upon the GAP function of the molecule (Manchinelly et al., 2010; Su et al., 2003) and can be rescued by co-overexpression of a RhoGEF, Ect2 (Mikawa et al., 2008), indicating that p190's function in cytokinesis is through its regulation of Rho's activity. However, the pathways that p190 regulates downstream of Rho still remain to be identified.

p190 and Apoptosis:

The link between p190 and apoptosis was first made when Morrissey *et. al.* reported an increase in both p190 protein and mRNA levels in epithelial cells undergoing apoptosis following castration of rats (Morrissey et al., 1999). At that time it was not known if the increase in p190 levels was causative or an effect of the ensuing apoptosis. Since then, multiple labs have overexpressed p190 in epithelial cells, fibroblasts, and neuronal cell lines of transformed and non-transformed status, and have noticed that cells which overexpress p190 often display chromatin condensation (B. Dukes & S.J. Parsons,

unpublished data; personal communications), a hallmark of apoptosis (Kerr et al., 1972). Additionally, many labs have attempted to generate a cell line which stably overexpresses p190; however, all attempts yielded cells which eventually died (S. Diaz & S.J. Parsons, unpublished data; personal communications). Together all of these data suggest that p190 may play a role in regulating apoptosis; however, this had not been experimentally determined. Therefore, a major part of this dissertation work was devoted to addressing the role of p190 in initiating apoptosis, and how the transformation status of a cell affected the outcome.

It is important to note that established, immortalized cell lines are used throughout this study, yet they are classified as transformed or non-transformed cells. The criteria used to determine the transformation status of a cell line was based upon the guidelines established by the American Tissue Culture Collection in 1990 (Schaeffer, 1990). *In vivo* tumorgenicity and *in vitro* soft agar assay are two ways to assess the neoplastic properties of an established cell line. Colony formation in soft agar indicates anchorage independent growth, while tumor formation in mice indicates tumorigenicity. A cell line must be tumorigenic and have soft agar colony formation to be considered transformed. Even though established cell lines are immortalized, generally through transfection of viral genes, if they did not display both criteria they were considered non-transformed for the purposes of this study.

p190 and Neurite Outgrowth:

Studies in knock-out mouse models have demonstrated a clear role for p190 in neuronal development. For example, mice expressing a partial knock-out mutant of

p190RhoGAP-A lacking the N-terminal GBD domain exhibit significant defects in neural development and abnormalities in forebrain hemisphere fusion, ventricle shape, optic cup formation, neural closure, and layering of cerebral cortex cells brought about by excessive actin polymerization in cells of the neural tube floor plate (Brouns et al., 2000). These mice also exhibit defects in axon guidance, with 95% of them dying within 2 days of birth, while the remaining 5% are runted and die within 3 weeks (Brouns et al., 2001). However, Nemeth *et.al.* recently generated a full-length p190 null mouse and found that they die within one week of birth from encephalopathy and spina bifida (Nemeth et al., 2010). Mice lacking p190-B have defects in the formation of major forebrain connections, which inhibit neurogenesis and ultimately survival of the mice. These mice also display a thinning of the neocortical intermediate zone with defects in neuronal differentiation and/or axonal outgrowth, along with impaired neuronal differentiation (Matheson et al., 2006). These effects of p190 deletion in animals are consistent with the known action of Rho in neurite retraction discussed above. Given the role of Rho in neurite retraction, we asked whether p190 would also regulate this process (Koh, 2006).

In support of this hypothesis, Liang *et.al.* found that overexpression of p190 in oligodendrocyte precursor cells resulted in dendrite formation, a phenotype similar to expression of DNRho, CARac1, or CACdc42, and that this phenotype was dependent upon activation of p190 by Fyn (Liang et al., 2004). Other upstream regulators of p190 have also been implicated in this phenomenon, including Arg (Sfakianos et al., 2007), PAR-6 (Zhang and Macara, 2008), and Src (Jeon et al., 2010a; Jeon et al., 2010b). That p190 induces dendrite formation through its down regulation of Rho is supported by

reports of p190-induced dendrite-formation resulting in a decrease in Rho activation (Billuart et al., 2001; Sfakianos et al., 2007; Zhang and Macara, 2008). These studies also reported a decrease in ROCK activation, with a corresponding decrease in rMLC phosphorylation (Billuart et al., 2001). Together, these findings suggest that p190 can stimulate dendrite extension by decreasing myosin II activity, decreasing retrograde flow, enhancing the growth of actin filaments at the tip of the dendrite, and promoting dendrite elongation.

Apoptosis:

Apoptosis, or programmed cell death, is a process wherein cells play an active role in their own death. Apoptosis is a form of "suicide" that occurs while the cell is in the context of an otherwise healthy environment, such as in a developing fetus. Necrosis, on the other hand is a passive cell death process, brought about by a hostile environment (Isaacs, 1993; Kerr et al., 1972; Wyllie et al., 1980). In apoptosis, the outer cell membrane generally remains intact, while in necrosis, the cell membrane is disrupted and releases cellular constituents into the surrounding environment (Isaacs, 1993; Kerr et al., 1972; Wyllie et al., 1980). Many inducers of apoptosis exist, but some of the most prominent ones in the literature are, fibroblast-associated ligand (FasL), tumor necrosis factor (TNF), TNF-related apoptosis inducing ligand (TRAIL), growth factor starvation, genotoxic agents (γ-irradiation), and oxidative stress (Kukhta et al., 2003; Medema et al., 1993). Apoptosis is a precisely choreographed series of steps, beginning with cell shrinkage, membrane inversion with the exposure of phosphatidylserine, membrane blebbing, nuclear fragmentation, chromatin condensation, and DNA fragmentation, after

which the remainder of the cell is digested by intracellular enzymes and other cells (Green and Reed, 1998; Medema et al., 1993). Apoptosis can be triggered by one of two pathways; at the mitochondria, via an intrinsic pathway (caspase-9) (Hockenbery et al., 1990), or at the plasma membrane, via an extrinsic pathway (caspase-8 and -10) (Zapata et al., 2001), although both converge to a final pathway that results in cleavage of caspase-3 (Ghobrial et al., 2005) (Fig. 4). Caspases, or cysteine proteases, act as the death effector molecules in this process. They are synthesized as inactive proforms and upon activation by the apoptosome, or DISC (Death-inducing signaling complex) formation, cleave substrates at cysteine residues next to aspartate residues. Signal amplification is achieved by caspases cleaving each other at identical sequences (Degterev et al., 2003; Fulda and Debatin, 2006). Active/cleaved caspases then degrade downstream targets, which include protein kinases, cytoskeletal proteins, DNA repair proteins, and inhibitory subunits of endonucleases, all of which ultimately leads to the morphological manifestation of apoptosis (Ghobrial et al., 2005; Mancini et al., 1998; Thornberry and Lazebnik, 1998). Caspase activation is regulated by IAP's (inhibitors of apoptosis) that directly bind and inhibit caspases, preventing cleavage, activation, and progression of apoptosis (Liston et al., 2003).

Intrinsic:

The intrinsic or mitochondrial pathway is initiated by intracellular stress stimuli such as genotoxic agents or oxidative stress (Kukhta et al., 2003; Medema et al., 1993). These stimuli result in permeabilization of the outer mitochondrial membrane which releases cytochrome *c*, Smac/DIABLO, Omi/HtrA2, and endonuclease G into the cytosol

Figure 4

A: Direct Binding

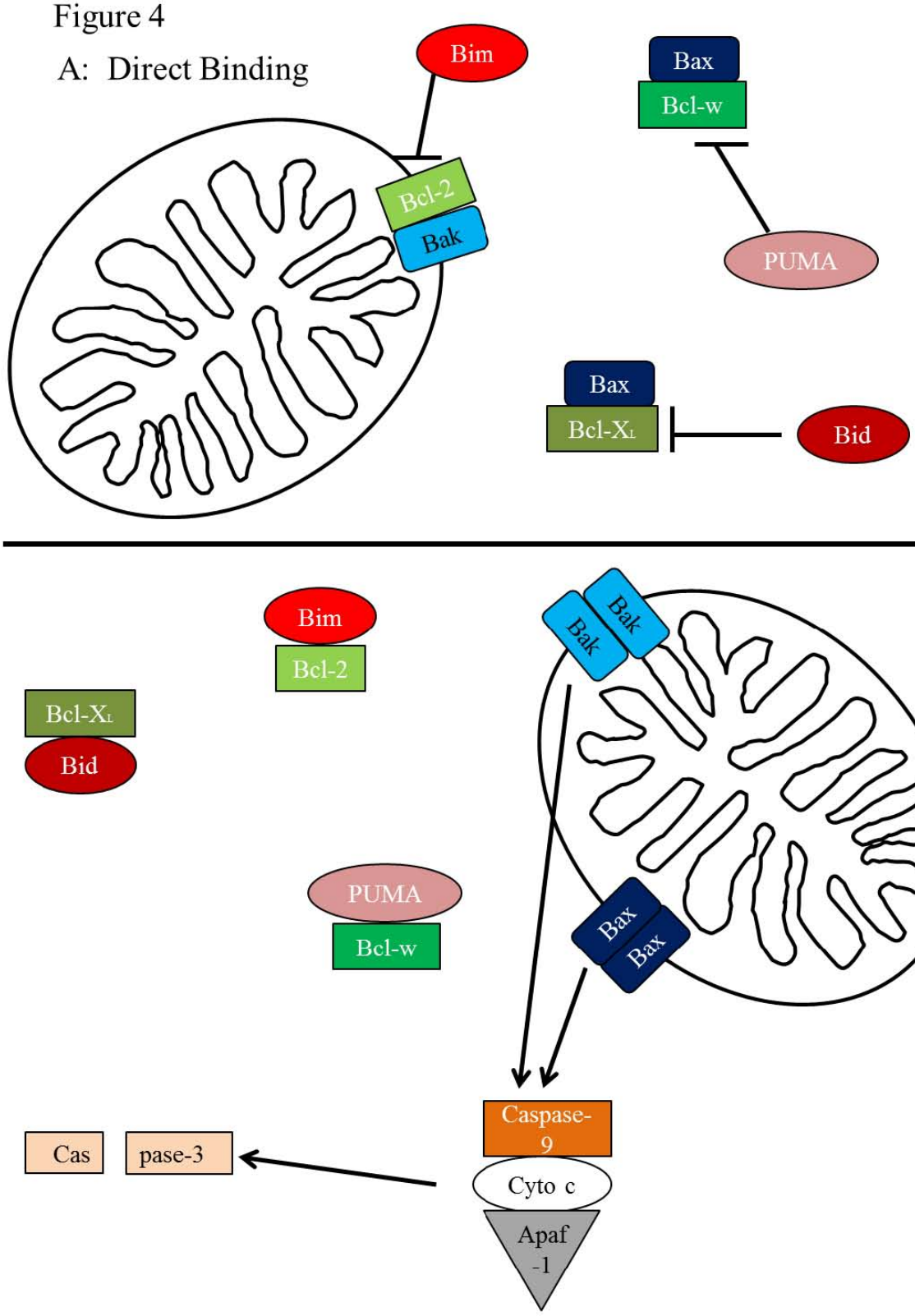

Figure 4: Mitochondrial apoptotic pathway

A: Direct binding model. Bax and Bak are constitutively active and inhibited by the anti-apoptotic Bcl-2 proteins, Bcl-2, Bcl-w, Bcl-X_L, and Bfl-1. The free pro-apoptotic BH3 only proteins, Bid, Bim, and Puma, bind and sequester the Bcl-2 proteins. This frees Bax and Bak from inhibition allowing them to oligomerize at the mitochondria and induce MOMP, resulting in cytochrome c release, binding to Apaf-1 and caspase-9 and activation of the caspase cascade, leading to apoptosis.

Figure 4

B: Displacement

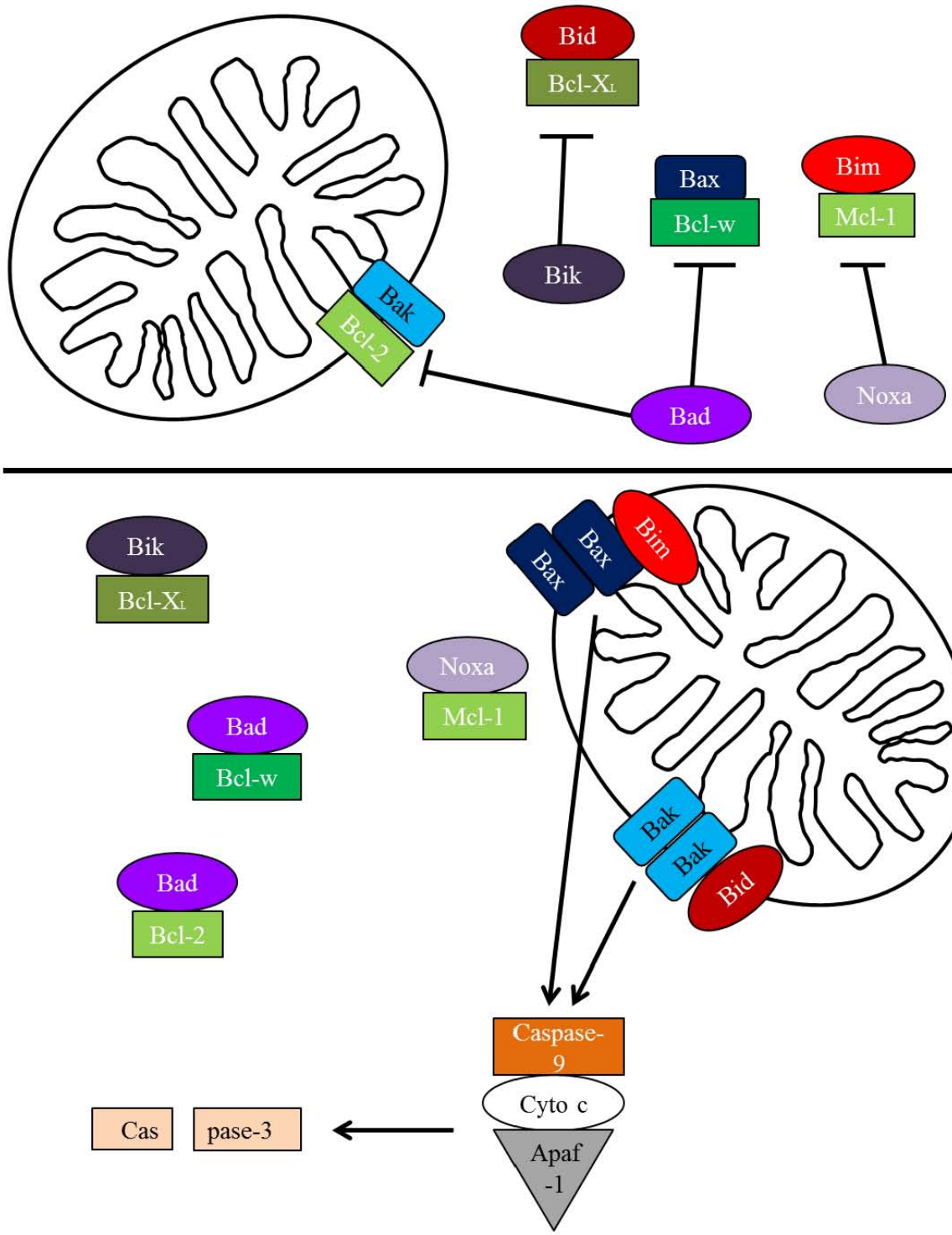

Figure 4: Mitochondrial apoptotic pathway

B: Displacement model. The pro-apoptotic BH3-only proteins are divided into activator (Bid and Bim) and inhibitor (Bik, Bad, and Noxa) proteins. Both Bax and Bak, along with activator pro-apoptotic proteins Bid and Bim, are inhibited by anti-apoptotic Bcl-2 proteins. Inhibitor pro-apoptotic BH3-only proteins bind and sequester anti-apoptotic Bcl-2 proteins, freeing Bax, Bak, Bid, and Bim. Before Bax and Bak can oligomerize, they need to be activated by Bid and Bim. Once activated they oligomerize at the mitochondria and induce MOMP. This stimulates release of cytochrome c which binds to Apaf-1 and caspase-9, activates the caspase cascade, and results in apoptosis.

(Fulda and Debatin, 2006; Saelens et al., 2004). Mitochondrial outer membrane permeabilization (MOMP) is controlled by Bcl-2 family member proteins (Green and Kroemer, 2004). Twenty or more members make up this family, which is defined by the presence of one or more Bcl-2 homology (BH) domains (Cory and Adams, 2002) and includes the anti-apoptotic proteins Bcl-2, Bcl-X_L, and Bcl-w (Skommer et al., 2007; Willis and Adams, 2005), or pro-apoptotic proteins Bax, Bak, Bad, Bim, and Bid (Coultas et al., 2003; Guo et al., 2001; Kataoka et al., 2001; Ke et al., 2001; Skommer et al., 2007). Within the pro-apoptotic family are two distinct groups: 1) Those that are structurally very similar to the anti-apoptotic proteins, especially in the BH1, BH2, and BH3 regions, such as the multi-domain Bcl-2 proteins, cytosolic Bax, and the mitochondrially located Bak; and 2) The BH3 only proteins, including Bad, Bim, Noxa, Bik, and Bid, which are homologous to the Bcl-2 proteins only in the short BH3 region (Skommer et al., 2007).

There are currently two prevailing theories as to how the Bcl-2 family proteins initiate apoptosis, the direct binding model or the displacement model (Skommer et al., 2007; Thomas et al., 2010). The direct binding model (Fig. 4A) proposes that the multi-domain pro-apoptotic proteins, Bax and Bak, are constitutively active, and inhibited by their association with the anti-apoptotic Bcl-2 proteins. Upon apoptotic stimulation the pro-apoptotic BH3 proteins, which exist in an unbound state, are thought to bind to the hydrophobic pocket of the anti-apoptotic Bcl2 proteins and release their repressive hold on Bax or Bak (Willis and Adams, 2005). This allows Bax and Bak to oligomerize at the mitochondria, resulting in a change in the MOMP and the subsequent release of

cytochrome c and other pro-apoptotic factors (Cory and Adams, 2002; Ghobrial et al., 2005; Skommer et al., 2007). Cytosolic cytochrome c then binds to Apaf-1 and caspase-9 to form the apoptosome complex (Cain et al., 2000; Fulda and Debatin, 2006). It is this complex that initiates caspase-3 cleavage and the ensuing caspase cascade that results in cell death.

The displacement model divides the BH3 pro-apoptotic proteins into inhibitor proteins, like Noxa, Bad and Bik, and activator proteins, such as Bid and Bim. This model proposes that Bax and Bak need to be stimulated by the activator BH3 proteins before they can induce MOMP. In a healthy cell the anti-apoptotic Bcl-2 proteins are bound to Bax, Bak, and activator BH3 proteins, Bid and Bim. Upon apoptotic stimulation, inhibitor BH3 proteins (Noxa, Bad, and Bik) bind anti-apoptotic Bcl-2 proteins, displacing the activator BH3 proteins. This frees the activator BH3 proteins so they can bind Bak and Bax, activate them to oligomerize, and initiate MOMP and the caspase-cleavage cascade (Akgul, 2009; Skommer et al., 2007; Thomas et al., 2010).

Bim:

Bim, or B-cell Lymphoma-2 Interacting Mediator of cell death, was discovered in 1998 by two separate labs (Pinon et al., 2008). The first used Bcl2 as bait in a bacteriophage λ cDNA screen (O'Connor et al., 1998), while the other identified Bim in a yeast two hybrid screen with Mcl-1 as bait (Hsu et al., 1998). Since then Bim has been established as a potent regulator of apoptosis, specifically involved in apoptosis induced by cytokine withdrawal, UV radiation, cell detachment, and taxol treatment (Akiyama et al., 2009; Strasser, 2005; Sunters et al., 2003). Many different isoforms of Bim have

been identified (O'Connor et al., 1998; U et al., 2001); however, the three most studied are the 196 a.a Bim_{EL} (Extra Long), the 140 a.a. Bim_L (Long), and the 110 a.a Bim_S (Short) (O'Connor et al., 1998; U et al., 2001)), all of which are cytotoxic. Of the three, Bim_{EL} is the most abundant and widely expressed isoform. Upon serum withdrawal, this isoform undergoes the most dramatic post-translational modifications of the three in the form of phosphorylation. Bim_{EL} expression often precedes the appearance of Bim_L and Bim_S, suggesting that Bim_{EL} may be a precursor to the shorter isoforms (Ewings et al., 2007; Weston et al., 2003).

Bim shows little sequence similarity to the other Bcl-2 family member proteins except for a 9 amino acid region of the BH domain which defines the family (O'Connor et al., 1998). Like other BH3 proteins, Bim contains a hydrophobic C-terminal domain and a transmembrane domain that is needed for localization and insertion into intra-cellular membranes, including the mitochondria (Akiyama et al., 2009; O'Connor et al., 1998; Pinon et al., 2008). Bim can bind and either inactivate all anti-apoptotic Bcl-2 proteins, which include Bcl-2, Bcl-w, Bcl-X_L, A1, and Mcl-1 (Skommer et al., 2007), or lead to the degradation of these proteins, as is the case for Mcl-1 and A1 (Pinon et al., 2008). However, Bim can also bind and activate the pro-apoptotic protein Bax (Pinon et al., 2008).

In healthy cells, Bim associates with microtubules (MTs) through its Dynein Light Chain 1 (DLC1) domain. Upon either UV radiation or loss of cell attachment, Bim disassociates from the MTs and can be found in complex with various Bcl-2 proteins at the mitochondria (Puthalakath et al., 1999; Puthalakath et al., 2001). One mechanism by

which this event is thought to be mediated is by phosphorylation of Bim on Thr112 by JNK. This residue lies within the DLC1 domain, and evidence suggests that phosphorylation at this site may compromise the protein-protein interaction between Bim and MT's. Phosphorylation would thus promote disassociation and increase Bim's affinity for Bcl-2 proteins or Bax (Hubner et al., 2008; Lei and Davis, 2003). Conversely, some evidence suggests that ERK phosphorylation at Ser55, 65, and 73 may target Bim for proteasomal degradation and promote cell survival (Hubner et al., 2008; Strasser, 2005).

Mcl-1:

Myeloid cell leukemia (Mcl-1) was identified as an immediate-early gene expressed during phorbol ester-induced differentiation of ML-1 myeloid leukemia cells (Kozopas et al., 1993) and was the second Bcl-2 family member to be identified (Thomas et al., 2010). It is the largest of the Bcl-2 proteins at 350 amino acids and is the only family member to contain multiple PEST domains (Kozopas et al., 1993). These domains, which are defined by the presence of proline (P), glutamic acid (E), serine (S), and threonine (T) residues, are common features of labile proteins (Akgul, 2009; Thomas et al., 2010). However Mcl-1 does share high structural and functional homology to both Bcl-2 and Bcl-X_L at its three BH domains. This homology allows Mcl-1 to bind other family members and in this way carry out its biological function (Lutz, 2000), which it does in two ways. First, Mcl-1 binds Bax and Bak, preventing oligomerization. For this interaction, the C-terminal transmembrane domain of Mcl-1 is required for localization and insertion into the mitochondrial membrane (Akgul et al., 2000). Mcl-1 can also

interact with the BH3 proteins Bim, NOXA, Bid, Puma, and Bik, sequestering them from the mitochondria and prohibiting their activation of Bax and Bak (Chen et al., 2005). In these ways Mcl-1 carries out its function as an anti-apoptoic Bcl-2 protein.

Mcl-1 has a very short half-life and upon apoptotic induction is rapidly down regulated (Akgul, 2009; Thomas et al., 2010), possibly as a mechanism of freeing pro-apoptotic proteins, and further promoting apoptosis. Mcl-1 expression levels and function are regulated by ubiquitin-mediated degradation, caspase cleavage, and phosphorylation (Akgul, 2009; Thomas et al., 2010). JNK has been shown to phosphorylate Mcl-1 at Thr92, Ser121, Ser159, and Thr163. ERK and GSK-3β have also been identified as kinases targeting Mcl-1. While most studies indicate that phosphorylation at these residues stabilizes Mcl-1 and promotes survival, numerous reports conclude that JNK phosphorylation at Thr163 results in degradation of Mcl-1 and promotes apoptosis (Inoshita et al., 2002).

Taxanes:

Taxanes are a class of anti-mitotic drugs used to treat Kaposi's sarcoma, breast, ovarian, prostate, gastric, and non-small cell lung cancer, among others (Baker et al., 2009). Taxanes were originally isolated from the bark of the Pacific yew *Taxus brevifloia* in 1962 (Wani et al., 1971). However it was not until an NCI screen on plant extracts in the 1970's that this extract was found to have anti-cancer activity (Schiff et al., 1979). Today, taxanes are produced by a semisynthetic method from 10-deacetylbaccatin III, a compound extracted from the needles of the European yew *Taxus baccata*. Taxanes are now classified into two main drug groups for use in the clinic: paclitaxel (Taxol),

which was approved for clinical use in 1992; and docetaxel (Taxotere), which was approved for use in 1996. Both Taxol and Taxotere are hydrophobic compounds with a taxane ring required for binding microtubules (MTs) (Francis et al., 1995; Yue et al., 2010). Binding of taxanes to MTs promotes MT polymerization in high concentrations of the drug and stabilizes MTs in low concentrations (Andreu et al., 1992; Buey et al., 2005; Jordan et al., 1993). However, docetaxel has a higher affinity for the taxane-binding site of MT than paclitaxel and as such has a different effect on cancer cells. While paclitaxel induces cell-cycle arrest at the G2-M phase, docetaxel induces maximal apoptosis during S-phase. Additionally, while both drugs cause significant side effects in the form of neutropenia, mucositis, neuropathy, and myelosuppression, docetaxel-induced neuropathy appears less frequently and is less severe than that of paclitaxel. (Montero et al., 2005)

Taxanes promote cell-cycle arrest and ultimately cell death by altering MT dynamics. Microtubules are long hollow tubes composed of molecules of tubulin, which is itself a heterodimer between α-tubulin and β-tubulin (Luduena, 1998; Verdier-Pinard et al., 2003). The α- and β-tubulin heterodimers polymerize to create protofilaments, 13 of which create the hollow cylinder known as a microtubule (Jordan and Wilson, 2004). These tubes can then grow or shrink by addition or removal of tubulin subunits, an event that is dependent on GTP (Nogales, 2001). Because MT are composed of tubulin dimers, the filaments are polarized, with the β-tubulin at the plus end, or the fast growing end, and the α-tubulin associated with the minus end, or the slow growing end. Both α- and β-tubulin bind GTP; however, only the β-subunit hydrolyses GTP upon incorporation into

the polymer. During polymerization, GTP hydrolysis lags behind by one subunit, which forms a GTP cap and stabilizes the molecule, thus promoting MT growth at the plus end. However, when the rate of subunit addition decreases and GTP hydrolysis catches up with the formation of the GTP cap, the cap is destabilized, resulting in MT depolymerization. The constant polymerization and depolymerization of MTs is known as dynamic instability, and this constant fluctuation is of vital importance to progression of the cell cycle (Gascoigne and Taylor, 2009; Jordan and Wilson, 2004).

During prometaphase, after the breakdown of the nuclear envelope, MTs probe the cytoplasm to attach to chromosomes at their kinetochores. This process, termed congression, connects chromosomes to the mitotic spindle and ensures proper alignment of chromosomes at the metaphase plate (Hayden et al., 1990). During this process, MTs emanate from the mitotic spindle and are extremely dynamic, growing up to 5-10 μm and then shortening almost completely. The presence of just one chromosome that is unable to achieve bipolar attachment is enough to trigger the spindle-assembly checkpoint (SAC) and prevent the cell from transitioning to anaphase. The cell will then remain blocked in metaphase and eventually undergo apoptosis (Jordan et al., 1996; Musacchio and Salmon, 2007).

In the presence of MT inhibitors, like taxanes, chromosomes are often captured at the spindle poles and unable to align at the metaphase plate. This event blocks the cell at the metaphase-anaphase transition and activates the SAC (Kelling et al., 2003). Taxanes inhibit MT depolymerization by binding along the length of the polymer and stabilizing the molecule. This binding occurs in the N-terminal 31 amino acids of the β-tubulin

subunit within the MT polymer (Rao et al., 1994), specifically requiring Arg282, His227, and Asp224 of β-tubulin (Nogales et al., 1999; Rao et al., 1999). Taxanes are thought to gain access to their binding sites by diffusing through small openings in the MT (Nogales, 2001). By an unknown mechanism, taxane binding stabilizes the MT polymer. One hypothesis suggests that binding induces a conformational change in the tubulin heterodimer which increases its affinity for neighboring tubulin molecules (Jordan et al., 1996; Nogales, 2001), thereby inhibiting depolymerization and ultimately resulting in apoptosis.

As previously discussed in this dissertation, active Rho promotes MT polymerization through mDia. However, studies have found that mDia1 can remain active in the presence of low RhoGTP levels (Arakawa et al., 2003; Ishizaki et al., 1997). Titration studies with the C3 endotoxin to inhibit Rho or the Y-27632 ROCK inhibitor with constitutively active mDia suggest an antagonistic relationship between ROCK and mDia1 (Morii and Narumiya, 1995; Tsuji et al., 2002; Watanabe et al., 1999). Results from these studies suggest that mDia1 is still active in the presence of decreased Rho activity, which can promote MT stabilization. This event can activate Rac through Src (Sahai and Marshall, 2002), which can then feedback to further decrease Rho and ROCK activity. Furthermore, Rac activation can decrease Rho activity by activating p190 through the inactivation of its phosphatase LMW-PWP (Nimnual et al., 2003). In this way, MT polymerization, through mDia, can decrease both Rho and ROCK activity.

Given these complex relationships, it follows that drugs which alter microtubule dynamics might affect Rho and its downstream effectors. Such was first demonstrated in

1996 when Enomoto treated Balb/c 3T3 cells with the MT depolymerizing drugs, colcemid and vinblastine, and noticed the rapid formation of actin stress fibers. However, treatment with taxol, a MT polymerizing agent, completely abrogated the formation of actin stress fibers, a phenotype mimicked by microinjection of the C3 Rho inhibitor (Enomoto, 1996). Since then, multiple groups have found that treatment with MT depolymerizing agents like colchicine, nocodazole, and vinblastine activate Rho, which is necessary for their action. The requirement for Rho was supported by the finding that MT depolymerization can be reduced by treatment with the ROCK inhibitor, Y-27632 (Chitaley and Webb, 2002; Niggli, 2003). Conversely, treatment with taxol results in MT polymerization and a decrease in Rho activation and ROCK activity (Birukova et al., 2004a; Birukova et al., 2004b; McGee et al., 2003; Ren et al., 1999). This in turn, inhibits the activation of myosin II, specifically through a decrease in levels of myosin light chain phosphatase (Birukova et al., 2004b; Niggli, 2003; Verin et al., 2001). While the activation of Rho in response to MT depolymerization has been well established, how its activation induces apoptosis in response to depolymerization of MTs is still poorly understood.

What is known about taxol-induced apoptosis is that it is mediated through the pro-apoptotic BH3 protein, Bim. Treatment of cells with taxol results in an increase in Bim, possibly through the phosphorylation of the MAPK pathway (Bull et al., 2010; Li et al., 2007; Tan et al., 2005) and the FOXO transcription factor (Sunters et al., 2003). Recently, it was found that treatment of breast cancer cells with taxol displaces Bim from anti-apoptotic proteins, allowing Bim to activate Bax and Bak and initiate apoptosis

(Kutuk and Letai, 2010). Accordingly, overexpression of Bim increases a cell's sensitivity to taxol-induced apoptosis, while knockdown of Bim confers taxol resistance (Janssen et al., 2007; Li et al., 2005). Moreover, increased levels of endogenous Bim in various NSCLC cell lines correlates with increased susceptibility to taxol-induced apoptosis (Li et al., 2005).

While treatment with taxol increases expression of the pro-apoptotic protein Bim, it decreases expression of the anti-apoptotic protein, Mcl-1. Expression of Mcl-1 is decreased upon taxol treatment in lymphoma, multiple myeloma, and ovarian carcinoma cell lines (Jazirehi and Bonavida, 2004; Poruchynsky et al., 2001), and the stability of the protein parallels the cell's sensitivity to the drug (Poruchynsky et al., 2001). Knockdown of Mcl-1 increases the amount of taxol-induced apoptosis in cell lines (Skoda et al., 2008; Yamanaka et al., 2006) and mice (Wertz et al., 2011). However, when Mcl-1 cannot be degraded, due to a mutant E3 ligase, taxol resistance is conferred (Wertz et al., 2011). The stability of Mcl-1 in response to taxol may also be regulated by JNK phosphorylation. Taxol treatment of human monocytic leukemia cells increases Mcl-1 phosphorylation by JNK, which corresponds with a decrease in expression levels (Poruchynsky et al., 2001). Recently, Wertz *et.al.* found that JNK phosphorylation can simulate taxol-dependent degradation of Mcl-1 through the E3 ligase FBW7 (Wertz et al., 2011). Together these data suggest that taxol stabilizes MT polymerization, which inactivates the Rho-ROCK pathway and up regulates the MLC phosphatase to decrease myosin II activation. While we do not currently understand how myosin II inactivation

leads to apoptosis, it is known that increased Bim expression and decreased Mcl-1 expression are required for taxol-induced apoptosis.

Extrinsic:

The extrinsic apoptotic pathway utilizes the caspase-8, caspase-3 pathway. Caspase-8 is activated through death receptors. Death receptors are members of the tumor necrosis factor (TNF) receptor gene superfamily that consists of more than 20 proteins, including CD95 (APO-1/Fas), TNF receptor 1, and TNF-related apoptosis-inducing ligand-receptor 1 (TRAIL) (Ashkenazi, 2002; Fulda and Debatin, 2006; Walczak and Krammer, 2000). When a death stimulus, such as FasL (Fas Ligand) activates this pathway, its specific receptor is activated (FasL receptor [CD95]) and trimerizes, recruiting adaptor proteins such as Fas-associated death domain (FADD) from the cytosol (Walczak and Krammer, 2000). This complex recruits caspase-8 to form the death-inducing signaling complex (DISC) (Kischkel et al., 1995). Oligomerization of caspase-8 upon DISC formation leads to self-cleavage, which can then activate downstream effector caspases (Fulda and Debatin, 2006). In some cases the amount of caspase-8 cleavage is insufficient to yield a robust apoptotic response. To circumvent this problem caspase-8 can also cleave Bid to its active form, tBid, which translocates to the mitochondria and causes release of cytochrome c and cleavage of caspases-9 and -3 (Fulda et al., 2002; Scaffidi et al., 1998).

Effectors:

The extrinsic and intrinsic pathways are major mediators of apoptosis; however, it is also known that apoptosis can be initiated by proteins such as p53, JNK, p38, Akt, and

NF-κB, all of which have been implicated in apoptosis mediated by Rho family members. The exact apoptotic initiating mechanisms of these proteins have yet to be fully determined; however, much evidence supports the concept that activation of p53, p38, and JNK or decreased levels of Akt leads to apoptosis though the intrinsic pathway. Decreased levels/activation of Akt can reduce its inhibitory effect on FKRHL, capsase-9 and Bad, resulting in apoptosis (Cantley, 2002; Ghobrial et al., 2005). NF-κB's role in apoptosis is more complicated, as it can be both pro-and anti-apoptotic. While most known NF-κB pathways function in survival by activating IAP, BCL-X_L, and FLIP, NF-κB is also activated in response to some apoptotic stimuli. Activated NF-κB can transcriptionally activate pro-apoptotic factors, such as *c-myc* and p53, to initiate the intrinsic pathway, or it can increase FasL production to induce an extrinsic apoptotic response.

p53:

p53 was discovered in 1979 as an SV40 large T-antigen binding protein (DeLeo et al., 1979) and is considered the quintessential tumor suppressor protein (Brady and Attardi, 2010; Farnebo et al., 2010). The ancestral function of p53 is to trigger apoptosis in response to DNA damage to preserve the integrity of the germ line (Lu et al., 2009). However, as organisms evolved, the protein also evolved to gain more functions including; apoptosis, senescence, cell-cycle arrest, DNA repair, autophagy, metabolism, angiogenesis, and fertility (Brady and Attardi, 2010; Brooks and Gu, 2010). To promote these biological functions, p53 is activated by a variety of stimuli, which include DNA damage, hypoxia, oncogene expression, nutrient deprivation, and ribosome dysfunction

(Brady and Attardi, 2010; Brooks and Gu, 2010; Farnebo et al., 2010). Upon activation p53 forms tetramers, translocates to the nucleus, and promotes transcription of mRNA and microRNA which give rise to specific biological outcomes (Kruse and Gu, 2009; Laptenko and Prives, 2006). What is transcribed upon p53 activation depends not only upon the cell-type and environment, but also upon the nature of the stress which activates the protein. For instance severe stress on the cell may lead to an apoptotic response which will induce the transcription of Bax, FasL, Noxa, or Puma (Riley et al., 2008; Zilfou and Lowe, 2009), or it may lead to cellular senescence through the transcription of p21 or PML (Kortlever et al., 2006; Riley et al., 2008). Conversely, if the cellular stress is less severe, p53 activation may result in either cell-cycle arrest or DNA repair through the transcription of Reprimo, 14-3-3, and GADD45 (Brady and Attardi, 2010).

p53 is structurally similar to most other transcription factors, in that it contains transcriptional activator domains which enhance the transcription of its target genes (Gamper and Roeder, 2008; Joerger and Fersht, 2007). The central core of the protein is the DNA binding domain, which binds to sequence-specific regions of the DNA (response elements) (Liu and Kulesz-Martin, 2006). At the C-terminus of the molecule are the tetramerization domain and a basic, lysine-rich domain, which facilitates selection of its response elements. This basic domain is also subject to a multitude of post-translational modifications which affect the protein's activation, stability, and sequence-specific DNA binding. These modifications include phosphorylation, acetylation, ubiquitination, methylation, sumoylation, and neddylation (Amaral et al., 2010; Riley et al., 2008). Some of the proteins reported to phosphorylate and activate p53 are ATM,

Chk1, Chk2, JNK, and p38 (Amaral et al., 2010; Bartkova et al., 2005; Gorgoulis et al., 2005). Normally p53 is bound and sequestered in the cytoplasm by the E3 ligase, MDM2, which associates with p53 at the transactivation domain. MDM2 ubiquitinates p53, resulting in its constant down regulation, keeping the endogenous levels of p53 low in a healthy cell (Brady and Attardi, 2010; Brooks and Gu, 2010). However, upon cellular stress, ATM or other kinases phosphorylate p53, promoting dissociation from MDM2. This stabilizes the protein, leading to a nuclear accumulation of the protein and transcription of p53 target genes (Bartkova et al., 2005; Farnebo et al., 2010; Gorgoulis et al., 2005). However, p53 has also been reported to have pro-apoptotic function independently of its transcriptional activity. Although it is still not fully understood, the current model suggests that p53 regulates the stability and expression of various Bcl-2 family member proteins in the mitochondrial membrane (Brady and Attardi, 2010; Brooks and Gu, 2010).

p38:

p38 is a member of the mitogen associated protein kinase (MAPK) family of proteins, which include ERK, JNK, and p38 (Keshet and Seger, 2010; Raman et al., 2007). The ERK pathway is generally thought to be involved in cell proliferation, while the other two pathways function mainly in apoptosis (Chang and Karin, 2001; Olson and Hallahan, 2004; Rennefahrt et al., 2005; Xia et al., 1995). The MAPK proteins are activated by a cascade of kinases starting with a membrane-proximal serine/threonine kinase (MAPKKK/MAP3K) that phosphorylates and activates a second kinase (MAPKK/MKK). This second kinase is a dual-specific kinase which phosphorylates the

sequence Thr-X-Tyr, with the X being specific for each of the respective MAPK family members and is located in the activation loop. Phosphorylation of the activation loop leads to a conformational change that alters the alignment of the hemispheric halves of the folded protein and enhances its access to subsequent substrates. The ability of the third and final kinase (ERK, JNK, or p38) to phosphorylate its downstream targets leads to a biological outcome, such as growth or apoptosis. (Ashwell, 2006; Bellon et al., 1999; Canagarajah et al., 1997; Wilson et al., 1996) p38 is predominantly phosphorylated by MKK 3 and 6 within minutes of exposure to tumor necrosis factor-α (TNF-α), interleukin-1 (IL-1), heat shock, cytokines, or high osmolarity (Kim et al., 2002; Rennefahrt et al., 2005). MKK3/6 are themselves activated by Mlk1-3, Dlk, Lzk, Mekk1-4, Tak1, Ask1-2, and Tp1-2 (Feng et al., 2009; Wagner and Nebreda, 2009). In many cellular contexts these latter proteins are activated by active Rac1 or Cdc42 (Hall, 2005; Verma et al., 2002), which is associated with decreased Rho activity (Georges et al., 2008; Koh, 2006).

p38 induces apoptosis either through the regulation of its downstream transcription factors, such as p53, ATF2, Elk1, C/EBPβ, MSK1, and MNK1-2, or by directly interacting with Bcl-2 proteins (Cuenda and Rousseau, 2007; Ono and Han, 2000). p38 phosphorylates Bcl-2, decreasing its anti-apoptotic ability (De Chiara et al., 2006), while p38 phosphorylation of Bax promotes its translocation to the mitochondria and initiates MOMP (Capano and Crompton, 2006; Choi et al., 2006).

JNK:

JNK, or Jun N-terminal kinase, is another member of the MAPK family of proteins that is best known for its role in promoting apoptosis. It is regulated in the same way as p38, by a cascade of kinases. It is activated in response to inflammatory cytokines, environmental stress, heat shock, DNA damage, and DNA and protein synthesis inhibition (Kyriakis and Avruch, 2001). These stimuli activate JNK through the upstream kinases MEK 4 and 7, which are in turn activated by many of the same kinases as p38 (Kyriakis and Avruch, 2001; Raman et al., 2007). Like p38, JNK is often activated by Rac1 or Cdc42 (Coso et al., 1995).

Also similar to p38, JNK promotes apoptosis in two ways, i.e., through regulation of transcription factors and Bcl-2 proteins. JNK phosphorylation can lead to an increased activity of p53, Elk1, ATF2, and FOXO (Wagner and Nebreda, 2009; Weston and Davis, 2007). JNK also activates c-Jun, which leads to the formation of the transcription factor AP-1, of which TNFα, FasL, and Bak, are all target genes (Fan and Chambers, 2001). Through phosphorylation, JNK has also been reported to inactivate Bcl-2 (Srivastava et al., 1999; Yamamoto et al., 1999) and activate Bid (Madesh et al., 2002) and Bad (Tsuruta et al., 2004). Furthermore, JNK phosphorylation of Bim releases the protein from the dynein and myosin V motor complex, allowing it to act as a pro-apoptotic protein (Lei and Davis, 2003). Finally, taxol-treatment increases JNK expression, and silencing of JNK confers resistance to taxol-induced apoptosis (Kolomeichuk et al., 2008). Thus, JNK activity mediates the apoptotic response of a cell through regulation and phosphorylation of transcription factors, and Bcl-2 proteins.

Akt:

Akt is a serine/threonine kinase which was discovered as a retroviral oncogene in 1991 (Bellacosa et al., 1991). Akt functions in protein synthesis, energy metabolism, and most notably, survival (Duronio, 2008; Miyamoto et al., 2009). Activation of receptor tyrosine kinases or G-protein coupled receptors activates PI3K, which results in an increase in PIP_3 production. Akt is recruited to the plasma membrane in response to the increase in PIP_3 where it can be phosphorylated at Thr308 by its upstream kinase, PDK1 (Sarbassov et al., 2005; Williams et al., 2000). Once activated, Akt dissociates from the plasma membrane to interact with its cytosolic targets, mTOR, GSK-3β, and FOXO, which function in translation, protein degradation, and transcription (Matsui and Rosenzweig, 2005; Morisco et al., 2000; Shioi et al., 2002; Skurk et al., 2005).

Akt is considered to be a pro-survival protein. This was first recognized when inhibition of the Akt pathway alone resulted in cell death (Scheid et al., 1995; Yao and Cooper, 1995). Akt maintains cell survival and preserves the mitochondrial outer membrane potential by directly or indirectly regulating the expression of the Bcl-2 family of proteins. As an indirect mechanism, Akt phosphorylates FOXO, resulting in its sequestration in the cytoplasm and degradation (Brunet et al., 1999). This prevents transcription of the pro-apoptotic proteins Bim and Fas L (Dijkers et al., 2000; Suhara et al., 2002). Akt is also an upstream regulator of the NF-κB pathway. By phosphorylating IKKα, Akt can stimulate its degradation and promote expression of the anti-apoptotic proteins Bcl-2, Bcl-X_L, and the caspase-8 inhibitor FLIP by nuclear NF-κB (Ozes et al., 1999; Romashkova and Makarov, 1999). Akt can also activate p53 by phosphorylating its inhibitor, MDM2, and promoting MDM2 degradation (Mayo and Donner, 2001).

Direct regulation of the stability and/or expression of the Bcl-2 proteins by Akt has also been described. Phosphorylation of Bad on Ser136 by Akt inactivates the pro-apoptotic protein by promoting it association with 14-3-3 (Blume-Jensen et al., 1998). Akt can also inactivate Bax through phosphorylation of Ser183 which prevents the conformation change required for translocation and insertion into the mitochondrial members (Gardai et al., 2004). All of these actions of Akt result in either the activation of anti-apoptotic proteins or inactivation of pro-apoptotic proteins. Thus, inactivation of Akt inactivates the anti-apoptotic proteins and activates the pro-apoptotic proteins, ultimately resulting in cell death.

NF-κB:

Deciphering the role of NF-κB in apoptosis has been perplexing, as NF-κB activity was originally reported to increase after exposure to DNA-damaging agents or TNFα exposure (Baichwal and Baeuerle, 1997). However, it is now believed that the increase in NF-κB activation is a recovery response by the cell in an attempt to salvage the damage induced by stress, inflammation, UV irradiation, or cytokines and prevent apoptosis (Baichwal and Baeuerle, 1997; Plantivaux et al., 2009). In contrast, there are reports of NF-κB activation promoting apoptosis (Kasibhatla et al., 1999; Lin et al., 1999; Zheng et al., 2001). As such, it appears that NF-κB has roles in promoting both cell survival and death. Nonetheless, the best characterized role of NF-κB is in cellular survival.

In healthy cells, NF-κB is sequestered in the cytoplasm by IκBα, which masks its nuclear localization sequence (Zandi et al., 1997). When the cell is under stressful

conditions, the IκB kinase complex (IKK) phosphorylates IκBα, targeting it for degradation. NF-κB can then translocate to the nucleus where it binds DNA as a heterodimer containing a p50 subunit and a p65 transactivator subunit, RelA. Once bound to DNA NF-κB can activate the transcription of its target genes (Baichwal and Baeuerle, 1997; Plantivaux et al., 2009). NF-κB promotes survival primarily through the transcription of the anti-apoptotic proteins, Bcl-2 and Bcl-X_L (Ozes et al., 1999; Romashkova and Makarov, 1999), or caspase inhibitors, c-IAP1 c-IAP2, or c-FLIP (Bakkar and Guttridge, 2010; Kucharczak et al., 2003). However, NF-κB can also promote apoptosis through increased expression of pro-apoptotic proteins Fas, FasL, DR4-6, p53, and Bcl-$_X$S (Bakkar and Guttridge, 2010; Kucharczak et al., 2003).

Rho:

It has been known for years that the inactivation of Rho results in cell death, as has already been discussed in this dissertation. However the apoptotic signaling pathways that are activated upon down regulation have yet to be elucidated. Treatment with *Clostridium difficile* toxins induces cytochrome c release (Matarrese et al., 2007; Nottrott et al., 2007), while inactivation of Rho through a variety of other methods decreases Bcl-2 (Badr et al., 2010; Costello et al., 2000; Fromigue et al., 2006; He et al., 2008; Hippenstiel et al., 2002a), Bcl-X_L(Badr et al., 2010), and Mcl-1 (Hippenstiel et al., 2002a) expression. Accordingly, several labs have reported that inhibition of Rho increases Bim expression (Le et al., 2005; Loucks et al., 2006) and activates Bid cleavage (Brito et al., 2002; Hippenstiel et al., 2002a). JNK, which is known to regulate the stability of both Bim and Mcl-1, can be activated upon prolonged decrease in Rho

activity (Le et al., 2005). However, an increase in p38 activation has also been reported when Rho is not geranylated, and hence is not activated (Khan et al., 2011; Schulz et al., 2009). p53 has also been implicated in the Rho inactivation apoptotic pathway, as an increase in p53 is seen upon a decrease in Rho and ROCK activation (Costello et al., 2000; Li et al., 2002).

Alternatively several reports implicate the pro-survival pathways, Akt and NF-κB, in Rho inactivation-induced apoptosis. Multiple methods of inactivating Rho result in either a decrease in IκBα phosphorylation or NF-κB DNA binding, suggesting a decrease in the pro-survival signals resulting from this pathway (Badr et al., 2010; Denoyelle et al., 2001; Hippenstiel et al., 2002b; Khan et al., 2011; Liu et al., 2004). However the most commonly reported pathway to be altered by Rho inactivation is Akt. Whether the Rho pathway is inactivated by bacterial toxins, siRNA, post-translational modifications, RhoGDI expression, or ROCK inhibition a significant decrease in Akt activation has been reported by multiple labs (Badr et al., 2010; Dreger et al., 2009; Hamid et al., 2007; Khwaja et al., 2006; Krijnen et al., 2010; Qi et al., 2008; Reuveny et al., 2004; Schulz et al., 2009; Stepan et al., 2004; Weiss et al., 1999). Finally, an increase in FasL production has also been seen upon Rho or ROCK inhibition (Ramaswamy et al., 2007; Sarrabayrouse et al., 2007).

While many reports have described activation of different apoptotic signaling pathways upon Rho inactivation, each study has used a different method to down regulate Rho. As such, this could have different effects on the cell, based upon Rho expression levels, localization, post-translational modifications, or modifications of Rho's upstream

or downstream effectors. Additionally, there is a great deal of cross-talk between the apoptotic signaling pathways. For instance, Akt can activate p53 and inactivate the NF-κB pathway, while JNK and p38 can activate the p53 pathway and inactivate the pathways downstream of Akt and NF-κB. All of these reasons could contribute to the numerous, sometimes confusing results reported regarding the apoptotic pathways responsible for the death of a cell upon loss of Rho activation.

Cytokinesis:

Cytokinesis is the final step in cell division where ingression of the cleavage furrow results in two separate daughter cells. The process initiates in anaphase and continues throughout telophase when membrane invagination at the equatorial cell cortex occurs. Cytokinesis is completed when intercellular membrane abscission separates daughter cells (Glotzer, 2001). The contractile forces required for furrow ingression are provided by a ring of filamentous actin and myosin II that is juxtaposed to the cell membrane at the equator of the dividing cell. Assembly and proper regulation of this contractile ring is critical for achieving proper cell division and is under the control of the small GTPase RhoA (Piekny et al., 2005) (Fig. 5). Rho's role in cytokinesis has already been discussed in this dissertation, and so will not be described here. Instead, this section will focus on regulators of cytokinesis that are upstream and downstream of Rho.

Microtubules:

In 1961, Raymond Rappaport displaced the mitotic spindle with a glass bead and found that the cleavage furrow and all subsequent cleavage furrows formed in response to the location of the mitotic spindle (Rappaport, 1961). These studies suggested that the

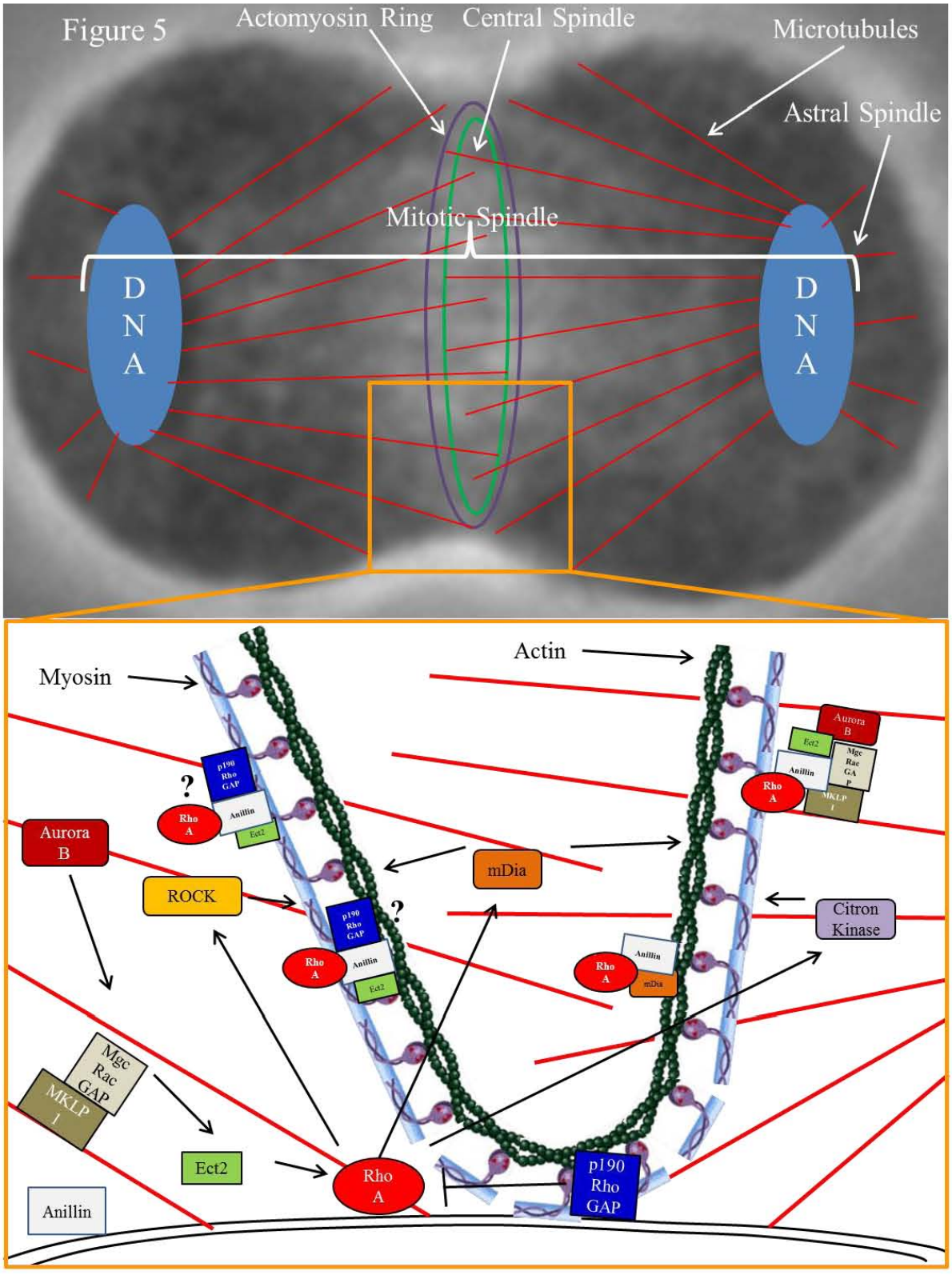
Figure 5
Actomyosin Ring
Central Spindle
Microtubules
Astral Spindle
Mitotic Spindle
D N A
D N A
Myosin
Actin
Aurora B
ROCK
mDia
Citron Kinase
Mgc Rac GAP
MKLP 1
Ect2
Rho A
Anillin
p190 Rho GAP
?

Figure 5: Cytokinetic pathways

Pathways active in cytokinesis. Daughter cells are separated by contraction of the actomyosin network, a ring of actin and myosin II filaments. Location of the cleavage furrow is initiated by signals emanating from the microtubules. (Upper panel) The centralspindlin, composed of the kinesin motor protein, MKLP1 and MgcRacGAP, are activated by Aurora B. Upon activation, this complex activates the RhoGEF, Ect2. RhoGTP levels are maintained by the dichotomous relationship between Ect2 and p190RhoGAP. When active, Rho organizes actin polymerization through mDia, myosin II activation through ROCK and citron kinase, and microtubule polymerization through mDia. Anillin is a scaffold protein which binds actin, myosin II, Ect2, MgcRacGAP, mDia, ROCK, and Rho. Whether anillin and p190 associate is not currently known. Possible anillin complexes are shown around the actomyosin ring. (Lower panel)

positioning of the cleavage furrow was not determined by chromosomes or cytoplasm but by the location of microtubules. Today, there is some debate as to whether the cue for cleavage furrow positioning is determined by aster MTs or the mitotic spindle, and there are three leading theories. The first theory, called polar or astral relaxation, proposes that astral MTs provide an inhibitory signal to the cortical regions of the cell. This results in inhibition of contraction and establishes a gradient of cortical tension with the highest tension and cortical furrowing located at the center of the cell. The second theory is based on the classic Rappaport experiments and is termed astral stimulation. This model suggests that furrowing is determined by the equatorial zone where MT asters converge at the cortex. It is proposed that a subpopulation of mitotic asters position the cleavage furrow through the delivery of specific factors that move along the MTs. The last model is a refinement of the astral stimulation model. This model, called the central spindle stimulation model, puts forth the idea that cleavage furrow formation is determined by the position of the central spindle. (Oliferenko et al., 2009; von Dassow, 2009) The merits and pitfalls of each of these models are beyond the scope of this dissertation; however, it is clear from each that positioning cues from MTs establish the position of the cleavage furrow.

However, positioning of the cleavage furrow is not the only thing altered if MTs in the mitotic spindle are displaced. Active Rho is concentrated at the cleavage furrow in what is called the Rho zone. The width of the Rho zone correlates almost exactly with the width of the central spindle. Lengthening or contracting of the mitotic spindle also results in a corresponding alteration in the width of the Rho zone. Moreover, if the

central spindle is displaced from one side of the cell to another, Rho activity quickly dissipates from the old Rho zone, and an increase in Rho activation is seen at the new corresponding appropriate position relative to the new spindle (Bement et al., 2005). This phenomenon is most likely regulated through the activity of the centralspindlin complex, comprised of the plus-end-directed kinesin MKLP1, and the RhoGAP, MgcRacGAP (Mishima et al., 2002). This complex is required for activation of the cytokinetic RhoGEF, Ect2 (Somers and Saint, 2003; Zhao and Fang, 2005b), which is required for the activation of Rho at the cleavage furrow (Yuce et al., 2005). All three proteins, MKLP1, MgcRacGAP, and Ect2, are required for the completion of cytokinesis (Kamijo et al., 2006; Nishimura and Yonemura, 2006; Yuce et al., 2005). Through action of the motor component of MKLP1 in anaphase, the centralspindlin complex accumulates at the cleavage furrow. Thus, MKLP1 is thought to localize the complex to the cleavage furrow (Nishimura and Yonemura, 2006).

Downstream of Rho, several lines of evidence suggest that the mDia proteins may have some function in the regulation of MT dynamics during mitosis. mDia1 localizes to the mitotic spindle and is thought to regulate its position (Ishizaki et al., 2001; Kato et al., 2001). mDia3 is required for bipolar MT attachment and chromosome segregation (Yasuda et al., 2004), while mDia2 has been found to associated with taxol-stabilized MTs (Palazzo et al., 2001). However, little is currently known about the exact mechanisms of action of the mDia proteins in these processes.

Aurora B:

Three members of the Ser/Thr Aurora kinases family have been described. Aurora A, B, and C share 70% sequence identity in the catalytic domain (Carmena et al., 2009; Kollareddy et al., 2008). However, despite this similarity, they have very distinct functions in mitosis. Aurora A functions primarily in mitotic entry and centrosome maturation (Barr and Gergely, 2007), while Aurora B is the catalytically active member of the Chromosomal Passenger Complex (CPC) and is required for cytokinesis (Carmena et al., 2009). Aurora C is the newest member of the family, and its functions are still under investigation; however, the data at present suggest it may have similar functions as Aurora B (Kollareddy et al., 2008).

Aurora B is a 343 amino acid bipolar protein, with a β-strand N-terminal involved in regulation of the protein and an α-helical C-terminus which acts as a docking site for its various substrates (Sessa et al., 2005). The kinase domain and activation loop are located in the center of the protein (Brown et al., 2004). Activation of Aurora B is dependent upon binding to specific protein cofactors, which can induce a conformational change in the activation loop of Aurora B and trigger the kinase activity. This conformational change puts Aurora B into an intermediate state; however, the protein is not fully active until a threonine residue in the T (activation)-loop is auto-phosphorylated (Bishop and Schumacher, 2002; Honda et al., 2003).

Aurora B functions in spindle assembly, tension promotion of bi-oriented chromosomes, spindle assembly checkpoint, sister chromatid cohesion, and cleavage furrow ingression and cytokinesis (Carmena et al., 2009). To carry out so many diverse mitotic functions, Aurora B localization is very dynamic and has been very well defined.

During prophase, Aurora B localizes along the chromosome arms and at the centromeres, from prometaphase to metaphase it is confined to the inner centromere region, and in anaphase it moves to the central spindle and cortex, eventually accumulating in the midbody during telophase (Lens et al., 2010).

Aurora B activity and localization are regulated by Borealin, Survivin, and INCEP, all of which together make-up the CPC (Chromosomal Passenger Complex) (Carmena et al., 2009; Lens et al., 2010). Borealin is thought to promote clustering which may lead to Aurora B auto-activation at the centromere (Kelly et al., 2007; Sessa et al., 2005), while Survivin targets the CPC to centromeres (Vader et al., 2006). INCEP is the scaffold protein which keeps this complex together and allows for complete activation of Aurora B through a positive feedback loop (Bishop and Schumacher, 2002; Sessa et al., 2005). Some evidence suggests that Aurora B promotes completion of cytokinesis through the indirect activation of Rho. Aurora B phosphorylates and activates the centralspindlin complex, which activates Ect2 and ultimately Rho (Minoshima et al., 2003; Mishima et al., 2002). Interestingly, when Aurora B is depleted, the kinesin-like protein of the central spindle responsible for the complex's localization (MKLP1) is no longer found at the cleavage furrow, and cytokinesis does not proceed (Giet and Glover, 2001; Kaitna et al., 2000; Severson et al., 2000). Inhibition or depletion of Aurora B also results in defects in chromosome congression, abnormal chromosome segregation, failure to induce the SAC, and ultimately cytokinesis failure as evidenced by the presence of multinucleated cells (Adams et al., 2001; Ditchfield et al., 2003; Hauf et al., 2003; Kallio et al., 2002)

Anillin:

Anillin is a scaffold protein of 190 kDa, required for the completion of cytokinesis (D'Avino, 2009; Hickson and O'Farrell, 2008a; Piekny and Maddox, 2010). It contains multiple nuclear localization sequences (NLS), SH3 binding sites, a PH domain, Rhotekin binding domain, and an anillin Homology Region (AHR) (Oegema et al., 2000). Anillin was first identified in 1989 by F-actin affinity chromatography (Miller et al., 1989). Since then, anillin has been shown to bind mDia2 (Watanabe et al., 2010), myosin II (Straight et al., 2005), F-actin (Oegema et al., 2000), MgcRacGAP (Zhao and Fang, 2005b), Ect2 (Zhao and Fang, 2005b), Rho (Piekny and Glotzer, 2008), microtubules (Sisson et al., 2000), and the APC (Zhao and Fang, 2005a).

Anillin is a cell-cycle regulated protein whose expression is highest during mitosis and falls dramatically upon entry into interphase through ubiquitin-mediated degradation by the APC. As the cell progresses through interphase, anillin levels slowly increase, peaking in mitosis (Field and Alberts, 1995; Monzo et al., 2005; Zhao and Fang, 2005a). Anillin is also phosphorylated in a mitosis-specific manner; however, the significance of the phosphorylation is still not understood (Field and Alberts, 1995; Monzo et al., 2005). It is known, however, that anillin contains putative phosphorylation sites for the kinases Cdk1, Aurora B, and Polo-like Kinase 1 (A.S. Maddox, unpublished observations). The localization of anillin is also regulated in a cell-cycle dependent manner. During interphase, the NLSs restrict anillin to the nucleus of the cell (Field and Alberts, 1995; Oegema et al., 2000). In mitosis, concurrent with breakdown of the nuclear envelope, anillin localizes to peripheral stress fibers (Kinoshita et al., 2002).

After the onset of anaphase, anillin rapidly accumulates at the cortex, where it associates with various cytokinetic regulators. Anillin remains enriched at the cleavage furrow throughout cytokinesis and accumulates in the midbody towards the end of mitosis (Field and Alberts, 1995; Field et al., 2005; Silverman-Gavrila et al., 2008).

While anillin is a scaffold protein for actin and myosin, it does not appear to act as a recruiting factor for either protein (Hickson and O'Farrell, 2008b; Kinoshita et al., 2002; Straight et al., 2003), instead acting as a contractility organizer. This is exemplified by the fact that anillin binds only active myosin (phosphorylated on the rMLC) (Straight et al., 2005) and that binding of anillin to active myosin II promotes the organization of myosin into discrete intact rings (Field et al., 2005). Importantly, depletion of anillin alters the temporal and spatial stability of myosin at the cell equator during cytokinesis. Specifically, knockdown of anillin does not inhibit the formation of the cleavage furrow, nor does it inhibit initial contraction; however, without anillin the organization of the actomyosin ring cannot be maintained, and the furrow begins to oscillate back and forth across the equator, eventually resulting in cytokinetic failure (Piekny and Glotzer, 2008; Straight et al., 2005; Zhao and Fang, 2005a). There also appears to be a feedback loop from the actomyosin network regulating the localization of anillin, in that perturbation of myosin II activation results in anillin mislocalization from the cleavage furrow (Kinoshita et al., 2002).

While myosin II is activated by the Rho pathway during cytokinesis and binds anillin (Piekny and Glotzer, 2008), there is some confusion as to whether Rho recruits anillin to the cleavage furrow or anillin recruits Rho. A study by Piekny and Glotzer in

2008 found that anillin depletion results in a mislocalization of Rho away from the cleavage furrow. However, depletion of either Rho or Ect2 resulted in a decrease in anillin localization at the cleavage furrow (Piekny and Glotzer, 2008). Furthermore, knockdown of Rho causes anillin to maintain its metaphase distribution around the entire cells cortex, a phenotype similar to inactivation of Ect2 (D'Avino et al., 2008; Somma et al., 2002). Together these findings suggest that active Rho and anillin are required for the activation and organization of the actomyosin network of the cleavage furrow. If, however myosin is not phosphorylated and activated, due to a down regulation of Rho, a mislocalization of anillin can result.

Actomyosin Network:

Cytokinesis is mediated by the ingression of the contractile ring, which is a band of actin and non-muscle myosin II filaments cross-linked to the cell membrane. The actomyosin network begins to form in anaphase with positional cues from the microtubules, and constriction begins in telophase. (D'Avino et al., 2005; Glotzer, 2001; von Dassow, 2009) Constriction occurs as myosin walks along actin fibers in an ATP hydrolysis-dependent manner. Rayment *et.al.* proposed a model for actomyosin contraction in muscle based upon myosin movement on actin cables and the three dimensional structure of myosin (Rayment et al., 1993; Sheetz and Spudich, 1983a; Sheetz and Spudich, 1983b). In an inactive muscle the myosin head is bound to the actin filament, and in response to appropriate cues an ATP molecule binds to the myosin head causing an immediate change in conformation, which releases the myosin head from the actin filament. At this point, ATP hydrolysis occurs, causing the myosin head to be

displaced by about 5nm. Although the ATP nucleotide is hydrolysed, both products, ADP and the inorganic phosphate, remain bound to the myosin head. The newly positioned myosin head weakly binds a new actin molecule on the actin filament, which triggers the release of the inorganic phosphate produced by ATP hydrolysis. The phosphate release stimulates the force-generating conformational change in myosin, which walks the molecule down the actin filament and increases the association between the two proteins. At the end of this cycle myosin is now in a position to bind another ATP nucleotide and begin the process again (Rayment et al., 1993).

Myosin II is a hexamer composed of two 230 kDa heavy chains, two 20kDa regulatory light chains, and two 17kDa essential light chains which stabilize the heavy chains. The globular heads of the heavy chains bind both ATP and actin and are connected to the rest of the molecule by the neck domain. The neck domain acts as a lever and provides the mechanical force responsible for the motor action of the protein. It is also at the neck region that both light chains bind. The neck domain is followed by long α-helical coiled-coil domains, which are responsible for the dimerization of the protein. (Niederman and Pollard, 1975; Vicente-Manzanares et al., 2009) Myosin is activated by phosphorylation of the regulatory light chain on Ser19. This phosphorylation greatly increases the ATPase activity of myosin in the presence of actin by controlling the conformation of the myosin head; however, it has little to no effect on the affinity for actin (Sellers et al., 1982; Wendt et al., 2001). Phosphorylation of the heavy chain in either the coiled-coil or tail region results in dissociation of the myosin complex from actin or completely inhibits the formation of the complex (Bosgraaf and

van Haastert, 2006; Vicente-Manzanares et al., 2009). Cells which are not able to form myosin filaments cannot complete cytokinesis in suspension (Egelhoff et al., 1990).

Myosin II was first thought to play a role in cleavage furrow contraction when Yamakita *et. at.* reported that the activating phosphorylation, Ser19, decreased during metaphase, but increased 20-fold during cytokinesis and was practically undetectable during interphase, suggesting that the myosin activity was critical during cytokinesis (Yamakita et al., 1994). Since then, active myosin has been found to accumulate at the cleavage furrow during anaphase and telophase (Matsumura et al., 1998), and myosin activation is required for completion of cytokinesis (Jordan and Karess, 1997), as overexpression of a non-phosphorylatable form of myosin results in failure of cytokinesis (Komatsu et al., 2000).

Perspectives:

The biological role of Rho and its negative regulator p190 have been described as they are currently found in the literature. Through its inactivation of Rho, p190 regulates progression through cytokinesis and neurite growth; however, the role p190 plays in apoptosis, if any, is still not clearly defined. Overexpression studies designed to understand the biological role of p190 indicated that the protein might induce apoptosis. This hypothesis was strengthened when chromatin condensation, a hallmark of apoptosis, was observed in cells that overexpressed p190. These studies also revealed that p190 overexpression results in multinucleation in epithelial transformed cells and dendrite-like formation in non-transformed fibroblasts. In further support of the hypothesis that p190 might initiate apoptosis, attempts to generate a cell line that stably overexpressed p190

failed. Therefore, the goal of this dissertation was to investigate the role of p190 in mediating apoptosis and understand how apoptosis was related to the other phenotypes observed upon p190 overexpression.

This dissertation shows that p190 overexpression results in caspase- and Rho-dependent apoptosis, possibly mediated through the secondary phenotypes, multinucleation and dendrite-like formation, which are dependent upon transformation status of the cell (multinucleation in transformed cells and dendrite-like formation in non-transformed cells). Preliminary data suggest that the differential response to p190 overexpression may be due to the differential activation of the NF-κB pathway in transformed vs. non-transformed cells. Evidence is also provided that p190-induced apoptosis may activate the JNK-Bim/Mcl-1 apoptotic pathway. Finally, studies reveal that p190 confers sensitivity to docetaxel through its down regulation of Rho.

The multinucleation phenotype elicited upon p190 overexpression suggested that increased levels of p190 result in failure to complete cytokinesis. Further studies revealed that multinucleation was a consequence of insufficient RhoGTP levels at the cleavage furrow, which result in failure of the daughter cells to separate. However, how p190 overexpression affected the downstream targets of Rho was still unknown, and this question became a major point of investigation in this dissertation. Studies revealed that decreased RhoGTP levels resulting from p190 overexpression diminish myosin II activation, which is required for completion of cytokinesis. p190 overexpression also prevents anillin localization to the cleavage furrow, while silencing of anillin results in p190 mislocalization. This yin and yang suggests that anillin is required for p190

localization, but a feedback loop maintains the localization of anillin. The feedback signal may be a contractility signal, as p190 and anillin physically interact in a contractility-dependent manner. As a whole, these studies more accurately define the role of Rho and p190 in cytokinesis and apoptosis. These data also provide further evidence for p190's role as a tumor suppressor and strengthen the Rho pathway as a cancer therapeutic target.

CHAPTER 2

Materials and Methods

Chapter 2
Materials and Methods:

Reagents:

The following chemicals were used throughout this study: Thymidine, Nocodazole, DAPI, (all from Sigma, St. Louis, MO), Blebbistatin (Calbiochem, San Diego, CA), and Doxycycline (Clontech, Mountain View, CA). All monoclonal and polyclonal antibodies used in this work and their sources and concentrations are identified in Tables 2 and 3 of this chapter.

Cell culture and synchronization:

MDA-MB-231, MDA-MB-468, BT-549, MCF7, HeLa, C3H10T1/2, NIH-3T3, vSrc NIH-3T3, and vSrc Rat1 cells were maintained by serial passage in Dulbecco's Modified Eagle Medium (DMEM) (Gibco, Carlsbad, CA) containing 10% fetal calf serum (Gibco) and 1% penicillin/streptomycin (Gibco) at 37ºC in a 5% CO_2, humidified environment. MDA-MB-468 Tet-on cells were maintained in DMEM with 10% fetal calf serum (Gibco), 1% penicillin/streptomycin, 130 ng/ml puromycin (Sigma), and 400 µg/ml geneticin (G418) (Sigma). MDA-MB-361 cells were cultured in Leibovitz's L-15 Medium (Gibco) containing 20% fetal calf serum (Gibco) and 1% penicillin/streptomycin (Gibco). MCF10A cells were maintained in DMEM/F12 (Gibco) with 5% Horse Serum (Gibco), 1% penicillin/streptomycin (Gibco), 100 µg/ml EGF (Sigma), 1 mg/ml hydrocortisone (Sigma), 1 mg/ml cholera toxin (Calbiochem, Gibbstown, NJ), and 10 mg/ml insulin (Sigma). RWPE-1 cells were grown in Keratinocyte Serum Free Medium (Gibco), with L-glutamine (Gibco), 0.2 ng/ml EGF, and 25 µg/ml bovine pituitary extract

(Gibco). Cell lines were obtained from American Tissue Culture Collection (Manassas, VA) except for v-Src NIH3T3 and v-Src Rat-1 cells, which were gifts from Dr. J.T. Parsons. Cells were synchronized for arrest in mitosis by treatment with 50 ng/mL nocodazole for 14-16 hrs, released from the nocodazole block for 40 mins, and harvested by mitotic shake off at indicated times. G1 arrest was achieved by treatment with 2 mM thymidine for 14-16 hrs, release for 8 hrs, followed by an additional treatment of 14-16 hrs of 2 mM thymidine, at which time cells were collected for analysis.

Transient transfection:

MDA-MB-468, HeLa, NIH-3T3, vSrc NIH-3T3, and vSrc Rat1 cells were transfected with Polyfect Transfection Reagent (Qiagen Inc., Valencia, CA), and C3H10T1/2 cells were transfected using Superfect Transfection Reagent (Qiagen Inc.). Fugene Transfection Reagent (Roche, Indianapolis, IN) was used to transfect MCF10A and MCF7 cells, while RWPE-1 cells were transfected with Lipofectamine Plus Transfection Reagent (Invitrogen, Eugene, OR). All cells were transfected according to the manufacturer's protocol. Plasmids used were: pKH3 plasmid encoding triple HA-tagged p190 (gift from Dr. Ian Macara), or the indicated p190 mutants; pTriEX plasmid encoding CARho (Q63L) or DNRho (T19N); or GFP plasmid containing GFP-p190 or CA MLC (phosphomimetic T18D, S19D). Cells were plated in either 100mm or 6-well dishes (Corning). Mock-transfected cells were treated with transfection reagents alone. When two or more plasmids were co-transfected, total plasmid levels were equalized with empty vector. Vector control experiments were performed with empty pKH3 HA-vectors or empty GFP vectors with equivalent amount of vector for each experiment.

siRNA transfection:

The p190 RNAi oligos were double stranded and custom made by Dharmacon to silence the expression of human p190-A protein by targeting a unique sequence at the N-terminus of the protein. The sequence of the double stranded oligos was 5' AAG AUG CAC AUU GUG GAG CAG 3'. The Anillin RNAi oligo was from the Dharmacon ANLN ON-TARGETplus SMARTpool targeted to human Anillin. Cells were treated with the p190 siRNA oligos (200 pmol), or the Anillin siRNA oligos (200 pmol) using the RNAiMax reagent (Invitrogen), as per the manufacturer's instructions. After 24 hrs, cells were either treated with Dox to induce HA-p190 expression or fixed for confocal microscopy as described below.

Mutant constructs:

The ΔGAP, ΔGBD, Middle Domain, and GAP-only domain mutants of p190 were constructed using primers purchased from Integrated DNA Technologies, Inc (Table 1). pkH3 triple-HA tagged full-length p190RhoGAP plasmid served as the template for PCR amplification. Using restriction sites for *Bam*HI and *Eco*RI full-length p190 was excised, and the amplified deletion mutants were ligated into the pkH3 vector using the Rapid DNA Ligation Kit (Roche). All mutants obtained by PCR were confirmed by sequencing prior to use. Verified plasmids were purified from competent DH5α E.Coli using Maxi-prep (Qiagen) according to manufacturer's protocol.

Table 1: Primers for Mutant Constructs

Mutant	Sense primer sequence	Anti-sense primer sequence
ΔGAP	CGGGATCCATGATGATGGCAAGAAAGCAA	GCGAATTCTCAATCACTCCCAACACTGAAGCT
ΔGBD	CGGGATCCTTTGTTGTACTTGAAGAGACA	GCGAATTCTCAAGAAGACAACTGATTTTC
Middle Domain	CGGGATCCTTTGTTGTACTTGAAGAGACA	GCGAATTCTCAATCACTCCCAACACTGAAGCT
GAP	CGGGATCCATACCCATTTTCATTGAAAGA	GCGAATTCTCAAGAAGACAACTGATTTTC

Immunofluorescence:

For phenotypic studies, cells were seeded on coverslips (Fisher, Pittsburgh, PA) in 6-well dishes (Corning) at the following densities to accommodate different time points of analysis: 24 hrs, 7.5 x 10^5 cells/well; 48 hrs, 5 x 10^5 cells/well; or 72 hrs, 2.5 x 10^5 cells/well. The next day cells were transfected as described above and at the designated times were fixed for 5 min with 4% paraformaldehyde and permeated with 0.2% Triton-X 100 for 20 min at room temperature. Slides were blocked for 1 hr at room temperature in 20% filtered goat serum in phosphate buffered saline (PBS) (0.14M NaCl, 4.2mM Na_2HPO_4, 2.7mM KCl, and 1.5mM KH_2PO_4, pH 7.3) and incubated with primary mouse antibody αHA.11 mAb (Covance, Berkeley, CA) (2 μg/ml in 20% goat serum) to detect

HA-p190, followed by Alexafluor 594-conjugated goat anti-mouse IgG (Jackson Immuno Research Laboratories, Inc., West Grove, PA) for 1 hr at room temperature. To test for apoptosis, cells were stained for DNA fragmentation using TUNEL, *In Situ* Cell Death Kit, Fluorescein (Roche), as per the manufacturer's protocol. For all immunofluorescence (IF) studies, cells were stained for DNA with 2 μg/ml DAPI (Sigma-Aldrich) in PBS for 3 min. Cover slips were mounted on slides and viewed on a Leica-Leitz DM RBE microscope equipped with a Sensys camera (Photometric, Beaverton, OR) controlled by Inovision software (ISee, Raleigh, NC). Mutant p190, Z-VAD, CA-Rho, dose-dependent, Image J, and Docetaxel studies were visualized using the same protocol 48 hrs post-transfection.

Quantification of p190 overexpression by immunofluorescence pixel intensity:

Cells were seeded, transfected with HA-p190 plasmid, and prepared for IF 48 hrs post transfection as described above. Images of p190-overexpressing cells exhibiting normal morphology, multinucleation, or dendrite-like formation were captured with a Photometric's Sensys camera controlled by Inovision's ISee software. Exposure times were consistent for each channel throughout individual experiments, and no images were altered after capture. The area of a cell was outlined using the phase image to determine the region of interest (ROI). The ROI was then applied to the HA-p190 image to determine the average pixel intensity within the ROI, represented as a random numerical value. These values were then grouped by phenotype, and an average pixel intensity for each phenotype was determined using the cells analyzed from one individual experiment.

Between 10-40 cells per phenotype were analyzed for each experiment. Average pixel intensities were then normalized to normal morphology, which was set to 1.

Time-lapse microscopy:

Four x 10^5 MDA-MB-468, MCF10A, NIH-3T3, or vSrc NIH-3T3 cells were plated in 0.17mm Delta T dishes (Fisher Scientific) and transfected with 3μg (MDA-MB-468, NIH-3T3, vSrc NIH-3T3) or 2μg (MCF10A) GFP-p190RhoGAP plasmid using Polyfect (Qiagen Inc.) or Fugene (Roche) Transfection Reagent as per the manufacturer's protocol. Twenty four hrs later cells were incubated for 30 min at 37ºC in 5% CO_2 in the dark with 2μg Hoechst 33342 (Molecular Probes, Invitrogen Detection Technologies, Eugene, OR) in serum free DMEM (Gibco) to visualize the DNA. Cells were maintained for the next 24 hrs in Leibovitz's L-15 medium (Gibco). GFP-p190 expressing cells were identified by immunofluorescence microscopy of live cells. DIC images were captured every 10 min (starting time 24 hrs. post-transfection) with a Nikon Eclipse TE200 microscope equipped with a heated stage and a Hammamatsu CCD camera controlled by Improvision's Openlab software.

Confocal Microscopy:

HeLa cells were grown to 60% confluency in normal growth media, treated with Nocodazole for 14-16 hours to induce mitotic arrest, and released for 40 minutes onto poly-L-lysine-coated coverslips in culture dishes supplemented with fresh media. After release, cells were fixed for 20 min with 4% paraformaldehyde, permeabilized for 5 min with 0.2% Triton X-100 and blocked with 20% goat serum at room temperature for 1 hr. After blocking, samples were incubated with appropriate primary antibodies (see Table 2)

for 1 hr at room temperature. Coverslips were mounted onto glass microscope slides using ProLong® Gold antifade reagent with DAPI as the mounting medium. After overnight drying at 4˚C, cells were analyzed in a Zeiss LSM510 confocal head (Carl Zeiss MicroImaging GmbH) mounted on an Axiovert 200 wide-field fluorescence microscope, fitted with a purple diode laser for 405 nm excitation; an argon laser with 458, 477, 514, and 488 nm lines; a 543 nm HeNe laser; and a 633 nm HeNe laser. Images were captured using the accompanying LSM software (Carl Zeiss MicroImaging GmbH).

Table 2: Antibodies for Confocal Microscopy

Antibody	Company	Type	Dilution
p190	BD Transduction Lab	Mouse mAb	1:200
Anillin	Santa Cruz	Rabbit pAb	1:250
MLC II (MY-21)	Sigma	Mouse IgM	1:200
p-MLC II	Cell Signaling	Rabbit pAb	1:100
Aurora B (AIM-1)	BD Transduction Lab	Mouse mAb	1:200
Phalloidin AF Conj 647	Molecular Probes	Mouse mAb	1:1000
AF 594 Conj GαM	Molecular Probes	Goat	1:1000
AF 594 Conj GαR	Molecular Probes	Goat	1:1000
AF 647 Conj GαM	Molecular Probes	Goat	1:1000
AF 488 Conj GαM	Molecular Probes	Goat	1:1000
AF Conj 568 GαIgM	Molecular Probes	Goat	1:1000

Western blotting:

Cells were seeded at the following densities per time of analysis: Mock, 1.6 x 10^6 cells/100mmplate; 24 hrs, 1.8 x 10^6 cells/100mm plate; 48 hrs, 1.6 x10^6 cells/100mm plate; or 72 hrs, 1.4 x 10^6 cells/100mm plate and transfected as described above with HA-p190RhoGAP plasmid. At the indicated times, cells were lysed and sonicated. Cell debris was removed by centrifugation at 13,000 x *g* for 10 min at 4 ºC. Protein was quantified using the BioRad Protein Assay (BioRad, Hercules, CA). 50 μg protein per treatment group was separated on an SDS-PAGE gel and transferred to a Nitrocellulose membrane (Whatman, Dassel, Germany), which was then blocked for 1 hr at room temperature. The blocked membrane was washed three times with TBST buffer (9.98mM Tris, 150.58mM NaCl, 0.1% Tween-20 [Fisher Scientific,]) and incubated overnight at 4 ºC with the respective primary antibodies listed in Table 3 below. Membranes were again washed three times with TBST buffer and incubated for 1 hr at room temperature with HRP (horseradish peroxidase)-conjugated anti-mouse or anti-rabbit IgG secondary antibody (1:5,000) (Amersham Biosciences, Piscataway, NJ), or anti-mouse IgM secondary antibody (1:5,000) (Rockland). Antigen-antibody complexes were visualized by ECL (enhanced chemiluminescence) (Amersham Biosciences), radiographed, and quantified by densitometric analysis using AlphaEase FC.

Table 3: Antibodies for Western blot and Immunoprecipitation

Antibody	Company	Type	Dilution
p190 (8C10)	S. Parsons Lab	Mouse mAb	1:4,500 in 5% milk

p190	BD Transduction Lab	Mouse mAb	1:1,000 in 5% milk
HA.11 (18B12)	Covance	Mouse mAb	1:1,000 in 5% milk
Caspase-3 (8G10)	Cell Signaling	Rabbit mAb	1:1,000 in 5% milk
Akt	Cell Signaling	Rabbit pAb	1:1,000 in 5% milk
p-Akt	Cell Signaling	Rabbit pAb	1:1,000 in 5% milk
p38 (L53F8)	Cell Signaling	Mouse mAb	1:1,000 in 5% BSA
p-p38 (28B10)	Cell Signaling	Mouse mAb	1:1,000 in 5% BSA
JNK	Cell Signaling	Rabbit pAb	1:1,000 in 5% BSA
p-JNK (G9)	Cell Signaling	Mouse mAb	1:1,000 in 5% BSA
IKB	Cell Signaling	Mouse mAb	1:1,000 in 5% BSA
p-IKB	Cell Signaling	Mouse mAb	1:1,000 in 5% BSA
p53 (1C12)	Cell Signaling	Mouse pAb	1:1,000 in 5% BSA
p-p53	Cell Signaling	Rabbit pAb	1:1,000 in 5% BSA
Bim (C34C5)	Cell Signaling	Rabbit mAb	1:1,000 in 5% milk
Mcl-1 (D35A5)	Cell Signaling	Rabbit mAb	1:1,000 in 5% milk
MLC II (MY-21)	Sigma	Mouse IgM	1:1,000 in 5% BSA & 3%milk
p-MLC II	Rockland	Rabbit pAb	1:1,000 in 5% BSA
Anillin	Santa Cruz	Rabbit pAb	1:1,000 in 5% milk
Actin	Sigma	Mouse mAb	1:10,000 in 5% milk

Immunoprecipitation:

Cell lysates were prepared as described above and incubated with 5 μg of the indicated immunoprecipitating antibody overnight. After primary antibody incubation, immunecomplexes were precipitated by protein G agarose (Invitrogen) and separated by centrifugation at 5,000 rpm for 1 min. After cold PBS washes, SDS sample buffer was added to each sample, boiled for 5 mins, and subjected to Western blotting analysis, as described above.

CHAPTER 3

The Tumor Suppressor, p190RhoGAP, Differentially Initiates Apoptosis and Confers Docetaxel Sensitivity.

Chapter 3:
The Tumor Suppressor, p190RhoGAP, Differentially Initiates Apoptosis and Confers Docetaxel Sensitivity.

INTRODUCTION:

Through GTP binding, RhoGTPases directly and indirectly regulate a myriad of down-stream effectors, including Rho kinase (ROCK) and mDia, which in turn regulate actomyosin and microtubule cytoskeletal dynamics (Hall, 2009). Numerous biological processes are modulated by Rho's effects on cytoskeletal dynamics including proliferation, migration, differentiation, and survival (Heasman and Ridley, 2008). Of particular importance to the work described in this report are the roles Rho plays in cytokinesis (proliferation) (Kishi et al., 1993) and neurite retraction/extension (differentiation) (Jalink et al., 1994).

Due to their multiple functions in cells, aberrant expression or function of any of the RhoGTPases can result in malignant transformation. Overexpression of several members of the Rho family of GTPases, their upstream regulators, or downstream effectors has been observed in a variety of malignancies, including; pancreatic, breast, brain, and prostate cancer (Aznar et al., 2004). It has also been shown that Rho- and Rac1-transformed murine fibroblasts develop distant metastases in the lung, spleen, lymph nodes, and other tissues when injected into immuno-compromised mice, suggesting a role for these GTPases in malignant progression (Gomez del Pulgar et al., 2005).

RhoGAPs are a large family of proteins that stimulate the intrinsic GTPase activity of the Rho proteins, leading to Rho inactivation. To date, 67 GAP domain-

containing proteins have been identified (Hall, 2009), among which is p190RhoGAP (p190). p190 is a multi-domain protein with an N-terminal GTP Binding Domain (GBD), a Middle Domain containing critical phosphorylation and protein-protein interaction motifs, and a C-terminal region that includes the GAP domain (Ludwig et al., 2009). Through inactivation of Rho, p190 plays a critical role in regulating actin cytoskeleton dynamics (Ridley et al., 1993) in response to growth factors (Chang et al., 1995), integrin engagement (Arthur and Burridge, 2001), and v-Src transformation (Fincham et al., 1999). In these processes, Src phosphorylates p190 at tyrosine 1105 (Y1105) and promotes p190 binding to p120RasGAP, enhancing p190's RhoGAP activity and Rho inactivation (Haskell et al., 2001a). As a result of its negative regulation of Rho, p190 has also been shown to negatively control tumor growth (Wolf et al., 2003), transformation (Wang et al., 1997), metastasis, invasion (Kusama et al., 2006), and angiogenesis (Mammoto et al., 2009), suggesting that it may function as a tumor suppressor *in vivo* (Ludwig et al., 2009).

Previous studies designed to understand the tumor suppressive role of p190 employed an overexpression approach. In epithelial cells (MDA-MB-468), overexpression of p190 resulted in multinucleation (Su et al., 2003), suggestive of an involvement in mitosis, while in fibroblasts or neuronal cells overexpression produced a dendritic-like phenotype (Tatsis et al., 1998), implicating a role in differentiation. This chapter describes for the first time that p190 is also a regulator of apoptosis, that the multinucleation and dendritic phenotypes can be intermediates to apoptosis, and that p190 functions through Rho and its downstream effectors (including caspases) to mediate

this process. Furthermore, we found that elevated levels of p190 can sensitize breast cancer cells to docetaxel-induced apoptosis, consistent with its function as a tumor suppressor.

RESULTS:

p190RhoGAP overexpression leads to apoptosis.

To test for the ability of p190 to regulate apoptosis and to assess the frequency of apoptosis relative to multinucleation and dendrite-like formation, HA-tagged p190 was transiently transfected into MDA-MB-468 cells, a transformed cell of epithelial origin, and allowed to express for 24, 48 or 72 hrs. Cells were then immuno-stained for HA to identify those overexpressing p190 and tested for apoptosis via TUNEL immunofluorescence. Concurrently, we quantitated the occurrence of the two other p190-reported phenotypes: multinucleation (2 or more nuclei), postulated to occur in epithelial cells, and dendrite-like formation (protrusions the length of the cell body or greater), postulated to occur in fibroblasts. As seen in Fig. 6A, upon p190 overexpression in MDA-MB-468 cells, all three phenotypes (multinucleation, dendrite-like formation, and apoptosis) were observed. Of interest was the finding that the predominant phenotype was apoptosis at all times examined, occurring in 30% of the cells that overexpressed p190 (Fig 6B) at 72 hrs post transfection, with a secondary phenotype of multinucleation (9%), and only 3% of cells displaying dendritic processes, a phenomenon which had been reported previously only in non-transformed fibroblasts or neuronal cell lines (Tatsis et al., 1998; Troller et al., 2004). To investigate whether p190 overexpression could invoke the same pattern of morphological changes in a non-

Figure 6

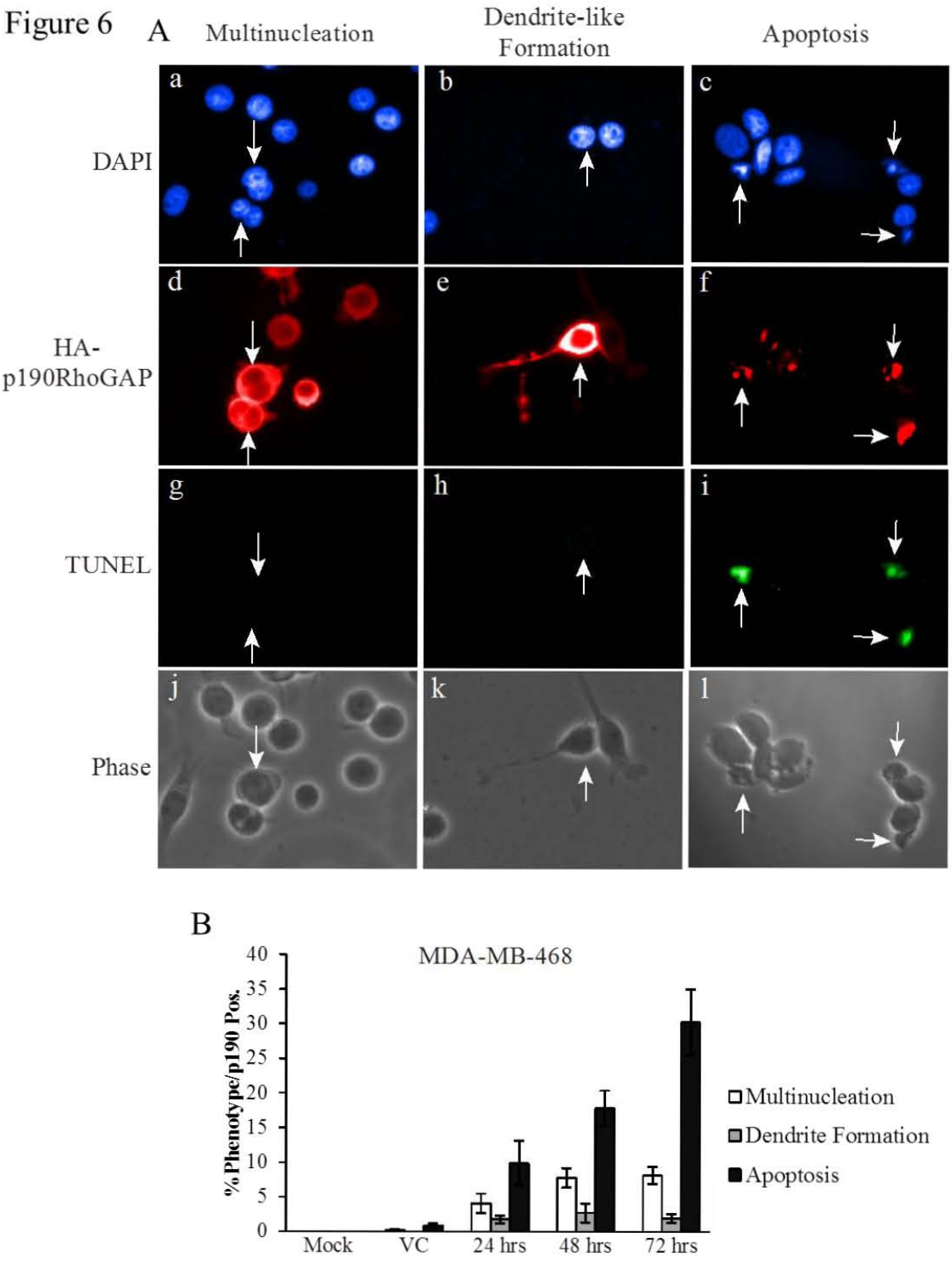
A
Multinucleation
Dendrite-like Formation
Apoptosis
DAPI
HA-p190RhoGAP
TUNEL
Phase
a
b
c
d
e
f
g
h
i
j
k
l
B
MDA-MB-468
% Phenotype/p190 Pos.
0
5
10
15
20
25
30
35
40
Mock
VC
24 hrs
48 hrs
72 hrs
Multinucleation
Dendrite Formation
Apoptosis

Figure 6: p190RhoGAP overexpression leads to apoptosis in MDA-MB-468 cells.

A: Immunofluorescent images of MDA-MB-468 cells transiently overexpressing HA-p190 represent the three observed phenotypes: multi-nucleation, dendrite-like formation, and apoptosis. Panels a-c: DAPI-stained DNA; panels d-f: triple HA-tagged p190; panels g-i: TUNEL, and panels j-l: phase. Arrows identify p190 overexpressing cells that are multinucleated (panels a, d, g, and j), dendritic-like (panels b, e, h, and k), or apoptotic (panels c, f, i, and l).

B: Quantitation of the respective phenotypes observed in mock-treated, vector-control (VC) or p190-transfected MDA-MB-468 cells. Results are expressed as the mean percent total cells (Mock or VC) or cells positive for HA-p190 that exhibited the observed phenotypes +/- standard error of the mean (SEM), n>3.

transformed epithelial cell line, the same experiment was performed with MCF10A cells. Again all three phenotypes were observed (Fig. 7A), and apoptosis was the most common phenotype at all time points, with 30% apoptosis at 72 hrs post transfection. However, in contrast to the transformed epithelial cell line, p190 overexpression elicited a secondary phenotype of dendrite like-formation (8%), with only a few cells displaying multinucleation (3%) (Fig. 7B).

To determine whether this same pattern would hold true for a pair of transformed and non-transformed fibroblasts, the preceding protocol was repeated in vSrc transformed NIH-3T3 cells (Fig. 8A) and NIH-3T3 cells (Fig. 9A). In both cell lines apoptosis was the most abundant phenotype at all times observed with 34% in vSrc NIH-3T3s (Fig. 8B) and 32% in NIH-3T3 (Fig. 9B) at 72 hrs post transfection. In the transformed cell line (vSrc NIH-3T3), multinucleation was the second most common phenotype (16%) with only a small percentage of cells displaying dendrite-like extensions (4%). Conversely, the non-transformed cell line (NIH-3T3) exhibited more dendrite-like protrusions (18%) than multinucleated cells (5%). Based on these results, it appears that transformation status determines the phenotype rather than fibroblast or epithelial cellular lineage.

To further examine the relationship between the transformation status of the cell and the secondary phenotype induced by p190 overexpression, an eight cell line (Table 4) survey was performed using two non-transformed epithelial cells (MCF10A and RWPE-1), two transformed epithelial cells (MDA-MB-468 and HeLa), two non-transformed fibroblasts (NIH-3T3 and C3H 10T1/2) and two transformed fibroblasts (vSrc transformed NIH-3T3 and vSrc transformed Rat-1). All cell lines were transiently

Figure 7

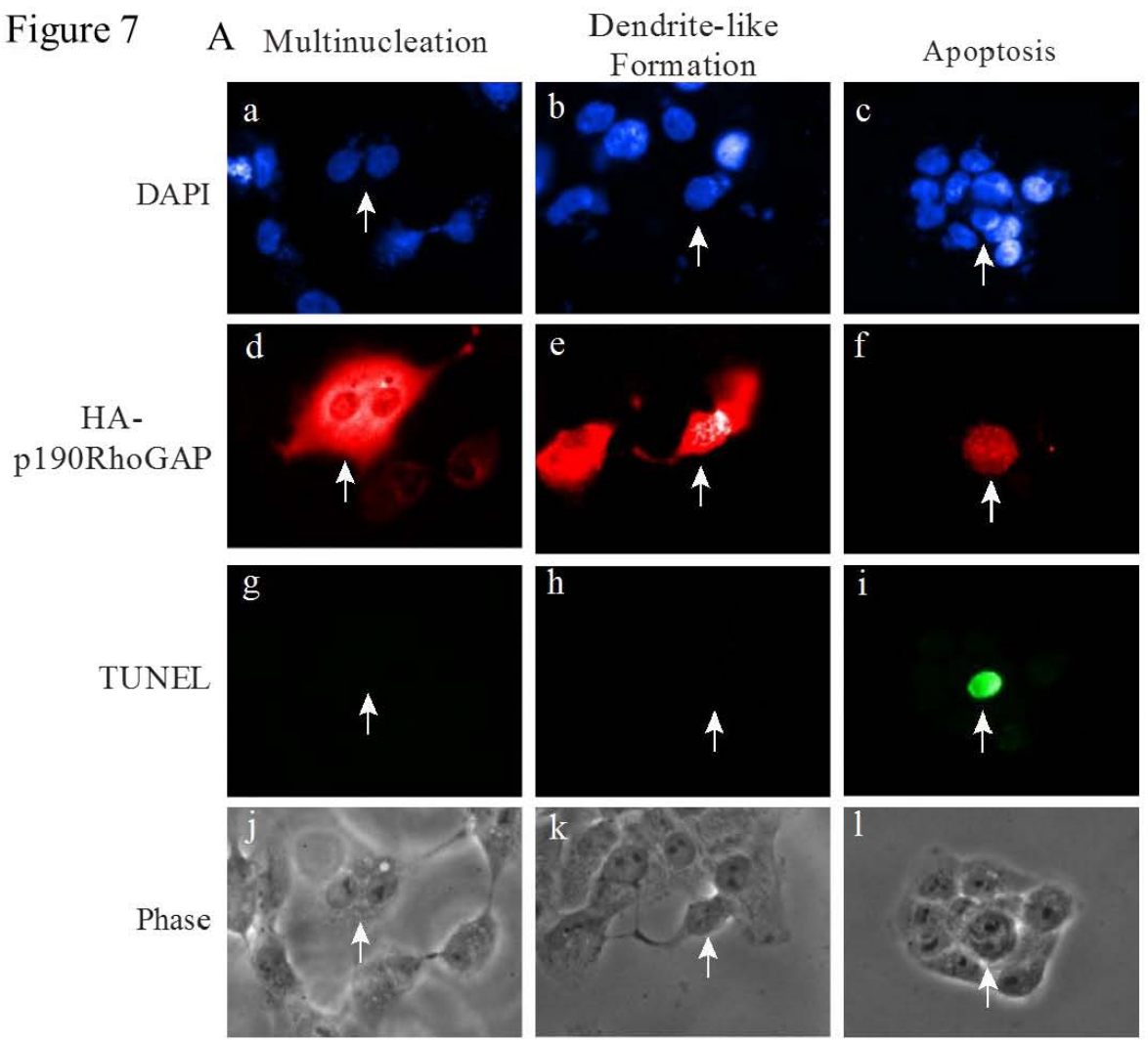
A
Multinucleation
Dendrite-like Formation
Apoptosis
DAPI
HA-p190RhoGAP
TUNEL
Phase
a
b
c
d
e
f
g
h
i
j
k
l

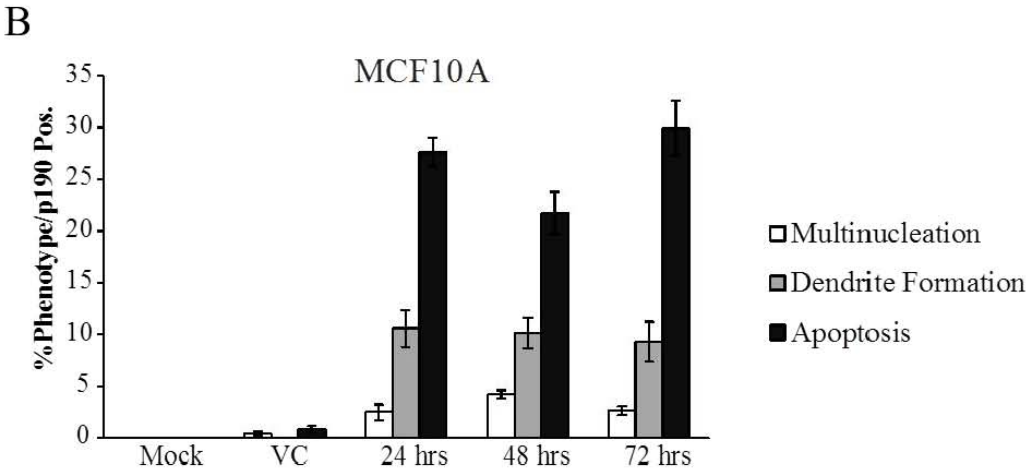
B
MCF10A
%Phenotype/p190 Pos.
35
30
25
20
15
10
5
0
Mock
VC
24 hrs
48 hrs
72 hrs
Multinucleation
Dendrite Formation
Apoptosis

Figure 7: p190RhoGAP overexpression leads to apoptosis in MCF10A cells.

A: Immunofluorescent images of MCF10A cells transiently overexpressing HA-p190 represent the three observed phenotypes: multi-nucleation, dendrite-like formation, and apoptosis. Panels a-c: DAPI-stained DNA; panels d-f: triple HA-tagged p190; panels g-i: TUNEL, and panels j-l: phase. Arrows identify p190 overexpressing cells that are multinucleated (panels a, d, g, and j), dendritic-like (panels b, e, h, and k), or apoptotic (panels c, f, i, and l).

B: Quantitation of the respective phenotypes observed in mock-treated, vector-control (VC) or p190-transfected MCF10A cells. Results are expressed as the mean percent total cells (Mock or VC) or cells positive for HA-p190 that exhibited the observed phenotypes +/- standard error of the mean (SEM), n>3.

Figure 8

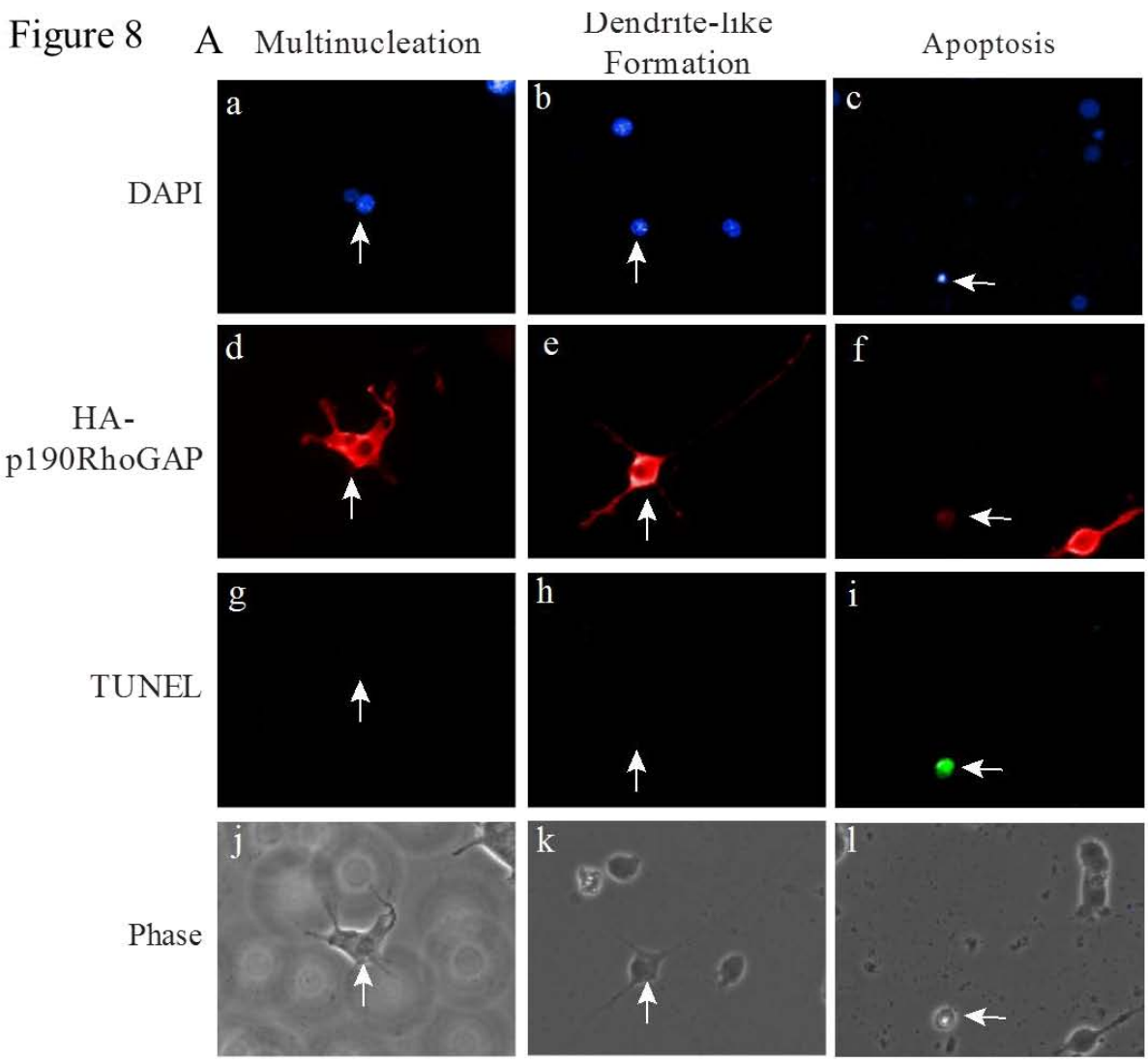
A
Multinucleation
Dendrite-like Formation
Apoptosis
DAPI
HA-p190RhoGAP
TUNEL
Phase
a
b
c
d
e
f
g
h
i
j
k
l

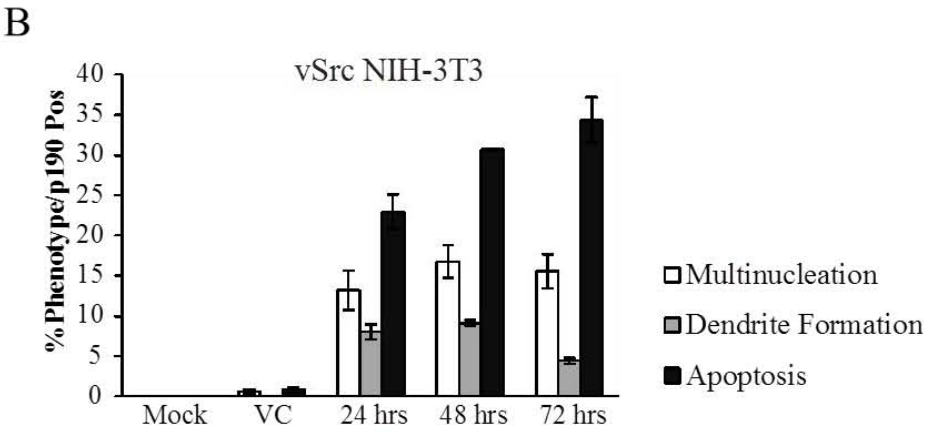
B
vSrc NIH-3T3
% Phenotype/p190 Pos
40
35
30
25
20
15
10
5
0
Mock
VC
24 hrs
48 hrs
72 hrs
Multinucleation
Dendrite Formation
Apoptosis

Figure 8: p190RhoGAP overexpression leads to apoptosis in vSrc NIH-3T3 cells.

A: Immunofluorescent images of vSrc NIH-3T3 cells transiently overexpressing HA-p190 represent the three observed phenotypes: multi-nucleation, dendrite-like formation, and apoptosis. Panels a-c: DAPI-stained DNA; panels d-f: triple HA-tagged p190; panels g-i: TUNEL, and panels j-l: phase. Arrows identify p190 overexpressing cells that are multinucleated (panels a, d, g, and j), dendritic-like (panels b, e, h, and k), or apoptotic (panels c, f, i, and l).

B: Quantitation of the respective phenotypes observed in mock-treated, vector-control (VC) or p190-transfected vSrcNIH3T3 cells. Results are expressed as the mean percent total cells (Mock or VC) or cells positive for HA-p190 that exhibited the observed phenotypes +/- standard error of the mean (SEM), n>3.

Figure 9

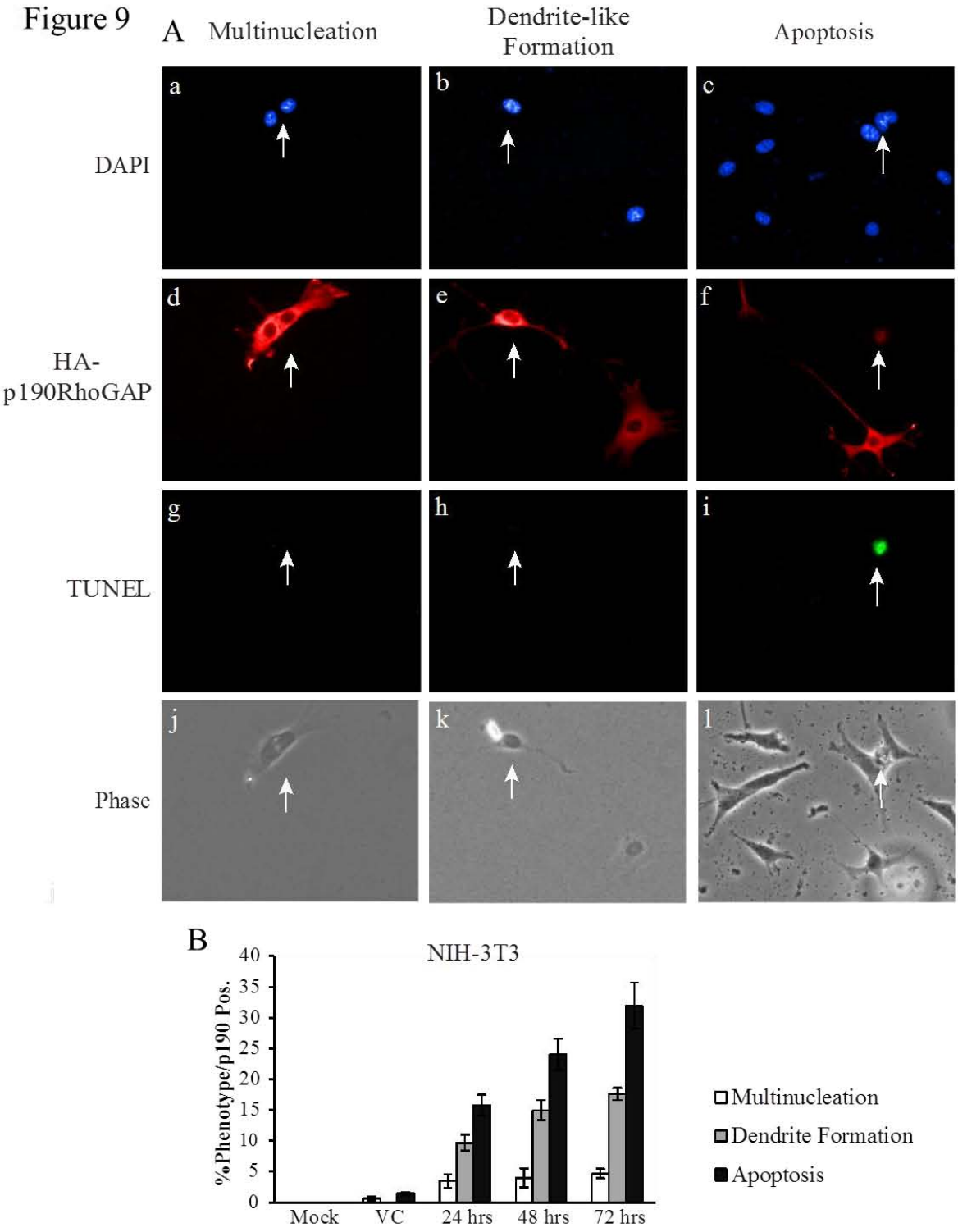
A
Multinucleation
Dendrite-like Formation
Apoptosis
DAPI
HA-p190RhoGAP
TUNEL
Phase
a
b
c
d
e
f
g
h
i
j
k
l
B
NIH-3T3
%Phenotype/p190 Pos.
40
35
30
25
20
15
10
5
0
Mock
VC
24 hrs
48 hrs
72 hrs
Multinucleation
Dendrite Formation
Apoptosis

Figure 9: p190RhoGAP overexpression leads to apoptosis in NIH-3T3 cells.

A: Immunofluorescent images of NIH-3T3 cells transiently overexpressing HA-p190 represent the three observed phenotypes: multi-nucleation, dendrite-like formation, and apoptosis. Panels a-c: DAPI-stained DNA; panels d-f: triple HA-tagged p190; panels g-i: TUNEL, and panels j-l: phase. Arrows identify p190 overexpressing cells that are multinucleated (panels a, d, g, and j), dendritic-like (panels b, e, h, and k), or apoptotic (panels c, f, i, and l).

B: Quantitation of the respective phenotypes observed in mock-treated, vector-control (VC) or p190-transfected NIH3T3 cells. Results are expressed as the mean percent total cells (Mock or VC) or cells positive for HA-p190 that exhibited the observed phenotypes +/- standard error of the mean (SEM), n>3.

Table 4

	Epithelial Cell	Fibroblast
Non-transformed	MCF10A, RWPE-1	10T1/2, NIH-3T3
Transformed	HeLa MDA-MB-468	vSrc NIH-3T3 vSrc Rat1

Table 4: Cell lines used in this study

Cell lines were grouped according to transformation status (transformed or non-transformed) and lineage (epithelial cell or fibroblast). Epithelial, non-transformed cell lines used were the breast cells, MCF10A, and the prostate cells, RWPE-1. Transformed epithelial cell lines used were the breast cancer cell lines, MCF7 and MDA-MB-468. The fibroblasts used in this study were the non-transformed mouse cell lines, C3H 10T1/2 and NIH-3T3, and the cell lines transformed by vSrc, vSrc Rat1 and vSrc NIH-3T3.

transfected with HA-tagged p190RhoGAP for 24, 48, or 72 hrs, stained for expression of HA-p190 and TUNEL, and scored for the frequency of multinucleation, dendrite-like formation, and apoptosis by immunofluorescence. As seen in Figure 10, apoptosis was the primary phenotype in all cell lines. However, the secondary phenotype was determined by transformation status, with transformed cells exhibiting a greater frequency of multinucleation than dendrite-like formation, and non-transformed cells, the reverse. These results indicate that overexpression of p190 induces apoptosis, regardless of cell type or transformation status while the secondary phenotype (multinucleation or dendrite-like formation) depends upon the transformation status of the cell.

p190-induced multinucleation and dendrite-like formation can result in apoptosis.

These findings raised the question of whether the two secondary morphologies, multinucleation and dendrite-like formation, could result in apoptosis, or if they represented distinct phenotypes. To initially address this question, we re-examined our previous experiments to determine what percentage of multinucleated cells were apoptotic and by so doing determine whether the phenotypes were mutually exclusive events. Figure 11 shows that at 72 hrs post transfection approximately 80% of cells overexpressing p190 and exhibiting a multinucleated phenotype stained positively for TUNEL in the three cell lines tested. This result indicated that the majority of p190-induced multinucleated cells were undergoing apoptosis, suggesting that multinucleation may be a concomitant or intermediate phenotype in the p190-induced apoptotic pathway. Attempts to detect dendritic cells that also stained positively for TUNEL were unsuccessful, suggesting that either dendrite-like formation and apoptosis were mutually

Figure 10

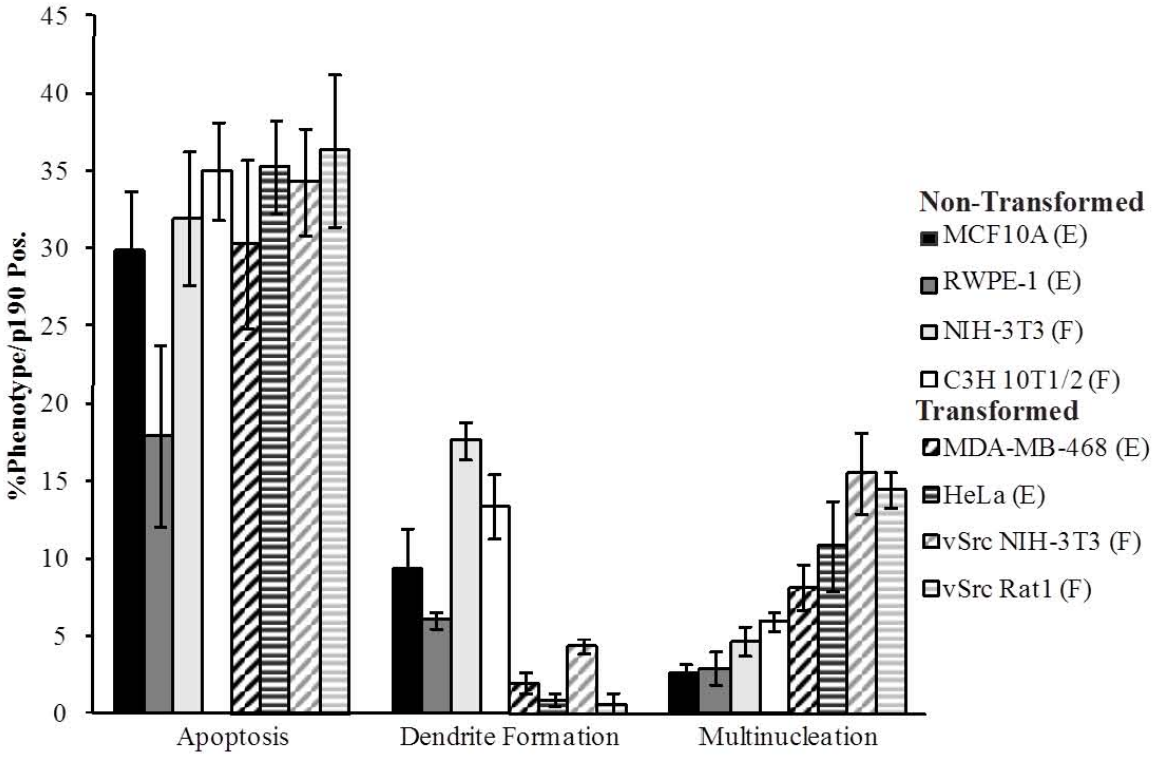
%Phenotype/p190 Pos.
45
40
35
30
25
20
15
10
5
0
Apoptosis
Dendrite Formation
Multinucleation
Non-Transformed
MCF10A (E)
RWPE-1 (E)
NIH-3T3 (F)
C3H 10T1/2 (F)
Transformed
MDA-MB-468 (E)
HeLa (E)
vSrc NIH-3T3 (F)
vSrc Rat1 (F)

Figure 10: The secondary phenotype of p190 overexpression is transformation-dependent.

Quantitation of the respective phenotypes observed in the indicated cell lines overexpressing p190 for 72 hrs. Cells were transfected and analyzed as in Figures 5-8. Results are expressed as the mean percent cells positive for HA-p190 that exhibited the observed phenotypes +/- SEM, n>3. E=epithelial cell, F=fibroblast.

Figure 11

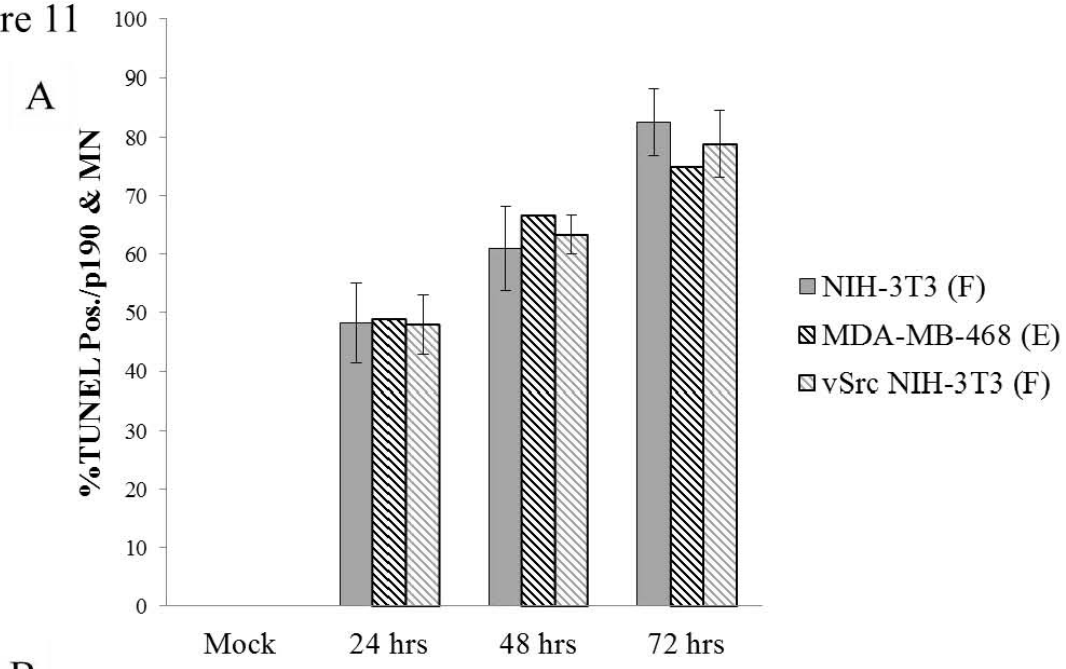
A
%TUNEL Pos./p190 & MN
100
90
80
70
60
50
40
30
20
10
0
Mock
24 hrs
48 hrs
72 hrs
NIH-3T3 (F)
MDA-MB-468 (E)
vSrc NIH-3T3 (F)

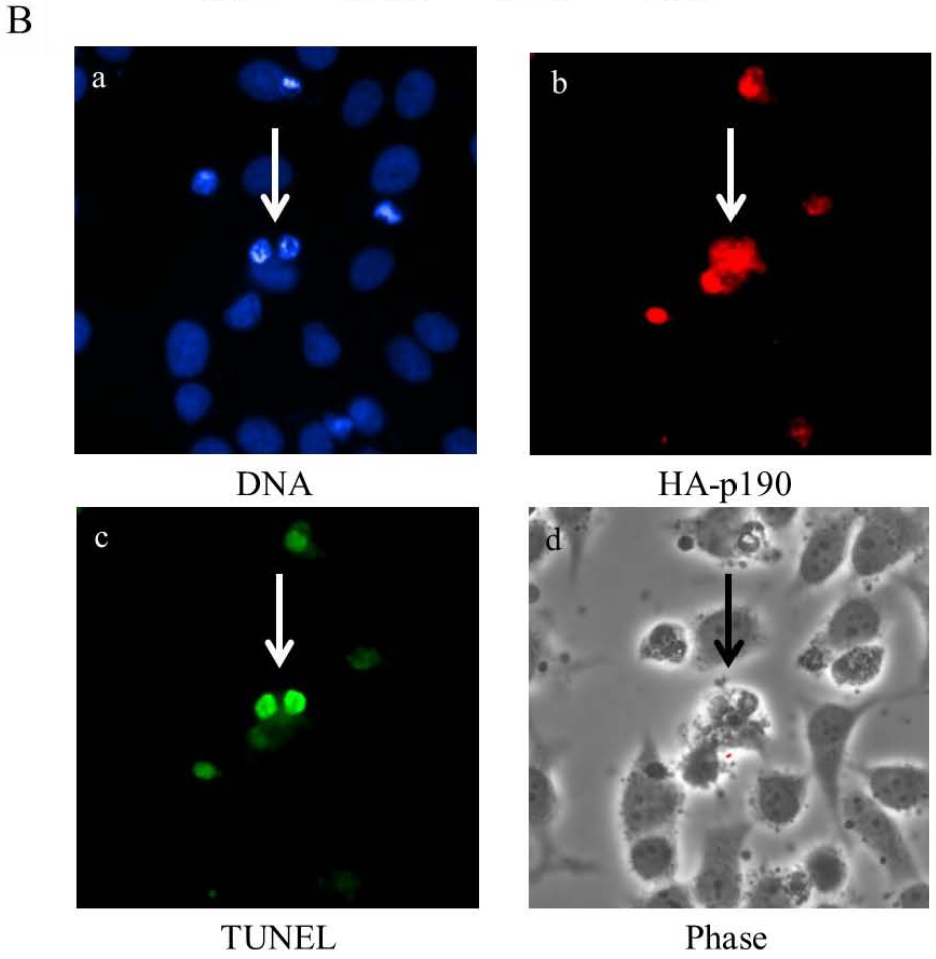
B
a
b
DNA
HA-p190
c
d
TUNEL
Phase

Figure 11: p190-induced multinucleated cells are also apoptotic.

A: Quantitation of p190 overexpressing cells that exhibit a multinucleated phenotype that are also apoptotic at 24, 48, and 72 hrs. Cells were transfected and analyzed as in Figures 5-8. Results are expressed as the mean percent cells positive for HA-p190 and multinucleation that exhibited apoptosis +/- SEM, n>3.

B: Immunofluorescent images of MDA-MB-468 cells transiently overexpressing HA-p190 are both multinucleated and apoptotic. Image in a: DAPI-stained DNA; b: triple HA-tagged p190; c: TUNEL, and panel d: phase. Arrow identifies p190 overexpressing cell that is multinucleated and apoptotic.

exclusive events, or that TUNEL positivity and dendrite processes could not be detected simultaneously. TUNEL stains double stranded breaks within the DNA, which is expected to occur after cellular condensation. Thus, it is possible that p190-apoptotic cells lose their dendritic phenotype as a result of cellular condensation.

To directly address the question of whether multinucleation and dendrite-like formation led to apoptosis, we used real-time microscopy to follow p190-induced phenotypic changes over time. GFP-tagged p190 was transiently transfected into MDA-MB-468 (Figs. 12A) cells to assess multinucleation and into NIH-3T3 (Figs. 13A) and MCF10A cells to assess dendrite-like formation. Twenty-four hrs post transfection, p190 positive cells were identified, and DIC images were captured every 10 mins for the next 24 hrs. Apoptosis was defined as cellular condensation and membrane blebbing. Figure 12A shows that p190-expressing multinucleated cells (solid arrows) underwent apoptosis within 3 hrs (panels d-e), followed by the p190-positive mononucleated cells (dashed arrows) (panel f), and the non-p190 overexpressing cells, which did not undergo apoptosis until near the end of the time course. (Eventually all cells, regardless of their p190 status, died from CO_2 deprivation due to the extended time required for video microscopy.) Quantifying the time to apoptotic induction for the three groups of cells from multiple experiments, a significant difference in the number of minutes to apoptotic induction was observed between the various groups, with the p190 overexpressing multinucleated cells displaying the shortest time to apoptosis (Fig. 12B).

Similar results were seen with the dendritic-like phenotype in NIH-3T3 and MCF10A cells (Fig. 13A). The dendritic NIH-3T3 cell seen in Fig. 13 (solid arrow)

Figure 12

A

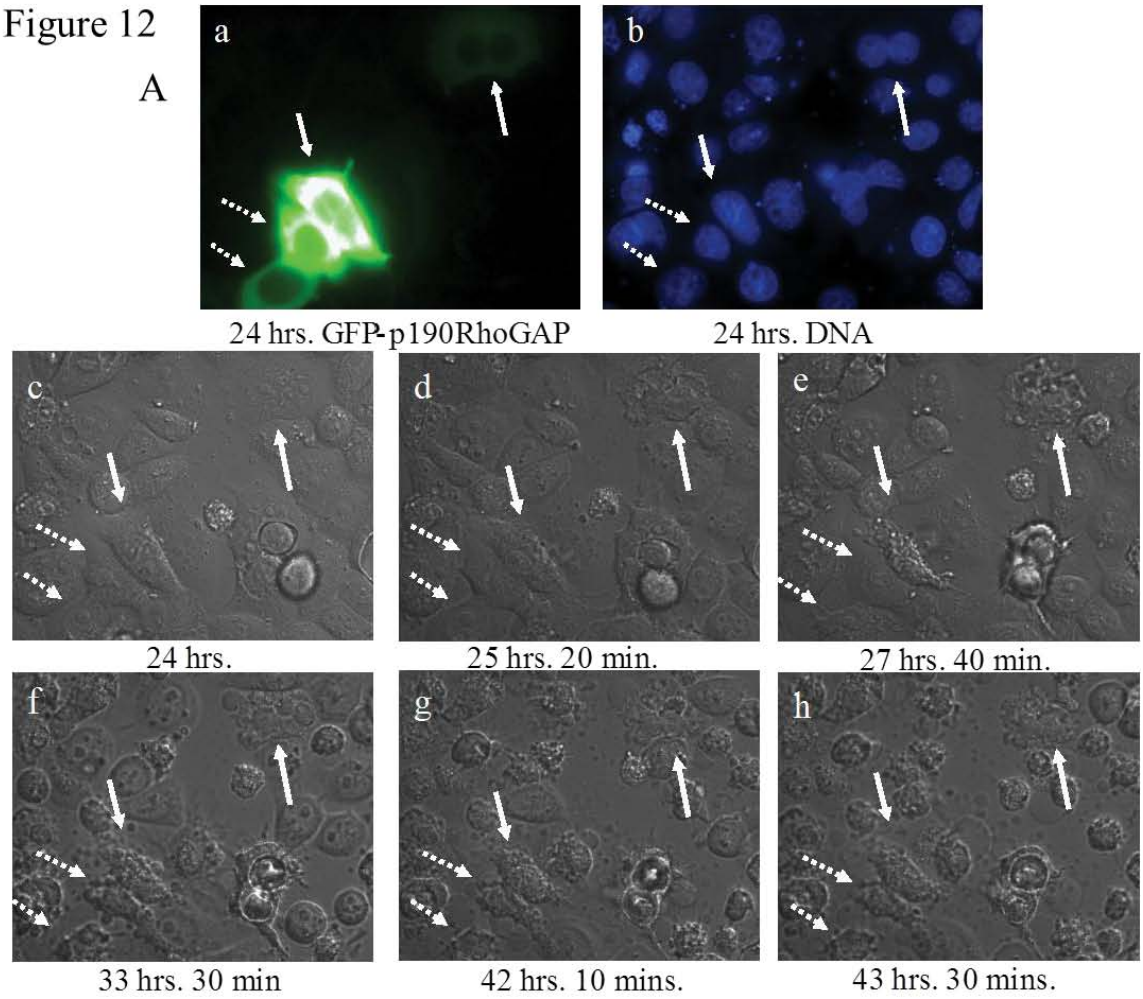
a
b
24 hrs. GFP-p190RhoGAP
24 hrs. DNA
c
d
e
24 hrs.
25 hrs. 20 min.
27 hrs. 40 min.
f
g
h
33 hrs. 30 min
42 hrs. 10 mins.
43 hrs. 30 mins.

B

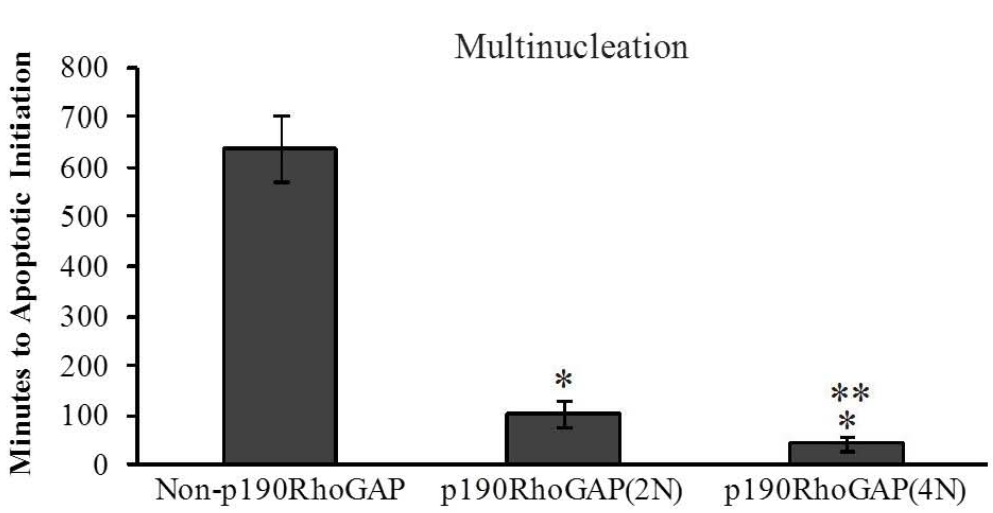
Multinucleation
Minutes to Apoptotic Initiation
800
700
600
500
400
300
200
100
0
*
**
*
Non-p190RhoGAP
p190RhoGAP(2N)
p190RhoGAP(4N)

Figure 12: p190-induced multinucleation can result in apoptosis.

A: Still images from real-time microscopy of MDA-MB-468 multinucleated cells undergoing apoptosis. Panel a shows GFP-tagged p190 24 hrs post transfection. Solid arrows indicate p190 multinucleated cells; dashed arrows indicate p190 mono-nucleated cells. Panel b depicts Hoechst 33342-stained images of DNA taken 24 hrs post transfection. Panels c-h represent the DIC images taken at designated times.

B: Multinucleated, p190 overexpressing MDA-MB-468 cells initiate apoptosis more rapidly than p190 mono-nucleated cells or non-overexpressors. The first image, 24 hrs post transfection, was defined as time-0, and a cell was measured as positive for apoptotic initiation at the first sign of cellular condensation. Cells were grouped as non-p190-overexpressing (normal, n=25), p190-overexpressing mononucleated (2N, n=14), or p190-overexpressing multinucleated (4N or greater, n=7), and results are expressed as the mean time in min to apoptosis +/- SEM. *=$p< 0.005$ as compared to Non-p190 overexpressing, **=$p<0.05$ as compared to p190 overexpressing mononucleated (2N).

Figure 13

A

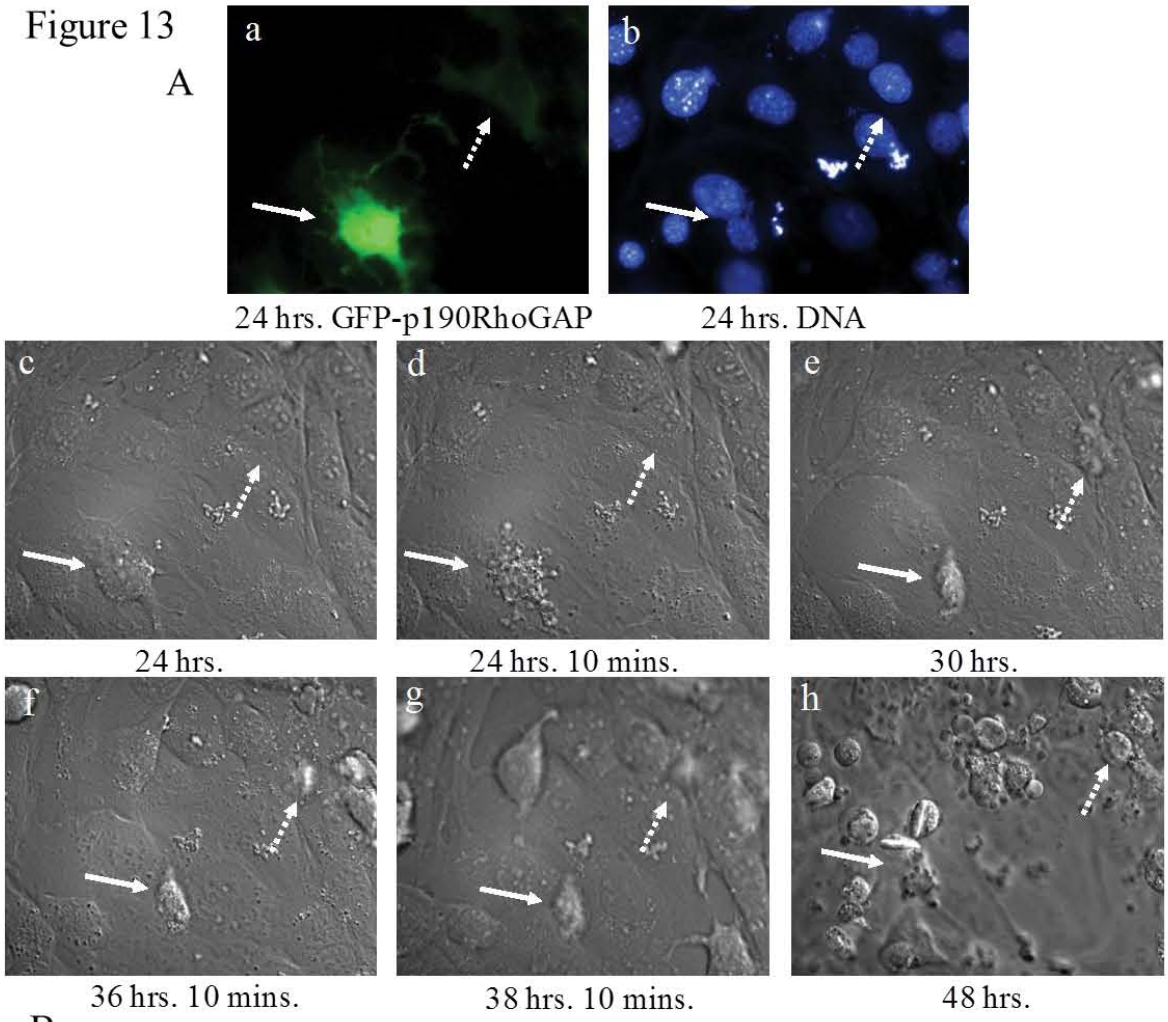
a
b
24 hrs. GFP-p190RhoGAP
24 hrs. DNA
c
d
e
24 hrs.
24 hrs. 10 mins.
30 hrs.
f
g
h
36 hrs. 10 mins.
38 hrs. 10 mins.
48 hrs.

B

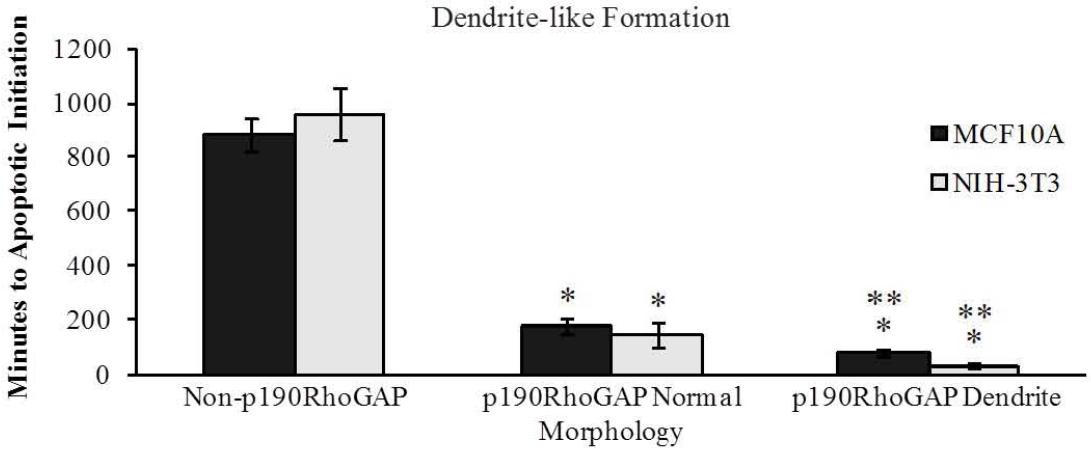
Dendrite-like Formation
Minutes to Apoptotic Initiation
1200
1000
800
600
400
200
0
MCF10A
NIH-3T3
*
*
**
*
**
*
Non-p190RhoGAP
p190RhoGAP Normal Morphology
p190RhoGAP Dendrite

Figure 13: p190-induced dendrite-like formation can result in apoptosis.

A : Still images from real-time microscopy of a NIH-3T3 dendritic cell undergoing apoptosis. Panel a shows GFP-tagged p190 24 hrs post transfection. Solid arrow indicates a p190 dendritic cell, and the dashed arrow indicate a p190 cell with normal morphology. Panel b depicts Hoechst 33342-stained images of DNA taken 24 hrs post transfection. Panels c-h represent the DIC images taken at designated times.

B: Dendritic, p190-overexpressing NIH-3T3 or MCF10A cells initiate apoptosis more rapidly than p190 normal morphology or non-p190 overexpressing cells. Cells (NIH-3T3, MCF10A) were grouped as non-p190-overexpressing (normal, n=23, 28), p190-overexpressing mononucleated normal morphology (n=12, 7), or p190-overexpressing dendritic (n=8, 4), and results are expressed as the mean time in min to apoptosis +/- SEM. Statistical significance was determined within individual cell lines. *=$p< 0.005$ as compared to non-p190 overexpressing, **=$p<0.05$ as compared to p190 overexpressing normal morphology.

Images (Su et al., 2003) were also taken of vSrc NIH-3T3 and vSrc Rat1 cells; however, all cells began apoptosis within 2 hours of the time course, whether or not they had been transfected with p190RhoGAP, most likely due to the pro-apoptotic nature of vSrc (Frame, 2004).

began the apoptotic process within 10 mins of the experiment (panel d), while the p190 overexpressing "normal" morphology cell (arrowhead) began apoptosis after 6 hrs. Non-p190 overexpressing cells did not initiate apoptosis until 14 hours. Quantification revealed (Fig. 13B) a similar pattern as that seen for multinucleation (Fig. 13B). Together these data indicate that multinucleation and dendrite-like formation can result in apoptosis and suggest that these phenotypes may be priming or sensitizing stages in the p190-induced apoptotic pathway. However, these findings do not preclude the possibility that p190 may induce apoptosis independently of multinucleation or dendrite-like formation.

p190-induced apoptosis is caspase-dependent.

To determine whether p190-induced death was mediated by caspases, 4 cell lines (MDA-MB-468, MCF10A, vSrc NIH-3T3, and NIH-3T3) were transiently transfected with HA-p190 and examined at 24, 48, and 72 hrs for caspase-3 cleavage by Western blot analysis. As seen in Figure 14A-D, caspase-3 cleavage was detected at all time points following p190 overexpression, indicating apoptosis. To determine whether caspase cleavage was required for apoptosis, cells were treated with the pan-caspase inhibitor, Z-VAD 1 hr post-transfection. Forty-seven hours later cells were immuno-stained for HA to identify those overexpressing p190 and tested for apoptosis via TUNEL immunofluorescence. Figure 14E shows that apoptosis was significantly reduced in all cell lines treated with Z-VAD, indicating that p190-induced apoptosis is caspase-dependent

Figure 14

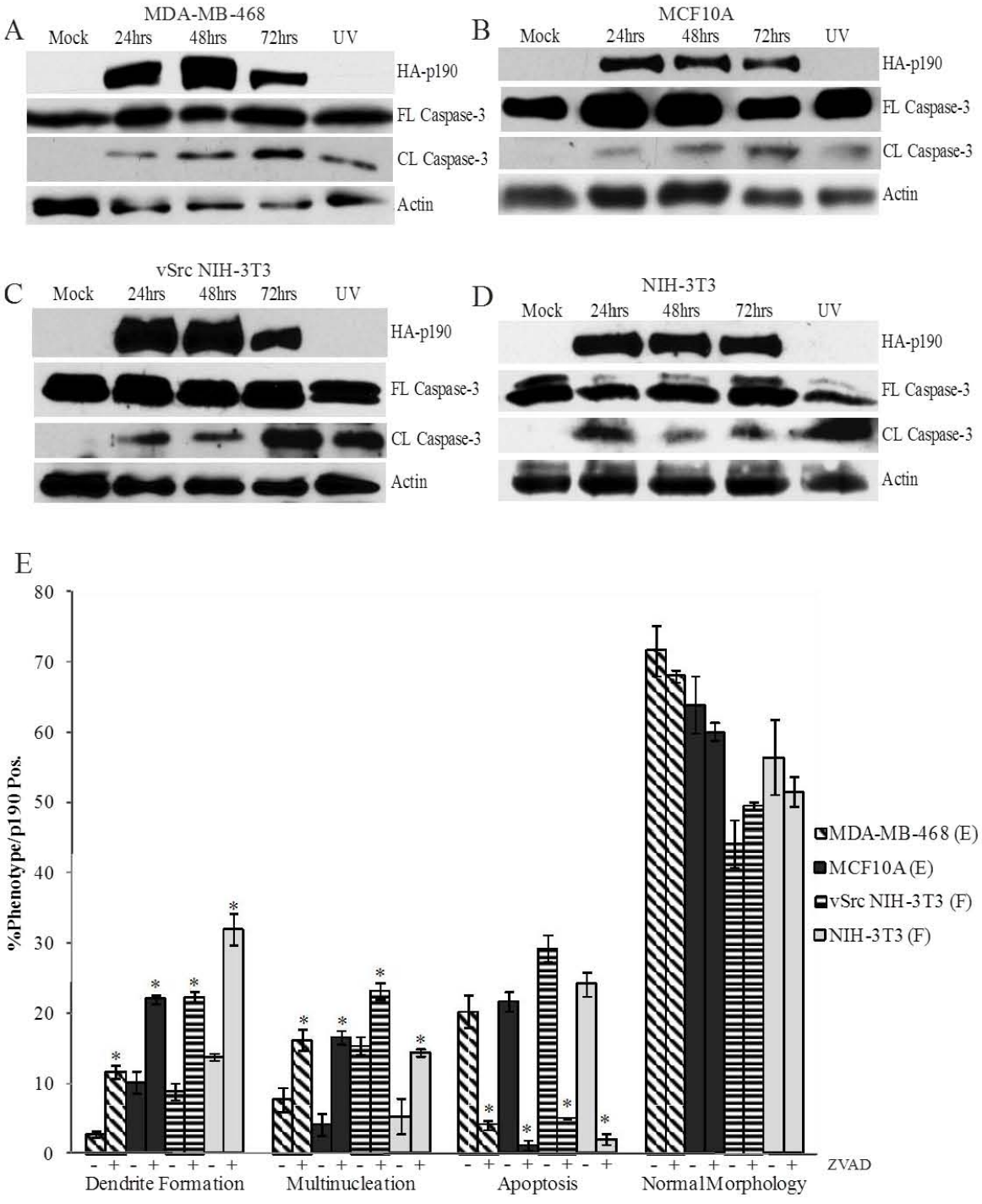
A
MDA-MB-468
Mock
24hrs
48hrs
72hrs
UV
HA-p190
FL Caspase-3
CL Caspase-3
Actin
B
MCF10A
Mock
24hrs
48hrs
72hrs
UV
HA-p190
FL Caspase-3
CL Caspase-3
Actin
C
vSrc NIH-3T3
Mock
24hrs
48hrs
72hrs
UV
HA-p190
FL Caspase-3
CL Caspase-3
Actin
D
NIH-3T3
Mock
24hrs
48hrs
72hrs
UV
HA-p190
FL Caspase-3
CL Caspase-3
Actin
E
%Phenotype/p190 Pos.
80
70
60
50
40
30
20
10
0
MDA-MB-468 (E)
MCF10A (E)
vSrc NIH-3T3 (F)
NIH-3T3 (F)
- + - + - + - +
ZVAD
Dendrite Formation
Multinucleation
Apoptosis
NormalMorphology

Figure 14: p190-induced apoptosis is caspase-dependent.

A: MDA-MB-468 cells were transfected with HA-p190 or Mock-treated, and extracts were subjected to Western blotting as described in Materials and Methods. UV-treated cells were used as a positive control for caspase cleavage. Mock and UV-treated cells were collected at the 48 hr time point.

B-D: MCF10A (B), vSrc NIH-3T3 (C), and NIH-3T3 (D) cells were treated as in panel A.

E: Cells were transiently transfected with HA-tagged p190. One hr post-transfection cells were treated with 50μM Z-VAD-FMK (BD Pharmingen) and scored for the respective phenotype 47 hrs later. Results are expressed as mean percent of p190 overexpressing cells that exhibited the indicated phenotype +/- SEM, $n>3$. Statistical significance was determined within individual cell lines; *=$p<0.005$ comparing Z-VAD treated to Z-VAD non-treated partner.

Based upon real-time images (Fig. 12 & 13), we speculated that multinucleation and dendrite-like formation may be priming intermediate phenotypes leading to p190-induced apoptosis. If that were the case, then inhibiting apoptosis would result in an accumulation of the intermediate phenotypes, without a significant change in the percentage of p190 overexpressing cells exhibiting normal morphology. When all cell lines were transiently transfected with p190, and treated with Z-VAD, a decrease in apoptosis was seen, along with an increase in multinucleation and dendrite-like formation; however no change in p190 positive normal morphology cells was seen. Together these results further support the conclusion that multinucleation and dendrite-like formation may be intermediate phenotypes to p190-induced apoptosis.

p190-induced phenotypes are dose-dependent.

To determine if p190-induced apoptosis was an experimental artifact of transient transfection, p190 was overexpressed in the Dox-inducible Tet-on cell line described in Su *et.al.* (Su et al., 2003). p190 overexpression by Dox induction (which increased p190 levels two-fold), also induced caspase-3 cleavage (Fig. 15, lane 2), suggesting that apoptosis is a result of p190 overexpression and not an experimental artifact. In support of this, reconstitution of endogenous levels of p190 with Dox-inducible p190 after silencing of endogenous p190 abolished caspase-3 cleavage (Fig. 15, lane 4). These results suggest that apoptosis is due to the overexpression of p190 and may be dose-dependent.

To further explore the possibility that p190-induced apoptosis is dose-dependent, increasing amounts of HA-p190 plasmid were transfected into MDA-MB-468 cells for 48

Figure 15

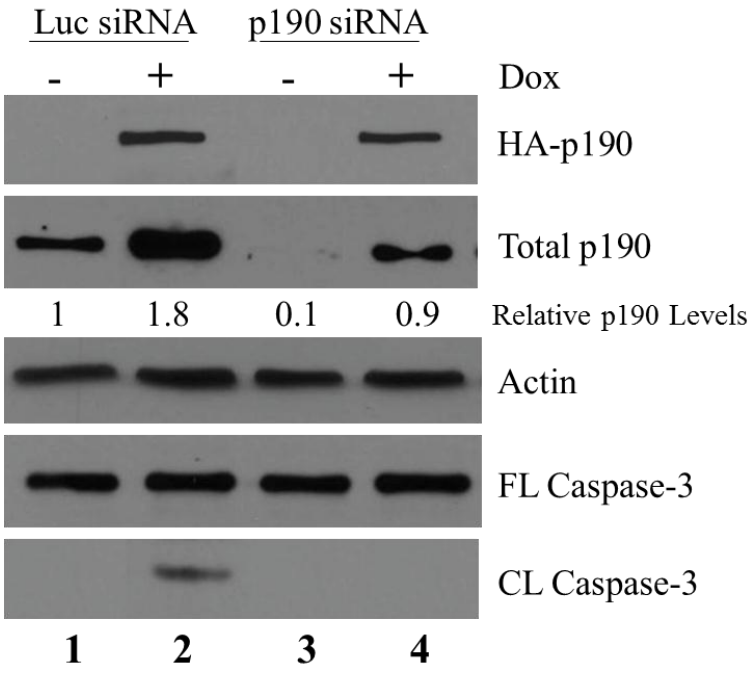
Luc siRNA
p190 siRNA
- + - +
Dox
HA-p190
Total p190
1 1.8 0.1 0.9
Relative p190 Levels
Actin
FL Caspase-3
CL Caspase-3
1 2 3 4

Figure 15: p190-induced caspase-3 cleavage in tet-on MDA-MB-468 cells is dose-dependent.

Western blot of HA-p190 and caspase-3. Dox-inducible (Tet-on) MDA-MB-468 cells were transfected with 200 pM of Luc or p190 siRNA for 24 hrs, followed by addition of 1 µg Dox to the Luc siRNA treatment group and 0.5µg Dox to the p190 siRNA treatment group for another 24 hrs to achieve equal levels of HA-p190 expression. Controls in each siRNA-treated group were left untreated by Dox. Cells were then lysed and subjected to Western blot analysis to determine the levels of total and HA-p190 and full-length and cleaved caspase-3, as described in Materials and Methods. Values noted for total p190 were normalized to actin.

hrs. Both the amount of p190 in the cell (Fig. 16A) and apoptosis (Fig. 16B), as measured by TUNEL immunofluorescence, increased with 0.5 µg, 2 µg, and 4 µg of HA-p190 plasmid. These results were compared to the amount of p190 expressed (Fig. 16A) and the corresponding apoptosis (Fig. 16B) induced by 2 µg of Dox treatment in the Dox-inducible cell line. Figure 16A & B shows that 2 µg of Dox treatment induce nearly equivalent levels of p190 expression as 2 µg HA-p190 plasmid (that amount used throughout this study), and both treatments elicit the same amount of apoptosis (~20%). These data confirm the results shown in Figure 15, namely, that apoptosis is due to overexpression of p190 and is dose-dependent.

These findings raised the question of whether the secondary phenotypes may also be dose-dependent. To test this possibility, Image J pixel intensity analysis was performed on the four cell lines described above to determine the relative amount of exogenous p190 in cells exhibiting multinucleated, dendrite-like formation, or normal morphology. Figure 17 shows that cells with dendritic-like processes expressed 2.75 to 4 fold higher amounts of exogenous p190 than cells with a normal morphology in all cell lines tested. Conversely, multinucleated cells expressed about half as much exogenous p190 as normal morphology cells. These results suggest that the secondary p190-induced phenotypes, like apoptosis are dose-dependent.

p190-induced dendrite-like formation may be due to a G1 arrest.

The multinucleation phenotype we observed suggested that p190 overexpression induces a block in mitosis. This block correlated with decreased p190 levels presumably

Figure 16

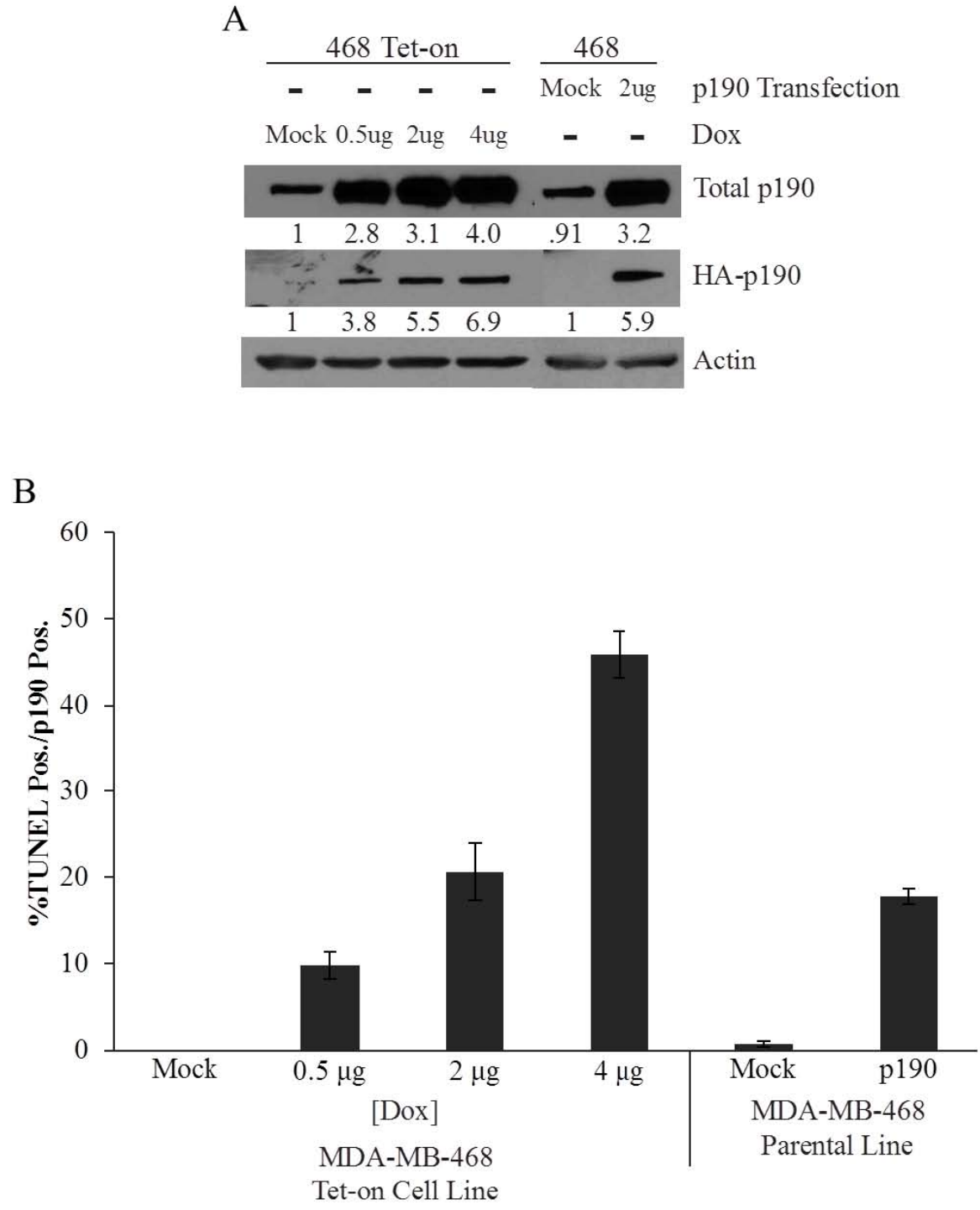
A
468 Tet-on
468
- - - - Mock 2ug
p190 Transfection
Mock 0.5ug 2ug 4ug - -
Dox
Total p190
1 2.8 3.1 4.0 .91 3.2
HA-p190
1 3.8 5.5 6.9 1 5.9
Actin
B
%TUNEL Pos./p190 Pos.
60
50
40
30
20
10
0
Mock
0.5 µg
2 µg
4 µg
[Dox]
MDA-MB-468
Tet-on Cell Line
Mock
p190
MDA-MB-468
Parental Line

Figure 16: p190-induced apoptosis of tet-on MDA-MB-468 cells is dose-dependent.

A: Western blot of total- and HA-p190. Dox-inducible (Tet-on) MDA-MB-468 cells were mock-treated or treated with 0.5, 2.0, or 4.0 µg Doxycycline to induce exogenous p190 expression, while parental MDA-MB-469 cells were transiently transfected with 2µg of HA-p190 according to Materials and Methods. HA- and total levels of p190RhoGAP were determined by densitometric analysis of Western blots prepared 48 hrs. post treatment. Indicated levels of p190 were normalized to actin as described in Materials and Methods.

B: Quantitation of apoptosis in MDA-MB-468 and Dox-inducible MDA-MB-468 cells. Apoptosis was detected by TUNEL immunofluorescence in the treatment groups described above. Results are expressed as the mean percent cells overexpressing p190 that are TUNEL positive +/- standard error of the mean (SEM), n=3.

Figure 17

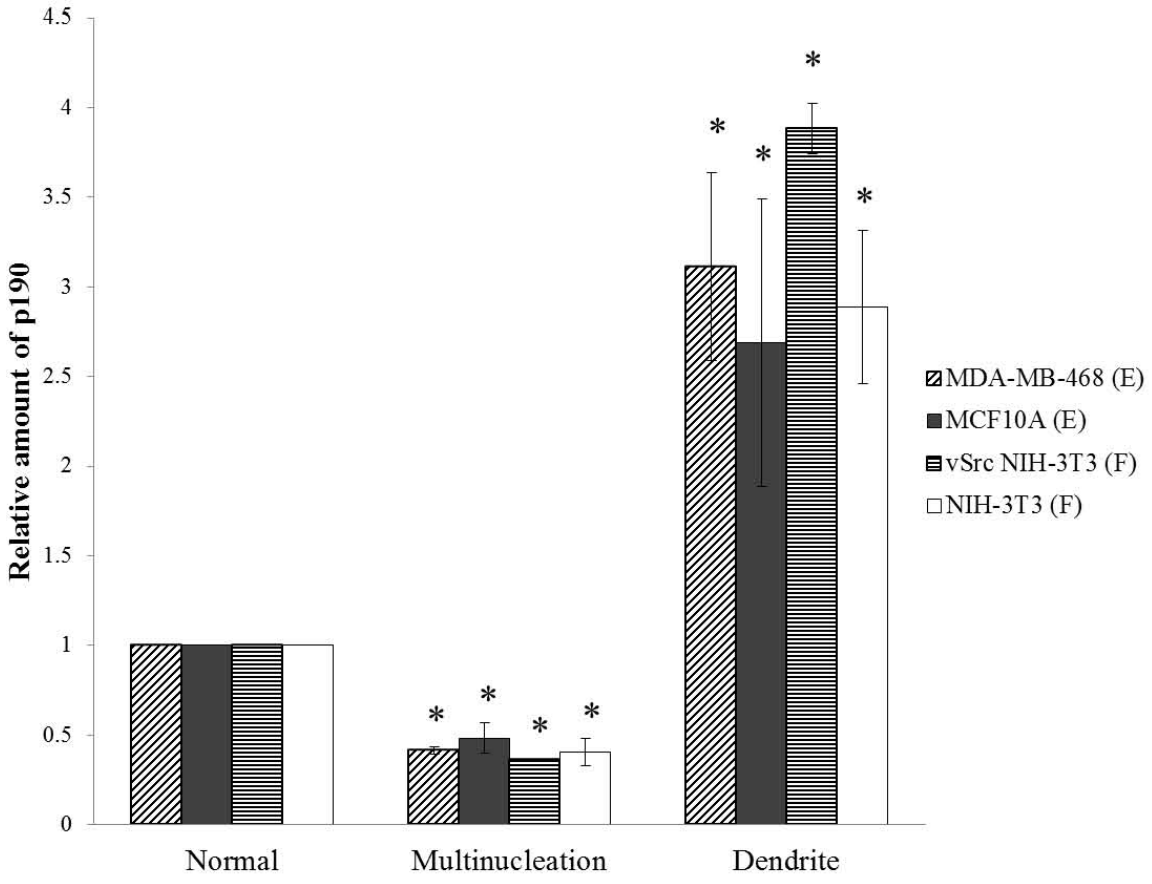
Relative amount of p190
4.5
4
3.5
3
2.5
2
1.5
1
0.5
0
Normal
Multinucleation
Dendrite
MDA-MB-468 (E)
MCF10A (E)
vSrc NIH-3T3 (F)
NIH-3T3 (F)

Figure 17: p190-induced multinucleation and dendrite-like phenotypes are dose-dependent.

Quantitation of Image J pixel intensity analysis. MDA-MB-468, MCF10A, vSrc NIH-3T3, and NIH-3T3 cells were transiently transfected with HA-p190 for 48 hrs, fixed, and stained for HA-p190 and DNA. Images were captured, and pixel intensity was determined as described in Materials and Methods. Values for normal morphology were set to 1. Results are expressed as the mean pixel intensity value for each phenotype +/- standard error of the mean (SEM) relative to normal morphology, n>3.

due to ubiquitin-mediated degradation of p190 as previously demonstrated (Manchinelly et al., 2010; Su et al., 2003). However, a block before mitosis, in G1, could result in an accumulation of p190, since the protein would still be expressed from the plasmid, but no degradation would occur. Therefore, a block in G1 could explain the increased levels seen in Fig. 17. Because dendrite-like formation occurs primarily in non-transformed cells, which have intact cell-cycle checkpoints, we hypothesized that the non-transformed cells were unable to bypass these checkpoints and were therefore arrested in G1. This arrest would result in more cells accumulating p190 and displaying dendrite-like processes. To test this theory, a G1 arrest was induced in transformed cells (which are postulated to have disabled checkpoints) with a double thymidine block and concurrent p190 overexpression for 48 hrs, and the incidence of dendrite-like formation was assessed. Figure 18 shows that when transformed cells were arrested in G1 and p190 was overexpressed, a significant increase in the number of cells exhibiting dendrite-like formation was observed. These results suggest that p190-induced dendrite-like formation may be a result of a block in G1.

<u>p190-induced phenotypes are Rho-dependent.</u>

Because p190 is a negative regulator of Rho, we hypothesized that the three phenotypes were Rho-dependent. To examine this, two approaches were taken. First, deletion and point mutants of p190 were generated (Fig. 19A), and each mutant's ability to induce multinucleation, dendrite-like formation, or apoptosis was determined by immunofluorescence. Prior to this analysis, mutants were shown to be expressed at

Figure 18

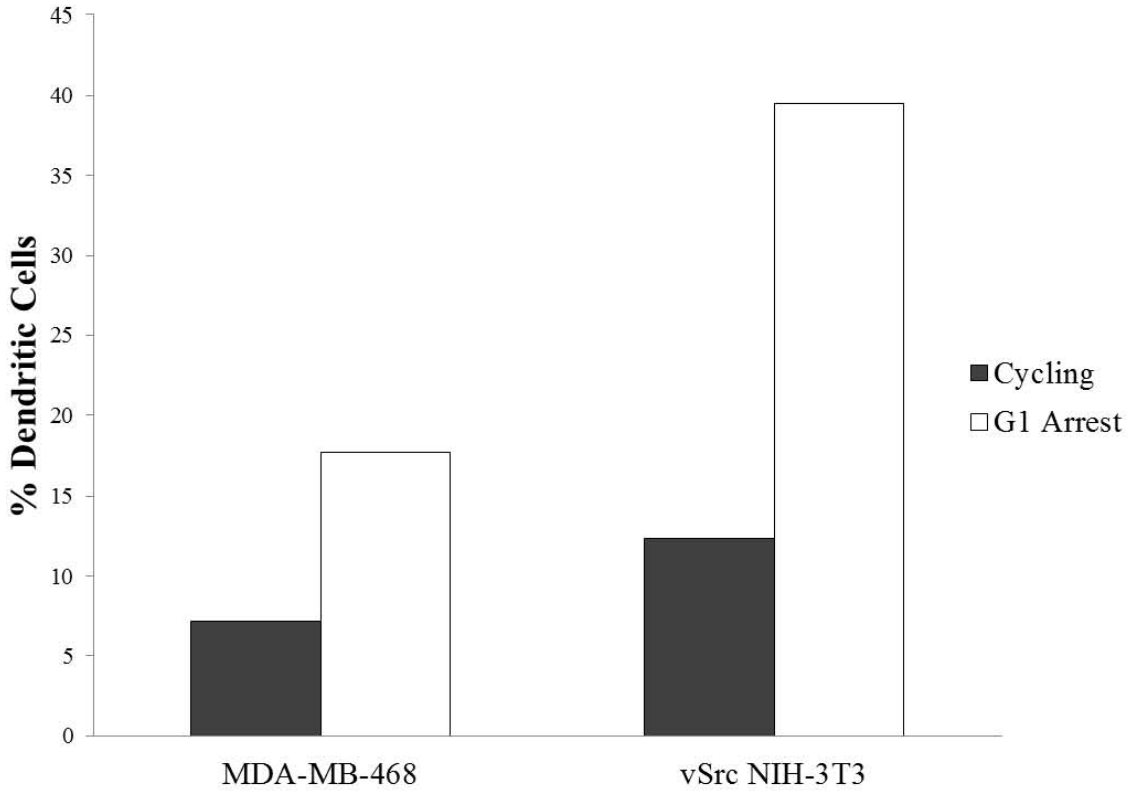
45
40
35
30
25
20
15
10
5
0
% Dendritic Cells
Cycling
G1 Arrest
MDA-MB-468
vSrc NIH-3T3

Figure 18: G1 arrest increases incidence of dendrite-like formation in transformed cells.

Quantitation of dendrite-like formation in transformed cells. MDA-MB-468 and vSrc NIH-3T3 cells were either arrested in G1 with a double thymidine block, or not arrested, and both groups were transiently transfected with HA-p190 for 48 hrs. Cells were fixed, stained for HA-p190 and DNA, and the occurrence of cells exhibiting dendrite-like formations was determined. Results are expressed as the mean percent cells overexpressing p190 that have dendritic-like protrusions, n=1.

Figure 19

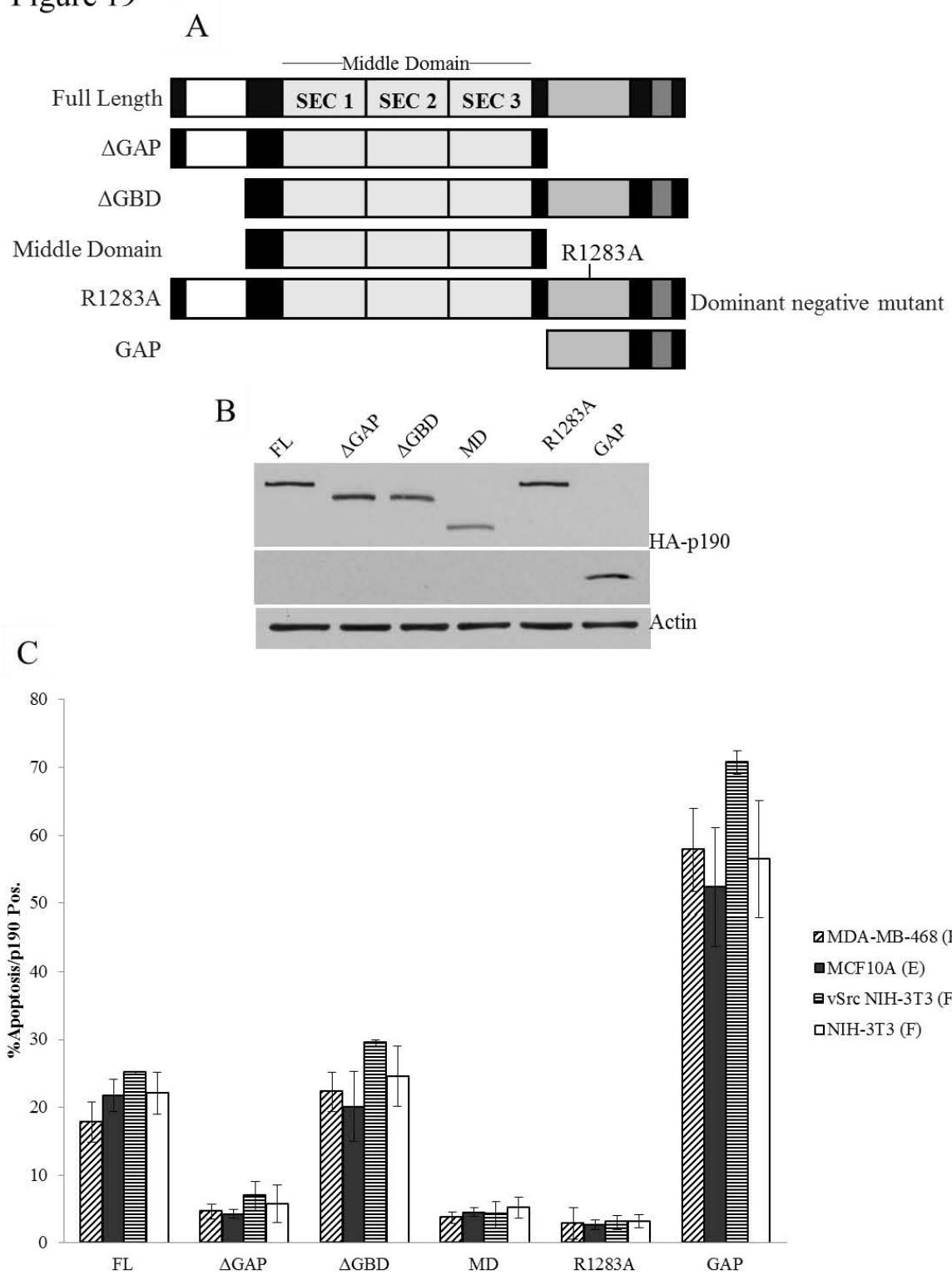
A
Middle Domain
Full Length
SEC 1
SEC 2
SEC 3
ΔGAP
ΔGBD
Middle Domain
R1283A
R1283A
Dominant negative mutant
GAP
B
FL
ΔGAP
ΔGBD
MD
R1283A
GAP
HA-p190
Actin
C
%Apoptosis/p190 Pos.
80
70
60
50
40
30
20
10
0
FL
ΔGAP
ΔGBD
MD
R1283A
GAP
MDA-MB-468 (E)
MCF10A (E)
vSrc NIH-3T3 (F)
NIH-3T3 (F)

Figure 19: p190-induced phenotypes are dependent on the RhoGAP activity.

A: Diagram of the p190RhoGAP mutants: Full-length (FL), ΔGAP, ΔGBD, Middle Domain (MD), dominant negative GAP inactive R1283A, and GAP-only Domain (GAP).

B: Western blot analysis of HA-p190RhoGAP mutants: MDA-MB-468 cells were transfected with plasmids encoding the indicated mutants of p190, and 48 hrs later cell lysates were immunoblotted with anti-HA antibody.

C: Effect of p190 mutations on induction of apoptosis. Indicated cells were transfected and analyzed 48 hrs later as in Fig. 1. Results are expressed as the mean percent of p190 overexpressing cells that were TUNEL positive +/- SEM, n>3.

Figure 19

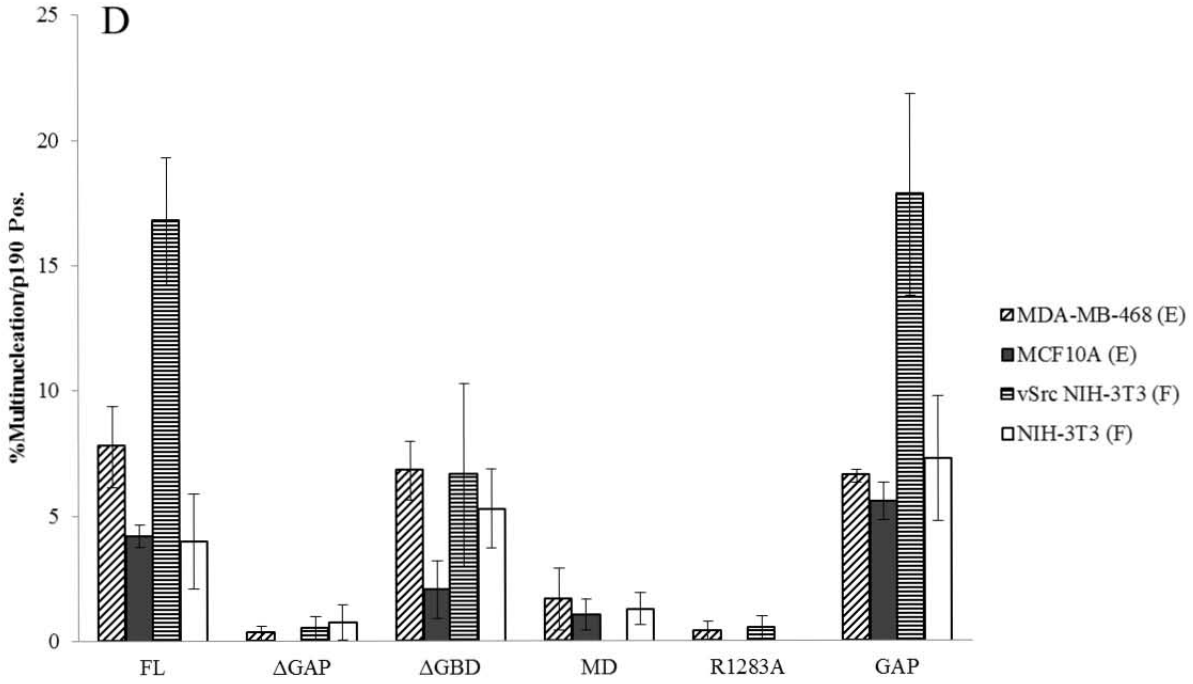
D
%Multinucleation/p190 Pos.
25
20
15
10
5
0
FL
ΔGAP
ΔGBD
MD
R1283A
GAP
MDA-MB-468 (E)
MCF10A (E)
vSrc NIH-3T3 (F)
NIH-3T3 (F)

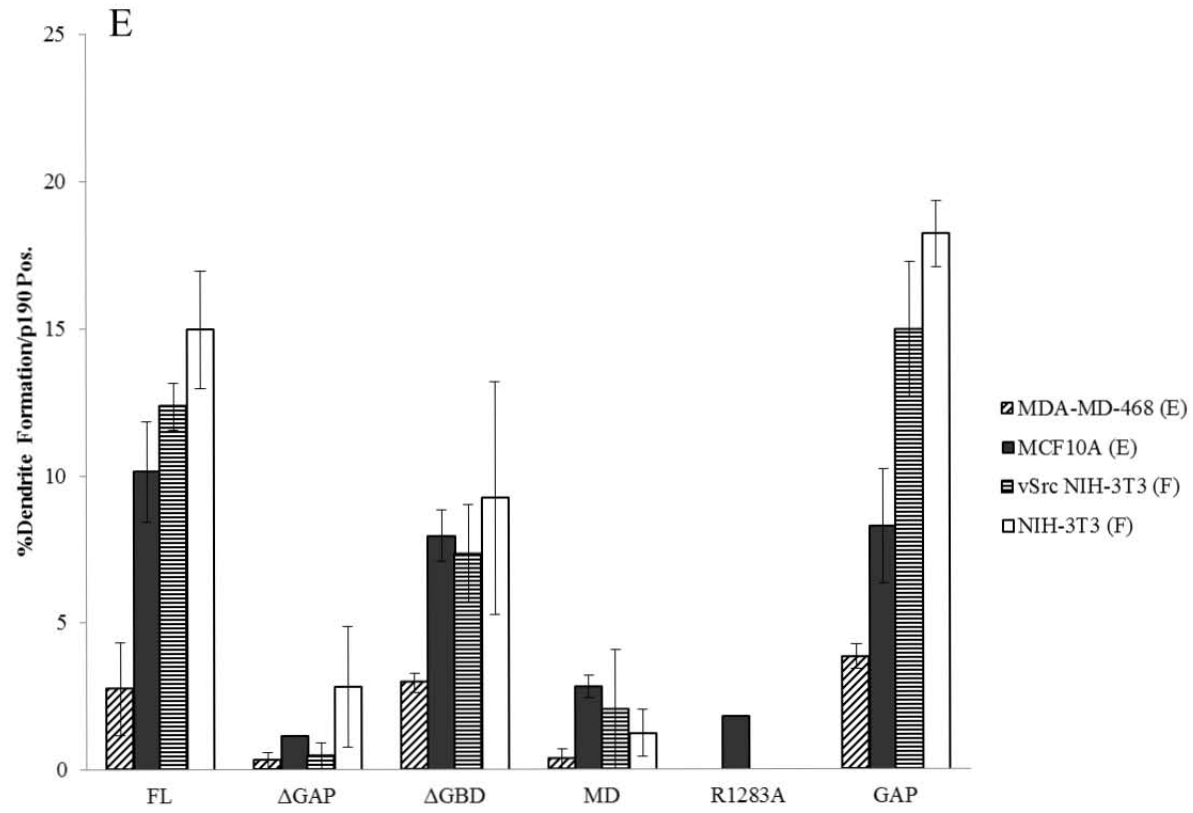
E
%Dendrite Formation/p190 Pos.
25
20
15
10
5
0
FL
ΔGAP
ΔGBD
MD
R1283A
GAP
MDA-MD-468 (E)
MCF10A (E)
vSrc NIH-3T3 (F)
NIH-3T3 (F)

Figure 19: p190-induced phenotypes are dependent on the RhoGAP activity.

D: Effect of p190 mutations on induction of multinucleation. Indicated cells were transfected and analyzed 48 hrs later as in Fig. 1. Results are expressed as the mean percent of p190 overexpressing cells that were positive for multinucleation, +/- SEM, n>3.

E: Effect of p190 mutations on induction of dendrite-like formation. Indicated cells were transfected and analyzed 48 hrs later as in Fig. 1. Results are expressed as the mean percent of p190 overexpressing cells that were positive for dendritic processes, +/- SEM, n>3.

nearly equivalent levels (Fig. 19B) and to exhibit appropriate GTPase activities (Haskell et al., 2001a; Mikawa et al., 2008; Su et al., 2009). Figure 19C shows that transient transfection of these mutants into the 4 indicated cell lines result in a significant decrease in the amount of apoptosis seen with those mutants that were unable to down regulate Rho (ΔGAP, Middle Domain, and R1283A– GAP inactive) as compared to the full length (FL) and ΔGBD proteins. In contrast, the isolated GAP domain showed a significant increase in the amount of apoptosis in all cell types, suggesting that p190-induced apoptosis is elicited through p190's regulation of Rho. Similar patterns were seen with both multinucleation and dendrite-like formation (Figs. 19D & E, respectively), indicating that these phenotypes also required the RhoGAP domain of p190.

The second approach to test the Rho-dependency of the p190-induced phenotypes was to determine the ability of CARho to rescue the effects of p190 overexpression. Figure 20 shows that when equivalent molar amounts of CARho (Q63L) were co-transiently transfected with p190 into the four cell lines, a rescue of all three phenotypes was seen.

<u>p190 confers docetaxel sensitivity through Rho.</u>

Rho activity can be modulated by drugs that regulate both microtubule (MT) polymerization and depolymerization (Niggli, 2003). Docetaxel, an agent that inhibits depolymerization of MT, is frequently employed therapeutically for a variety of cancers (Baker et al., 2009), suggesting that both Rho and p190 might play a role in docetaxel-mediated apoptosis. To address this question, a panel of breast cancer cell lines was examined to determine the relative levels of endogenous p190 in each, as compared to the

Figure 20

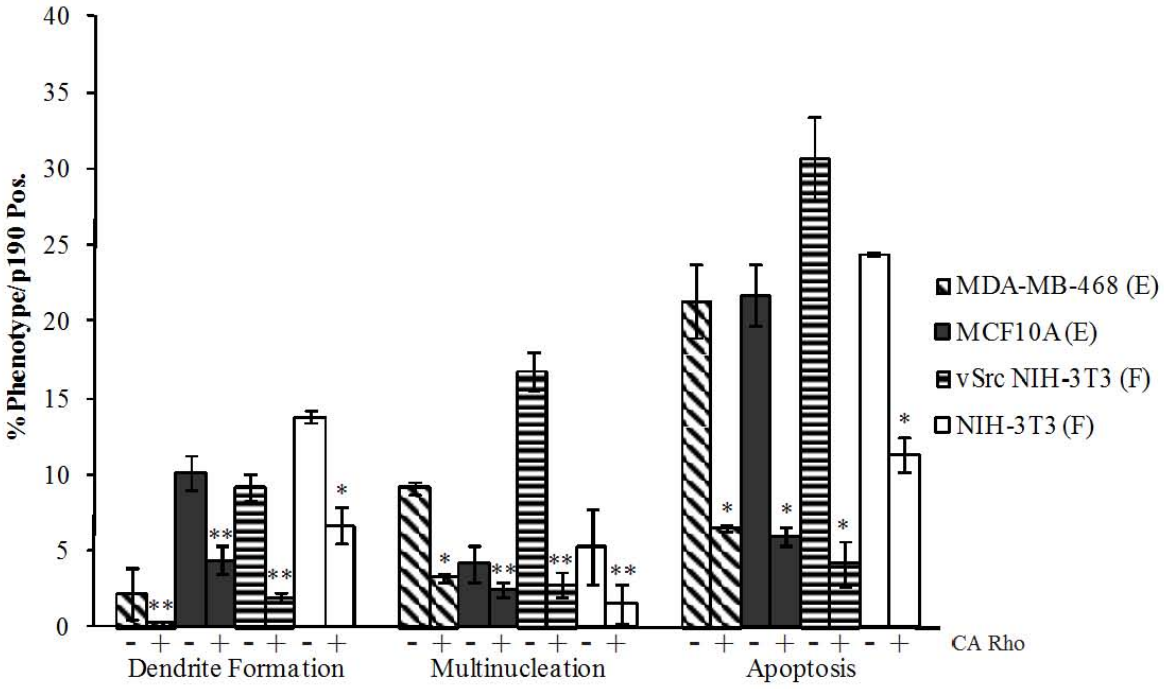
% Phenotype/p190 Pos.
40
35
30
25
20
15
10
5
0
MDA-MB-468 (E)
MCF10A (E)
vSrc NIH-3T3 (F)
NIH-3T3 (F)
CA Rho
Dendrite Formation
Multinucleation
Apoptosis

Figure 20: p190-induced phenotypes are Rho-dependent.

Rescue of p190-induced phenotypes by CARho. Indicated cells were co-transfected with equivalent molar amounts of p190 and CARho (Q63L) or with p190RhoGAP alone and cultured for 48 hrs. Where indicated, only cells expressing FLp190 alone or both FLp190 and CARho were assessed for apoptosis, multinucleation, or dendrite-like formation. Results are expressed as the mean percent HA-p190 or HA-p190/CARho expressing cells that exhibited the indicated phenotype +/- SEM, $n>3$. Statistical significance is determined within individual cell lines: *=$p<0.005$ or **=$p<0.05$, comparing presence of CARho to its absence in p190 overexpressing cells.

non-transformed MCF10A cell line (Figs. 21A). Figure 21B shows that when these cell lines were treated with increasing doses of docetaxel for 24 hrs and tested for apoptosis by TUNEL immunofluorescence, a direct relationship was seen between the level of endogenous p190 and sensitivity of the cell line to docetaxel-induced apoptosis. To further investigate whether p190 and Rho levels or activities altered sensitivity to docetaxel-induced apoptosis, MDA-MB-468 cells were transiently transfected with CARho (Q63L), DNRho (T19N), FLp190, or DNp190 (R1283A) for 24 hrs. Cells were then treated with either 10 nM or 100 nM docetaxel for an additional 24 hrs, and apoptosis was determined by TUNEL immunofluorescence. Figure 22A shows that CARho and DNp190, which increase the activation status of Rho, decreased docetaxel-induced apoptosis, while DNRho and FLp190, which decrease Rho activity, increased docetaxel-induced apoptosis. Interestingly, in MDA-MB-231 cells, a breast cancer cell line with low levels of endogenous p190 and a relatively moderate apoptotic response to docetaxel, the overexpression of p190 resulted in a significantly more profound effect at both the 10 nM and 100 nM dosages (Fig. 22B). Accordingly, silencing of p190 reduced docetaxel-induced caspase-3 cleavage (Fig. 23), suggesting that p190 plays an integral role in docetaxel-induced apoptosis. Taken together these results indicate that p190 confers enhanced sensitivity to docetaxel through its ability to down-regulate Rho.

DISCUSSION:

Multiple lines of evidence indicate p190RhoGAP can function as a tumor suppressor. It has been mapped to chromosome 19q13.3, a region deleted or rearranged in pancreatic, glioma, ovarian, and thyroid tumors (Tikoo et al., 2000). p190 suppresses

Figure 21

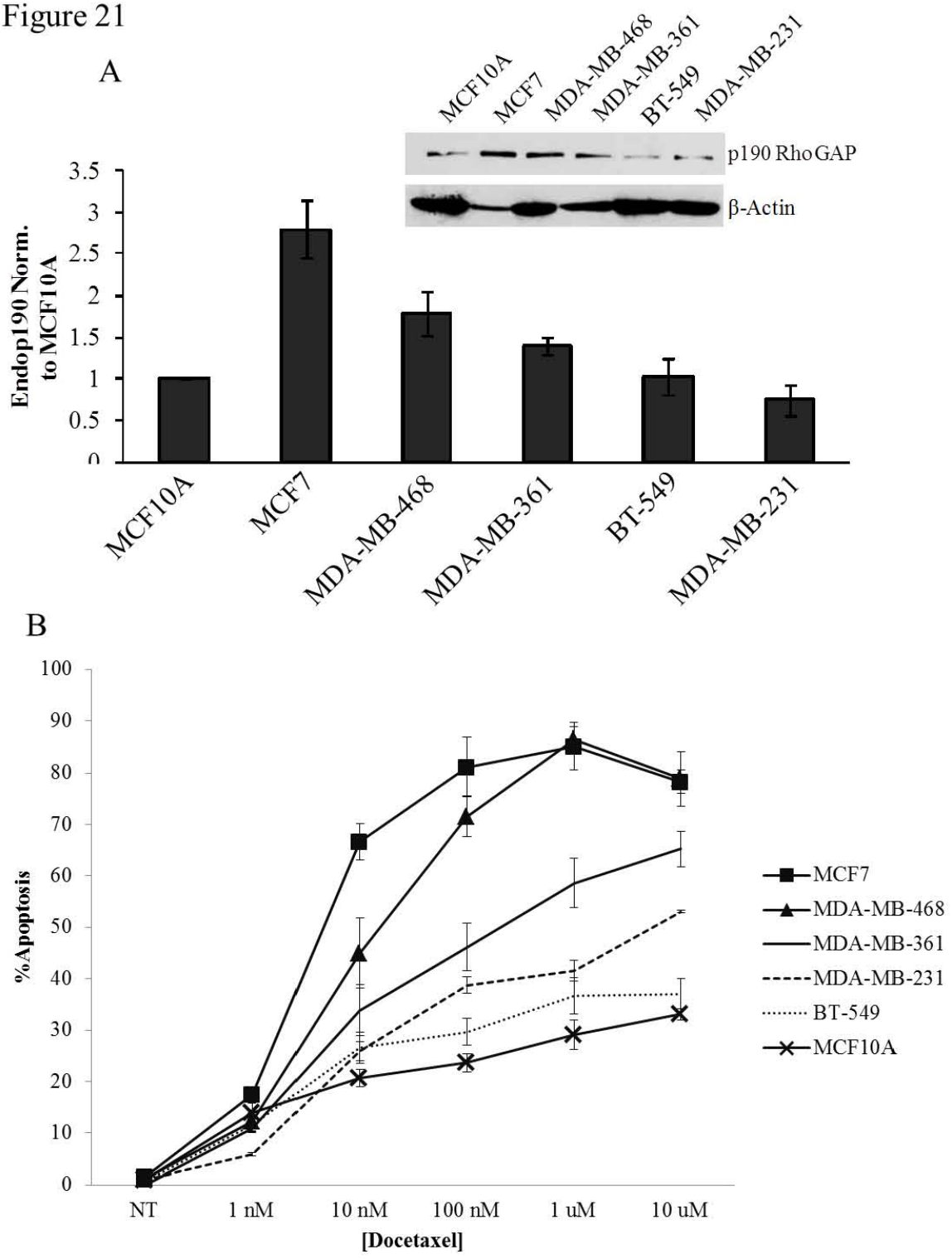
A
MCF10A
MCF7
MDA-MB-468
MDA-MB-361
BT-549
MDA-MB-231
p190 RhoGAP
β-Actin
Endop190 Norm. to MCF10A
3.5
3
2.5
2
1.5
1
0.5
0
MCF10A
MCF7
MDA-MB-468
MDA-MB-361
BT-549
MDA-MB-231
B
%Apoptosis
100
90
80
70
60
50
40
30
20
10
0
NT
1 nM
10 nM
100 nM
1 uM
10 uM
[Docetaxel]
MCF7
MDA-MB-468
MDA-MB-361
MDA-MB-231
BT-549
MCF10A

Figure 21: Amount of endogenous p190 determines sensitivity to docetaxel.

A: Quantitation of levels of endogenous p190 in the indicated cell lines. p190 levels were quantified as described in Materials and Methods. Values were related to β-actin and then normalized to p190 levels in MCF10A cells, which were set to 1. Results are expressed as the mean fold over MCF10A levels +/- SEM, n>3. Inset: Representative immunoblot of endogenous p190 in the indicated breast cancer cell lines.

B: Quantitation of docetaxel-induced apoptosis in breast cancer cell lines. Indicated cells were treated with increasing amounts of docetaxel for 24 hrs, and apoptosis was determined by TUNEL immunofluorescence. Results are expressed as the mean percent of apoptotic cells +/- SEM, n>3.

Figure 22

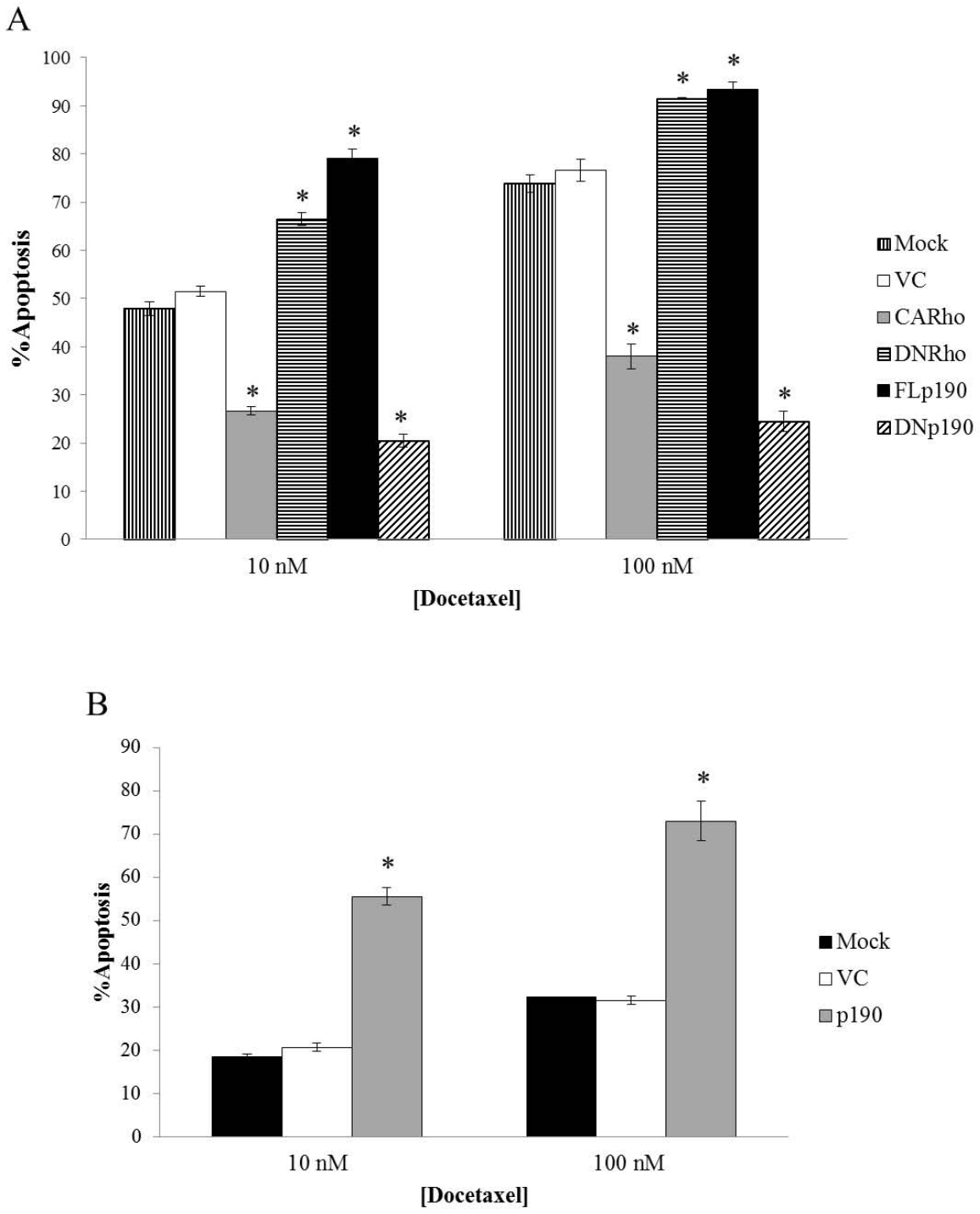
A
%Apoptosis
100
90
80
70
60
50
40
30
20
10
0
10 nM
100 nM
[Docetaxel]
Mock
VC
CARho
DNRho
FLp190
DNp190
B
%Apoptosis
90
80
70
60
50
40
30
20
10
0
10 nM
100 nM
[Docetaxel]
Mock
VC
p190

Figure 22: p190 confers docetaxel sensitivity through Rho in breast cancer cell lines.

A: Quantitation of apoptotic MDA-MB-468 cells transiently overexpressing mutants of Rho or p190 and treated with docetaxel. MDA-MB-468 cells were mock treated or transfected with VC, CARho, DNRho, FLp190, or DNp190 encoding plasmids. Twenty-four hrs later cells were treated with 10 nM or 100 nM docetaxel for another 24 hrs. Apoptosis was determined by TUNEL immunofluorescence. Results are expressed as the mean percent total cells (VC) or cells overexpressing p190 or Rho that were apoptotic +/- SEM, n>3. *=p<0.005 as compared to VC.

B: Quantitation of apoptosis in MDA-MB-231 cells transiently overexpressing p190RhoGAP and treated with docetaxel. MDA-MB-231 cells were mock treated or transfected with VC or p190 plasmids. Twenty-four hrs later cells were treated with 10nM or 100nM docetaxel for another 24 hrs. Apoptosis was determined by TUNEL immunofluorescence. Results are expressed as the mean percent total cells (Mock or VC) or cells positive for HA-p190 that were apoptotic +/- SEM, n>3. *=p<0.005 as compared to Mock treated.

Figure 23

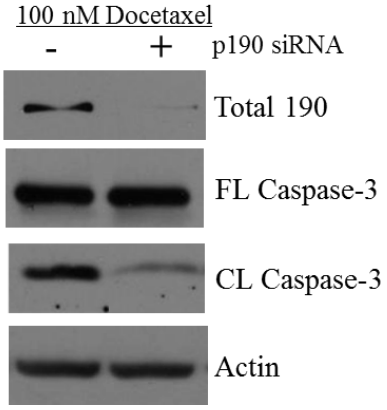
100 nM Docetaxel
-
+
p190 siRNA
Total 190
FL Caspase-3
CL Caspase-3
Actin

Figure 23: p190 is necessary for docetaxel-induced caspase-3 cleavage.

Western blot of docetaxel-induced caspase-3 after p190 knockdown in MDA-MB-468 cells. Cells were either mock-treated or treated with p190 siRNA as described in Materials and Methods, and 24 hrs. later 100 nM docetaxel was added to both treatment groups. Twenty-four hrs post docetaxel treatment, cells were lysed and subjected to Western blot analysis to determine levels of total p190, full-length caspase-3, and cleaved caspase-3. Actin was used as a loading control.

Ras-induced transformation in NIH-3T3 cells (Wang et al., 1997), and overexpression inhibits PDGF-induced gliomas in a mouse model (Wolf et al., 2003). A Rho/p190 chimera reduces human pancreatic cancer invasion and metastasis in mice (Kusama et al., 2006), while p190 negatively regulates angiogenesis (Mammoto et al., 2009). Like other tumor suppressor proteins, p190 has been implicated in apoptotic initiation. Specifically, epithelial prostate cells of mice undergo programmed cell death following castration. This correlates with an increase in p190 mRNA and protein levels upon apoptotic initiation (Morrissey et al., 1999). While these studies are supportive of apoptosis as a tumor suppressive activity of p190, they do not directly test the question.

The current study was conducted to determine whether p190 functions as a tumor suppressor by inducing apoptosis and to elucidate the relationship between apoptosis and the secondary p190-induced phenotypes, multinucleation and dendrite-like formation. We demonstrated that p190 induces apoptosis and further showed that overexpression most frequently results in apoptosis in all cell lines tested. Surprisingly, the secondary phenotype was found to be dependent upon transformation status rather than fibroblast or epithelial cellular origin. Specifically, the secondary phenotype of p190 overexpression in transformed cells was multinucleation, an outcome that suggests a defect in mitosis or cytokinesis, as previously shown by our lab (Su et al., 2003). Transformed cells are known to harbor flaws in cell cycle checkpoints, allowing transit through cell cycle in the presence of strong arrest signals (such as aberrant RhoGTP levels due to p190 overexpression). We postulate that transformed cells overexpressing p190 are able to bypass one or more checkpoints before undergoing apoptosis or failing to complete

cytokinesis. In support of this hypothesis are the findings that multiple cell cycle checkpoint proteins have pro-apoptotic function, many of which have been implicated in Rho-induced apoptosis, including p53 (Muller et al., 2006), CDK1 (Maddika et al., 2007), and the cyclins D (Sofer-Levi and Resnitzky, 1996), B (Porter et al., 2000), and E (Mazumder et al., 2002). Thus, fidelity of cell cycle checkpoints may be one factor that determines the route to apoptosis in cells of different malignant status that harbor dysregulated Rho signaling.

The secondary phenotype prevalent in non-transformed cells was dendrite-like formation. Studies in neuronal cells expressing CARho revealed that Rho induces neurite retraction, through ROCK activation. Conversely, Rho inactivation results in neurite outgrowth (Koh, 2006). The effect of Rho's activation status on neurite outgrowth supports observations reported here regarding p190-induced dendrite-like formation in non-transformed cells. While we do not have a complete understanding of the mechanism of p190-induced dendrite (neurite) formation, quantitation of the amount of p190 overexpressed suggests that cells with a dendritic phenotype have 4 times more p190 than p190-overexpressing cells with a normal phenotype. Non-transformed cells are assumed to have intact cell cycle checkpoints; accordingly, perturbations within the cell are sensed, and cell cycle progression is arrested. While arrested, p190 could still be transcribed and translated, leading to an accumulation of the protein. The p190-dendritic cells are often mono-nucleated with normal sized nuclei, suggesting they have not entered the S phase of the cell cycle and may have been arrested in G1. In support of this theory, forcing a G1 arrest in transformed cells increased the incidence of dendrite-like

formation, suggesting that G1 arrest may be a defining characteristic for the differential effect of p190 overexpression on transformed vs. non-transformed cells. Activation of the p53/p21 cell cycle checkpoint is consistent with a G1/S block (Agarwal et al., 1995). Indeed, several reports have implicated p53 in Rho-inactivation induced apoptosis (Costello et al., 2000), suggesting that p190-induced apoptosis in non-transformed cells may be elicited through the p53 pathway.

Real-time microscopy revealed that both secondary phenotypes result in apoptosis and do so more readily than p190-overexpressing cells with a normal morphology. Inhibition of apoptosis by the pan caspase inhibitor, ZVAD, increased both multinucleated and dendritic-like cells, consistent with the hypothesis that the two secondary phenotypes may be priming intermediates which lead to apoptosis. CARho rescued p190-induced apoptosis, along with multinucleation and dendrite-like formation, suggesting that all three phenotypes are Rho-dependent, a conclusion supported by a structure/function analysis with mutants of p190. The Rho-dependency of all three p190-induced phenotypes raises the question of whether the same signaling pathways downstream of Rho can generate the different phenotypes. We would posit that the pathways utilized by transformed vs. non-transformed cells are distinct, due to the fact that different secondary phenotypes are preferentially evoked. Prolonged inactivation of Rho can result in apoptosis (Hippenstiel et al., 2002a); however, reports are conflicting regarding which apoptotic signaling pathways are activated. For example, Akt has been implicated (Khwaja et al., 2006) along with the NK-κB (Hippenstiel et al., 2002b), JNK (Park et al., 2009), p38 (Schulz et al., 2009), ERK (Khwaja et al., 2006), and p53

pathways (Costello et al., 2000). However, it is not clear whether these pathways are specific to transformed or non-transformed cells. Further work is needed to clarify the mechanisms of Rho-induced apoptosis in cells with different transformation status with the goal of minimizing bystander effects of potential p190/Rho-based therapeutics.

Finally, we showed that p190 sensitized cells to docetaxel-induced apoptosis in a Rho-dependent manner. Rho is a master regulator of both actomyosin and microtubule dynamics (Hall, 2009). Dysregulation of these cytoskeletal elements can give rise to the phenotypes described in this report. Two main effector proteins mediate Rho's modulation of cytoskeletal processes; mDia, and ROCK (Piekny et al., 2005). Rho activates mDia to facilitate actin nucleation and polymerization in addition to microtubule alignment and stabilization (Narumiya and Yasuda, 2006). Rho's activation of ROCK results in actin filament (Ichetovkin et al., 2000) and microtubule stability (Takesono et al.) through its regulation of myosin II (Verin et al., 2001). The activation of both mDia and ROCK are required for actin stress fiber formation, a phenotypic characteristic of Rho activation (Watanabe et al., 1999), which is abolished with the overexpression of p190 (Begum et al., 2004; Chang et al., 1995). The fact that Rho is an important cytoskeletal regulator prompted us to test whether p190 affected the efficacy of docetaxel, a chemotherapeutic agent used to treat breast, lung, prostate, gastric, and head and neck cancers (Baker et al., 2009). Taxanes bind along the entire length of microtubules and prevent their depolymerization. This action results in failure of the mitotic spindle to effect chromosomal segregation, leading to mitotic catastrophe and ultimately cell death (Earhart, 1999).

The literature suggests a close link between Rho, ROCK and microtubule disrupting agents. In cells treated with MT de-polymerizing agents, Rho and ROCK activity increases (Niggli, 2003), whereas a MT stabilizer decreases Rho and ROCK activity (Birukova et al., 2004a). Conversely, CARho and ROCK induce MT depolymerization (Birukova et al., 2004a), while the ROCK inhibitor Y-27632 results in MT stability (Takesono et al.). Additionally, a myosin II inhibitor stabilizes microtubules (Takesono et al.), prompting investigators to look at the role of myosin II in MT regulation. They found that cells treated with MT destabilizing drugs exhibit an increase in rMLC phosphorylation (Verin et al., 2001), while Taxol treatment abolishes rMLC phosphorylation (Yin et al.), suggesting that MT organization is regulated through a Rho/ROCK/myosin II pathway. Our work shows that the sensitivity of MDA-MB-468 and MDA-MB-231 breast cancer cells to docetaxel-induced apoptosis is modulated through Rho and p190, possibly through the ROCK and rMLC pathway.

For over 30 years the cancer biology field has focused on kinases as therapeutic targets, while transcription factors, G-protein coupled receptors, and small-G proteins have received considerably less attention, despite the fact that they play important roles in the genesis and progression of tumors. Rho, for example, is up-regulated at the RNA or protein level in many solid tumors (Gomez del Pulgar et al., 2005); yet only one clinically available drug is targeted to the pathway at this time. The drug Fasudil (Olson, 2008), a ROCK inhibitor, is currently used in the treatment of cardiovascular diseases. Recently, however, several groups have shown that Fasudil may have a promising future as a cancer therapeutic. Fasudil treatment can inhibit liver, lung, and breast tumor

progression (Ying et al., 2006), reduce glioma invasion and growth (Deng et al.), and decrease ovarian tumor burden in mice (Ogata et al., 2009), all of which support the concept of targeting Rho and its regulators as cancer therapeutics. We have shown that both p190 and Rho are important modulators of at least one chemotherapeutic agent, docetaxel. Cells with elevated levels of p190 were more sensitive to docetaxel, suggesting that analysis of p190 levels may predict response rates and decrease off-target effects of drugs that target Rho and the Rho pathways which regulate microtubule and actin dynamics.

CHAPTER 4

Apoptotic Signaling Regulated by p190

Chapter 4:
Apoptotic Signaling Regulated by p190

INTRODUCTION:

RhoA is a member of the RhoGTPase family whose primary function is regulation of cytoskeletal dynamics (Hall, 2005). When active, Rho regulates a variety of cellular functions ranging from cell morphology (Paterson et al., 1990), axon guidance and extension (Jalink et al., 1994; Nishiki et al., 1990), smooth-muscle contraction (Hirata et al., 1992) and formation of stress fibers and focal adhesions (Nobes and Hall, 1994; Ridley and Hall, 1992), to cytokinesis (Kishi et al., 1993; Mabuchi et al., 1993), cell-cycle progression (Khosravi-Far et al., 1995; Olson et al., 1995; Yamamoto et al., 1993), transformation (Qiu et al., 1997; Qiu et al., 1995a; Qiu et al., 1995b), and survival (Miyoshi J., 2009). Of these, Rho's role in survival and apoptosis is the least well defined.

Many groups have found that prolonged inactivation of RhoGTPases leads to aberrant cellular function and ultimately cell death. Treatment of cerebellar granule neurons with *Clostridium difficile* toxin (Tox B), a specific Rho family inhibitor, leads to cytochrome c release and the activation of both caspases-9 and -3. Dominant negative Rac1, can also initiate apoptosis in these same cells in a c-Jun dependent manner (Le et al., 2005), while dominant negative Rac1 or Cdc42 induces apoptosis in Balb/c 3T3 murine fibroblasts in a p53-dependent manner (Lassus et al., 2000). Specific inhibition of RhoA by C3 toxin in EL4 T lymphoma cells results in 95% cell death by apoptosis (Moorman et al., 1996). Finally, cell lines stably expressing a RhoGAP have yet to be

generated, presumably due to deleterious effects on RhoGTP levels. Together, these findings support the conclusions that the Rho pathway is a critical regulator of cell death and survival.

The link between p190 and apoptosis was first suggested when Morrisey reported an increase in both p190 protein and mRNA levels in epithelial cells undergoing apoptosis following castration of rats (Morrissey et al., 1999). At that time it was not known if the increase in levels was causative or an effect of the ensuing apoptosis. Since then, p190 overexpression has been shown to initiate caspase-dependent apoptosis through its down regulation of Rho (Ludwig and Parsons, 2011). Interestingly, overexpression of p190 also elicits two other phenotypes; multinucleation, seen most often in transformed cells, and dendrite-like formation, more commonly seen in non-transformed cells. Both phenotypes can result in apoptosis and may serve as intermediates, priming the cells for p190-induced apoptosis. However, aside from the role of Rho in p190-induced apoptosis, little is known about the apoptotic signaling pathways activated upon overexpression of p190RhoGAP.

Attempts to molecularly characterize apoptosis initiated by Rho inactivation have yielded many candidate pathways, including a decrease in active Akt (Khwaja et al., 2006; Stepan et al., 2004) or NF-κB (Hippenstiel et al., 2002b; Liu et al., 2004), and an increase in p53 (Costello et al., 2000; Li et al., 2002), p38 (Khan et al., 2011; Schulz et al., 2009), and JNK (Le et al., 2005). Some groups have reported an increase in Bim levels (Le et al., 2005; Loucks et al., 2006), while others have seen a decrease in Mcl-1 expression levels (Hippenstiel et al., 2002a). It is clear that decreased Rho activity is

detrimental for cell survival; however, what specific signaling molecules regulate this effect appear to be quite complex and are still poorly defined. Given the importance of Rho activation in tumorigenesis and the need for new drug targets, the implications of Rho-targeted apoptosis are profound. By understanding the apoptotic signaling mechanisms responsible for inducing apoptosis upon inactivation of Rho, new drug targets may be identified.

In this study we show that inactivation of Rho through overexpression of p190RhoGAP resulted in an increase in the NF-κB pathway in transformed cells, but a decrease of this pathway in non-transformed cells, suggesting that NF-κB may be key to the differential apoptotic phenotypes seen in transformed vs. non-transformed cells. We also report that all cells, regardless of transformation status, exhibited a significant increase in JNK activation upon p190 overexpression. Finally we show that p190-induced apoptosis increased the cytotoxic isoforms of Bim, Bim_L and Bim_S, while decreasing cellular levels of the anti-apoptotic protein, Mcl-1. Together, these data suggest that JNK, Bim, and Mcl-1 function in p190-induced apoptosis regardless of transformation status, while NF-κB may play a role in the differential secondary phenotypes seen with p190 overexpression.

RESULTS:

Overexpression of p190 does not activate p53 or p38, or down regulate Akt.

Apoptosis can be initiated by increased levels or activation of pro-apoptotic proteins, such as p53 or p38, or the inactivation of pro-survival proteins, like Akt. To gain insights into the pathway by which p190 initiates apoptosis, two transformed (MDA-

MB-468 and vSrc NIH-3T3) and two non-transformed (MCF10A and NIH-3T3) cell lines were transiently transfected with HA-p190RhoGAP for 12, 24, 36, and 48 hrs., and the activation status (as judged by altered protein levels or specific phosphorylation) of each of the above-mentioned proteins was determined by Western blot. Figure 24 depicts representative blots of 3-5 experiments showing that neither the levels nor phosphorylation status of p53, p38, or Akt changed significantly upon p190 overexpression in MDA-MB-468 (Fig. 24A), vSrc NIH-3T3 (Fig. 24B), MCF10A (Fig. 24C), or NIH-3T3 (Fig. 24D) cells. These data suggest that neither the p53 nor the p38 apoptotic pathways are activated upon p190 overexpression, while the Akt pathway remains active and its suppression of pro-apoptotic proteins remains intact.

IKB is differentially activated by p190 in transformed cells vs. non-transformed cells.

p190 overexpression can induce apoptosis through different intermediate phenotypes (multinucleation and dendrite-like formation) depending upon the transformation status of the cell (Ludwig and Parsons, 2011). We therefore asked whether these different phenotypes corresponded to differential activation of apoptotic signaling pathways. To address this question, the same four cell lines analyzed above were again transiently transfected with HA-p190 for 12, 24, 36, and 48 hrs, and Western blot analysis was used to determine the levels of phospho-IKB and total IKB as a read-out for the activation of the pro-survival NF-κB pathway (Bakkar and Guttridge, 2010). Figure 25 shows a marked increase in the phosphorylation of IKB with time in the transformed cell lines, MDA-MB-468 (Panel A) and vSrc NIH-3T3 (Panel C). This phosphorylation promotes ubiquitin-mediated degradation of IKB and allows NF-κB to

Figure 24

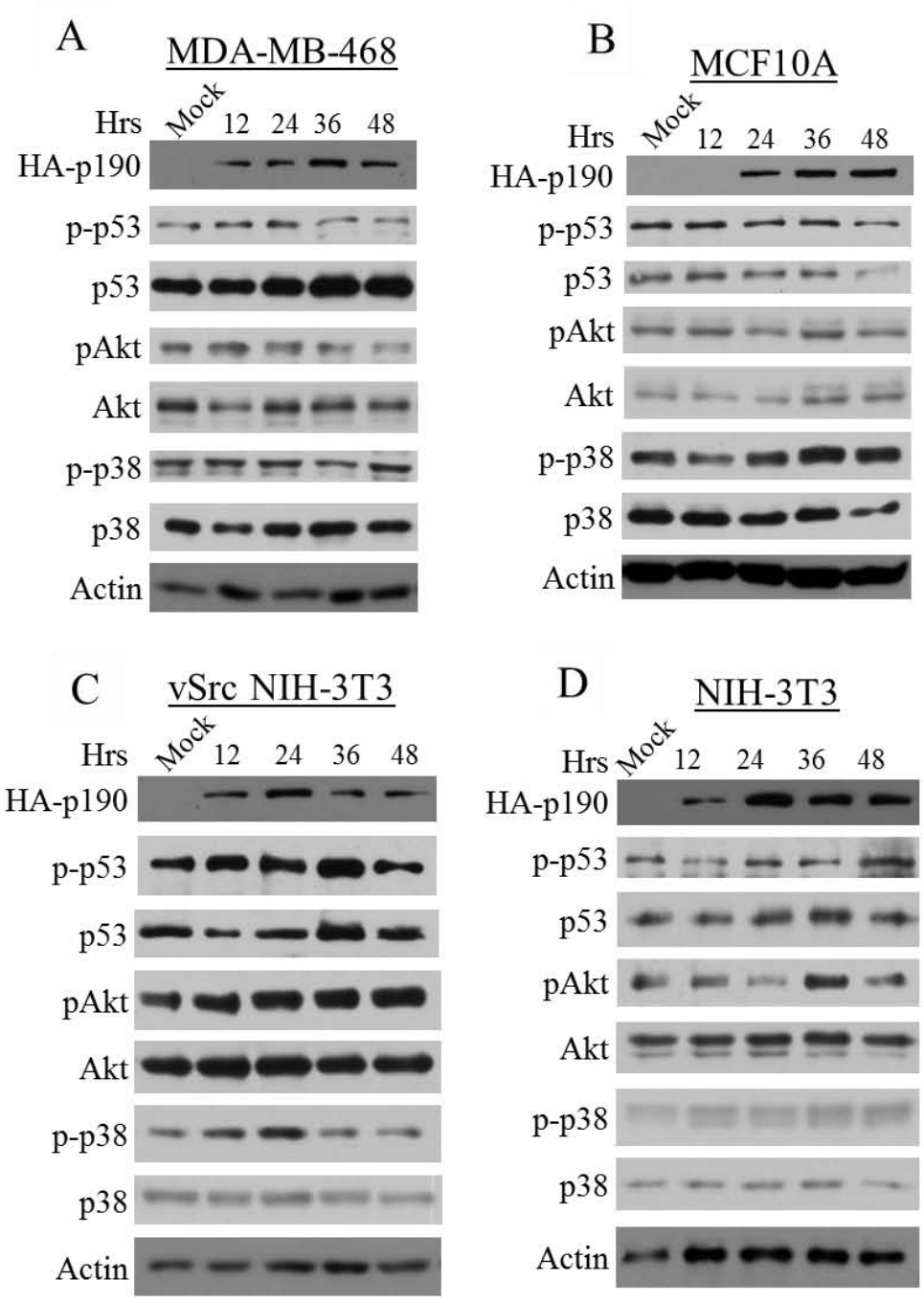
A
MDA-MB-468
Hrs
Mock
12
24
36
48
HA-p190
p-p53
p53
pAkt
Akt
p-p38
p38
Actin
B
MCF10A
Hrs
Mock
12
24
36
48
HA-p190
p-p53
p53
pAkt
Akt
p-p38
p38
Actin
C
vSrc NIH-3T3
Hrs
Mock
12
24
36
48
HA-p190
p-p53
p53
pAkt
Akt
p-p38
p38
Actin
D
NIH-3T3
Hrs
Mock
12
24
36
48
HA-p190
p-p53
p53
pAkt
Akt
p-p38
p38
Actin

Figure 24: Overexpression of p190 does not activate p53, or p38, or down regulate Akt.

A: Western blot of p53, p38, and Akt activation. MDA-MB-468 cells were transfected with HA-p190 or Mock-treated, and extracts were subjected to Western blotting with the indicated antibodies as described in Materials and Methods. Cells were lysed at 12, 24, 36, and 48 hrs after transfection. Mock time point was collected at 48 hrs. Western blots shown are representative of n>3.

B-D: MCF10A (B), vSrc NIH-3T3 (C), and NIH-3T3 (D) cells were treated as in panel A.

Figure 25

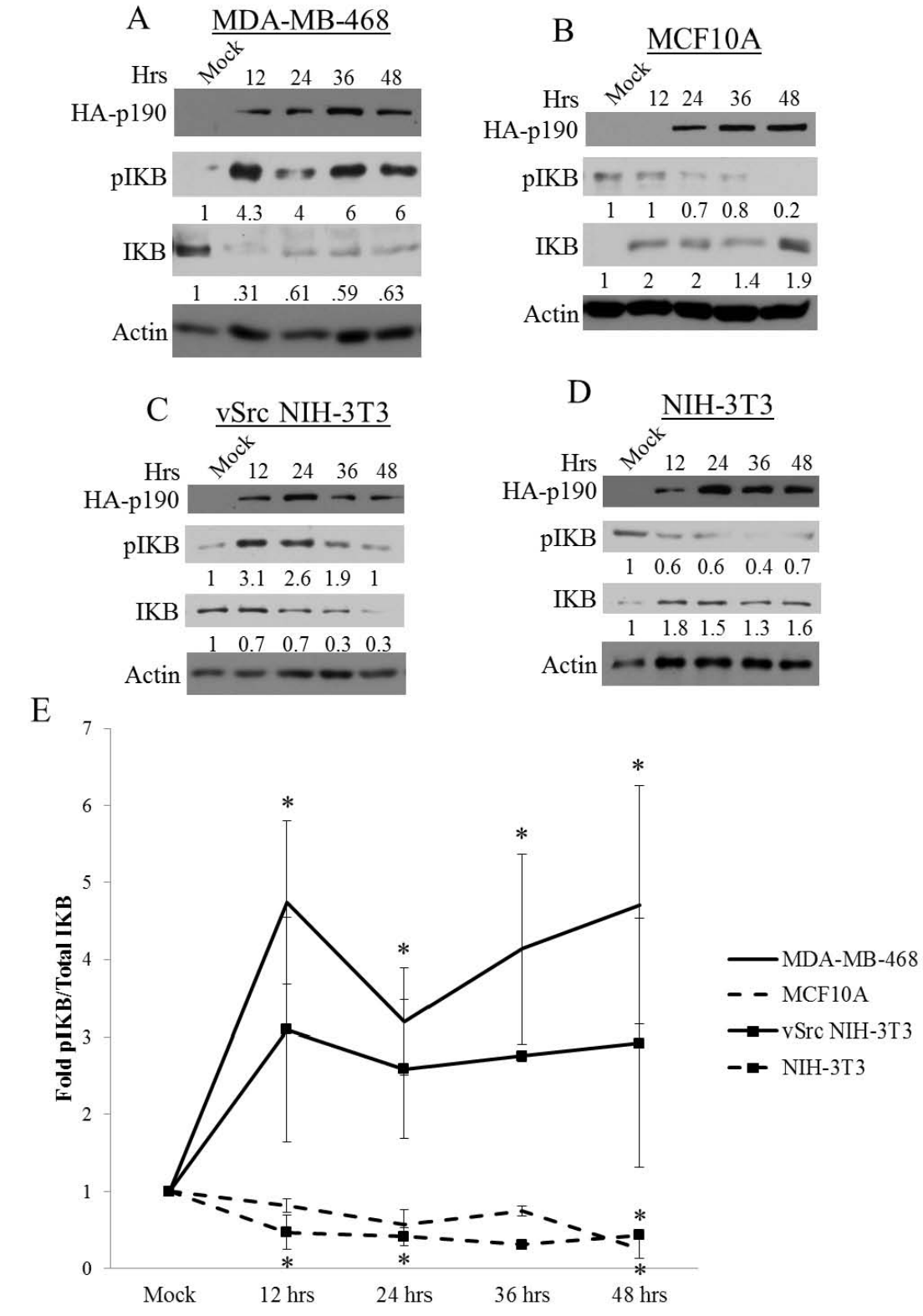
A
MDA-MB-468
Hrs
Mock
12
24
36
48
HA-p190
pIKB
1
4.3
4
6
6
IKB
1
.31
.61
.59
.63
Actin
B
MCF10A
Hrs
Mock
12
24
36
48
HA-p190
pIKB
1
1
0.7
0.8
0.2
IKB
1
2
2
1.4
1.9
Actin
C
vSrc NIH-3T3
Hrs
Mock
12
24
36
48
HA-p190
pIKB
1
3.1
2.6
1.9
1
IKB
1
0.7
0.7
0.3
0.3
Actin
D
NIH-3T3
Hrs
Mock
12
24
36
48
HA-p190
pIKB
1
0.6
0.6
0.4
0.7
IKB
1
1.8
1.5
1.3
1.6
Actin
E
Fold pIKB/Total IKB
0
1
2
3
4
5
6
7
Mock
12 hrs
24 hrs
36 hrs
48 hrs
MDA-MB-468
MCF10A
vSrc NIH-3T3
NIH-3T3

Figure 25: IKB is differentially regulated by p190 in transformed vs. non-transformed cells.

A: Western blot of phosphorylated and total IKB. MDA-MB-468 cells were transfected with HA-p190 or Mock-treated, and extracts were subjected to Western blotting as described in Materials and Methods. Cells were lysed at 12, 24, 36, and 48 hrs and total and phospho-levels of IKB were normalized to Actin (mean of n>3 are shown below the blot). Mock time point was collected at 48 hrs. Western blots shown are representative of 3 or more experiments.

B-D: MCF10A (B), vSrc NIH-3T3 (C), and NIH-3T3 (D) cells were treated as in panel A.

E: Quantitation of specific phospho-IKB in MDA-MB-468, MCF10A, vSrc NIH-3T3, and NIH-3T3 cells upon p190 overexpression. Cells were treated as described in A and the ratio of pIKB to IKB was determined. Results are expressed as the mean fold over Mock treatment, +/- SEM, n>3. *=$p<0.05$ as compared to Mock. Solid line=transformed cells, dashed line=non-transformed cells.

translocate to the nucleus and transcribe pro-survival factors (Kucharczak et al., 2003). In accordance with the increase in IKB phosphorylation, a significant decrease in total IKB was seen upon p190 overexpression (Panel A & C), resulting in a striking fold increase in pIKB vs. total IKB (Panel E). This finding suggests that the NF-κB pathway plays a role in p190-induced apoptosis. However, NF-κB regulates both pro-apoptotic and pro-survival pathways, and thus it remains to be determined which are activated upon p190 overexpression. NF-κB can initiate apoptosis by increasing expression of FasL, Fas, DR4-6, and p53, all of which initiate apoptosis. However, increased activation of the NF-κB pathway through decreased IKB protein could also represent a response similar to that seen with TNF-α treatment. It is hypothesized that this pathway is activated upon apoptotic stimuli as a rescue mechanism to prevent cell death. (Bakkar and Guttridge, 2010)

Conversely, phosphorylation of IKB in the non-transformed cell lines, MCF10A (Panel B) and NIH-3T3 (Panel D) decreased, while levels of total IKB remained unchanged or increased. In contrast to transformed cells, the ratio of pIKB to IKB decreased (Panel E). These results suggest that NF-κB is excluded from the nucleus in non-transformed cells. NF-κB nuclear exclusion decreases expression of pro-survival factors, such as caspase inhibitors and the anti-apoptosis proteins Bcl-2 and Bcl-X_L (Kucharczak et al., 2003), tipping the balance between cell survival and death towards apoptosis. These results also suggest that in non-transformed cells, p190 disables the pro-survival actions of the NF-κB pathway, eventually inducing apoptosis. Taken together, these data further support the idea that p190-induced apoptosis is differentially

regulated in transformed vs. non-transformed cells, and this difference may be regulated through the NF-κB pathway.

p190 overexpression activates JNK.

JNK is a pro-apoptotic protein that is activated (by phosphorylation) in response to cytokines and DNA damage (Kyriakis and Avruch, 2001). Examination of its phosphorylation in response to p190 overexpression revealed that all cells, regardless of transformation status, exhibited an increase in JNK activation at all time-points examined (Fig. 26A-D). Quantification revealed an increase in JNK activation between 1.5-4 fold, depending upon the time examined and cell line (Fig. 26E). These data suggest that JNK may play an active role in p190-induced apoptosis.

p190 overexpression modulates Bim and Mcl-1 levels.

JNK can phosphorylate Bim, promoting its dissociation from microtubules and activating its pro-apoptotic function (Hubner et al., 2008; Lei and Davis, 2003). Conversely, several reports indicate that JNK phosphorylation of the anti-apoptotic protein, Mcl-1, promotes its degradation (Wertz et al., 2011). Additionally, both an increase in Bim expression and a decrease in Mcl-1 protein have been reported following exposure to taxol, a microtubule depolymerizing agent (Bull et al., 2010; Jazirehi and Bonavida, 2004). Chapter 3 details how a cell's sensitivity to taxol is dependent upon the amount of endogenous p190 within the cell and that p190 can sensitize breast cancer cells to taxol through its down regulation of Rho (Ludwig and Parsons, 2011). Given this information, we hypothesized that p190-induced apoptosis may be mediated through the Bcl-2 family proteins, Bim and/or Mcl-1. To assess this possibility, MDA-MB-468 cells

Figure 26

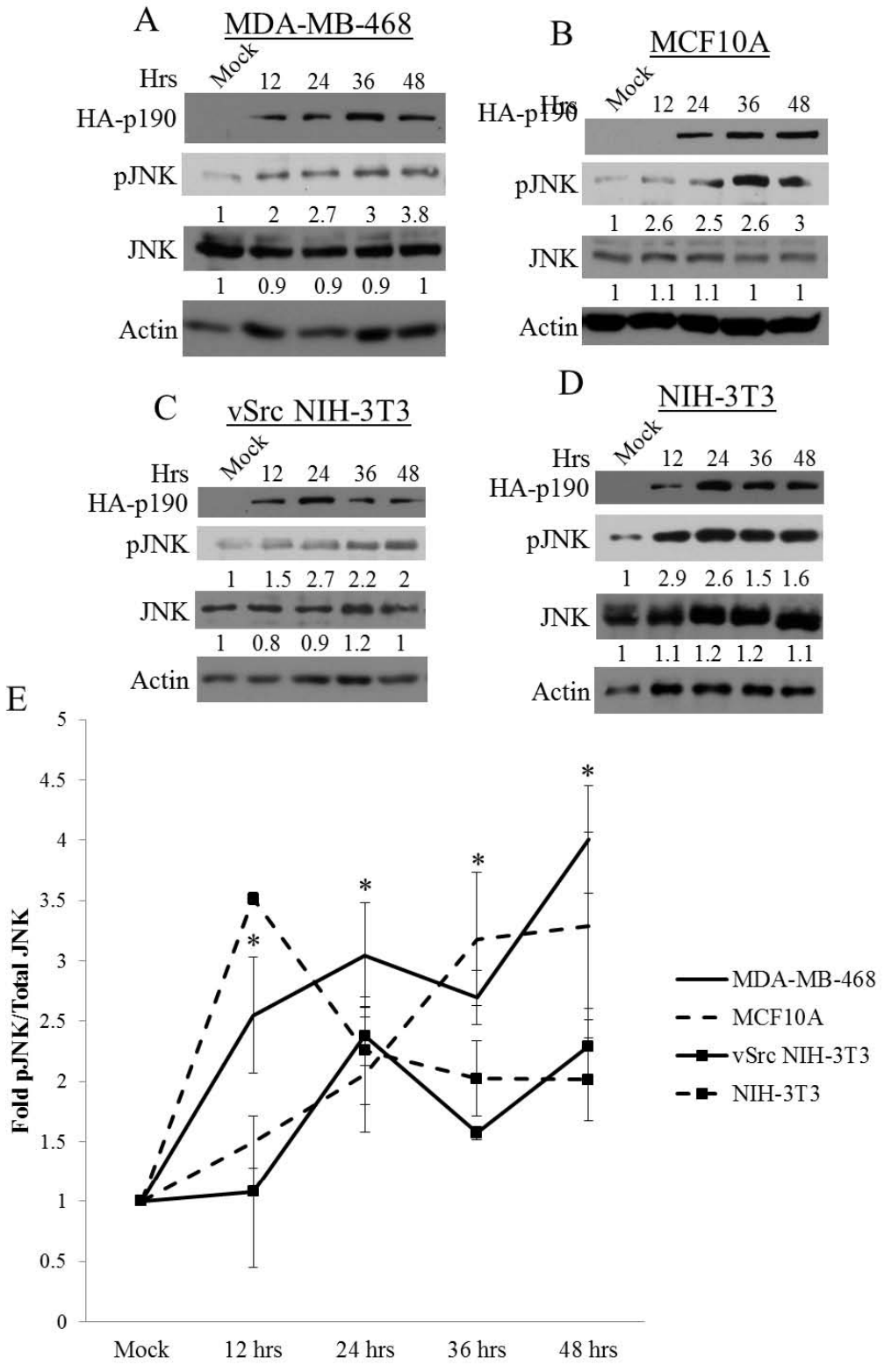
A
MDA-MB-468
Hrs
Mock
12
24
36
48
HA-p190
pJNK
1
2
2.7
3
3.8
JNK
1
0.9
0.9
0.9
1
Actin
B
MCF10A
Hrs
Mock
12
24
36
48
HA-p190
pJNK
1
2.6
2.5
2.6
3
JNK
1
1.1
1.1
1
1
Actin
C
vSrc NIH-3T3
Hrs
Mock
12
24
36
48
HA-p190
pJNK
1
1.5
2.7
2.2
2
JNK
1
0.8
0.9
1.2
1
Actin
D
NIH-3T3
Hrs
Mock
12
24
36
48
HA-p190
pJNK
1
2.9
2.6
1.5
1.6
JNK
1
1.1
1.2
1.2
1.1
Actin
E
Fold pJNK/Total JNK
0
0.5
1
1.5
2
2.5
3
3.5
4
4.5
5
Mock
12 hrs
24 hrs
36 hrs
48 hrs
MDA-MB-468
MCF10A
vSrc NIH-3T3
NIH-3T3

Figure 26: p190 overexpression activates JNK.

A: Western blot of phosphorylated and total JNK. MDA-MB-468 cells were transfected with HA-p190 or Mock-treated, and extracts were subjected to Western blotting as described in Materials and Methods. Cells were lysed at 12, 24, 36, and 48 hrs and total and phospho-levels of JNK were normalized to Actin (mean of n>3 are shown below the blot). Mock time point was collected at 48 hrs. Western blots shown are representative of 3 or more experiments.

B-D: MCF10A (B), vSrc NIH-3T3 (C), and NIH-3T3 (D) cells were treated as in panel A.

E: Quantitation of specific phospho-JNK in MDA-MB-468, MCF10A, vSrc NIH-3T3, and NIH-3T3 cells upon p190 overexpression. Cells were treated as described in A and the ratio of pJNK to JKN was determined. Results are expressed as the mean fold over Mock treatment, +/- SEM, n>3. *=$p<0.05$ as compared to Mock. Solid line=transformed cells, dashed line=non-transformed cells.

were transiently transfected with HA-p190, and 48 hrs later the levels of Mcl-1 and the three isoforms of Bim were assessed by Western blot analysis. As seen in Fig. 27A a significant decrease in Mcl-1 was seen upon p190 overexpression, suggesting that p190-induced apoptosis may be mediated through Mcl-1 inactivation.

Bim has three isoforms, Bim_{EL}, Bim_L, and Bim_S. While Bim_{EL} is the most abundant, it may be a precursor for the more toxic isoforms, Bim_L and Bim_S (Ewings et al., 2007; Weston et al., 2003). Figure 27A shows that p190 overexpression slightly decreased the levels of Bim_{EL}, which corresponded to increased levels of the cytotoxic isoforms, Bim_L and Bim_S, as compared to mock-transfected cells. Together these data suggest that p190-induced apoptosis increases Bim_L and Bim_S levels, while decreasing the levels of the anti-apoptotic protein, Mcl-1. Both of these events promote release of cytochrome c from the mitochondria and caspase-3 cleavage, a cellular response of p190 overexpression (Chapter 3). Results shown in Figures 26 and 27, thus, provide a possible mechanism for p190-induced apoptosis.

DISCUSSION:

RhoGTPases have been implicated in the progression and metastasis of multiple tumor types (Karlsson et al., 2009). Unfortunately, targeting this pathway has proven difficult, due to both the regulation of RhoGTPases and the complexity of the downstream signaling pathways involved. Prolonged inhibition of Rho results in apoptosis; however, how a cell activates this process, and the mechanisms involved in regulating this response are still poorly defined. To validate the Rho pathway as a cancer

Figure 27

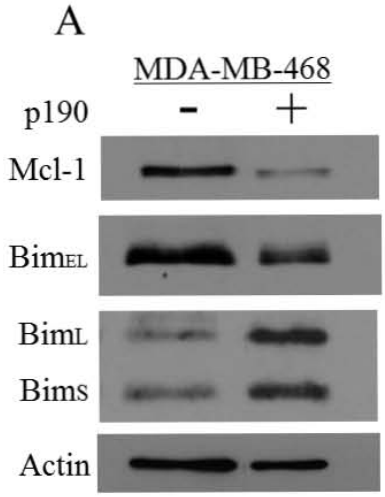

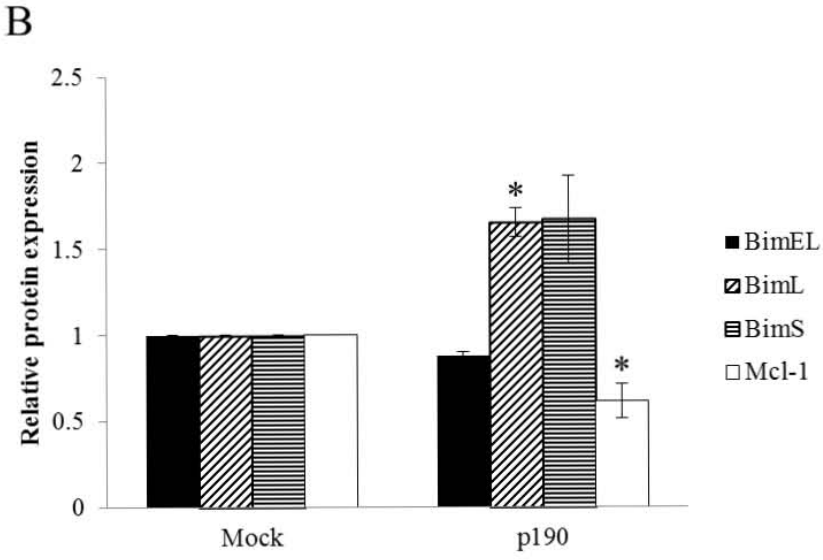

C. Kelley

Figure 27: p190 overexpression activates Bim and Mcl-1.

A: Western blot of Bim and Mcl-1 expression. MDA-MB-468 cells were mock transfected or transfected with HA-p190 and lysed 48 hrs later. Cell extracts were subjected to Western blot analysis as described in Materials and Methods to determine expression levels of Bim_{EL}, Bim_{L}, Bim_{S}, and Mcl-1. Western blots shown are representative of n=3

B: Quantitation of Bim_{EL}, Bim_{L}, Bim_{S}, and Mcl-1 in MDA-MB-468 cells upon p190 overexpression. Cells were treated as described in A and levels of Bim_{EL}, Bim_{L}, Bim_{S}, and Mcl-1 were normalized to Actin. Results are expressed as the mean fold levels of indicated protein over Mock treatment, +/- SEM, n=3. *=$p<0.05$ as compared to Mock.

target, a better understanding of the regulators and activators involved in Rho-induced apoptosis is needed.

p190RhoGAP, a negative regulator of Rho, induces apoptosis in both transformed and non-transformed cells upon overexpression. p190-induced apoptosis is regulated through p190's down regulation of Rho and is mediated through caspase-3 cleavage (Chapter 3). Interestingly, p190 overexpression in transformed cells preferentially elicits a multinucleated phenotype due to a failure to successfully complete cytokinesis (Su et al., 2003) (Chapter 5). Conversely, p190 overexpression in non-transformed cells tends to result in dendrite-like formation. This phenotype appears to coincide with increased expression of p190, which may indicate G1 arrest. However overexpression of p190 in all cells, regardless of transformation status, ultimately results in apoptosis, suggesting that multinucleation and dendrite-like formation may be intermediate phenotypes, eventually leading to p190-induced apoptosis. (Chapter 3) This raises the possibility that different apoptotic signaling pathways are activated upon p190 overexpression in transformed and non-transformed cells. The current study was undertaken to define how p190 elicits apoptosis, and thus enhance our knowledge of Rho-induced apoptosis, as well as determine if p190 activates the same pathways in transformed and non-transformed cells alike.

Previous studies focused on characterizing the apoptotic response seen with prolonged inactivation of Rho have yielded several candidate apoptotic pathways, including p53, p38, JNK, Akt, and NF-κB. Our studies showed no significant change p53, p38 or Akt in any cell lines examined upon overexpression of p190 (Fig. 24A-D),

suggesting that these pathways are not involved in p190-induced apoptosis. However, alterations in the NF-κB and JNK pathways were observed.

Figure 25 shows that the activity of IKB, a regulator of the NF-κB pathway, was modulated upon p190 overexpression, suggesting that this pathway may function in p190-induced apoptosis. Interestingly, the level of IKB activity was dependent upon the transformation status of the cell, similar to the secondary phenotypes of p190 overexpression. IKB phosphorylation increased in response to elevated p190 expression in transformed cells, which correlated with decreased levels of IKB. However, decreased pIKB was observed in non-transformed cells. IKB binds and sequesters NF-κB in the cytoplasm. Phosphorylation and degradation of IKB releases NF-κB, allowing it to translocate to the nucleus where it can bind κB DNA binding sites and promote transcription of a variety of proteins such as the caspase inhibitors, c-IAP1, c-IAP2, XIAP, and c-FLIP (Kucharczak et al., 2003). NF-κB also promotes transcription of the anti-apoptotic Bcl-2 proteins, Bcl-2, Bcl-X_L, and Bfl-1. (Bakkar and Guttridge, 2010) Interestingly, NF-κB has been reported to promote expression of apoptotic proteins as well. From as early as 1998, NF-κB has been implicated in the transcription of FasL, TRAIL, Fas, DR4-6, p53, and the pro-apoptotic protein Bcl-X_S (Bakkar and Guttridge, 2010). Since NF-κB can enhance expression of pro-apoptotic proteins, it is possible that the increase in IKB phosphorylation and the corresponding decrease in its protein levels that we see in transformed cells could signify promotion of cell death. In support of this notion, NF-κB activation has been reported to induce apoptosis in T cells (Kasibhatla et

al., 1999; Lin et al., 1999; Zheng et al., 2001) and rat neuronal cells (Barkett and Gilmore, 1999).

However, an increase in the NF-κB pathway could also signify a protective response by the cell to apoptotic stimuli, similar to that seen upon TNF-α treatment. NF-κB activity increases after treatment of TNF-α, and for many years this was believed to be a pro-apoptotic response. However, experiments in fibroblast and macrophages showed that cells with mutant NF-κB were more sensitive to TNFα treatment and died within 8 hrs, whereas wild type cells normally survived treatment (Beg and Baltimore, 1996). These and similar experiments with silencing or inhibition of the NF-κB pathway indicate that NF-κB is activated to increase pro-survival proteins in an attempt to prevent apoptosis (Baichwal and Baeuerle, 1997). Therefore, the decrease in IKB levels seen upon p190 overexpression, which indicate activation of the NF-κB pathway, could represent a survival response. Which proteins will be up-regulated upon NF-κB activation, are not completely understood. It has been suggested that recruitment of different transcriptional co-factors determine whether NF-κB will promote transcription of pro-survival or pro-apoptotic proteins (Barkett and Gilmore, 1999). Another theory is that different subunits of NF-κB may have differential effects on the expression pattern regulated by NF-κB. In either case, p190 overexpression clearly induces degradation of IKB in transformed cells, which is hypothesized to promote translocation of NF-κB to the nucleus. The ultimate biological outcome of this event, and how it affects p190-induced apoptosis in transformed cells remains to be determined; however, there is clearly an effect of p190 on IKB itself, which suggests an involvement of the NF-κB pathway.

Conversely, p190 overexpression in non-transformed cells decreased IKB phosphorylation and increased expression of the protein, suggesting stability of the IKB/NF-κB complex and sequestration of NF-κB from the nucleus (Fig. 25B, D & E). This inactivation would result in a decrease in the pro-survival factors normally controlled by NF-κB and eventually lead to apoptosis. Indeed, inhibition of NF-κB in a variety of cell types results in apoptosis, primarily through a decrease in the anti-apoptotic proteins Bcl-2, Bcl-X_L, and Bfl-1 (Bakkar and Guttridge, 2010; Kucharczak et al., 2003; Namba et al., 2007). Such studies would indicate that p190-induced apoptosis in non-transformed cells may be due to a decrease in expression of pro-survival factors regulated by NF-κB. In support of this hypothesis, some studies suggest that Rho activation may promote degradation of IKB and NF-κB translocation to the nucleus (Cowell et al., 2009; Riganti et al., 2008; Shimada and Rajagopalan, 2010; Wang and Kitajima, 2007). Through Rho's activation of ROCK (Shimada and Rajagopalan, 2010; Wang and Kitajima, 2007), both IKB and NF-κB are phosphorylated, either directly, or indirectly through the Akt pathway (Cowell et al., 2009). This phosphorylation leads to activation of the NF-κB pathway and increased expression of pro-survival proteins. In this way p190 overexpression could decrease Rho and ROCK activation and result in stabilization of the IKB protein and decreased NF-κB signaling.

Additionally, NF-κB can regulate expression of cyclins D and E, important mediators of G1 progression. p190 overexpression in non-transformed cells therefore, could decrease levels of cyclin D or E through NF-κB regulation and induce a G1 block. As discussed in Chapter 3, a G1 block would prevent p190 degradation, resulting in p190

accumulation, the dendritic phenotype, and ultimately cell death. In fact, knockdown of certain subunits of NF-κB from B cells results in G1 arrest (Hsia et al., 2002; Kontgen et al., 1995; Pohl et al., 2002). Together these data suggest that in non-transformed cells, p190 overexpression decreases IKB. This inhibition may decrease cyclin D expression and induce a G1 arrest, resulting in the dendrite-like phenotype. Decreased NF-κB signaling would also result in decreased levels of pro-survival proteins and caspase inhibitors, ultimately leading to apoptosis.

Chapter 3 revealed that p190 overexpression can sensitize cells to docetaxel-induced apoptosis. Taxane treatment, either with paclitaxel or docetaxel, also induces activation of the NF-κB pathway (Huang et al., 2002; Huang et al., 2000; Kubo et al., 2005), a phenomenon similar to that seen with p190 overexpression in transformed cells. This increase in activation is most likely a pro-survival response, as inhibition of the pathway can increase taxol-induced apoptosis (Kang et al., 2009; Lee et al., 2009; Zhang et al., 2009). This latter result would suggest that the degradation of IKB induced by p190 overexpression in transformed cells may be a pro-survival. This response differs from non-transformed cells where the NF-κB pathway may play an active role in p190-induced apoptosis by decreasing expression of pro-survival proteins as a result of decreased Rho-ROCK activation. Interestingly, NF-κB may also be differentially activated in response to taxane treatment in transformed vs. non-transformed cells. IKB and NF-κB phosphorylation, NF-κB localization to the nucleus, and NF-κB DNA binding are all decreased in non-transformed cells (Bava et al., 2005; Li et al., 2010; Spencer et al., 1999). All together, these data suggest that the NF-κB pathway may be responsible

for the differential effects of p190 overexpression in transformed vs. non-transformed cells, in that the pathway has a direct role in p190-induced apoptosis in non-transformed cells, and an in-direct role in transformed cells. These data also strengthen the connection between the p190-Rho pathway and docetaxel-induced apoptosis.

In addition to the NF-κB pathway, p190 overexpression also activated JNK. In both transformed and non-transformed cells JNK activity increased at all time points examined (Fig. 25), suggesting that JNK may be involved in p190-induced apoptosis in both of these cell types. It is well-established that JNK can be activated by both Rac1 and Cdc42 (Coso et al., 1995; Keshet and Seger, 2010). As was discussed in Chapter 1, the activation of RhoGTPase proteins is often inversely related, meaning that a decrease in Rho activation often results in an increase in Rac1 and Cdc42 activation (Bustos et al., 2008; Pestonjamasp et al., 2006; Rosenfeldt et al., 2006). This inverse relationship may be responsible for the increase in JNK activity resulting from Rac1 and Cdc42 activation.

JNK can initiate apoptosis by phosphorylating and activating the pro-apoptotic protein Bim (Hubner et al., 2008; Lei and Davis, 2003). In concordance with these reports, increases in both Bim_L and Bim_S levels were found in MDA-MB-468 cells after 48 hrs of p190 overexpression (Fig. 4A-C). Bim_L and Bim_S are the more cytotoxic isoforms of Bim, and evidence suggests that BimEL may be a precursor to Bim_L and Bim_S (Ewings et al., 2007; Weston et al., 2003), thus explaining the slight decrease in Bim_{EL} seen with p190 overexpression.

In addition, expression levels of the anti-apoptotic protein, Mcl-1, decreased upon overexpression of p190, a response similar to that seen upon taxol treatment (Jazirehi and

Bonavida, 2004). While controversial, several studies indicate that JNK phosphorylation of Mcl-1 ultimately results in its degradation (Wertz et al., 2011; Yu et al., 2001). Inhibition of this phosphorylation prevents Mcl-1 degradation and confers taxol resistance to cells (Wertz et al., 2011). Together, our preliminary results suggest that p190-induced apoptosis may also be mediated through a JNK-Bim/Mcl-1 pathway, although more studies need to be done to both validate and clarify this pathway.

Finally, it is important to note that the JNK and NF-κB pathways can regulate one another. It is well established that activation of the NF-κB pathway can inhibit JNK activation, although most of these studies are in response to TNF-α treatment (Kucharczak et al., 2003; Namba et al., 2007). However, it is possible that such a cross-talk exists in non-transformed cells, whereby decreased NF-κB activity promotes increased activation of JNK, whose activity is normally repressed under healthy conditions. In this way, the signal initiating from NF-κB could differentiate the apoptotic signal from JNK seen in transformed vs. non-transformed cells. However, currently we have no evidence for this type of interaction in our system, and more studies are needed to determine if NF-κB repression promotes or allows JNK-induced apoptosis in non-transformed cells.

Together, the data in this Chapter suggest that p190-induced apoptosis may be mediated through a JNK-Bim/Mcl-1 pathway in all cells; however, the NF-κB pathway may play a role in the differential responses seen in transformed and non-transformed cells. While all of these results are preliminary and no strong conclusions can be drawn,

these pathways are now implicated and provide a starting ground for further experimentation.

CHAPTER 5

Regulation of pMLC II and Anillin in Cytokinesis by p190RhoGAP

Chapter 5:
Regulation of pMLC II and Anillin in Cytokinesis by p190RhoGAP

INTRODUCTION:

Cytokinesis is the final step in cell division where ingression of the cleavage furrow results in separation of two daughter cells. The process initiates in anaphase, continues throughout telophase when membrane invagination at the equatorial cell cortex occurs, and is completed upon membrane abscission (Glotzer, 2001). The contractile forces required for furrow ingression are provided by a ring of filamentous actin and myosin II that is juxtaposed to the cell membrane at the equator of the dividing cell. Assembly and regulation of this contractile ring is critical for achieving proper cell division, which is under the control of the small GTPase RhoA (Piekny et al., 2005).

As described in the overall Introduction to this dissertation, RhoA is a molecular switch that cycles between active (GTP-bound) and inactive (GDP-bound) states. Transitions between activation states are facilitated by GEFs (activators), GAPs (inactivators), and GDIs (inactivators). RhoA localizes to the cleavage furrow formation site (Nishimura et al., 1998; Takaishi et al., 1995), and inhibition of RhoA activity prevents cleavage furrow formation (Kishi et al., 1993; Mabuchi et al., 1993). During the latter stages of mitosis, RhoGTP levels increase at the contractile ring (Kimura et al., 2000; Maddox and Burridge, 2003; Yoshizaki et al., 2004). This increase in is necessary for cleavage furrow formation and contraction (Bement et al., 2005; Bement et al., 2006; Su et al., 2009), suggesting that increased Rho activity at the equatorial midzone during cytokinesis is required for cell division.

Active RhoA mediates contractile ring assembly through its downstream effectors, mDia2, ROCK and Citron Kinase (Piekny et al., 2005). mDia2 functions as an actin nucleator that induces the polymerization of long, unbranched actin filaments (Watanabe et al., 2008), along with microtubule alignment and stabilization (Narumiya and Yasuda, 2006). ROCK and citron kinase both activate the contractile mechanism of myosin II by phosphorylating Ser19 of the regulatory light chain of myosin II (MLC II) (Matsumura, 2005). Upon phosphorylation of Ser19 on MLC II, myosin II crosslinks with newly created actin filaments to form a fully functional contractile ring (Vavylonis et al., 2008; Wu et al., 2006). Activation of MLC II triggers its motor activity and provides the mechanical force required for furrow contraction and ingression (Bresnick, 1999).

Actomyosin filaments are assembled on a network of cytoskeletal proteins at the cell cortex that act as a scaffold and connect the filaments to the plasma membrane. Anillin, an actin-binding protein of 120kDa in mass, is a crucial component of this scaffold and is required for cytokinesis (Oegema et al., 2000; Zhao and Fang, 2005b). Anillin has been shown to interact with actin, myosin II, microtubules, mDia, Ect2, MgcRacGAP, and RhoA (Piekny and Maddox, 2010). Additionally, overexpression of anillin increases Rho activation, suggesting that anillin functions in the regulation of Rho during cytokinesis (Suzuki et al., 2005). Together, these findings support the conclusion that anillin plays a vital role in linking the structural components of the contractile ring to Rho-regulated signaling proteins and events that govern cytokinesis.

In addition to Rho and anillin, a number of other proteins are involved in the regulation of cytokinesis. Microtubules form the mitotic spindle that provides the framework for chromosome segregation and the signals for positioning of the cleavage furrow formation site at the equatorial midzone, thereby directing contractile ring formation (Bement et al., 2005). Aurora B, as a member of the chromosomal passenger complex (CPC), is essential for assembly and stability of the bipolar mitotic spindle, chromosome-kinetochore attachment and chromosome segregation through its regulation of the spindle assembly checkpoint (SAC) (Ruchaud et al., 2007). Moreover, through its interactions with the centralspindlin complex, Aurora B mediates the recruitment of the RhoGEF Ect2 to the cleavage furrow where it activates RhoA, initiating the downstream signaling pathways that direct contractile ring establishment and function (Zhao and Fang, 2005a).

In opposition to Ect2's activity at the cleavage furrow is p190RhoGAP (p190), a negative regulator of RhoGTP activity (Ludwig et al., 2009). p190 localizes to the cleavage furrow during cytokinesis where it associates with Ect2 (Mikawa et al., 2008). Because of the cyclical nature of RhoA activation, this paradoxical association between Rho's activating and inactivating enzymes is important for the careful regulation of RhoGTP levels needed for cell division. Furthermore, proteasome-dependent degradation of p190 in late mitosis provides an additional mechanism by which the necessary increase in RhoGTP levels is achieved (Manchinelly et al., 2010; Su et al., 2003). Overexpression of p190 therefore results in decreased RhoGTP levels at the cleavage furrow and multinucleation, a phenotype indicative of cytokinesis failure (Su et

al., 2009). However, the mechanism of p190 action and identification of which components of the contractile ring are affected by p190 are unknown.

Thus, a greater understanding of RhoA regulation and its effect on downstream targets is required before the complex nature of cytokinesis is clearly revealed. Here, we use a p190 overexpression approach to test its effect on cytokinesis and identify affected downstream Rho effectors or pathways. In this study, we show that p190 overexpression results in decreased cleavage furrow localization of anillin and activated myosin II, the latter determined by decreased phosphorylation of its regulatory light chain (pMLC II) at Ser19. We also find that p190 and anillin co-localize during cytokinesis, and that anillin is required for p190 localization to the cleavage furrow. Moreover, we report that endogenous p190 interacts with endogenous anillin in mitotic cell extracts in a contractility-dependent fashion, providing clues to their potential involvement in a contractility pathway that can regulate anillin association with p190, localize both anillin and p190 to the cleavage furrow, and ultimately regulate the activation status of Rho in the cleavage furrow and successful completion of cytokinesis.

RESULTS:

Overexpression of p190 does not affect the cytokinetic localization of RhoA, Actin, Aurora B or Microtubules.

Successful completion of cytokinesis requires the proper localization and activation of several proteins which are critical for cell division, including RhoA, anillin, Actin, Aurora B, and microtubules. To determine the mechanism by which p190 overexpression causes cytokinesis failure and induces multinucleation, HeLa cells were

mock-transfected or transiently transfected with GFP-p190 plasmids, and the effect of this treatment on the localization of the aforementioned proteins was assessed by confocal immunofluorescence microscopy. Figure 28A-C revealed that after p190 overexpression RhoA (Panel A) and actin (Panels A-C) continued to localize to the cell cortex at the cleavage furrow, where they are normally observed after anaphase onset. Likewise, Aurora B (Panel B) localization followed its usual pattern as a chromosomal passenger complex protein, i.e., it was found associated with the metaphase plate and remained at the equator of the cell after anaphase onset, aligned with the spindle midzone, the future site of cleavage furrow formation. Microtubules also formed functional mitotic spindles and appeared unaffected by p190 overexpression (Panel C). As described in Materials and Methods, similar results were found with vector-transfected cells as described for Mock-treated cells. Together, these data indicate that p190 overexpression and its corresponding decrease in Rho activation (Su et al., 2009) does not affect the localization of mitotic RhoA, actin, Aurora B, or microtubules.

MLC activation is regulated by p190 and required for completion of cytokinesis

Examination of myosin localization revealed that p190 overexpression did not affect its ability to localize to the cleavage furrow (Fig. 29A). However, activation of myosin, as determined by phosphorylation of the regulatory light chain, was altered upon overexpression of p190 (Fig. 29B). In mock-treated and vector transfected cells, a clear enrichment of active, phosphorylated myosin light chain II (pMLC II) is found at the cleavage furrow and cortex. With overexpression of p190, the accumulation of pMLC II at both sites is abrogated. Quantification revealed that the majority (68%) of mock-

Figure 28

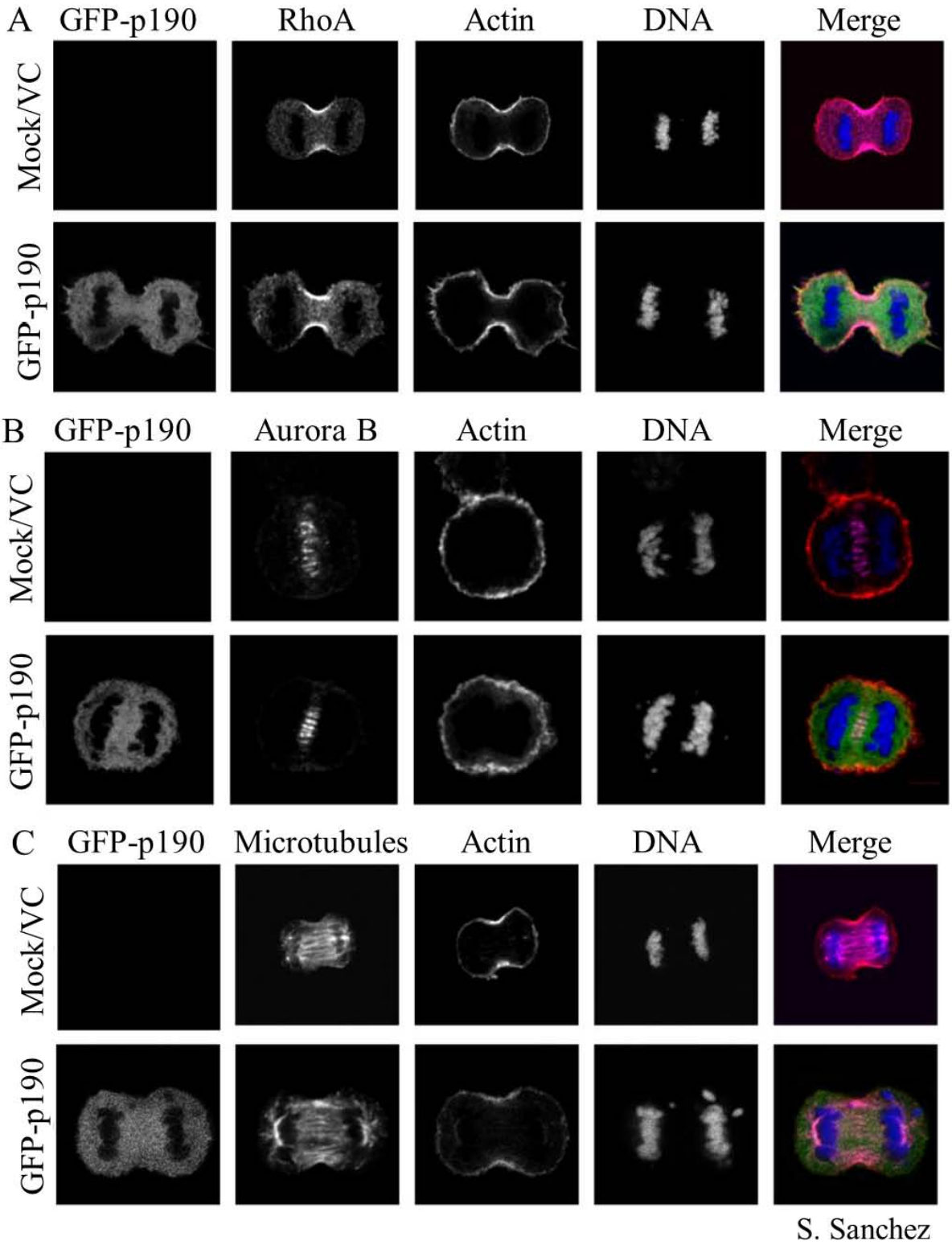

S. Sanchez

Figure 28: p190RhoGAP overexpression does not affect the cytokinetic localization of RhoA, Actin, Aurora B, or Microtubules.

Images of RhoA (A), Aurora B (B), microtubules (C) or actin (A-C) localization during cytokinesis. HeLa cells were either Mock-treated or transiently transfected with GFP-empty plasmid or GFP-p190 plasmid, synchronized with Nocodazole, fixed, and immuno-stained for the indicated proteins and DNA as described in Materials and Methods. Mock and vector only transfected cells gave similar results. Images shown are representative of n>30.

Figure 29

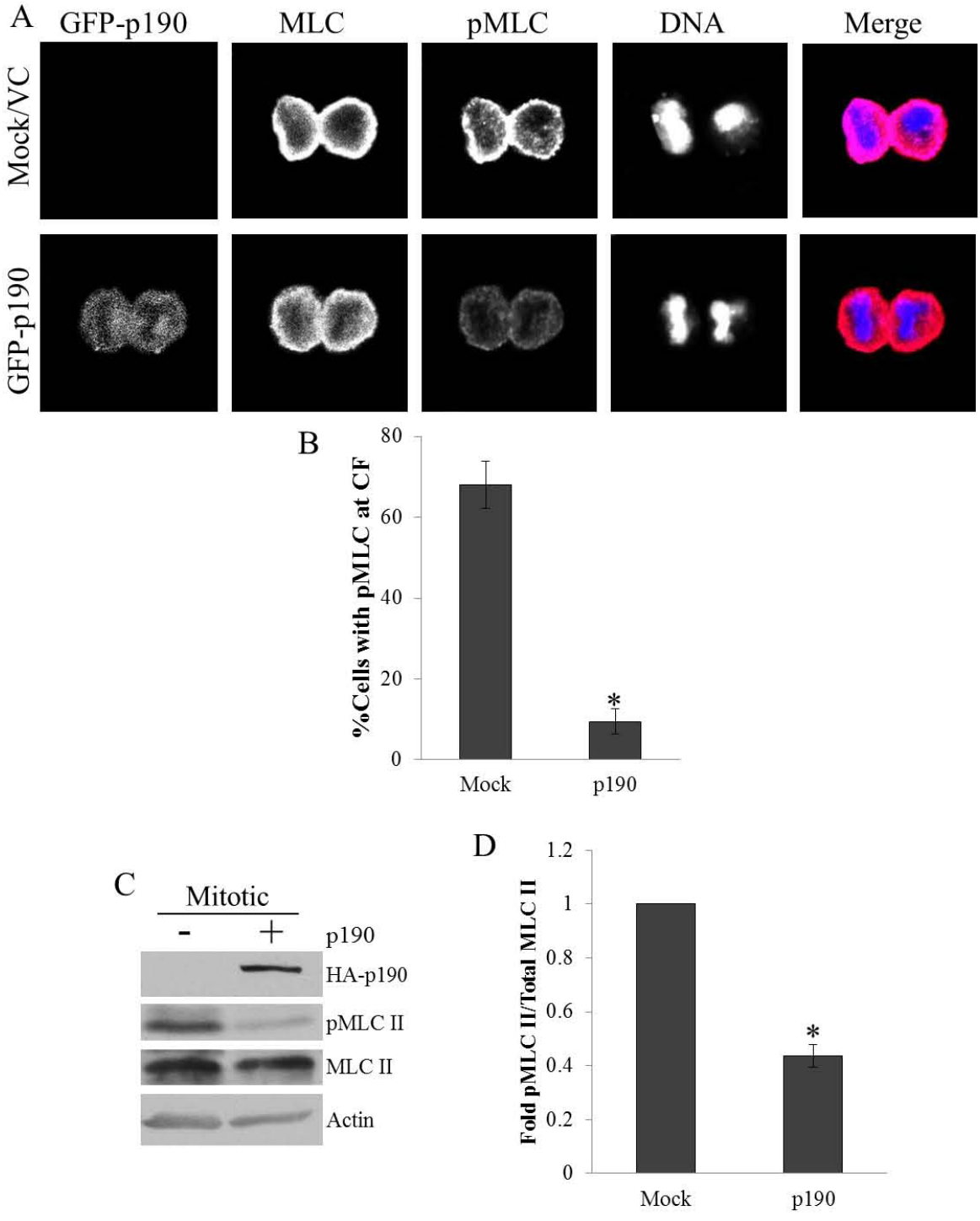
A
GFP-p190
MLC
pMLC
DNA
Merge
Mock/VC
GFP-p190
B
%Cells with pMLC at CF
80
60
40
20
0
*
Mock
p190
C
Mitotic
-
+
p190
HA-p190
pMLC II
MLC II
Actin
D
Fold pMLC II/Total MLC II
1.2
1
0.8
0.6
0.4
0.2
0
*
Mock
p190

Figure 29: p190 regulates MLC II phosphorylation in the cleavage furrow.

A: Images of total- and phospho-myosin light chain II (pMLC II) localization during cytokinesis. HeLa cells were either Mock-treated of transiently transfected with GFP-empty plasmid or GFP-p190 plasmid. Cells were synchronized with Nocodazole, fixed, and stained for total mMLC II, pMLC II, and DNA as described in Materials and Methods. Mock and vector only transfected cells gave similar results. Images shown are representative of n>30.

B: Quantitation of HeLa cells exhibiting enrichment of phospho-MLC II at the cleavage furrow during cytokinesis. Cells were prepared as above, and results are expressed as the mean percent of total cytokinetic cells (Mock) or cytokinetic cells positive for GFP-p190 with localization of phospho-MLC II at the cleavage furrow +/- SEM, n>3 with n>30 cells per experiment. *=$p<0.001$ as compared to Mock treated.

C: Western blot of total MLC II and pMLC II during cytokinesis. Mitotic populations of HeLa cells were either Mock-treated or transiently transfected with HA-p190 plasmid. Twenty four hrs post-transfection, cells were lysed and levels of total MLC II, pMLC II, and HA-p190 were assessed by Western blot analysis as described in Materials and Methods. Actin was immunoblotted as a loading control.

D: Quantitation of specific pMLC II. Total- and phospho-MLC II levels were quantified densitometrically as described in Materials and Methods and normalized to Actin. The ration of pMLC II/total MLC II was then determined and normalized to the ratio in Mock-treated cells, which was set to 1. Results are expressed as the mean fold ratio over that of Mock treated cells +/- SEM, n>3. *=$p<0.05$ as compared to Mock.

treated cells displayed enrichment of pMLC II at the cleavage furrow, while only 9.5% of p190 overexpressing cells exhibited such enrichment. Western blot analysis of mitotic cells, either mock-treated or overexpressing p190, further corroborated results obtained from confocal microscopy (Fig. 29C & D).

To determine if the decrease in pMLC II might be a mechanism by which p190 overexpression was inducing cytokinesis failure, a rescue experiment with mutationally activated MLC was conducted. HeLa cells were transfected with p190, a constitutively active form of MLC (CA MLC), or the two together, and scored for cytokinesis failure as assessed by multinucleation. This form of MLC has phospho-mimetic residues at threonine 18 and serine 19, resulting in constant activation (Vicente-Manzanares et al., 2009). Figure 30 shows that p190 overexpression alone induced cytokinetic failure (Panel A, image b & Panel B), while CA MLC alone did not (Panel A, image c & Panel B). However, concomitant overexpression of p190 and CA MLC reduced p190-induced multinucleation (Panel A, images d-f & Panel B), suggesting that p190-regulated MLC activation is required for completion of cytokinesis. Together, these results indicate that a potential mechanism by which p190 overexpression causes cytokinesis failure is by decreasing the phosphorylation levels of MLC II at the cleavage furrow and cortex, thus inactivating the molecular motor of myosin II and inhibiting initiation and/or sustained contractility.

p190 and anillin regulate each other's localization

As a molecular scaffold, anillin creates a molecular complex where effector and substrate proteins are placed within close proximity to one another, allowing for efficient

Figure 30

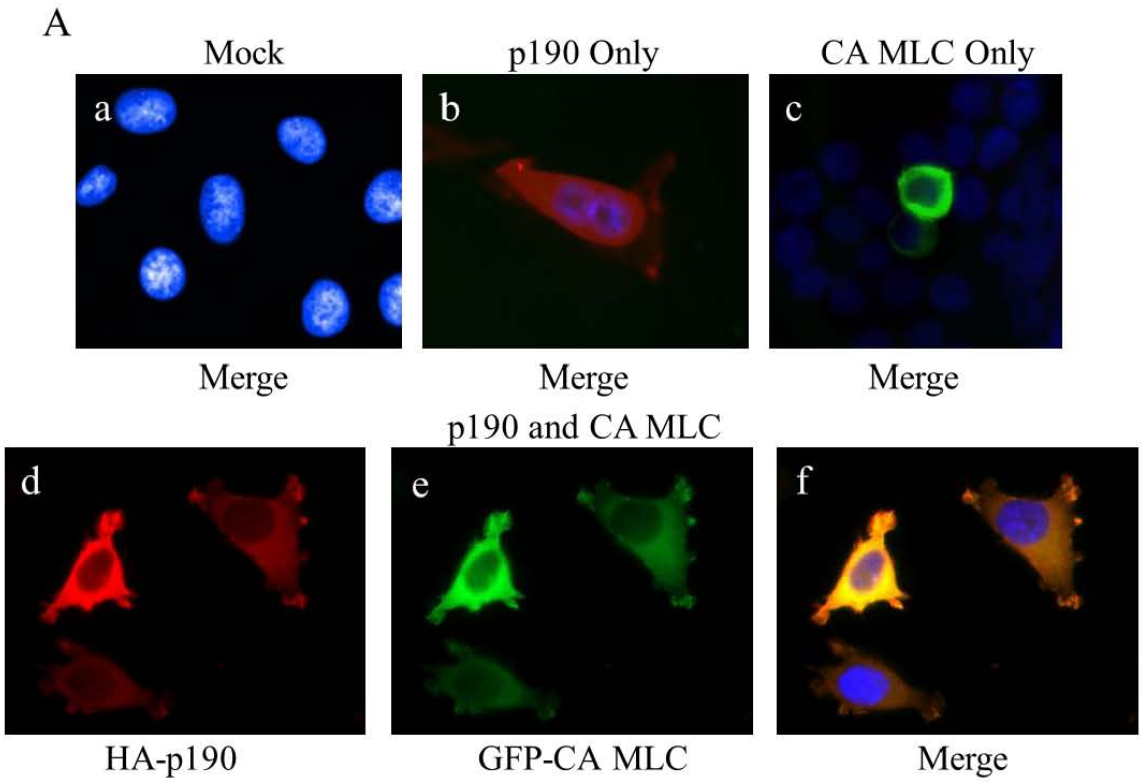
A
Mock
p190 Only
CA MLC Only
a
b
c
Merge
Merge
Merge
p190 and CA MLC
d
e
f
HA-p190
GFP-CA MLC
Merge

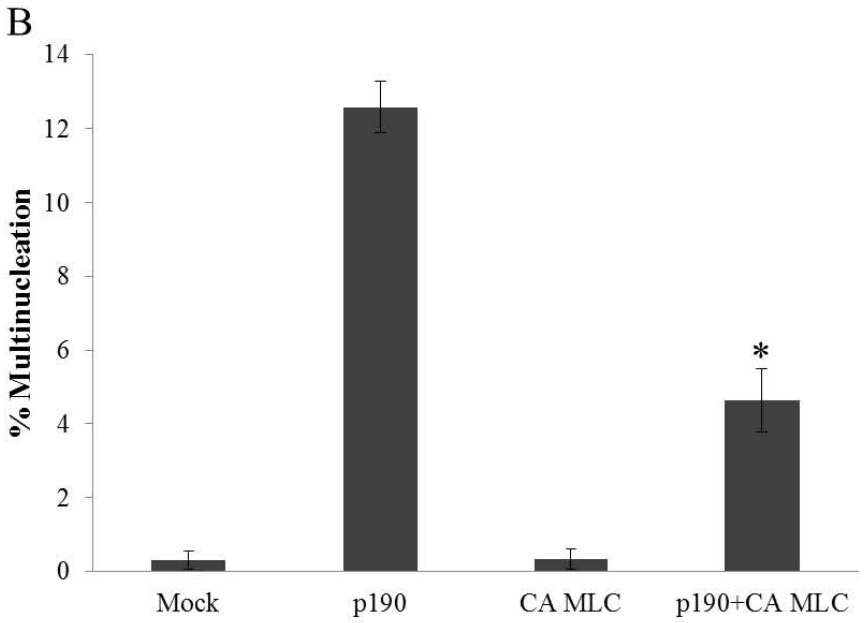
B
% Multinucleation
14
12
10
8
6
4
2
0
*
Mock
p190
CA MLC
p190+CA MLC

Figure 30: p190 mediates its effects on cytokinesis through pMLC II.

A: Images of HeLa cells Mock-treated or transiently transfected with HA-p190 or constitutively active (CA) MLC II plasmids singly or in combination. Molar equivalents of plasmid were transfected, levels being augmented with empty vector where appropriate. Merged, representative images are shown of Mock-treated DNA alone (a), HA-p190 (b), and CA MLC II (c) single transfections. HA-p190 (d), CA MLC II (e), and Merge (f) images are shown of the dual transfection. Forty-eight hrs after transfection cells were fixed and stained as described in Materials and Methods. Images shown are representative of n=3.

B: CA MLC II rescues p190-induced multinucleation. HeLa cells were prepared as described above, and the occurrence of multinucleation was assessed by immunofluorescence. Results are expressed as the mean percent total cells (Mock) or cells positive for HA-p190 and or CA MLC II that were multinucleated +/- SEM, $n>3$ with $n>100$ cells per experiment. *=$p<0.005$ as compared to Mock-treated.

completion of cytokinesis (Piekny and Glotzer, 2008). While anillin is a well-established scaffold protein, its role in recruiting proteins to the cleavage furrow is still unclear. For example, anillin regulates localization of Rho to the cleavage furrow, as exemplified by mislocalization of Rho upon knockdown of anillin. However, by an unknown mechanism, active Rho is also required for anillin localization to the cleavage furrow, as determined by anillin mislocalization silencing of either Rho or Ect2 (Piekny and Glotzer, 2008). This finding suggests that a feedback mechanism may be involved, wherein Rho-dependent signals may feedback to anillin, thus affecting anillins localization. Because anillin performs such an essential role in cytokinesis, and Rho activity is required for proper anillin localization, we examined whether p190 overexpression in HeLa cells affected anillin localization to the cleavage furrow by confocal microscopy imaging. Figure 31A-B demonstrate that p190 overexpression resulted in a decrease in anillin localization to the cleavage furrow in approximately 42% of p190 overexpressing cells as compared to mock-treated or vector transfected cells, suggesting that p190 may play a role in Rho-regulated anillin localization to the cleavage furrow.

That Rho affects localization of anillin to the cleavage furrow is well documented; however, the effect of p190 on anillin's localization remains unclear. Figure 32 shows confocal images of endogenous anillin and p190 at all stages of cytokinesis. Results reveal that both proteins co-localize at the cleavage furrow throughout cytokinesis. However, silencing of anillin with siRNA resulted in a mislocalization of p190 (Fig. 33), and ultimately failure of cytokinesis (Straight et al., 2005; Zhao and Fang, 2005a)

Figure 31

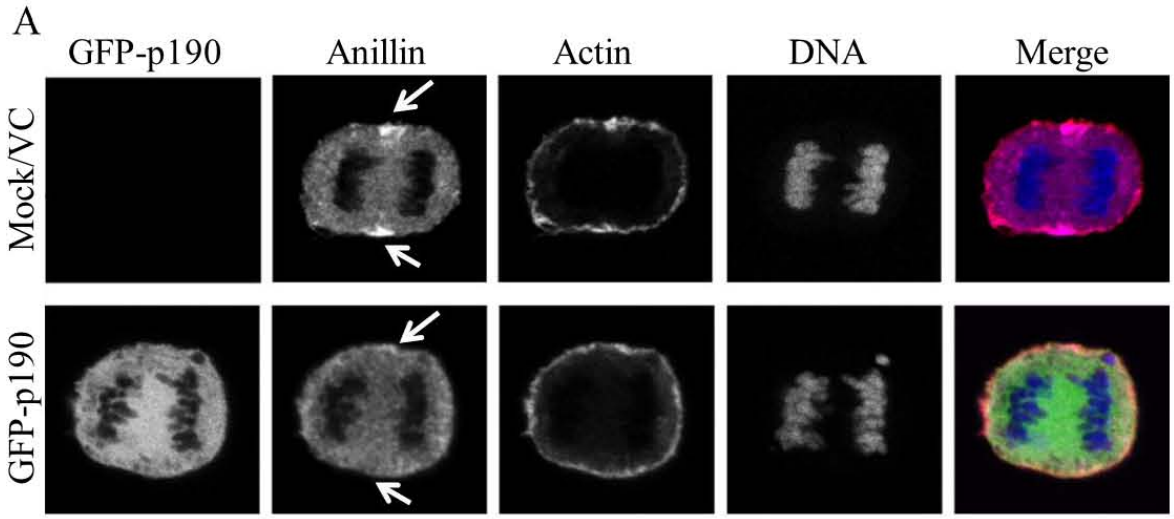

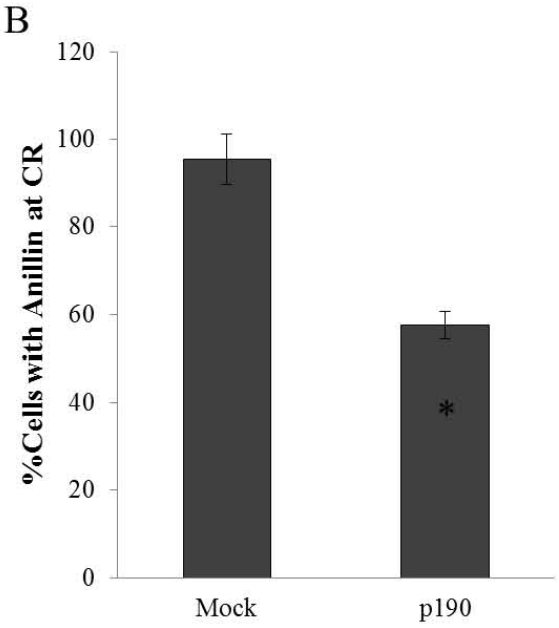

S. Sanchez

Figure 31: p190 overexpression reduces localization of anillin to the cleavage furrow.

A: Images of anillin and actin localization during cytokinesis. HeLa cells were either Mock-treated or transiently transfected with GFP-empty plasmid or GFP-p190 plasmid. Cells were synchronized with Nocodazole, fixed, and stained for anillin, actin, and DNA as described in Materials and Methods. Mock and vector only transfected cells gave similar results. Images shown are representative of $n>30$.

B: Quantitation of HeLa cells with anillin accumulation at the cleavage furrow during cytokinesis. Cells were prepared as above, and results are expressed as the mean percent of total cytokinetic cells (Mock) or cytokinetic cells positive for GFP-p190 with anillin accumulation at the cleavage furrow +/- SEM, $n=6$, with $n>5$ cells per experiment. *=$p<0.001$ as compared to Mock-treated.

Figure 32

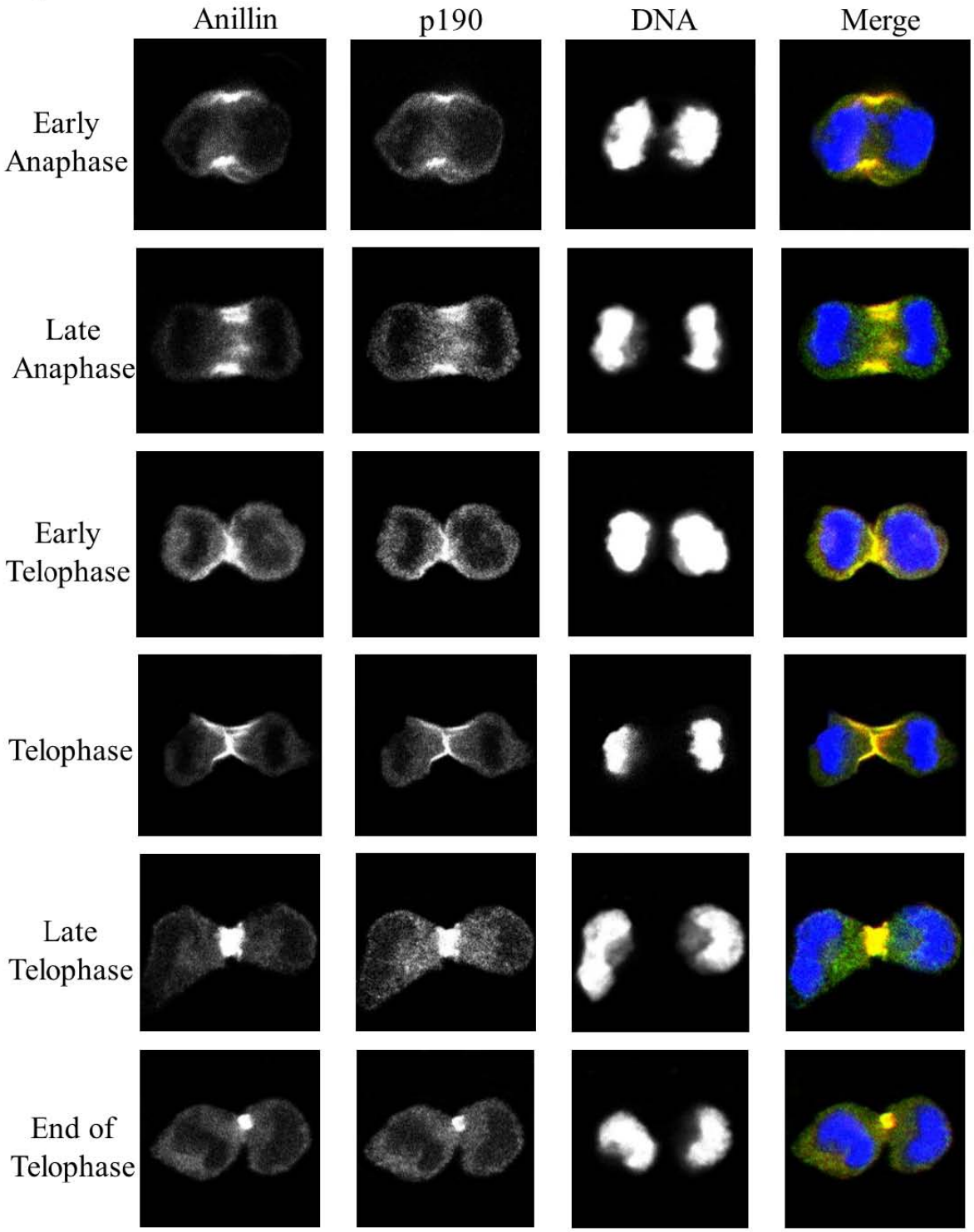
Anillin
p190
DNA
Merge
Early Anaphase
Late Anaphase
Early Telophase
Telophase
Late Telophase
End of Telophase

Figure 32: p190 and anillin co-localize during cytokinesis.

Images of p190 and anillin during each stage of cytokinesis. HeLa cells were fixed and stained for endogenous p190, endogenous anillin, and DNA as described in Materials and Methods. Confocal images were captured of cells at all stages of cytokinesis. Images shown are representative of n>30.

Figure 33

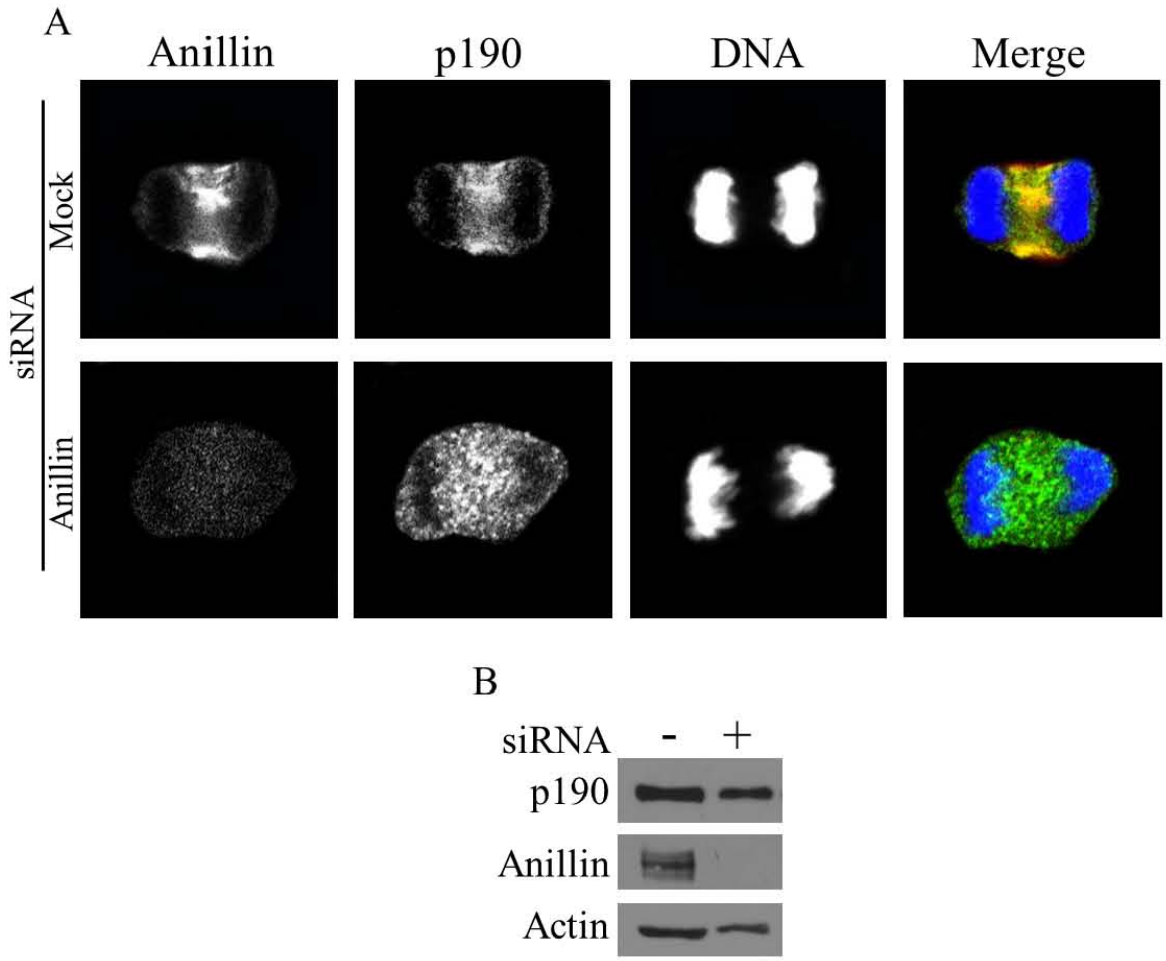
A
Anillin
p190
DNA
Merge
siRNA
Mock
Anillin
B
siRNA - +
p190
Anillin
Actin

Figure 33: Anillin is required for p190 localization to the cleavage furrow.

A: Images of p190 and anillin during cytokinesis. Anillin was silenced by siRNA transfection of HeLa cells as described in Materials and Methods. Thirty-six hrs later, cells were fixed and stained for endogenous p190, endogenous anillin, and DNA as described in Materials and Methods. Images shown are representative of n>30.

B: Western blot of anillin silencing. HeLa cells were treated as described in A, lysed, and subjected to Western blot analysis.

and (data not shown), suggesting that anillin mediates p190's localization during cytokinesis, which is known to be required for cytokinetic completion (Manchinelly et al., 2010). Together, these results from figures 32 and 33 suggest that p190 and anillin regulate each other's localization to the cleavage furrow, similar to Rho and anillin. Since anillin and p190 play crucial roles during cytokinesis, the feedback mechanism between these two proteins has the potential for significant effects on cytokinesis.

The association between anillin and p190 is contractility dependent

Anillin also binds both actin and myosin and is thought to increase the interaction between the cytoskeletal components responsible for cleavage furrow contraction (Piekny and Maddox, 2010). In this way anillin is postulated to act as a "contractility organizer". We hypothesized that because p190 and anillin regulate localization of one another at the cleavage furrow, this regulation could be mediated through a potential interaction between the two proteins. Such a possibility was examined by co-immunoprecipitation of endogenous proteins in asynchronous and mitotic HeLa cells. Figure 34 revealed that endogenous p190 and anillin associated in a cytokinesis-specific manner.

Biochemical signals provided by increased RhoGTP levels initiate the contractile deformation of the cleavage furrow that permits progression through cytokinesis and eventual cell division. To avoid errors in the process, a feedback mechanism has been proposed that involves pMLC II (Effler et al., 2007). Because p190 negatively regulates RhoA (Su et al., 2009) and myosin II activity at the cleavage furrow (Fig. 29) and endogenously associates with anillin during mitosis (Fig. 32), we hypothesized that the p190-anillin interaction could be involved in a contractility feedback loop and may be

Figure 34

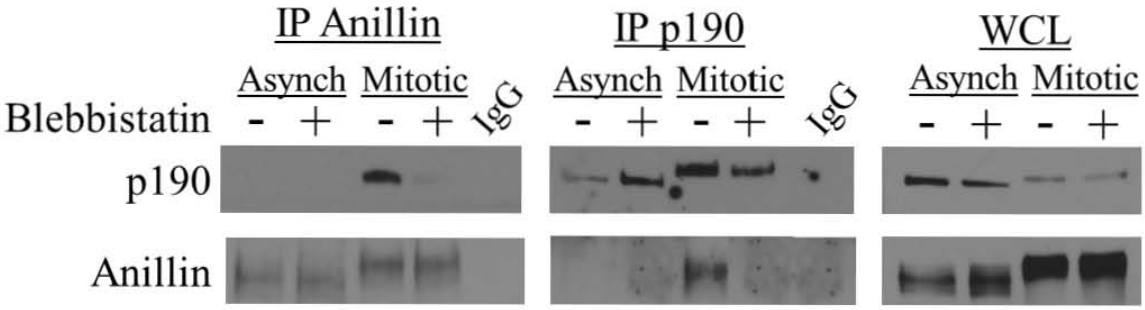
IP Anillin
IP p190
WCL
Asynch
Mitotic
IgG
Asynch
Mitotic
IgG
Asynch
Mitotic
Blebbistatin
- + - + - + - + - + - +
p190
Anillin

Figure 34: Contractility regulates association between anillin and p190 during cytokinesis.

Immunoprecipitation of anillin and p190 in Asynchronous or mitotic HeLa cells. HeLa cells were either untreated or synchronized with Nocodazole. Each mitotic or asynchronous group was then either mock-treated or treated with 50 μM of blebbistatin for 40 min to inhibit myosin association with actin. Immunoprecipitations (IPs) were performed as described in Materials and Methods, with anti-rabbit IgG as a negative antibody control. Extracts were subjected to Western blot analysis and levels of endogenous p190 and anillin were detected. Western blots shown are representative of n>3. WCL=Whole cell lysate.

sensitive to perturbations in contractility. To test this hypothesis we disrupted the contractile forces required for ingression of the cleavage furrow by treating synchronized HeLa cells with the myosin II inhibitor blebbistatin, and determining if the p190-anillin complex was affected. Figure 34 shows that the interaction between p190 and anillin was lost when contractility was decreased by blebbistatin treatment. Together, these results show that p190 is capable of disrupting anillin localization, possibly through p190-anillin complex formation. Furthermore, the sensitivity of this association to blebbistatin suggests that the p190-anillin complex may be part of a feedback mechanism that regulates contractile forces in the cleavage furrow through the modulation of RhoGTP levels and myosin II activation. That blebbistatin treatment is well-documented to induce multinucleation (Durcan et al., 2008) further supports this hypothesis.

DISCUSSION:

Cytokinesis is a critical process in the cell cycle, which is regulated by numerous proteins whose mechanism of action and associations are complex. The results outlined in this report focus on one such regulator, p190RhoGAP. We report that overexpression of p190 results in decreased activity of myosin II in the cleavage furrow and cortex, as determined by a reduction in phosphorylation of myosin light chain II (pMLC II), and decreased anillin localization to the cleavage furrow during cytokinesis. We further demonstrate that p190 and anillin regulate the localization of the reciprocal protein in a possible feedback mechanism. This mechanism may be dependent upon downstream effectors of Rho, as anillin regulates Rho's accumulation in the cleavage furrow (Piekny and Glotzer, 2008), and p190 regulates Rho's activity (Mikawa et al., 2008). These

effects on Rho's downstream targets could then feed back to regulate the anillin/p190 complex and contractility.

Previous studies have shown that p190 negatively affects cytokinesis in a RhoGAP-dependent fashion (Manchinelly et al., 2010; Mikawa et al., 2008; Su et al., 2003). Throughout the years, numerous studies have confirmed the critical involvement of RhoA in cytokinesis and have shown that its inhibition results in cytokinesis failure (Kishi et al., 1993; Mabuchi et al., 1993). Many of those studies have made use of dominant negative mutants, inhibitors, and RNAi to ablate RhoA activity and analyze its role in cytokinesis (Drechsel et al., 1997; Jantsch-Plunger et al., 2000; O'Connell et al., 1999). The present study also employs a Rho-inhibitory approach but with a significant difference. First, it utilizes a naturally occurring negative regulator of Rho, p190, and second, rather than a complete inactivation, an attenuation of Rho activity is achieved by p190 overexpression. Previous work in our laboratory demonstrated, by FRET analysis, that overexpression of p190 results in decreased RhoGTP levels at the cleavage furrow during cytokinesis (Su et al., 2009) but not a complete inactivation of Rho signaling, as observed in C3 endotoxin- and Rho siRNA-treated cells.

This partial decrease affords us an opportunity to ask further questions regarding Rho signaling in cytokinesis, including which, if any, downstream effectors of Rho are more sensitive to decreased RhoGTP levels at the cleavage furrow. The primary effectors of Rho activation in cytokinesis are mDia, ROCK and Citron Kinase (Narumiya and Yasuda, 2006). mDia directs actin nucleation needed for contractile ring formation, while ROCK and Citron kinases phosphorylate MLC II, among other substrates, and thus

stimulate myosin II-dependent contractility. Our results consistently showed normal actin localization and enrichment at the cleavage furrow in cells overexpressing p190 (Fig. 28A-C), suggesting that mDia function is not significantly dampened by a decrease in RhoGTP levels during cytokinesis. However, the observation that decreased pMLC II levels occur after p190 overexpression (Fig. 29) suggests that the RhoA-activated kinases, ROCK and Citron, and their downstream pathways are more susceptible to disturbances in RhoGTP levels at the cleavage furrow. Both ROCK and Citron kinase target the same residue, Ser19, in MLC II and therefore we are unable to identify which of these two effectors is most affected upon p190 overexpression. Because overall phosphorylation levels detected by a phospho-specific antibody are decreased, it is possible that the activity or localization of both kinases is affected.

During cytokinesis, anillin concentrates at the equatorial cell cortex (Fig. 31), where it co-localizes with Rho, Ect2, actin, myosin and numerous other proteins (Piekny and Maddox, 2010). Our results indicate that overexpression of p190 affects anillin localization in nearly half of transfected cells (Fig. 31A-B). These results are in accordance with, and further support, previous studies reporting that a pool of active RhoA is necessary for proper anillin localization to the equatorial cell cortex (Piekny and Glotzer, 2008). Specifically, silencing of Ect2 prevents proper anillin localization as it results in a complete loss of RhoGTP at the cleavage furrow. As previously noted, p190 overexpression does not completely ablate RhoGTP levels but instead attenuates them. Fitting with the current model of anillin localization, the overexpression of p190 mediates a moderate decrease in RhoGTP levels during early cytokinesis which in turn results in a

concomitant increase in the number of observed anillin mislocalization events. Additionally, we show that in mock-treated cells anillin and p190 co-localize at the cleavage furrow (Fig. 31), similar to the pattern seen with anillin and Rho co-localization (Piekny and Glotzer, 2008). However, when anillin is silenced, p190 becomes dispersed throughout the cytoplasm, suggesting that anillin is required for correct localization of p190 during cytokinesis (Fig. 33).

Since both p190 and anillin localize to the cleavage furrow and both are associated with Rho, we hypothesized that p190 could be interacting with anillin. Furthermore, we believed that an interaction between the two proteins was likely, as anillin associates with numerous other cytokinesis-related proteins and serves as an anchor for the contractile ring machinery. Our results show that the endogenous proteins do interact by co-immunoprecipitation (Fig. 34) during cytokinesis, when both proteins localize to the cleavage furrow, as observed by immunofluorescence microscopy. It is possible that this interaction is a means by which p190 is localized and "anchored" at the equatorial cortex where it is then well placed to carry out its regulatory functions toward RhoGTP enriched in that zone.

Biochemical signals provided by increased RhoGTP levels initiate the contractile deformation of the cleavage furrow that permits progression through cytokinesis and eventual cell division. To ensure that membrane furrowing is proceeding appropriately, feedback mechanisms allowing correction of errors which may occur during the process are required. Such feedback mechanisms are proposed to follow changes in cell shape and contractility at the cleavage furrow and involve myosin II (Effler et al., 2007).

Anillin acts as a bridge between contractile ring structural components and the biochemical signal transducer that regulates them. In this way, anillin is well positioned to act as a convergence point between both biochemical and contractility inputs, and as such, is considered a contractility organizer. Because p190 negatively regulates RhoA (Su et al., 2009) and myosin II activity at the cleavage furrow (Fig. 29) and endogenously associates with anillin during mitosis (Fig. 34), we hypothesize that the p190-anillin interaction could be involved in a contractility feedback loop and may be sensitive to perturbations in contractility. This raises the possibility that anillin is required for p190 recruitment to the cleavage furrow. During cytokinesis, Rho signals to its downstream effectors, activating contraction of the actomyosin ring. Strong contraction signals feedback to the anillin-p190 complex, keeping the two proteins in complex and anillin localized to the cleavage furrow. However, a decrease in RhoGTP levels, due to p190 overexpression, would result in a decrease in contraction of the actomyosin ring (due to decreased myosin II activation) which feeds back to the anillin-p190 complex, possibly resulting in mis-localization of anillin. In this way anillin could mediate the localization of p190, while overexpression of p190 would result in occlusion of anillin from the cleavage furrow.

Actomyosin filaments are assembled on a network of cytoskeletal proteins at the cell cortex that act as a scaffold and connect the filaments to the plasma membrane. Anillins' interaction with a myriad of cytokinetic regulators, both cytoskeletal and signaling molecules, places it in a unique position to act as a regulator of contraction during cytokinesis (Piekny and Maddox, 2010). Contraction is achieved by active

myosin 2 “walking” along actin fibers, ultimately leading to ingression of the cleavage furrow (Matsumura, 2005). Both the polymerization of actin and the activation of myosin 2 are controlled by appropriate levels of RhoGTP (Piekny et al., 2005), which allow for completion of cytokinesis. Perturbation of RhoGTP levels, either an increase or a decrease, results in incomplete cytokinesis (Mikawa et al., 2008; Piekny et al., 2005).

Because anillin and p190 physically interact in a contractility-, cytokinetic-dependent manner, their association may be a means to detect proper or sufficient contractility of the actomyosin ring at the cleavage furrow and act in a feedback loop to regulate Rho activation. Figure 35 is a model in which optimal RhoGTP levels are ensured by the contractility sensing nature of the p190-anillin complex. During cytokinesis, RhoGTP is enriched at the cleavage furrow by specific localization of Ect2 and decreased levels of p190RhoGAP, resulting in activation of mDia, ROCK, and Citron Kinase. This in turn leads to actin polymerization and myosin II activation, allowing the cleavage furrow to contract and successfully complete cytokinesis. While contractility is strong, reduced levels of p190 that remain in mitotic cells associate with anillin at the cleavage furrow and maintain RhoGTP at biologically appropriate levels. (Fig. 35A)

However, if RhoGTP levels decrease, (as in the case of p190 overexpression) a cascade of events are initiated that ultimately result in a decrease in actin polymerization and myosin activation. This event would result in a decrease in the contractility forces of the cleavage furrow, incomplete cytokinesis, and onset of multinucleation. In such a situation, weak contractility forces would feedback to the p190-anillin association,

Figure 35

A

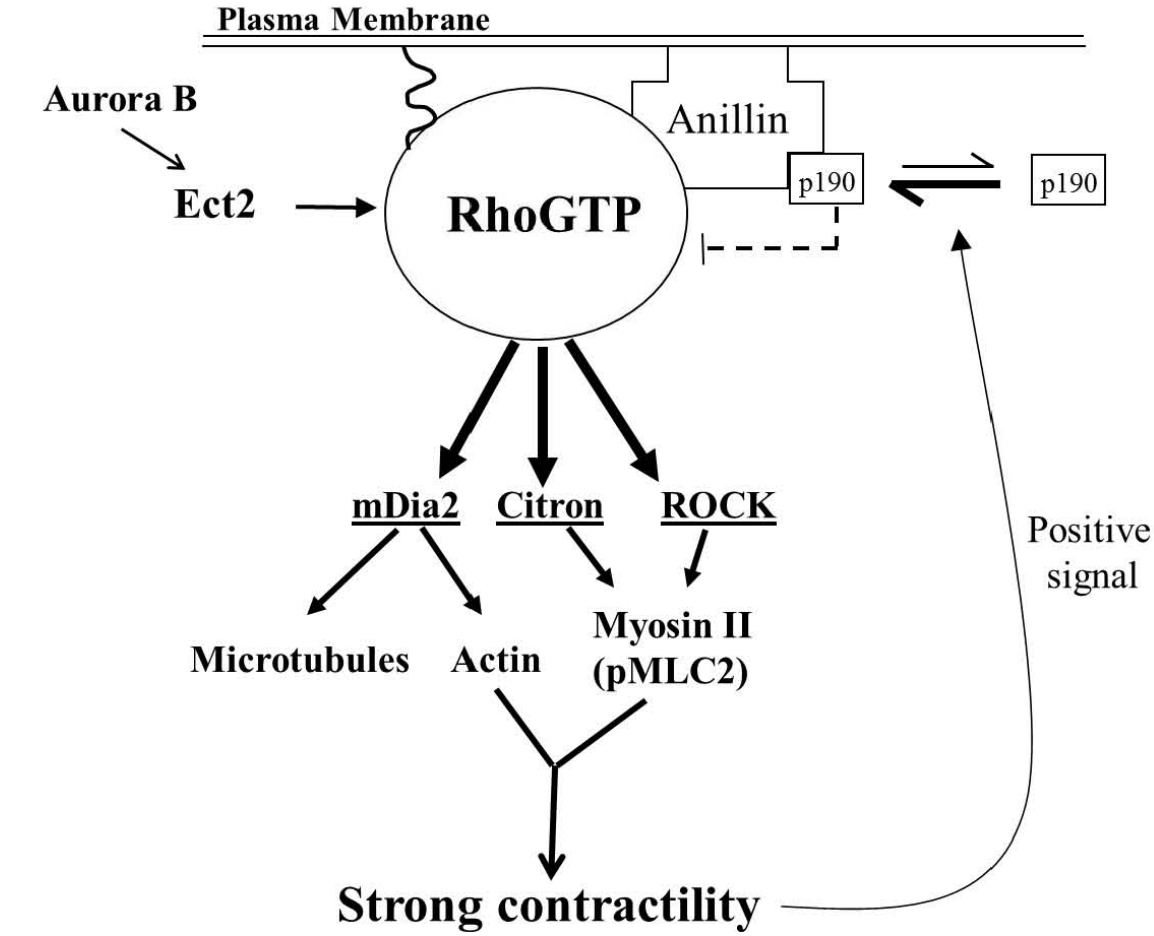

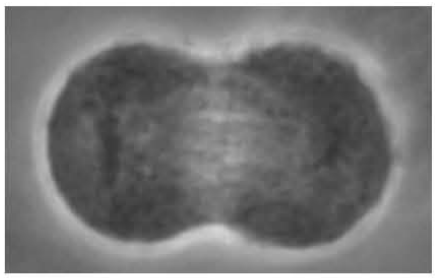

S. Sanchez

Figure 35: Proposed model of cleavage furrow dynamics.

A: In normal dividing cells p190 is partially degraded in late mitosis, and only a small pool persists (~30% of interphase levels). Remaining p190 is localized to the cleavage furrow and found in association with the molecular scaffold anillin. Decreased p190 levels allow RhoGTP levels to appropriately increase and activate of actomyosin contractility through its downstream effectors. The contractility of the actomyosin ring feeds back to the p190-anillin complex, signaling for continued association and completion of cytokinesis.

Figure 35
B

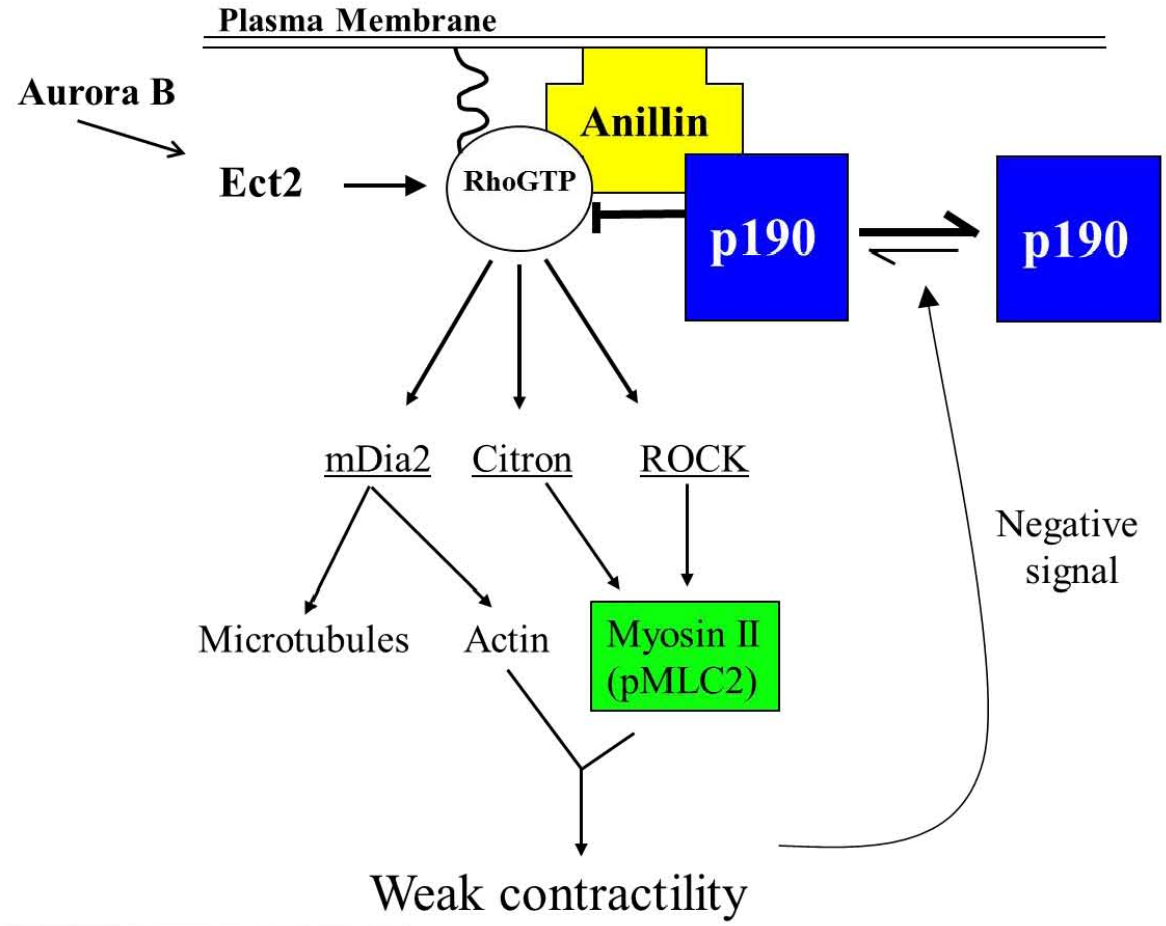

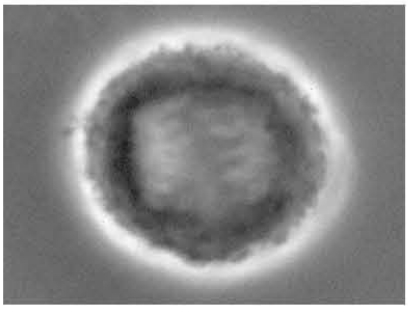

S. Sanchez

Figure 35: Proposed model of cleavage furrow dynamics.

B: Overexpression of p190 leads to decreased RhoGTP levels and weak contractility of the actomyosin network through decreased activation of Rho's downstream effectors. Less contractility at the cleavage furrow feeds back to the anillin-p190 interaction, resulting in dissociation between the two proteins and releasing p190 from the cleavage furrow complex. This, in turn, releases Rho from GAP mediated down-regulation, restoring RhoGTP levels to normal levels, activation of downstream effectors, and contractility of the actomyosin network. These events ultimately result in cleavage furrow ingression and successful completion of cytokinesis.

inducing dissociation between the two proteins (such as seen in Fig. 34). Since anillin also binds Rho, the dissociation between p190 and anillin may lead to a dissociation between p190 and Rho. This would allow a RhoGEF, like Ect2, to have a greater influence on RhoGTP levels, restoring them to biologically appropriate levels, re-activating downstream cascades and completing of cytokinesis. (Fig. 35B) In such a manner, the p190-anillin association could regulate myosin-mediated contractility. However, mislocalization of anillin would prevent transmission of the signal, inhibiting the feedback loop, and preventing biologically appropriate levels of RhoGTP from being restored and progression through cytokinesis.

Together, our results provide additional insight into the events involving RhoA during cytokinesis. We propose that decreased p190 levels during cytokinesis, previously reported by our laboratory (Manchinelly et al., 2010; Su et al., 2003), allow for RhoA-dependent phosphorylation of MLC II, inducing myosin activity and cleavage furrow contraction, which in turn facilitate the interaction between p190 and anillin at the equatorial cortex. This interaction allows p190 to exert appropriate levels of inhibitory activity toward RhoA and prevent uncontrolled Rho activation, mediated by Ect2RhoGEF. Association of anillin with p190 ensures that Rho activity is kept at an optimal level and in a proper location, as it is well known that either constitutive activation or inhibition of the Rho signaling pathway results in cytokinesis failure.

CHAPTER 6

Summary and Perspectives

Chapter 6
Summary and Perspectives:

Summary:

It was first hypothesized that p190 may have a role in apoptosis when attempts to generate a cell line stably expressing p190 failed. This result raised the idea that increased levels of p190, and the ensuing decrease in RhoGTP levels, may be detrimental to the cell. To study the biological role of p190, investigators employed an overexpression system and reported the formation of dendritic protrusions in neuronal and fibroblast cells (Liang et al., 2004; Troller et al., 2004) and multinucleation in epithelial cells (Su et al., 2003). Chromatin condensation, a hallmark of apoptosis was also described (unpublished data). The initial goals of this study were to determine if increased levels of p190 in a cell could indeed initiate apoptosis and to determine if the other reported phenotypes, dendrite-like formation and multinucleation, were exclusive to either fibroblasts or epithelial cells.

The current study demonstrates that p190 overexpression primarily results in dose-dependent and caspase-mediated apoptosis. However, p190 also induces secondary phenotypes, multinucleation and dendrite-like formation, in all cell lines examined. Using a panel of transformed and non-transformed, fibroblast and epithelial cells, it was determined that the frequency of the secondary phenotypes of p190 overexpression were dependent upon the transformation status of the cell, not cell lineage, as had been previously thought. In transformed cells, p190 overexpression preferentially induces multinucleation, a phenotype indicative of a defect in progress through cytokinesis.

However non-transformed cells more often form dendrite-like protrusions upon p190 overexpression. Additionally, all three phenotypes, apoptosis, multinucleation, and dendrite-like formation, are dependent on p190's down-regulation of Rho. These findings were not surprising, since Rho had previously been shown to function in neurite retraction, cytokinesis, and survival (Miyoshi J., 2009). However, how p190 overexpression differentially induced the secondary phenotypes in transformed vs. non-transformed cells was still not understood. Figure 36 is a proposed model for p190-induced apoptosis in transformed (Fig. 36A) and non-transformed (Fig. 36B) cells compiling the data gathered from Chapters 3 and 4 and further discussed below.

Real-time microscopy and caspase inhibition studies raised the possibility that multinucleation and dendrite-like formation may be intermediate phenotypes, eventually leading to p190-induced apoptosis. These results imply that the apoptotic signaling pathways activated in response to p190 overexpression are different in transformed and non-transformed cells. In an attempt to understand these pathways, apoptotic signaling pathways implicated in apoptosis initiated by prolonged inactivation of Rho were screened for changes in activation upon overexpression of p190. All cell lines examined display an increase in JNK activation, suggesting a role for this protein in p190-induced apoptosis. An increase in Bim_L and Bim_S expression levels are also observed, which correspond with a decrease in Mcl-1 levels. Both Bim and Mcl-1 have been reported to be downstream targets of JNK, and their phosphorylation by JNK promotes apoptosis (Hubner et al., 2008; Lei and Davis, 2003; Wertz et al., 2011). However, further investigation needs to be done to determine if this pathway is required for p190-induced

Figure 36

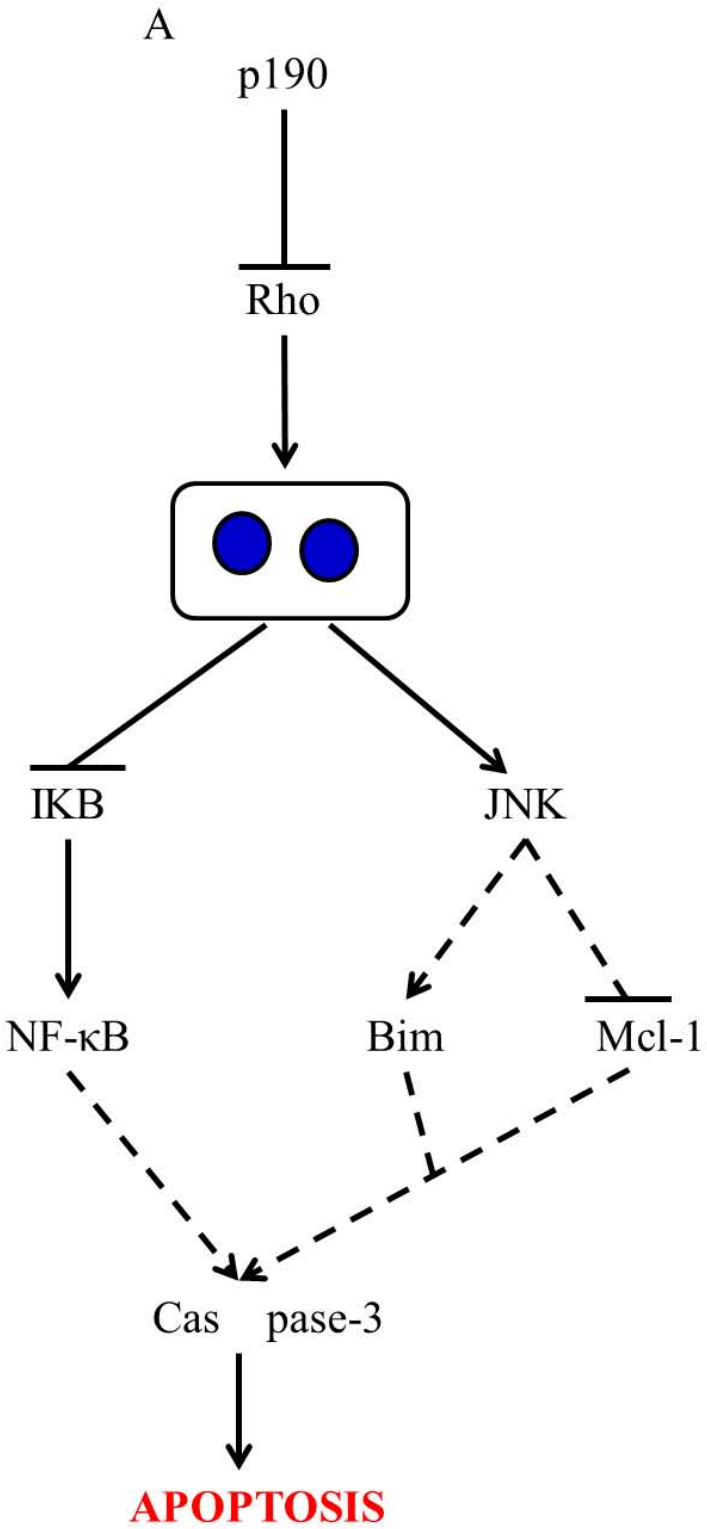

Figure 36: Proposed model for p190 overexpression in transformed and non-transformed cells.

A: In transformed cells p190 overexpression inhibits Rho activation, inducing cytokinesis failure and multinucleation. Overexpression of p190 promotes IKB degradation which would activate the NF-κB pathway. NF-κB can promote the expression of pro-apoptotic proteins and induce apoptosis. p190 overexpression also activates JNK, increases levels of the pro-apoptotic protein Bim and decreases levels of the anti-apoptotic protein Mcl-1. JNK may regulate the apoptotic function of each of these proteins by affecting their stability through phosphorylation. The resulting increased ratio of Bim to Mcl-1 induces cleavage of caspase-3 and eventually apoptosis.

Figure 36

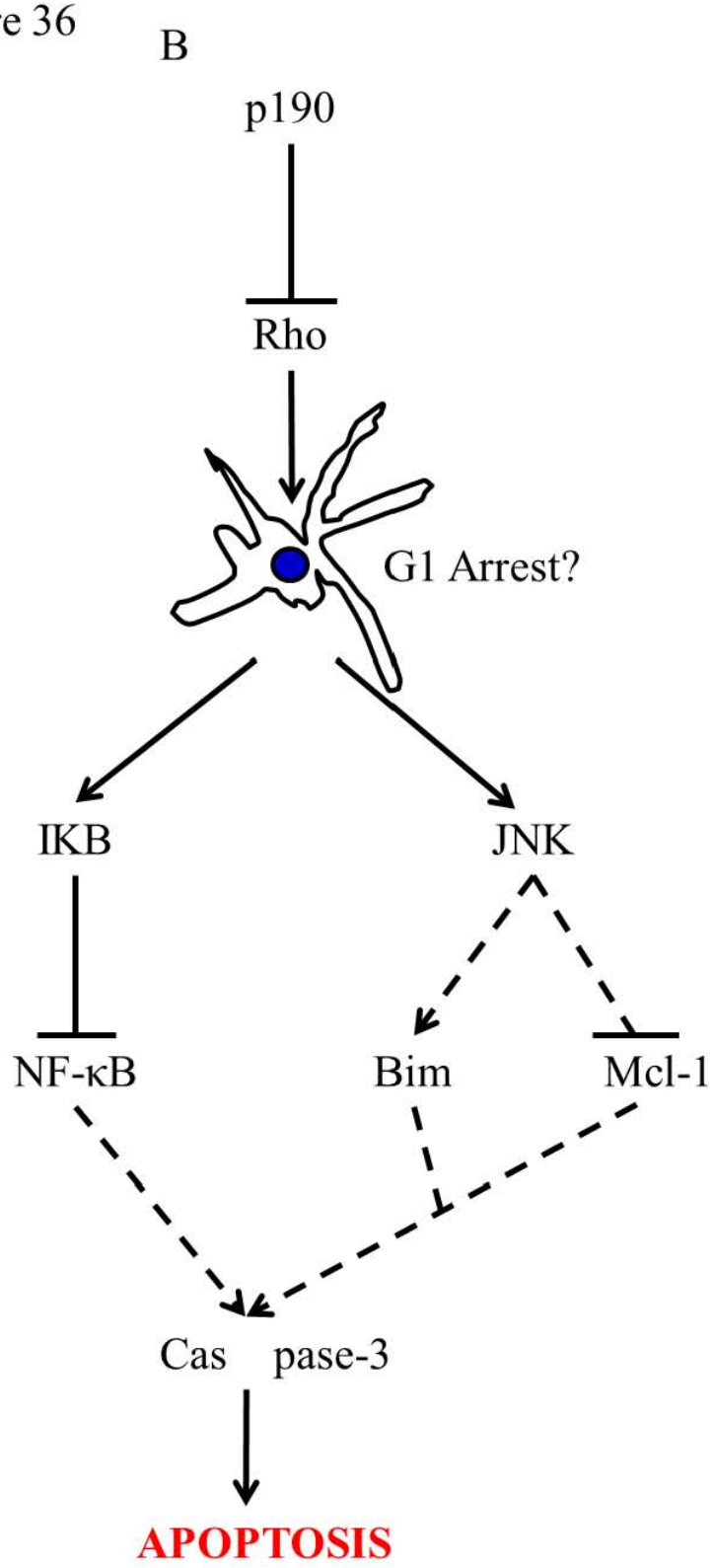
B
p190
Rho
G1 Arrest?
IKB
JNK
NF-κB
Bim
Mcl-1
Cas pase-3
APOPTOSIS

Figure 36: Proposed model for p190 overexpression in transformed and non-transformed cells.

B: In non-transformed cells p190 overexpression inhibits Rho activation, inducing dendrite-like formation, which may be a result of arrest in G1. Overexpression of p190 also inhibits IKB degradation, which would inactivate the NF-κB pathway and promote apoptosis through reduced expression of pro-survival proteins. p190 overexpression also activates JNK, increases levels of the pro-apoptotic protein Bim and decreases levels of the anti-apoptotic protein Mcl-1. Active NF-κB can inhibit JNK activity, so decreased NF-κB, through p190 overexpression, may further promote JNK activation and enhance apoptosis through caspase-3 cleavage.

apoptosis, or if it is simply an effect of the apoptotic pathway. Intriguingly, overexpression of p190 has opposing effects on IKB, a regulator of the NF-κB pathway, in transformed and non-transformed cells, suggesting that the NF-κB pathway may play a role in the differential responses seen in the two cell types. What role NF-κB plays in p190-induced apoptosis and if this pathway may be responsible for the differential response seen in transformed and non-transformed cells needs to be further examined before any significant conclusions can be made about the role of the NF-κB pathway in the p190 pathway.

Docetaxel is a microtubule depolymerizing drug used for treatment of numerous cancers (Baker et al., 2009). The fact that Rho can both regulate organization of microtubules and be modulated by microtubule dynamics (Birukova et al., 2004b; Niggli, 2003) prompted the idea that p190 might play a role in docetaxel-induced apoptosis. Results in Chapter 3 indicate that breast cancer cell lines with more endogenous p190 are more sensitive to docetaxel-induced apoptosis, while cell lines with less p190 are more resistant. Accordingly, introducing either full length p190 or DNRho increases the amount of docetaxel-induced apoptosis, while introducing DNp190 or CARho has the opposite effect, measured either by TUNEL immunofluorescence or caspase-3 cleavage. That p190 plays an integral role in docetaxel-induced apoptosis is evidenced by the finding that knocking-down p190 significantly decreases caspase-3 cleavage by docetaxel.

While the majority of this dissertation focused primarily on the role of p190 in apoptosis, p190 also plays an instrumental role in cell-cycle progression. This is

exemplified by the fact that knock-down of p190 results in arrest at G2 (Maddox and Burridge, 2003) (and unpublished results), while overexpression ultimately results in failure to complete cytokinesis (Su et al., 2003; Su et al., 2009). p190 expression levels are normally down regulated upon entry into mitosis in a ubiquitin-dependent manner, and this degradation is required for successful completion of cytokinesis (Manchinelly et al., 2010). If p190 levels are not decreased, RhoGTP levels at the cleavage furrow are diminished, resulting in unsuccessful abscission of the cleavage furrow (Su et al., 2009). How p190 affects Rho during cytokinesis is well understood; however, how p190 affects the downstream effectors of Rho involved in cytokinesis was undetermined until our study. We found that p190 overexpression decreases the activity of myosin II, without altering localization of actin, microtubules, Rho, or Aurora B, and that active myosin II was required for completion of cytokinesis. Increased expression levels of p190 also inhibit localization of the scaffold protein, anillin to the cleavage furrow. Confocal images of endogenous anillin and p190 show that both proteins co-localize to the cleavage furrow at all stages of cytokinesis. Knockdown of anillin results in mislocalization of p190 to the cleavage furrow, suggesting that anillin is required for p190 localization to the cleavage furrow. However, given the fact that both proteins regulate localization of the other, a feedback loop may be responsible for anillin's continued localization to the cleavage furrow. This feedback may be dependent upon contractility signals, as p190 and anillin are shown to physically interact in a mitotic- and contractility-dependent manner.

Perspectives:

p190-induced apoptosis:

Work presented in this dissertation established that p190 overexpression induced caspase-dependent apoptosis due to decreased Rho activity. Overexpression of p190 also elicited secondary phenotypes of multinucleation in transformed cells and dendrite-like formation in non-transformed cells. Moreover, evidence suggested that p190-induced apoptosis was mediated through the secondary phenotypes, indicating that they may act as intermediate steps in the p190-induced apoptotic pathway. If the secondary phenotypes are indeed intermediate steps, then understanding the differences between multinucleation and dendrite-like formation upon p190 overexpression may provide clues as to the apoptotic signaling pathways activated by overexpression of p190 in transformed and non-transformed cells.

To more directly address this question, apoptosis rescue experiments could be performed by inhibiting the secondary phenotypes to decrease the amount of p190-induced apoptosis. Z-VAD experiments presented in Chapter 3 reveal that inhibiting apoptosis increases the incidence of the secondary phenotypes, suggesting an accumulation of an intermediate stage. However, inhibiting the intermediate phenotypes to inhibit p190-induced apoptosis would more directly address the question. Chapter 5 shows that p190-induced multinucleation is due to a decrease in myosin II activation, and that this phenotype could be rescued with a CA MLC mutant. If p190-induced multinucleation is an intermediate step leading to p190-induced apoptosis in transformed cells, then p190 co-transfection with CA MLC would rescue p190-induced apoptosis,

indicating that multinucleation is an intermediate step in the p190-apoptotic pathway. Similar results would be expected by inhibiting dendrite-like formation in non-transformed cells. DNRac1 or DNCdc42 stimulate neurite retraction through decreased activation of their downstream effectors and increased activation of Rho (Sarner et al., 2000). Co-transfection of these mutants with p190 should reduce p190-induced apoptosis if dendrite-like formation is an intermediate step. This information would more firmly establish the two phenotypes as intermediate steps and help define p190-induced apoptotic pathways in transformed and non-transformed cells.

However, to understand the different apoptotic signaling pathways activated by p190 overexpression in transformed vs. non-transformed cells, we need to have a greater understanding of the signaling differences between the two secondary phenotypes. Data presented in Chapter 3 and previous publications from our lab indicate that p190 overexpression in transformed cells results in a block in mitosis and cytokinesis failure, in the form of multinucleated cells (Manchinelly et al., 2010; Mikawa et al., 2008; Su et al., 2003; Su et al., 2009). Data in Chapter 3 also suggested that p190 overexpression in non-transformed cells elicits a G1 arrest. However, further experimentation needs to be done to fully understand the differential role of p190 overexpression in transformed vs. non-transformed cells. Pixel intensity analysis indicates that cells with dendrite-like protrusion have around 4-times more exogenous p190 than cells with normal morphology. Conversely multinucleated cells have about half as much exogenous p190 as normal morphology cells. Our lab has previously shown that p190 is degraded upon entry into mitosis (Manchinelly et al., 2010; Su et al., 2003), which would explain the

decrease in p190 levels in transformed, multinucleated cells. If, however, cells never progress to mitosis due to a block in G1, p190 levels could accumulate. The increase in p190 would decrease RhoGTP levels and promote dendrite-like extension, a well-established phenomenon of decreased RhoGTP levels (Jalink et al., 1994; Koh, 2006; Kozma et al., 1997).

In support of this hypothesis, Figure 18 in Chapter 3 shows that in transformed cells, forcing a block in G1 increases the incidence of dendrite-like formation. While this is only one experiment and needs to be repeated, it further supports the idea that p190-induced dendrite-like formation is due to a block in G1. A corollary to this experiment would be to bypass the G1 arrest in non-transformed cells by knocking down p27. p27 is a negative regulator of the cyclin D-CDK4 complex, whose activation is required for progression through G1 (Jackson et al., 2002). By inhibiting p27, cells can bypass the G1 block in the presence of arrest signals and promote cell cycle progression (Nakayama et al., 1996; Polyak et al., 1994). If p190-induced dendrite-like formation is a result of p190 accumulation due to G1 arrest, then forcing non-transformed cells out of G1 by silencing p27 should rescue this phenotype. These experiments would attempt to switch the phenotype with regard to the transformation status, and by doing so, provide evidence that the differential effects of p190 overexpression in transformed vs. non-transformed cells may be due to cell-cycle checkpoints, which are known to be compromised in cancer cells. If p190 overexpression, through the Rho pathway, elicits apoptosis by activating different cell-cycle checkpoints in transformed vs. non-transformed cells, this

pathway could be exploited as a useful tool for cancer treatment once the signaling pathways are fully understood.

Another strategy to determine if p190 overexpression induces G1 arrest in non-transformed cells is to analyze cell cycle stages by flow cytometry. If p190 overexpression is inducing a block in G1, then a greater percentage of non-transformed cells should be in G1 than transformed cells upon p190 overexpression. This would quickly address the question as to whether or not p190 overexpression induced a G1 block in non-transformed cells. Another way to address this question would be through the use of immunofluorescence. If the dendrite-like phenotype is a result of arrest in G1, then cells with dendrite-like formations should either express cyclin D or have decreased Rb phosphorylation, both of which indicate that a cell is in G1. Normally, in a population of cycling cells, the majority of cells are in G1. However, if dendrite-like formation occurs as a result of G1 arrest, then almost 100% of dendritic-like cells should either express cyclin D or have decreased Rb phosphorylation. These experiments would directly test the correlation between cell cycle stage and p190-induced dendrite-like formation.

It is, however, possible that results of the proposed experiments would indicate that either the secondary phenotypes do not act as intermediate steps or they are not initiated by cues from cell-cycle checkpoints. If either is the case, it is still possible that p190-induced apoptosis may activate different signaling pathways in transformed vs. non-transformed cells, given the fact that p190 clearly has differential effects on morphology. As such, another way to address the question would be to investigate the

activation of known apoptotic proteins implicated in Rho-induced apoptosis. Such an approach was taken in Chapter 4, and results revealed that NF-κB was differentially activated by p190 overexpression in transformed and non-transformed cells.

NF-κB plays a role in cell survival, death, and cell cycle progression (Bakkar and Guttridge, 2010; Kucharczak et al., 2003), but how this pathway functions in p190-induced apoptosis needs to be more fully investigated. Data presented in Chapter 4 indicate that upon p190 overexpression IKB is degraded in transformed cells, activating the NF-κB pathway, and stabilized in non-transformed cells, inhibiting the pathway. These findings imply that apoptosis is initiated through decreased expression of NF-κB-dependent pro-survival factors in non-transformed cells. However, this dissertation provides no direct evidence for this theory. Experiments need to be performed examining the expression levels of Bcl-2, Bcl-X_L, Bfl-1, XIAP, c-IAP, and c-FLIP. A decrease in any of these proteins would suggest an involvement of the NF-κB pathway in p190-induced apoptosis in non-transformed cells. If any of these proteins do have decreased levels as a result of p190 overexpression, a rescue experiment with co-overexpression of p190 and the identified protein would indicate a direct involvement in p190-induced apoptosis. Additionally, the NF-κB pathway itself should be examined. This could be done using a constitutively active subunit of NF-κB or knocking down IKB. Either method would promote NF-κB translocation to the nucleus and increase expression of its pro-survival targets. If NF-κB is in fact involved in p190-induced apoptosis, either method should rescue the apoptotic response resulting from p190 overexpression.

How the NF-κB pathway may be involved in p190-induced apoptosis in transformed cells also needs to be more closely examined. Several groups have shown that NF-κB can promote expression of Fas, FasL, p53, DR4-6, and TRAIL, so expression levels of all of these proteins should be examined after p190 overexpression. A similar experiment as described above would again indicate involvement of both the identified protein and the NF-κB pathway. However in this case, knocking down the identified protein to decrease apoptosis would indicate its involvement in p190-induced apoptosis. Additionally, either knocking down NF-κB, using a proteasomal inhibitor to prevent degradation of IKB or using a non-degradable mutant of IKB, would inhibit expression of NF-κB dependent proteins and could prevent p190-induced apoptosis. Conversely, an increase in NF-κB activation upon apoptotic stimulation could also be a pro-survival response by the cell to prevent cell death. In this case, the pro-survival proteins mentioned in the above paragraph would increase, and their expression levels should be examined. If p190 overexpression is activating the pro-survival pathway in transformed cells, inhibiting this pathway might increase the amount of apoptosis reported upon overexpression of p190.

Unlike NF-κB, JNK activity increases in transformed and non-transformed cells alike. However, it is not known if p190-induced apoptosis requires the pro-apoptotic functions of JNK. If JNK is required for p190-induced apoptosis, inhibiting the activity of JNK with the chemical inhibitor SP600125 should rescue p190-induced apoptosis. This would provide more direct evidence for the role of JNK in p190-induced apoptosis. Additionally, knockdown of JNK with siRNA should give similar results. It is possible

that inhibiting JNK activity would not affect p190-induced apoptosis, which would indicate that while JNK may be activated in response to p190 overexpression, it is not required for p190-induced apoptosis. In this case, the roles of Bim and Mcl-1 in p190-induced could be examined.

Chapter 4 also reported an increase in the expression levels of Bim_L and Bim_S, along with a decrease in Mcl-1. While these findings suggest that both proteins may play a role in p190-induced apoptosis, more direct evidence is needed. If silencing Bim rescued p190-induced apoptosis, this would suggest a requirement for this protein in the apoptotic response seen with p190 overexpression. Conversely, inhibiting the degradation of Mcl-1, with either a non-degradable mutant or proteasomal inhibition should decrease apoptosis upon overexpression of p190. If apoptosis is decreased, more direct evidence for the role of Mcl-1 in p190-induced apoptosis would be provided. If neither rescue experiment succeeds in reducing p190-induced apoptosis, such a result would suggest that Bim and Mcl-1 are not required and other Bcl-2 proteins may be mediating caspase-3 cleavage. In that case the role of Bcl-2 and Bcl-X_L, proteins which have been implicated in apoptosis due to prolonged inactivation of Rho, could be examined for changes in expression levels by Western blot analysis.

Finally, current literature suggests that JNK phosphorylation of Bim promotes its pro-apoptotic function (Hubner et al., 2008; Lei and Davis, 2003), while JNK phosphorylation of Mcl-1 results in its degradation (Wertz et al., 2011). If JNK phosphorylation, as a result of p190 overexpression is mediating the alterations of Bim and Mcl-1 levels, then inhibition of JNK should also inhibit the increase in Bim_L and

Bim_S, while stabilizing Mcl-1. Additionally, mutants of both Bim and Mcl-1 are available that are mutated at the JNK phosphorylation sites. Co-transfection of p190 with each mutant protein, which act as dominant negative mutants, should rescue p190-induced apoptosis if either protein is required for the apoptotic response.

Understanding the apoptotic pathways activated in response to p190 overexpression and the corresponding decrease in Rho activation could provide new targets for cancer therapy. As discussed in Chapter 1, RhoGTPases are involved in the malignant progression of numerous tumors; however, only one drug targets a Rho effector. Fasudil, a ROCK inhibitor, is used for cardiovascular diseases. However, new data suggest that the drug may have a promising future in the treatment of cancer (Olson, 2008). By understanding how a decrease in Rho activation promotes apoptosis we could more accurately trigger apoptosis. Additionally, if p190 overexpression and decreased Rho activation activate different apoptotic signaling pathways in transformed cells vs. non-transformed cells, this may allow physicians to more accurately target transformed cells and minimize off-target effects. In this way, targeting the p190-Rho pathway may prove to not only provide new pathways for drug development but also minimize killing of non-tumorigenic cells.

To this point, the discussion in this chapter has focused on identifying new targets for drug discovery; however, this dissertation also presents data which indicate that p190 can sensitize breast cancer cells to the action of a well-established chemotherapeutic drug, docetaxel. These preliminary data suggest that cell sensitivity to docetaxel, and theoretically, paclitaxel, is dependent upon the amount of endogenous p190 in the cell.

To further study this relationship, a retrospective study of archival patient samples could be done to determine the levels of endogenous p190 and correlate that to the response to taxanes. These data would provide additional information regarding the levels of p190 and docetaxel responses. With this information, physicians might then have another prognostic marker to help determine which drugs a patient would respond best to and how to tailor treatments to best suit their patients.

Chapter 3 also provided data which suggest that altering the levels of active Rho through expression of p190 can modulate a cell's response to docetaxel; however, events downstream of Rho are still uncharacterized. If the increased sensitivity to docetaxel is through the Rho effector, ROCK, than using the ROCK inhibitor Fasudil, in combination with taxanes, may improve a patient's response to taxane-induced apoptosis. This could be determined by treating cells in tissue culture with taxanes in combination with the ROCK inhibitor Y-27632 or constitutively active and dominant negative mutants of ROCK. If decreased ROCK activity increases taxane-induced apoptosis in tissue culture, this relationship could be further explored in mouse models looking at combination treatments of Fasudil and taxanes on breast, ovarian, prostate, gastric, and lung cancer (cancers that taxanes are currently used for treatment). If promising results are found with mouse models, the combination of Fasudil and taxanes could progress to a Phase I clinical trial.

p190-induced multinucleation:

p190 also plays a significant role in progression through cytokinesis. This function was first demonstrated when overexpression of p190 resulted in cytokinesis

failure (Su et al., 2003). Since then, our lab has demonstrated that p190 modulates RhoGTP levels in concert with Ect2 (Mikawa et al., 2008) at the cleavage furrow (Su et al., 2003). Normally, p190 levels are down regulated upon entry into mitosis, and this down regulation is required for completion of cytokinesis (Manchinelly et al., 2010; Su et al., 2009). In the presence of continued p190, RhoGTP levels are decreased at the cleavage furrow, which inhibits abscission and prevents completion of cytokinesis (Su et al., 2009). However, how p190 overexpression affects the downstream effectors of Rho were not understood when this dissertation work was initiated.

Data presented in Chapter 5 shows that p190 overexpression in HeLa cells decreases myosin II activation at the cleavage furrow and that this activation is required for completion of cytokinesis. However, these data do not address which downstream target of Rho is responsible for decreased MLC II phosphorylation. Two effectors of Rho can activate myosin II, ROCK and Citron Kinase. Further clarification is needed to determine which kinase is responsible for the decrease in myosin II activation, as both kinases phosphorylate MLC at Ser19. The literature suggests that while ROCK activation is important for cytokinesis, it is not required, as treatment with the ROCK inhibitor Y-27632 does not inhibit progression through cytokinesis (Kosako et al., 2000; Madaule et al., 2000). To determine which kinase is responsible for the decrease in MLC II phosphorylation, co-transfection of p190 with either a constitutively active mutant of ROCK or Citron kinase should rescue the decrease in MLC II phosphorylation and multinucleation. Whichever mutant kinase increases MLC II phosphorylation levels over p190 alone would suggest it is responsible for the decrease seen upon p190

overexpression. It is also possible that neither mutant could rescue the decrease in MLC II phosphorylation. Such a result would argue that the decrease in MLC II phosphorylation levels may be mediated through an increase in the MLC phosphatase, which is inactivated by ROCK. By co-transfecting p190 with a DN MLC phosphatase mutant and assessing if there is an effect on MLC II phosphorylation, we could determine if this protein was involved in the decreased activation of myosin II upon p190 overexpression.

Finally, the association between p190 and anillin is a novel and interesting finding suggesting a contractility feedback loop to maintain biologically appropriate levels of RhoGTP during cytokinesis. This study provides evidence that when contractility decreases, due to decreased RhoGTP levels, the interaction between anillin and p190 is lost. This result suggests that the interaction between p190 and Rho might also be compromised in the presence of weak contractility signals. To further explore this hypothesis, one could directly examine the interaction between p190 and Rho under high and low contractility conditions. A dot-blot assay of the GAP domain of p190 and CARho show that both proteins physically interact (Li et al., 1997). If the addition of blebbistatin during cytokinesis disrupts this interaction between p190 and Rho, such a result would indicate that the contractility feedback loop which disrupts the p190 anillin interaction also affects the association between p190 and Rho, presumably to increase RhoGTP levels.

While the previous experiment investigates the interaction between p190 and Rho, it does not address the biological effect of this interaction. A decreased interaction

between p190 and Rho would allow an increased signal from the RhoGEF, Ect2, and increase RhoGTP levels, ultimately increasing contractility to promote completion of cytokinesis. This hypothesis can be addressed in a variety of ways. A Rho pull down assay shows that p190 overexpression decreases RhoGTP levels (Mikawa et al., 2008). In the presence of decreased contractility, RhoGTP levels should increase, if the feedback signal results in a p190-Rho dissociation and increased RhoGTP levels. Additionally, if decreased contractility during cytokinesis increases the influence of Ect2, FRET analysis using the Rho biosensor (Su et al., 2009) would show that cells overexpressing p190 and treated with blebbistatin have increased RhoGTP levels over cells simply overexpressing p190. These experiments could address the biological effect of decreased contractility on the p190-Rho association and how that affects the levels of RhoGTP.

Together the results presented in this dissertation increase our understanding of the biological functions of p190RhoGAP and provide further insight into the molecular mechanisms of cytokinesis. Furthermore, this work provides evidence for an exciting role for p190 and Rho in cancer therapy and suggests a novel means of specifically targeting tumorigenic cells.

CHAPTER 7

References

Adams, R.R., H. Maiato, W.C. Earnshaw, and M. Carmena. 2001. Essential roles of Drosophila inner centromere protein (INCENP) and aurora B in histone H3 phosphorylation, metaphase chromosome alignment, kinetochore disjunction, and chromosome segregation. *J Cell Biol*. 153:865-880.

Agarwal, M.L., A. Agarwal, W.R. Taylor, and G.R. Stark. 1995. p53 controls both the G2/M and the G1 cell cycle checkpoints and mediates reversible growth arrest in human fibroblasts. *Proc Natl Acad Sci U S A*. 92:8493-8497.

Agnew, B.J., L.S. Minamide, and J.R. Bamburg. 1995. Reactivation of phosphorylated actin depolymerizing factor and identification of the regulatory site. *J Biol Chem*. 270:17582-17587.

Akgul, C. 2009. Mcl-1 is a potential therapeutic target in multiple types of cancer. *Cell Mol Life Sci*. 66:1326-1336.

Akgul, C., D.A. Moulding, M.R. White, and S.W. Edwards. 2000. In vivo localisation and stability of human Mcl-1 using green fluorescent protein (GFP) fusion proteins. *FEBS Lett*. 478:72-76.

Akiyama, T., C.R. Dass, and P.F. Choong. 2009. Bim-targeted cancer therapy: a link between drug action and underlying molecular changes. *Mol Cancer Ther*. 8:3173-3180.

Aktories, K., U. Braun, S. Rosener, I. Just, and A. Hall. 1989. The rho gene product expressed in E. coli is a substrate of botulinum ADP-ribosyltransferase C3. *Biochem Biophys Res Commun*. 158:209-213.

Alberts, A.S. 2001. Identification of a carboxyl-terminal diaphanous-related formin homology protein autoregulatory domain. *J Biol Chem*. 276:2824-2830.

Alberts, A.S., N. Bouquin, L.H. Johnston, and R. Treisman. 1998. Analysis of RhoA-binding proteins reveals an interaction domain conserved in heterotrimeric G protein beta subunits and the yeast response regulator protein Skn7. *J Biol Chem*. 273:8616-8622.

Amano, M., K. Chihara, N. Nakamura, T. Kaneko, Y. Matsuura, and K. Kaibuchi. 1999. The COOH terminus of Rho-kinase negatively regulates rho-kinase activity. *J Biol Chem*. 274:32418-32424.

Amano, M., M. Ito, K. Kimura, Y. Fukata, K. Chihara, T. Nakano, Y. Matsuura, and K. Kaibuchi. 1996. Phosphorylation and activation of myosin by Rho-associated kinase (Rho-kinase). *J Biol Chem*. 271:20246-20249.

Amaral, J.D., J.M. Xavier, C.J. Steer, and C.M. Rodrigues. 2010. The role of p53 in apoptosis. *Discov Med*. 9:145-152.

Anderson, S.M., W.S. Hayward, B.G. Neel, and H. Hanafusa. 1980. Avian erythroblastosis virus produces two mRNA's. *J Virol*. 36:676-683.

Andreu, J.M., J. Bordas, J.F. Diaz, J. Garcia de Ancos, R. Gil, F.J. Medrano, E. Nogales, E. Pantos, and E. Towns-Andrews. 1992. Low resolution structure of microtubules in solution. Synchrotron X-ray scattering and electron microscopy of taxol-induced microtubules assembled from purified tubulin in comparison with glycerol and MAP-induced microtubules. *J Mol Biol*. 226:169-184.

Arakawa, Y., H. Bito, T. Furuyashiki, T. Tsuji, S. Takemoto-Kimura, K. Kimura, K. Nozaki, N. Hashimoto, and S. Narumiya. 2003. Control of axon elongation via an SDF-1alpha/Rho/mDia pathway in cultured cerebellar granule neurons. *J Cell Biol*. 161:381-391.

Arthur, W.T., and K. Burridge. 2001. RhoA inactivation by p190RhoGAP regulates cell spreading and migration by promoting membrane protrusion and polarity. *Mol Biol Cell*. 12:2711-2720.

Ashkenazi, A. 2002. Targeting death and decoy receptors of the tumour-necrosis factor superfamily. *Nat Rev Cancer*. 2:420-430.

Ashwell, J.D. 2006. The many paths to p38 mitogen-activated protein kinase activation in the immune system. *Nat Rev Immunol*. 6:532-540.

Aznar, S., P. Fernandez-Valeron, C. Espina, and J.C. Lacal. 2004. Rho GTPases: potential candidates for anticancer therapy. *Cancer Lett*. 206:181-191.

Badr, G., H. Waly, H.M. Eldien, H. Abdel-Tawab, K. Hassan, I.M. Alhazza, H. Ebaid, and S.H. Alwasel. 2010. Blocking type I interferon (IFN) signaling impairs antigen responsiveness of circulating lymphocytes and alters their homing to lymphoid organs: protective role of type I IFN. *Cell Physiol Biochem*. 26:1029-1040.

Baichwal, V.R., and P.A. Baeuerle. 1997. Activate NF-kappa B or die? *Curr Biol*. 7:R94-96.

Baker, J., J. Ajani, F. Scotte, D. Winther, M. Martin, M.S. Aapro, and G. von Minckwitz. 2009. Docetaxel-related side effects and their management. *Eur J Oncol Nurs*. 13:49-59.

Bakkar, N., and D.C. Guttridge. 2010. NF-kappaB signaling: a tale of two pathways in skeletal myogenesis. *Physiol Rev*. 90:495-511.

Barberis, D., A. Casazza, R. Sordella, S. Corso, S. Artigiani, J. Settleman, P.M. Comoglio, and L. Tamagnone. 2005. p190 Rho-GTPase activating protein associates with plexins and it is required for semaphorin signalling. *J Cell Sci*. 118:4689-4700.

Barker, T.H., H.E. Grenett, M.W. MacEwen, S.G. Tilden, G.M. Fuller, J. Settleman, A. Woods, J. Murphy-Ullrich, and J.S. Hagood. 2004. Thy-1 regulates fibroblast focal adhesions, cytoskeletal organization and migration through modulation of p190 RhoGAP and Rho GTPase activity. *Exp Cell Res*. 295:488-496.

Barkett, M., and T.D. Gilmore. 1999. Control of apoptosis by Rel/NF-kappaB transcription factors. *Oncogene*. 18:6910-6924.

Barone, M.V., L. Sepe, R.M. Melillo, A. Mineo, G. Santelli, C. Monaco, M.D. Castellone, D. Tramontano, A. Fusco, and M. Santoro. 2001. RET/PTC1 oncogene signaling in PC Cl 3 thyroid cells requires the small GTP-binding protein Rho. *Oncogene*. 20:6973-6982.

Barr, A.R., and F. Gergely. 2007. Aurora-A: the maker and breaker of spindle poles. *J Cell Sci*. 120:2987-2996.

Bartkova, J., Z. Horejsi, K. Koed, A. Kramer, F. Tort, K. Zieger, P. Guldberg, M. Sehested, J.M. Nesland, C. Lukas, T. Orntoft, J. Lukas, and J. Bartek. 2005. DNA damage response as a candidate anti-cancer barrier in early human tumorigenesis. *Nature*. 434:864-870.

Bartolini, F., J.B. Moseley, J. Schmoranzer, L. Cassimeris, B.L. Goode, and G.G. Gundersen. 2008. The formin mDia2 stabilizes microtubules independently of its actin nucleation activity. *J Cell Biol*. 181:523-536.

Bartolome, R.A., N. Wright, I. Molina-Ortiz, F.J. Sanchez-Luque, and J. Teixido. 2008. Activated G(alpha)13 impairs cell invasiveness through p190RhoGAP-mediated inhibition of RhoA activity. *Cancer Res*. 68:8221-8230.

Bass, M.D., M.R. Morgan, K.A. Roach, J. Settleman, A.B. Goryachev, and M.J. Humphries. 2008. p190RhoGAP is the convergence point of adhesion signals from alpha 5 beta 1 integrin and syndecan-4. *J Cell Biol*. 181:1013-1026.

Bava, S.V., V.T. Puliappadamba, A. Deepti, A. Nair, D. Karunagaran, and R.J. Anto. 2005. Sensitization of taxol-induced apoptosis by curcumin involves down-regulation of nuclear factor-kappaB and the serine/threonine kinase Akt and is independent of tubulin polymerization. *J Biol Chem*. 280:6301-6308.

Beg, A.A., and D. Baltimore. 1996. An essential role for NF-kappaB in preventing TNF-alpha-induced cell death. *Science*. 274:782-784.

Begum, R., E.K.M.S. Nur, and M.A. Zaman. 2004. The role of Rho GTPases in the regulation of the rearrangement of actin cytoskeleton and cell movement. *Exp Mol Med*. 36:358-366.

Bellacosa, A., J.R. Testa, S.P. Staal, and P.N. Tsichlis. 1991. A retroviral oncogene, akt, encoding a serine-threonine kinase containing an SH2-like region. *Science*. 254:274-277.

Bellon, S., M.J. Fitzgibbon, T. Fox, H.M. Hsiao, and K.P. Wilson. 1999. The structure of phosphorylated p38gamma is monomeric and reveals a conserved activation-loop conformation. *Structure*. 7:1057-1065.

Bement, W.M., H.A. Benink, and G. von Dassow. 2005. A microtubule-dependent zone of active RhoA during cleavage plane specification. *J Cell Biol*. 170:91-101.

Bement, W.M., A.L. Miller, and G. von Dassow. 2006. Rho GTPase activity zones and transient contractile arrays. *Bioessays*. 28:983-993.

Billuart, P., C.G. Winter, A. Maresh, X. Zhao, and L. Luo. 2001. Regulating axon branch stability: the role of p190 RhoGAP in repressing a retraction signaling pathway. *Cell*. 107:195-207.

Birukova, A.A., K.G. Birukov, K. Smurova, D. Adyshev, K. Kaibuchi, I. Alieva, J.G. Garcia, and A.D. Verin. 2004a. Novel role of microtubules in thrombin-induced endothelial barrier dysfunction. *FASEB J*. 18:1879-1890.

Birukova, A.A., K. Smurova, K.G. Birukov, P. Usatyuk, F. Liu, K. Kaibuchi, A. Ricks-Cord, V. Natarajan, I. Alieva, J.G. Garcia, and A.D. Verin. 2004b. Microtubule disassembly induces cytoskeletal remodeling and lung vascular barrier dysfunction: role of Rho-dependent mechanisms. *J Cell Physiol*. 201:55-70.

Bishop, A.L., and A. Hall. 2000. Rho GTPases and their effector proteins. *Biochem J*. 348 Pt 2:241-255.

Bishop, J.D., and J.M. Schumacher. 2002. Phosphorylation of the carboxyl terminus of inner centromere protein (INCENP) by the Aurora B Kinase stimulates Aurora B kinase activity. *J Biol Chem*. 277:27577-27580.

Blume-Jensen, P., R. Janknecht, and T. Hunter. 1998. The kit receptor promotes cell survival via activation of PI 3-kinase and subsequent Akt-mediated phosphorylation of Bad on Ser136. *Curr Biol*. 8:779-782.

Boerner, J.L., M.J. McManus, G.S. Martin, and N.J. Maihle. 2000. Ras-independent oncogenic transformation by an EGF-receptor mutant. *J Cell Sci*. 113 (Pt 6):935-942.

Bosgraaf, L., and P.J. van Haastert. 2006. The regulation of myosin II in Dictyostelium. *Eur J Cell Biol*. 85:969-979.

Bradley, W.D., S.E. Hernandez, J. Settleman, and A.J. Koleske. 2006. Integrin signaling through Arg activates p190RhoGAP by promoting its binding to p120RasGAP and recruitment to the membrane. *Mol Biol Cell*. 17:4827-4836.

Brady, C.A., and L.D. Attardi. 2010. p53 at a glance. *J Cell Sci*. 123:2527-2532.

Braga, V.M., A. Del Maschio, L. Machesky, and E. Dejana. 1999. Regulation of cadherin function by Rho and Rac: modulation by junction maturation and cellular context. *Mol Biol Cell*. 10:9-22.

Brandt, D., M. Gimona, M. Hillmann, H. Haller, and H. Mischak. 2002. Protein kinase C induces actin reorganization via a Src- and Rho-dependent pathway. *J Biol Chem*. 277:20903-20910.

Bresnick, A.R. 1999. Molecular mechanisms of nonmuscle myosin-II regulation. *Curr Opin Cell Biol*. 11:26-33.

Brito, G.A., J. Fujji, B.A. Carneiro-Filho, A.A. Lima, T. Obrig, and R.L. Guerrant. 2002. Mechanism of Clostridium difficile toxin A-induced apoptosis in T84 cells. *J Infect Dis*. 186:1438-1447.

Brooks, C.L., and W. Gu. 2010. New insights into p53 activation. *Cell Res*. 20:614-621.

Brouns, M.R., S.F. Matheson, K.Q. Hu, I. Delalle, V.S. Caviness, J. Silver, R.T. Bronson, and J. Settleman. 2000. The adhesion signaling molecule p190 RhoGAP is required for morphogenetic processes in neural development. *Development*. 127:4891-4903.

Brouns, M.R., S.F. Matheson, and J. Settleman. 2001. p190 RhoGAP is the principal Src substrate in brain and regulates axon outgrowth, guidance and fasciculation. *Nat Cell Biol*. 3:361-367.

Brown, J.R., K.K. Koretke, M.L. Birkeland, P. Sanseau, and D.R. Patrick. 2004. Evolutionary relationships of Aurora kinases: implications for model organism studies and the development of anti-cancer drugs. *BMC Evol Biol*. 4:39.

Brunet, A., A. Bonni, M.J. Zigmond, M.Z. Lin, P. Juo, L.S. Hu, M.J. Anderson, K.C. Arden, J. Blenis, and M.E. Greenberg. 1999. Akt promotes cell survival by phosphorylating and inhibiting a Forkhead transcription factor. *Cell*. 96:857-868.

Buey, R.M., I. Barasoain, E. Jackson, A. Meyer, P. Giannakakou, I. Paterson, S. Mooberry, J.M. Andreu, and J.F. Diaz. 2005. Microtubule interactions with chemically diverse stabilizing agents: thermodynamics of binding to the paclitaxel site predicts cytotoxicity. *Chem Biol*. 12:1269-1279.

Bull, V.H., E.M. Fargestad, M. Strozynski, and B. Thiede. 2010. Temporal proteome profiling of taxol-induced mitotic arrest and apoptosis. *Electrophoresis*. 31:1873-1885.

Burbelo, P.D., A.A. Finegold, C.A. Kozak, Y. Yamada, and H. Takami. 1998. Cloning, genomic organization and chromosomal assignment of the mouse p190-B gene. *Biochim Biophys Acta*. 1443:203-210.

Burbelo, P.D., S. Miyamoto, A. Utani, S. Brill, K.M. Yamada, A. Hall, and Y. Yamada. 1995. p190-B, a new member of the Rho GAP family, and Rho are induced to cluster after integrin cross-linking. *J Biol Chem*. 270:30919-30926.

Bustos, R.I., M.A. Forget, J.E. Settleman, and S.H. Hansen. 2008. Coordination of Rho and Rac GTPase function via p190B RhoGAP. *Curr Biol*. 18:1606-1611.

Cain, K., S.B. Bratton, C. Langlais, G. Walker, D.G. Brown, X.M. Sun, and G.M. Cohen. 2000. Apaf-1 oligomerizes into biologically active approximately 700-kDa and inactive approximately 1.4-MDa apoptosome complexes. *J Biol Chem*. 275:6067-6070.

Canagarajah, B.J., A. Khokhlatchev, M.H. Cobb, and E.J. Goldsmith. 1997. Activation mechanism of the MAP kinase ERK2 by dual phosphorylation. *Cell*. 90:859-869.

Cantley, L.C. 2002. The phosphoinositide 3-kinase pathway. *Science*. 296:1655-1657.

Capano, M., and M. Crompton. 2006. Bax translocates to mitochondria of heart cells during simulated ischaemia: involvement of AMP-activated and p38 mitogen-activated protein kinases. *Biochem J*. 395:57-64.

Carmena, M., S. Ruchaud, and W.C. Earnshaw. 2009. Making the Auroras glow: regulation of Aurora A and B kinase function by interacting proteins. *Curr Opin Cell Biol*. 21:796-805.

Caron, E., and A. Hall. 1998. Identification of two distinct mechanisms of phagocytosis controlled by different Rho GTPases. *Science*. 282:1717-1721.

Cerione, R.A., and Y. Zheng. 1996. The Dbl family of oncogenes. *Curr Opin Cell Biol*. 8:216-222.

Chang, J.H., S. Gill, J. Settleman, and S.J. Parsons. 1995. c-Src regulates the simultaneous rearrangement of actin cytoskeleton, p190RhoGAP, and p120RasGAP following epidermal growth factor stimulation. *J Cell Biol*. 130:355-368.

Chang, L., and M. Karin. 2001. Mammalian MAP kinase signalling cascades. *Nature*. 410:37-40.

Chen, L., S.N. Willis, A. Wei, B.J. Smith, J.I. Fletcher, M.G. Hinds, P.M. Colman, C.L. Day, J.M. Adams, and D.C. Huang. 2005. Differential targeting of prosurvival Bcl-2 proteins by their BH3-only ligands allows complementary apoptotic function. *Mol Cell*. 17:393-403.

Chiarugi, P., P. Cirri, L. Taddei, E. Giannoni, G. Camici, G. Manao, G. Raugei, and G. Ramponi. 2000a. The low M(r) protein-tyrosine phosphatase is involved in Rho-mediated cytoskeleton rearrangement after integrin and platelet-derived growth factor stimulation. *J Biol Chem*. 275:4640-4646.

Chiarugi, P., M.L. Taddei, P. Cirri, D. Talini, F. Buricchi, G. Camici, G. Manao, G. Raugei, and G. Ramponi. 2000b. Low molecular weight protein-tyrosine phosphatase controls the rate and the strength of NIH-3T3 cells adhesion through its phosphorylation on tyrosine 131 or 132. *J Biol Chem*. 275:37619-37627.

Chitaley, K., and R.C. Webb. 2002. Microtubule depolymerization facilitates contraction of rat aorta via activation of Rho-kinase. *Vascul Pharmacol*. 38:157-161.

Choi, S.Y., M.J. Kim, C.M. Kang, S. Bae, C.K. Cho, J.W. Soh, J.H. Kim, S. Kang, H.Y. Chung, Y.S. Lee, and S.J. Lee. 2006. Activation of Bak and Bax through c-abl-protein kinase Cdelta-p38 MAPK signaling in response to ionizing radiation in human non-small cell lung cancer cells. *J Biol Chem*. 281:7049-7059.

Continolo, S., A. Baruzzi, M. Majeed, E. Caveggion, L. Fumagalli, C.A. Lowell, and G. Berton. 2005. The proto-oncogene Fgr regulates cell migration and this requires its plasma membrane localization. *Exp Cell Res*. 302:253-269.

Cook, T.A., T. Nagasaki, and G.G. Gundersen. 1998. Rho guanosine triphosphatase mediates the selective stabilization of microtubules induced by lysophosphatidic acid. *J Cell Biol*. 141:175-185.

Cory, S., and J.M. Adams. 2002. The Bcl2 family: regulators of the cellular life-or-death switch. *Nat Rev Cancer*. 2:647-656.

Coso, O.A., M. Chiariello, J.C. Yu, H. Teramoto, P. Crespo, N. Xu, T. Miki, and J.S. Gutkind. 1995. The small GTP-binding proteins Rac1 and Cdc42 regulate the activity of the JNK/SAPK signaling pathway. *Cell*. 81:1137-1146.

Costello, P.S., S.C. Cleverley, R. Galandrini, S.W. Henning, and D.A. Cantrell. 2000. The GTPase rho controls a p53-dependent survival checkpoint during thymopoiesis. *J Exp Med*. 192:77-85.

Coultas, L., M. Pellegrini, J.E. Visvader, G.J. Lindeman, L. Chen, J.M. Adams, D.C. Huang, and A. Strasser. 2003. Bfk: a novel weakly proapoptotic member of the Bcl-2 protein family with a BH3 and a BH2 region. *Cell Death Differ*. 10:185-192.

Cowell, C.F., I.K. Yan, T. Eiseler, A.C. Leightner, H. Doppler, and P. Storz. 2009. Loss of cell-cell contacts induces NF-kappaB via RhoA-mediated activation of protein kinase D1. *J Cell Biochem*. 106:714-728.

Cuenda, A., and S. Rousseau. 2007. p38 MAP-kinases pathway regulation, function and role in human diseases. *Biochim Biophys Acta*. 1773:1358-1375.

D'Avino, P.P. 2009. How to scaffold the contractile ring for a safe cytokinesis - lessons from Anillin-related proteins. *J Cell Sci*. 122:1071-1079.

D'Avino, P.P., M.S. Savoian, and D.M. Glover. 2005. Cleavage furrow formation and ingression during animal cytokinesis: a microtubule legacy. *J Cell Sci*. 118:1549-1558.

D'Avino, P.P., T. Takeda, L. Capalbo, W. Zhang, K.S. Lilley, E.D. Laue, and D.M. Glover. 2008. Interaction between Anillin and RacGAP50C connects the actomyosin contractile ring with spindle microtubules at the cell division site. *J Cell Sci*. 121:1151-1158.

De Chiara, G., M.E. Marcocci, M. Torcia, M. Lucibello, P. Rosini, P. Bonini, Y. Higashimoto, G. Damonte, A. Armirotti, S. Amodei, A.T. Palamara, T. Russo, E. Garaci, and F. Cozzolino. 2006. Bcl-2 Phosphorylation by p38 MAPK: identification of target sites and biologic consequences. *J Biol Chem*. 281:21353-21361.

Degterev, A., M. Boyce, and J. Yuan. 2003. A decade of caspases. *Oncogene*. 22:8543-8567.

del Peso, L., R. Hernandez-Alcoceba, N. Embade, A. Carnero, P. Esteve, C. Paje, and J.C. Lacal. 1997. Rho proteins induce metastatic properties in vivo. *Oncogene*. 15:3047-3057.

DeLeo, A.B., G. Jay, E. Appella, G.C. Dubois, L.W. Law, and L.J. Old. 1979. Detection of a transformation-related antigen in chemically induced sarcomas and other transformed cells of the mouse. *Proc Natl Acad Sci U S A*. 76:2420-2424.

Deng, L., G. Li, R. Li, Q. Liu, Q. He, and J. Zhang. Rho-kinase inhibitor, fasudil, suppresses glioblastoma cell line progression in vitro and in vivo. *Cancer Biol Ther*. 9.

Denoyelle, C., M. Vasse, M. Korner, Z. Mishal, F. Ganne, J.P. Vannier, J. Soria, and C. Soria. 2001. Cerivastatin, an inhibitor of HMG-CoA reductase, inhibits the signaling pathways involved in the invasiveness and metastatic properties of highly invasive breast cancer cell lines: an in vitro study. *Carcinogenesis*. 22:1139-1148.

DeWard, A.D., and A.S. Alberts. 2008. Microtubule stabilization: formins assert their independence. *Curr Biol*. 18:R605-608.

Di Cunto, F., S. Imarisio, E. Hirsch, V. Broccoli, A. Bulfone, A. Migheli, C. Atzori, E. Turco, R. Triolo, G.P. Dotto, L. Silengo, and F. Altruda. 2000. Defective neurogenesis in citron kinase knockout mice by altered cytokinesis and massive apoptosis. *Neuron*. 28:115-127.

Dib, K., F. Melander, and T. Andersson. 2001. Role of p190RhoGAP in beta 2 integrin regulation of RhoA in human neutrophils. *J Immunol*. 166:6311-6322.

Diekmann, D., S. Brill, M.D. Garrett, N. Totty, J. Hsuan, C. Monfries, C. Hall, L. Lim, and A. Hall. 1991. Bcr encodes a GTPase-activating protein for p21rac. *Nature*. 351:400-402.

Dijkers, P.F., R.H. Medema, J.W. Lammers, L. Koenderman, and P.J. Coffer. 2000. Expression of the pro-apoptotic Bcl-2 family member Bim is regulated by the forkhead transcription factor FKHR-L1. *Curr Biol*. 10:1201-1204.

Ditchfield, C., V.L. Johnson, A. Tighe, R. Ellston, C. Haworth, T. Johnson, A. Mortlock, N. Keen, and S.S. Taylor. 2003. Aurora B couples chromosome alignment with anaphase by targeting BubR1, Mad2, and Cenp-E to kinetochores. *J Cell Biol*. 161:267-280.

Drechsel, D.N., A.A. Hyman, A. Hall, and M. Glotzer. 1997. A requirement for Rho and Cdc42 during cytokinesis in Xenopus embryos. *Curr Biol*. 7:12-23.

Dreger, S.C., F. Schulz, J. Huelsenbeck, R. Gerhard, F. Hofmann, I. Just, and H. Genth. 2009. Killing of rat basophilic leukemia cells by lethal toxin from Clostridium sordellii: critical role of phosphatidylinositide 3'-OH kinase/Akt signaling. *Biochemistry*. 48:1785-1792.

Durcan, T.M., E.S. Halpin, T. Rao, N.S. Collins, E.K. Tribble, J.E. Hornick, and E.H. Hinchcliffe. 2008. Tektin 2 is required for central spindle microtubule organization and the completion of cytokinesis. *J Cell Biol*. 181:595-603.

Duronio, V. 2008. The life of a cell: apoptosis regulation by the PI3K/PKB pathway. *Biochem J*. 415:333-344.

Earhart, R.H. 1999. Docetaxel (Taxotere): preclinical and general clinical information. *Semin Oncol*. 26:8-13.

Echard, A., G.R. Hickson, E. Foley, and P.H. O'Farrell. 2004. Terminal cytokinesis events uncovered after an RNAi screen. *Curr Biol*. 14:1685-1693.

Edwards, D.C., L.C. Sanders, G.M. Bokoch, and G.N. Gill. 1999. Activation of LIM-kinase by Pak1 couples Rac/Cdc42 GTPase signalling to actin cytoskeletal dynamics. *Nat Cell Biol*. 1:253-259.

Effler, J.C., P.A. Iglesias, and D.N. Robinson. 2007. A mechanosensory system controls cell shape changes during mitosis. *Cell Cycle*. 6:30-35.

Egelhoff, T.T., D.J. Manstein, and J.A. Spudich. 1990. Complementation of myosin null mutants in Dictyostelium discoideum by direct functional selection. *Dev Biol*. 137:359-367.

Ellerbroek, S.M., K. Wennerberg, and K. Burridge. 2003. Serine phosphorylation negatively regulates RhoA in vivo. *J Biol Chem*. 278:19023-19031.

Enomoto, T. 1996. Microtubule disruption induces the formation of actin stress fibers and focal adhesions in cultured cells: possible involvement of the rho signal cascade. *Cell Struct Funct*. 21:317-326.

Ewings, K.E., K. Hadfield-Moorhouse, C.M. Wiggins, J.A. Wickenden, K. Balmanno, R. Gilley, K. Degenhardt, E. White, and S.J. Cook. 2007. ERK1/2-dependent phosphorylation of BimEL promotes its rapid dissociation from Mcl-1 and Bcl-xL. *Embo J*. 26:2856-2867.

Fan, M., and T.C. Chambers. 2001. Role of mitogen-activated protein kinases in the response of tumor cells to chemotherapy. *Drug Resist Updat*. 4:253-267.

Farnebo, M., V.J. Bykov, and K.G. Wiman. 2010. The p53 tumor suppressor: a master regulator of diverse cellular processes and therapeutic target in cancer. *Biochem Biophys Res Commun*. 396:85-89.

Feng, Y., J. Wen, and C.C. Chang. 2009. p38 Mitogen-activated protein kinase and hematologic malignancies. *Arch Pathol Lab Med*. 133:1850-1856.

Field, C.M., and B.M. Alberts. 1995. Anillin, a contractile ring protein that cycles from the nucleus to the cell cortex. *J Cell Biol*. 131:165-178.

Field, C.M., M. Coughlin, S. Doberstein, T. Marty, and W. Sullivan. 2005. Characterization of anillin mutants reveals essential roles in septin localization and plasma membrane integrity. *Development*. 132:2849-2860.

Fincham, V.J., A. Chudleigh, and M.C. Frame. 1999. Regulation of p190 Rho-GAP by v-Src is linked to cytoskeletal disruption during transformation. *J Cell Sci*. 112 (Pt 6):947-956.

Fordjour, A.K., and E.O. Harrington. 2009. PKCdelta influences p190 phosphorylation and activity: events independent of PKCdelta-mediated regulation of endothelial cell stress fiber and focal adhesion formation and barrier function. *Biochim Biophys Acta*. 1790:1179-1190.

Forget, M.A., R.R. Desrosiers, D. Gingras, and R. Beliveau. 2002. Phosphorylation states of Cdc42 and RhoA regulate their interactions with Rho GDP dissociation inhibitor and their extraction from biological membranes. *Biochem J*. 361:243-254.

Fortier, M., F. Comunale, J. Kucharczak, A. Blangy, S. Charrasse, and C. Gauthier-Rouviere. 2008. RhoE controls myoblast alignment prior fusion through RhoA and ROCK. *Cell Death Differ*. 15:1221-1231.

Foster, R., K.Q. Hu, D.A. Shaywitz, and J. Settleman. 1994. p190 RhoGAP, the major RasGAP-associated protein, binds GTP directly. *Mol Cell Biol*. 14:7173-7181.

Frame, M.C. 2004. Newest findings on the oldest oncogene; how activated src does it. *J Cell Sci*. 117:989-998.

Francis, P.A., M.G. Kris, J.R. Rigas, S.C. Grant, and V.A. Miller. 1995. Paclitaxel (Taxol) and docetaxel (Taxotere): active chemotherapeutic agents in lung cancer. *Lung Cancer*. 12 Suppl 1:S163-172.

Fromigue, O., E. Hay, D. Modrowski, S. Bouvet, A. Jacquel, P. Auberger, and P.J. Marie. 2006. RhoA GTPase inactivation by statins induces osteosarcoma cell apoptosis by inhibiting p42/p44-MAPKs-Bcl-2 signaling independently of BMP-2 and cell differentiation. *Cell Death Differ*. 13:1845-1856.

Fukata, M., M. Nakagawa, and K. Kaibuchi. 2003. Roles of Rho-family GTPases in cell polarisation and directional migration. *Curr Opin Cell Biol*. 15:590-597.

Fukui, K., S. Tamura, A. Wada, Y. Kamada, Y. Sawai, K. Imanaka, T. Kudara, I. Shimomura, and N. Hayashi. 2006. Expression and prognostic role of RhoA GTPases in hepatocellular carcinoma. *J Cancer Res Clin Oncol*. 132:627-633.

Fulda, S., and K.M. Debatin. 2006. Extrinsic versus intrinsic apoptosis pathways in anticancer chemotherapy. *Oncogene*. 25:4798-4811.

Fulda, S., E. Meyer, and K.M. Debatin. 2002. Inhibition of TRAIL-induced apoptosis by Bcl-2 overexpression. *Oncogene*. 21:2283-2294.

Gamblin, S.J., and S.J. Smerdon. 1998. GTPase-activating proteins and their complexes. *Curr Opin Struct Biol*. 8:195-201.

Gamper, A.M., and R.G. Roeder. 2008. Multivalent binding of p53 to the STAGA complex mediates coactivator recruitment after UV damage. *Mol Cell Biol*. 28:2517-2527.

Gardai, S.J., D.A. Hildeman, S.K. Frankel, B.B. Whitlock, S.C. Frasch, N. Borregaard, P. Marrack, D.L. Bratton, and P.M. Henson. 2004. Phosphorylation of Bax Ser184 by Akt regulates its activity and apoptosis in neutrophils. *J Biol Chem*. 279:21085-21095.

Gascoigne, K.E., and S.S. Taylor. 2009. How do anti-mitotic drugs kill cancer cells? *J Cell Sci*. 122:2579-2585.

Georges, P.C., N.M. Hadzimichalis, E.S. Sweet, and B.L. Firestein. 2008. The yin-yang of dendrite morphology: unity of actin and microtubules. *Mol Neurobiol*. 38:270-284.

Ghobrial, I.M., T.E. Witzig, and A.A. Adjei. 2005. Targeting apoptosis pathways in cancer therapy. *CA Cancer J Clin*. 55:178-194.

Giet, R., and D.M. Glover. 2001. Drosophila aurora B kinase is required for histone H3 phosphorylation and condensin recruitment during chromosome condensation and to organize the central spindle during cytokinesis. *J Cell Biol*. 152:669-682.

Glise, B., and S. Noselli. 1997. Coupling of Jun amino-terminal kinase and Decapentaplegic signaling pathways in Drosophila morphogenesis. *Genes Dev*. 11:1738-1747.

Glomset, J.A., and C.C. Farnsworth. 1994. Role of protein modification reactions in programming interactions between ras-related GTPases and cell membranes. *Annu Rev Cell Biol*. 10:181-205.

Glotzer, M. 2001. Animal cell cytokinesis. *Annu Rev Cell Dev Biol*. 17:351-386.

Gomez del Pulgar, T., S.A. Benitah, P.F. Valeron, C. Espina, and J.C. Lacal. 2005. Rho GTPase expression in tumourigenesis: evidence for a significant link. *Bioessays*. 27:602-613.

Goode, B.L., and M.J. Eck. 2007. Mechanism and function of formins in the control of actin assembly. *Annu Rev Biochem*. 76:593-627.

Gorgoulis, V.G., L.V. Vassiliou, P. Karakaidos, P. Zacharatos, A. Kotsinas, T. Liloglou, M. Venere, R.A. Ditullio, Jr., N.G. Kastrinakis, B. Levy, D. Kletsas, A. Yoneta, M. Herlyn, C. Kittas, and T.D. Halazonetis. 2005. Activation of the DNA damage checkpoint and genomic instability in human precancerous lesions. *Nature*. 434:907-913.

Goulimari, P., T.M. Kitzing, H. Knieling, D.T. Brandt, S. Offermanns, and R. Grosse. 2005. Galpha12/13 is essential for directed cell migration and localized Rho-Dia1 function. *J Biol Chem*. 280:42242-42251.

Grande-Garcia, A., A. Echarri, J. de Rooij, N.B. Alderson, C.M. Waterman-Storer, J.M. Valdivielso, and M.A. del Pozo. 2007. Caveolin-1 regulates cell polarization and directional migration through Src kinase and Rho GTPases. *J Cell Biol*. 177:683-694.

Green, D.R., and G. Kroemer. 2004. The pathophysiology of mitochondrial cell death. *Science*. 305:626-629.

Green, D.R., and J.C. Reed. 1998. Mitochondria and apoptosis. *Science*. 281:1309-1312.

Guo, B., A. Godzik, and J.C. Reed. 2001. Bcl-G, a novel pro-apoptotic member of the Bcl-2 family. *J Biol Chem*. 276:2780-2785.

Haeusler, L.C., L. Blumenstein, P. Stege, R. Dvorsky, and M.R. Ahmadian. 2003. Comparative functional analysis of the Rac GTPases. *FEBS Lett*. 555:556-560.

Hall, A. 1990. The cellular functions of small GTP-binding proteins. *Science*. 249:635-640.

Hall, A. 2005. Rho GTPases and the control of cell behaviour. *Biochem Soc Trans*. 33:891-895.

Hall, A. 2009. The cytoskeleton and cancer. *Cancer Metastasis Rev*. 28:5-14.

Hamid, S.A., H.S. Bower, and G.F. Baxter. 2007. Rho kinase activation plays a major role as a mediator of irreversible injury in reperfused myocardium. *Am J Physiol Heart Circ Physiol*. 292:H2598-2606.

Hanahan, D., and R.A. Weinberg. 2000. The hallmarks of cancer. *Cell*. 100:57-70.

Harvey, J.J. 1964. An Unidentified Virus Which Causes the Rapid Production of Tumours in Mice. *Nature*. 204:1104-1105.

Haskell, M.D., A.L. Nickles, J.M. Agati, L. Su, B.D. Dukes, and S.J. Parsons. 2001a. Phosphorylation of p190 on Tyr1105 by c-Src is necessary but not sufficient for EGF-induced actin disassembly in C3H10T1/2 fibroblasts. *J Cell Sci*. 114:1699-1708.

Haskell, M.D., J.K. Slack, J.T. Parsons, and S.J. Parsons. 2001b. c-Src tyrosine phosphorylation of epidermal growth factor receptor, P190 RhoGAP, and focal adhesion kinase regulates diverse cellular processes. *Chem Rev*. 101:2425-2440.

Hauf, S., R.W. Cole, S. LaTerra, C. Zimmer, G. Schnapp, R. Walter, A. Heckel, J. van Meel, C.L. Rieder, and J.M. Peters. 2003. The small molecule Hesperadin reveals a role for Aurora B in correcting kinetochore-microtubule attachment and in maintaining the spindle assembly checkpoint. *J Cell Biol*. 161:281-294.

Hayden, J.H., S.S. Bowser, and C.L. Rieder. 1990. Kinetochores capture astral microtubules during chromosome attachment to the mitotic spindle: direct visualization in live newt lung cells. *J Cell Biol*. 111:1039-1045.

He, H., M. Yim, K.H. Liu, S.C. Cody, A. Shulkes, and G.S. Baldwin. 2008. Involvement of G proteins of the Rho family in the regulation of Bcl-2-like protein expression and caspase 3 activation by Gastrins. *Cell Signal*. 20:83-93.

Heasman, S.J., and A.J. Ridley. 2008. Mammalian Rho GTPases: new insights into their functions from in vivo studies. *Nat Rev Mol Cell Biol*. 9:690-701.

Hernandez, S.E., J. Settleman, and A.J. Koleske. 2004. Adhesion-dependent regulation of p190RhoGAP in the developing brain by the Abl-related gene tyrosine kinase. *Curr Biol*. 14:691-696.

Hickson, G.R., and P.H. O'Farrell. 2008a. Anillin: a pivotal organizer of the cytokinetic machinery. *Biochem Soc Trans*. 36:439-441.

Hickson, G.R., and P.H. O'Farrell. 2008b. Rho-dependent control of anillin behavior during cytokinesis. *J Cell Biol*. 180:285-294.

Hill, C.S., J. Wynne, and R. Treisman. 1995. The Rho family GTPases RhoA, Rac1, and CDC42Hs regulate transcriptional activation by SRF. *Cell*. 81:1159-1170.

Hippenstiel, S., B. Schmeck, P.D. N'Guessan, J. Seybold, M. Krull, K. Preissner, C.V. Eichel-Streiber, and N. Suttorp. 2002a. Rho protein inactivation induced apoptosis of cultured human endothelial cells. *Am J Physiol Lung Cell Mol Physiol*. 283:L830-838.

Hippenstiel, S., B. Schmeck, J. Seybold, M. Krull, C. Eichel-Streiber, and N. Suttorp. 2002b. Reduction of tumor necrosis factor-alpha (TNF-alpha) related nuclear factor-kappaB (NF-kappaB) translocation but not inhibitor kappa-B (Ikappa-B)-degradation by Rho protein inhibition in human endothelial cells. *Biochem Pharmacol*. 64:971-977.

Hirata, K., A. Kikuchi, T. Sasaki, S. Kuroda, K. Kaibuchi, Y. Matsuura, H. Seki, K. Saida, and Y. Takai. 1992. Involvement of rho p21 in the GTP-enhanced calcium ion sensitivity of smooth muscle contraction. *J Biol Chem*. 267:8719-8722.

Hirose, M., T. Ishizaki, N. Watanabe, M. Uehata, O. Kranenburg, W.H. Moolenaar, F. Matsumura, M. Maekawa, H. Bito, and S. Narumiya. 1998. Molecular dissection of the Rho-associated protein kinase (p160ROCK)-regulated neurite remodeling in neuroblastoma N1E-115 cells. *J Cell Biol*. 141:1625-1636.

Hockenbery, D., G. Nunez, C. Milliman, R.D. Schreiber, and S.J. Korsmeyer. 1990. Bcl-2 is an inner mitochondrial membrane protein that blocks programmed cell death. *Nature*. 348:334-336.

Hoffman, G.R., and R.A. Cerione. 2002. Signaling to the Rho GTPases: networking with the DH domain. *FEBS Lett*. 513:85-91.

Holinstat, M., N. Knezevic, M. Broman, A.M. Samarel, A.B. Malik, and D. Mehta. 2006. Suppression of RhoA activity by focal adhesion kinase-induced activation of p190RhoGAP: role in regulation of endothelial permeability. *J Biol Chem*. 281:2296-2305.

Honda, R., R. Korner, and E.A. Nigg. 2003. Exploring the functional interactions between Aurora B, INCENP, and survivin in mitosis. *Mol Biol Cell*. 14:3325-3341.

Horiuchi, A., N. Kikuchi, R. Osada, C. Wang, A. Hayashi, T. Nikaido, and I. Konishi. 2008. Overexpression of RhoA enhances peritoneal dissemination: RhoA suppression with Lovastatin may be useful for ovarian cancer. *Cancer Sci*. 99:2532-2539.

Horiuchi, H., M. Kawata, M. Katayama, Y. Yoshida, T. Musha, S. Ando, and Y. Takai. 1991. A novel prenyltransferase for a small GTP-binding protein having a C-terminal Cys-Ala-Cys structure. *J Biol Chem*. 266:16981-16984.

Hsia, C.Y., S. Cheng, A.M. Owyang, S.F. Dowdy, and H.C. Liou. 2002. c-Rel regulation of the cell cycle in primary mouse B lymphocytes. *Int Immunol*. 14:905-916.

Hsu, S.Y., P. Lin, and A.J. Hsueh. 1998. BOD (Bcl-2-related ovarian death gene) is an ovarian BH3 domain-containing proapoptotic Bcl-2 protein capable of dimerization with diverse antiapoptotic Bcl-2 members. *Mol Endocrinol*. 12:1432-1440.

Hu, K.Q., and J. Settleman. 1997. Tandem SH2 binding sites mediate the RasGAP-RhoGAP interaction: a conformational mechanism for SH3 domain regulation. *EMBO J*. 16:473-483.

Huang, Y., Y. Fang, J.M. Dziadyk, J.S. Norris, and W. Fan. 2002. The possible correlation between activation of NF-kappaB/IkappaB pathway and the susceptibility of tumor cells to paclitaxel-induced apoptosis. *Oncol Res*. 13:113-122.

Huang, Y., K.R. Johnson, J.S. Norris, and W. Fan. 2000. Nuclear factor-kappaB/IkappaB signaling pathway may contribute to the mediation of paclitaxel-induced apoptosis in solid tumor cells. *Cancer Res*. 60:4426-4432.

Hubner, A., T. Barrett, R.A. Flavell, and R.J. Davis. 2008. Multisite phosphorylation regulates Bim stability and apoptotic activity. *Mol Cell*. 30:415-425.

Huot, M.E., C.M. Brown, N. Lamarche-Vane, and S. Richard. 2009. An adaptor role for cytoplasmic Sam68 in modulating Src activity during cell polarization. *Mol Cell Biol*. 29:1933-1943.

Ichetovkin, I., J. Han, K.M. Pang, D.A. Knecht, and J.S. Condeelis. 2000. Actin filaments are severed by both native and recombinant dictyostelium cofilin but to different extents. *Cell Motil Cytoskeleton*. 45:293-306.

Inoshita, S., K. Takeda, T. Hatai, Y. Terada, M. Sano, J. Hata, A. Umezawa, and H. Ichijo. 2002. Phosphorylation and inactivation of myeloid cell leukemia 1 by JNK in response to oxidative stress. *J Biol Chem*. 277:43730-43734.

Institute, N.C. 2011. Clinical Trials. United States National Institutes of Health.

Isaacs, J.T. 1993. Role of programmed cell death in carcinogenesis. *Environ Health Perspect*. 101 Suppl 5:27-33.

Ishizaki, T., Y. Morishima, M. Okamoto, T. Furuyashiki, T. Kato, and S. Narumiya. 2001. Coordination of microtubules and the actin cytoskeleton by the Rho effector mDia1. *Nat Cell Biol*. 3:8-14.

Ishizaki, T., M. Naito, K. Fujisawa, M. Maekawa, N. Watanabe, Y. Saito, and S. Narumiya. 1997. p160ROCK, a Rho-associated coiled-coil forming protein kinase, works downstream of Rho and induces focal adhesions. *FEBS Lett*. 404:118-124.

Isomura, M., A. Kikuchi, N. Ohga, and Y. Takai. 1991. Regulation of binding of rhoB p20 to membranes by its specific regulatory protein, GDP dissociation inhibitor. *Oncogene*. 6:119-124.

Jackson, R.J., J. Adnane, D. Coppola, A. Cantor, S.M. Sebti, and W.J. Pledger. 2002. Loss of the cell cycle inhibitors p21(Cip1) and p27(Kip1) enhances tumorigenesis in knockout mouse models. *Oncogene*. 21:8486-8497.

Jaffe, A.B., and A. Hall. 2005. Rho GTPases: biochemistry and biology. *Annu Rev Cell Dev Biol*. 21:247-269.

Jalink, K., E.J. van Corven, T. Hengeveld, N. Morii, S. Narumiya, and W.H. Moolenaar. 1994. Inhibition of lysophosphatidate- and thrombin-induced neurite retraction and neuronal cell rounding by ADP ribosylation of the small GTP-binding protein Rho. *J Cell Biol*. 126:801-810.

Janiak, A., E.A. Zemskov, and A.M. Belkin. 2006. Cell surface transglutaminase promotes RhoA activation via integrin clustering and suppression of the Src-p190RhoGAP signaling pathway. *Mol Biol Cell*. 17:1606-1619.

Janssen, K., S. Pohlmann, R.U. Janicke, K. Schulze-Osthoff, and U. Fischer. 2007. Apaf-1 and caspase-9 deficiency prevents apoptosis in a Bax-controlled pathway and promotes clonogenic survival during paclitaxel treatment. *Blood*. 110:3662-3672.

Jantsch-Plunger, V., P. Gonczy, A. Romano, H. Schnabel, D. Hamill, R. Schnabel, A.A. Hyman, and M. Glotzer. 2000. CYK-4: A Rho family gtpase activating protein (GAP) required for central spindle formation and cytokinesis. *J Cell Biol*. 149:1391-1404.

Jazirehi, A.R., and B. Bonavida. 2004. Resveratrol modifies the expression of apoptotic regulatory proteins and sensitizes non-Hodgkin's lymphoma and multiple myeloma cell lines to paclitaxel-induced apoptosis. *Mol Cancer Ther*. 3:71-84.

Jeon, C.Y., H.J. Kim, J.Y. Lee, J.B. Kim, S.C. Kim, and J.B. Park. 2010a. p190RhoGAP and Rap-dependent RhoGAP (ARAP3) inactivate RhoA in response to nerve growth factor leading to neurite outgrowth from PC12 cells. *Exp Mol Med*. 42:335-344.

Jeon, C.Y., H.J. Kim, H. Morii, N. Mori, J. Settleman, J.Y. Lee, J. Kim, S.C. Kim, and J.B. Park. 2010b. Neurite outgrowth from PC12 cells by basic fibroblast growth factor (bFGF) is mediated by RhoA inactivation through p190RhoGAP and ARAP3. *J Cell Physiol*. 224:786-794.

Jiang, W., M. Betson, R. Mulloy, R. Foster, M. Levay, E. Ligeti, and J. Settleman. 2008. p190A RhoGAP is a glycogen synthase kinase-3-beta substrate required for polarized cell migration. *J Biol Chem*. 283:20978-20988.

Jiang, W., R. Sordella, G.C. Chen, S. Hakre, A.L. Roy, and J. Settleman. 2005. An FF domain-dependent protein interaction mediates a signaling pathway for growth factor-induced gene expression. *Mol Cell*. 17:23-35.

Joerger, A.C., and A.R. Fersht. 2007. Structural biology of the tumor suppressor p53 and cancer-associated mutants. *Adv Cancer Res*. 97:1-23.

Jordan, M.A., R.J. Toso, D. Thrower, and L. Wilson. 1993. Mechanism of mitotic block and inhibition of cell proliferation by taxol at low concentrations. *Proc Natl Acad Sci U S A*. 90:9552-9556.

Jordan, M.A., K. Wendell, S. Gardiner, W.B. Derry, H. Copp, and L. Wilson. 1996. Mitotic block induced in HeLa cells by low concentrations of paclitaxel (Taxol) results in abnormal mitotic exit and apoptotic cell death. *Cancer Res*. 56:816-825.

Jordan, M.A., and L. Wilson. 2004. Microtubules as a target for anticancer drugs. *Nat Rev Cancer*. 4:253-265.

Jordan, P., R. Brazao, M.G. Boavida, C. Gespach, and E. Chastre. 1999. Cloning of a novel human Rac1b splice variant with increased expression in colorectal tumors. *Oncogene*. 18:6835-6839.

Jordan, P., and R. Karess. 1997. Myosin light chain-activating phosphorylation sites are required for oogenesis in Drosophila. *J Cell Biol*. 139:1805-1819.

Just, I., H.P. Richter, U. Prepens, C. von Eichel-Streiber, and K. Aktories. 1994. Probing the action of Clostridium difficile toxin B in Xenopus laevis oocytes. *J Cell Sci*. 107 (Pt 6):1653-1659.

Just, I., J. Selzer, M. Wilm, C. von Eichel-Streiber, M. Mann, and K. Aktories. 1995. Glucosylation of Rho proteins by Clostridium difficile toxin B. *Nature*. 375:500-503.

Kaibuchi, K., S. Kuroda, and M. Amano. 1999. Regulation of the cytoskeleton and cell adhesion by the Rho family GTPases in mammalian cells. *Annu Rev Biochem*. 68:459-486.

Kaitna, S., M. Mendoza, V. Jantsch-Plunger, and M. Glotzer. 2000. Incenp and an aurora-like kinase form a complex essential for chromosome segregation and efficient completion of cytokinesis. *Curr Biol*. 10:1172-1181.

Kallio, M.J., M.L. McCleland, P.T. Stukenberg, and G.J. Gorbsky. 2002. Inhibition of aurora B kinase blocks chromosome segregation, overrides the spindle checkpoint, and perturbs microtubule dynamics in mitosis. *Curr Biol*. 12:900-905.

Kamijo, K., N. Ohara, M. Abe, T. Uchimura, H. Hosoya, J.S. Lee, and T. Miki. 2006. Dissecting the role of Rho-mediated signaling in contractile ring formation. *Mol Biol Cell*. 17:43-55.

Kang, H.J., S.H. Lee, J.E. Price, and L.S. Kim. 2009. Curcumin suppresses the paclitaxel-induced nuclear factor-kappaB in breast cancer cells and potentiates the growth inhibitory effect of paclitaxel in a breast cancer nude mice model. *Breast J*. 15:223-229.

Karlsson, R., E.D. Pedersen, Z. Wang, and C. Brakebusch. 2009. Rho GTPase function in tumorigenesis. *Biochim Biophys Acta*. 1796:91-98.

Kasibhatla, S., L. Genestier, and D.R. Green. 1999. Regulation of fas-ligand expression during activation-induced cell death in T lymphocytes via nuclear factor kappaB. *J Biol Chem*. 274:987-992.

Kataoka, T., N. Holler, O. Micheau, F. Martinon, A. Tinel, K. Hofmann, and J. Tschopp. 2001. Bcl-rambo, a novel Bcl-2 homologue that induces apoptosis via its unique C-terminal extension. *J Biol Chem*. 276:19548-19554.

Katayama, M., M. Kawata, Y. Yoshida, H. Horiuchi, T. Yamamoto, Y. Matsuura, and Y. Takai. 1991. The posttranslationally modified C-terminal structure of bovine aortic smooth muscle rhoA p21. *J Biol Chem*. 266:12639-12645.

Kato, T., N. Watanabe, Y. Morishima, A. Fujita, T. Ishizaki, and S. Narumiya. 2001. Localization of a mammalian homolog of diaphanous, mDia1, to the mitotic spindle in HeLa cells. *J Cell Sci*. 114:775-784.

Ke, N., A. Godzik, and J.C. Reed. 2001. Bcl-B, a novel Bcl-2 family member that differentially binds and regulates Bax and Bak. *J Biol Chem*. 276:12481-12484.

Kelling, J., K. Sullivan, L. Wilson, and M.A. Jordan. 2003. Suppression of centromere dynamics by Taxol in living osteosarcoma cells. *Cancer Res*. 63:2794-2801.

Kelly, A.E., S.C. Sampath, T.A. Maniar, E.M. Woo, B.T. Chait, and H. Funabiki. 2007. Chromosomal enrichment and activation of the aurora B pathway are coupled to spatially regulate spindle assembly. *Dev Cell*. 12:31-43.

Kerr, J.F., A.H. Wyllie, and A.R. Currie. 1972. Apoptosis: a basic biological phenomenon with wide-ranging implications in tissue kinetics. *Br J Cancer*. 26:239-257.

Keshet, Y., and R. Seger. 2010. The MAP kinase signaling cascades: a system of hundreds of components regulates a diverse array of physiological functions. *Methods Mol Biol*. 661:3-38.

Khan, O.M., M.X. Ibrahim, I.M. Jonsson, C. Karlsson, M. Liu, A.K. Sjogren, F.J. Olofsson, M. Brisslert, S. Andersson, C. Ohlsson, L.M. Hulten, M. Bokarewa, and M.O. Bergo. 2011. Geranylgeranyltransferase type I (GGTase-I) deficiency hyperactivates macrophages and induces erosive arthritis in mice. *J Clin Invest*. 121:628-639.

Khosravi-Far, R., P.A. Solski, G.J. Clark, M.S. Kinch, and C.J. Der. 1995. Activation of Rac1, RhoA, and mitogen-activated protein kinases is required for Ras transformation. *Mol Cell Biol*. 15:6443-6453.

Khwaja, A., C.C. Sharpe, M. Noor, and B.M. Hendry. 2006. The role of geranylgeranylated proteins in human mesangial cell proliferation. *Kidney Int*. 70:1296-1304.

Kim, B.C., J.Y. Yi, S.J. Yi, I.C. Shin, K.S. Ha, B.H. Jhun, S.B. Hwang, and J.H. Kim. 1998. Rac GTPase activity is essential for EGF-induced mitogenesis. *Mol Cells*. 8:90-95.

Kim, D.H., R. Feinbaum, G. Alloing, F.E. Emerson, D.A. Garsin, H. Inoue, M. Tanaka-Hino, N. Hisamoto, K. Matsumoto, M.W. Tan, and F.M. Ausubel. 2002. A conserved p38 MAP kinase pathway in Caenorhabditis elegans innate immunity. *Science*. 297:623-626.

Kim, Y., J.Y. Sung, I. Ceglia, K.W. Lee, J.H. Ahn, J.M. Halford, A.M. Kim, S.P. Kwak, J.B. Park, S. Ho Ryu, A. Schenck, B. Bardoni, J.D. Scott, A.C. Nairn, and P. Greengard. 2006. Phosphorylation of WAVE1 regulates actin polymerization and dendritic spine morphology. *Nature*. 442:814-817.

Kimura, K., M. Ito, M. Amano, K. Chihara, Y. Fukata, M. Nakafuku, B. Yamamori, J. Feng, T. Nakano, K. Okawa, A. Iwamatsu, and K. Kaibuchi. 1996. Regulation of myosin phosphatase by Rho and Rho-associated kinase (Rho-kinase). *Science*. 273:245-248.

Kimura, K., T. Tsuji, Y. Takada, T. Miki, and S. Narumiya. 2000. Accumulation of GTP-bound RhoA during cytokinesis and a critical role of ECT2 in this accumulation. *J Biol Chem*. 275:17233-17236.

Kinoshita, M., C.M. Field, M.L. Coughlin, A.F. Straight, and T.J. Mitchison. 2002. Self- and actin-templated assembly of Mammalian septins. *Dev Cell*. 3:791-802.

Kischkel, F.C., S. Hellbardt, I. Behrmann, M. Germer, M. Pawlita, P.H. Krammer, and M.E. Peter. 1995. Cytotoxicity-dependent APO-1 (Fas/CD95)-associated proteins form a death-inducing signaling complex (DISC) with the receptor. *EMBO J*. 14:5579-5588.

Kishi, K., T. Sasaki, S. Kuroda, T. Itoh, and Y. Takai. 1993. Regulation of cytoplasmic division of Xenopus embryo by rho p21 and its inhibitory GDP/GTP exchange protein (rho GDI). *J Cell Biol*. 120:1187-1195.

Koehler, J.A., and M.F. Moran. 2001. Regulation of extracellular signal-regulated kinase activity by p120 RasGAP does not involve its pleckstrin homology or calcium-dependent lipid

binding domains but does require these domains to regulate cell proliferation. *Cell Growth Differ*. 12:551-561.

Koh, C.G. 2006. Rho GTPases and their regulators in neuronal functions and development. *Neurosignals*. 15:228-237.

Kollareddy, M., P. Dzubak, D. Zheleva, and M. Hajduch. 2008. Aurora kinases: structure, functions and their association with cancer. *Biomed Pap Med Fac Univ Palacky Olomouc Czech Repub*. 152:27-33.

Kolomeichuk, S.N., D.T. Terrano, C.S. Lyle, K. Sabapathy, and T.C. Chambers. 2008. Distinct signaling pathways of microtubule inhibitors--vinblastine and Taxol induce JNK-dependent cell death but through AP-1-dependent and AP-1-independent mechanisms, respectively. *FEBS J*. 275:1889-1899.

Komatsu, S., T. Yano, M. Shibata, R.A. Tuft, and M. Ikebe. 2000. Effects of the regulatory light chain phosphorylation of myosin II on mitosis and cytokinesis of mammalian cells. *J Biol Chem*. 275:34512-34520.

Komuro, R., T. Sasaki, K. Takaishi, S. Orita, and Y. Takai. 1996. Involvement of Rho and Rac small G proteins and Rho GDI in Ca2+-dependent exocytosis from PC12 cells. *Genes Cells*. 1:943-951.

Kontgen, F., R.J. Grumont, A. Strasser, D. Metcalf, R. Li, D. Tarlinton, and S. Gerondakis. 1995. Mice lacking the c-rel proto-oncogene exhibit defects in lymphocyte proliferation, humoral immunity, and interleukin-2 expression. *Genes Dev*. 9:1965-1977.

Kortlever, R.M., P.J. Higgins, and R. Bernards. 2006. Plasminogen activator inhibitor-1 is a critical downstream target of p53 in the induction of replicative senescence. *Nat Cell Biol*. 8:877-884.

Kosako, H., T. Yoshida, F. Matsumura, T. Ishizaki, S. Narumiya, and M. Inagaki. 2000. Rho-kinase/ROCK is involved in cytokinesis through the phosphorylation of myosin light chain and not ezrin/radixin/moesin proteins at the cleavage furrow. *Oncogene*. 19:6059-6064.

Kovar, D.R., and T.D. Pollard. 2004. Insertional assembly of actin filament barbed ends in association with formins produces piconewton forces. *Proc Natl Acad Sci U S A*. 101:14725-14730.

Kozma, R., S. Ahmed, A. Best, and L. Lim. 1995. The Ras-related protein Cdc42Hs and bradykinin promote formation of peripheral actin microspikes and filopodia in Swiss 3T3 fibroblasts. *Mol Cell Biol*. 15:1942-1952.

Kozma, R., S. Sarner, S. Ahmed, and L. Lim. 1997. Rho family GTPases and neuronal growth cone remodelling: relationship between increased complexity induced by Cdc42Hs, Rac1, and acetylcholine and collapse induced by RhoA and lysophosphatidic acid. *Mol Cell Biol*. 17:1201-1211.

Kozopas, K.M., T. Yang, H.L. Buchan, P. Zhou, and R.W. Craig. 1993. MCL1, a gene expressed in programmed myeloid cell differentiation, has sequence similarity to BCL2. *Proc Natl Acad Sci U S A*. 90:3516-3520.

Krijnen, P.A., J.A. Sipkens, J.W. Molling, J.A. Rauwerda, C.D. Stehouwer, A. Muller, W.J. Paulus, G.P. van Nieuw Amerongen, C.E. Hack, A.J. Verhoeven, V.W. van Hinsbergh, and H.W. Niessen. 2010. Inhibition of Rho-ROCK signaling induces apoptotic and non-apoptotic PS exposure in cardiomyocytes via inhibition of flippase. *J Mol Cell Cardiol*. 49:781-790.

Kruse, J.P., and W. Gu. 2009. Modes of p53 regulation. *Cell*. 137:609-622.

Kubo, M., T. Morisaki, K. Matsumoto, A. Tasaki, N. Yamanaka, H. Nakashima, H. Kuroki, K. Nakamura, M. Nakamura, and M. Katano. 2005. Paclitaxel probably enhances cytotoxicity of natural killer cells against breast carcinoma cells by increasing perforin production. *Cancer Immunol Immunother*. 54:468-476.

Kucharczak, J., M.J. Simmons, Y. Fan, and C. Gelinas. 2003. To be, or not to be: NF-kappaB is the answer--role of Rel/NF-kappaB in the regulation of apoptosis. *Oncogene*. 22:8961-8982.

Kukhta, V.K., N.V. Marozkina, I.G. Sokolchik, and E.V. Bogaturova. 2003. Molecular mechanisms of apoptosis. *Ukr Biokhim Zh*. 75:5-9.

Kusama, T., M. Mukai, H. Endo, O. Ishikawa, M. Tatsuta, H. Nakamura, and M. Inoue. 2006. Inactivation of Rho GTPases by p190 RhoGAP reduces human pancreatic cancer cell invasion and metastasis. *Cancer Sci*. 97:848-853.

Kutuk, O., and A. Letai. 2010. Displacement of Bim by Bmf and Puma rather than increase in Bim level mediates paclitaxel-induced apoptosis in breast cancer cells. *Cell Death Differ*. 17:1624-1635.

Kyriakis, J.M., and J. Avruch. 2001. Mammalian mitogen-activated protein kinase signal transduction pathways activated by stress and inflammation. *Physiol Rev*. 81:807-869.

Lamaze, C., T.H. Chuang, L.J. Terlecky, G.M. Bokoch, and S.L. Schmid. 1996. Regulation of receptor-mediated endocytosis by Rho and Rac. *Nature*. 382:177-179.

Lamprecht, R., C.R. Farb, and J.E. LeDoux. 2002. Fear memory formation involves p190 RhoGAP and ROCK proteins through a GRB2-mediated complex. *Neuron*. 36:727-738.

Lang, P., F. Gesbert, M. Delespine-Carmagnat, R. Stancou, M. Pouchelet, and J. Bertoglio. 1996. Protein kinase A phosphorylation of RhoA mediates the morphological and functional effects of cyclic AMP in cytotoxic lymphocytes. *Embo J*. 15:510-519.

Laptenko, O., and C. Prives. 2006. Transcriptional regulation by p53: one protein, many possibilities. *Cell Death Differ*. 13:951-961.

Lassus, P., P. Roux, O. Zugasti, A. Philips, P. Fort, and U. Hibner. 2000. Extinction of rac1 and Cdc42Hs signalling defines a novel p53-dependent apoptotic pathway. *Oncogene*. 19:2377-2385.

Le, S.S., F.A. Loucks, H. Udo, S. Richardson-Burns, R.A. Phelps, R.J. Bouchard, H. Barth, K. Aktories, K.L. Tyler, E.R. Kandel, K.A. Heidenreich, and D.A. Linseman. 2005. Inhibition of Rac GTPase triggers a c-Jun- and Bim-dependent mitochondrial apoptotic cascade in cerebellar granule neurons. *J Neurochem*. 94:1025-1039.

Lee, S.Y., J.S. Cho, D.Y. Yuk, D.C. Moon, J.K. Jung, H.S. Yoo, Y.M. Lee, S.B. Han, K.W. Oh, and J.T. Hong. 2009. Obovatol enhances docetaxel-induced prostate and colon cancer cell death through inactivation of nuclear transcription factor-kappaB. *J Pharmacol Sci*. 111:124-136.

Lei, K., and R.J. Davis. 2003. JNK phosphorylation of Bim-related members of the Bcl2 family induces Bax-dependent apoptosis. *Proc Natl Acad Sci U S A*. 100:2432-2437.

Lens, S.M., E.E. Voest, and R.H. Medema. 2010. Shared and separate functions of polo-like kinases and aurora kinases in cancer. *Nat Rev Cancer*. 10:825-841.

Li, R., T. Moudgil, H.J. Ross, and H.M. Hu. 2005. Apoptosis of non-small-cell lung cancer cell lines after paclitaxel treatment involves the BH3-only proapoptotic protein Bim. *Cell Death Differ*. 12:292-303.

Li, R., B. Zhang, and Y. Zheng. 1997. Structural determinants required for the interaction between Rho GTPase and the GTPase-activating domain of p190. *J Biol Chem*. 272:32830-32835.

Li, X., L. Liu, J.C. Tupper, D.D. Bannerman, R.K. Winn, S.M. Sebti, A.D. Hamilton, and J.M. Harlan. 2002. Inhibition of protein geranylgeranylation and RhoA/RhoA kinase pathway induces apoptosis in human endothelial cells. *J Biol Chem*. 277:15309-15316.

Li, X.R., F. Ji, J. Ouyang, W. Wu, L.Y. Qian, and K.Y. Yang. 2006. Overexpression of RhoA is associated with poor prognosis in hepatocellular carcinoma. *Eur J Surg Oncol*. 32:1130-1134.

Li, Y., D. Xing, Q. Chen, and W.R. Chen. 2010. Enhancement of chemotherapeutic agent-induced apoptosis by inhibition of NF-kappaB using ursolic acid. *Int J Cancer*. 127:462-473.

Li, Z., J. Zhang, Z. Liu, C.W. Woo, and C.J. Thiele. 2007. Downregulation of Bim by brain-derived neurotrophic factor activation of TrkB protects neuroblastoma cells from paclitaxel but not etoposide or cisplatin-induced cell death. *Cell Death Differ*. 14:318-326.

Liang, X., N.A. Draghi, and M.D. Resh. 2004. Signaling from integrins to Fyn to Rho family GTPases regulates morphologic differentiation of oligodendrocytes. *J Neurosci*. 24:7140-7149.

Ligeti, E., M.C. Dagher, S.E. Hernandez, A.J. Koleske, and J. Settleman. 2004. Phospholipids can switch the GTPase substrate preference of a GTPase-activating protein. *J Biol Chem*. 279:5055-5058.

Ligeti, E., and J. Settleman. 2006. Regulation of RhoGAP specificity by phospholipids and prenylation. *Methods Enzymol*. 406:104-117.

Lin, B., C. Williams-Skipp, Y. Tao, M.S. Schleicher, L.L. Cano, R.C. Duke, and R.I. Scheinman. 1999. NF-kappaB functions as both a proapoptotic and antiapoptotic regulatory factor within a single cell type. *Cell Death Differ*. 6:570-582.

Liston, P., W.G. Fong, and R.G. Korneluk. 2003. The inhibitors of apoptosis: there is more to life than Bcl2. *Oncogene*. 22:8568-8580.

Liu, C.A., M.J. Wang, C.W. Chi, C.W. Wu, and J.Y. Chen. 2004. Overexpression of rho effector rhotekin confers increased survival in gastric adenocarcinoma. *J Biomed Sci*. 11:661-670.

Liu, Y., and M.F. Kulesz-Martin. 2006. Sliding into home: facilitated p53 search for targets by the basic DNA binding domain. *Cell Death Differ*. 13:881-884.

Loucks, F.A., S.S. Le, A.K. Zimmermann, K.R. Ryan, H. Barth, K. Aktories, and D.A. Linseman. 2006. Rho family GTPase inhibition reveals opposing effects of mitogen-activated protein kinase kinase/extracellular signal-regulated kinase and Janus kinase/signal transducer and activator of transcription signaling cascades on neuronal survival. *J Neurochem*. 97:957-967.

Lu, W.J., J.F. Amatruda, and J.M. Abrams. 2009. p53 ancestry: gazing through an evolutionary lens. *Nat Rev Cancer*. 9:758-762.

Luduena, R.F. 1998. Multiple forms of tubulin: different gene products and covalent modifications. *Int Rev Cytol*. 178:207-275.

Ludwig, K., S.A. Manchinelly, L. Su, M. Mikawa, and S.J. Parsons. 2009. p190RhoGAP-A. *UCSD-Nature Molecule Pages*.

Ludwig, K., and S.J. Parsons. 2011. The Tumor Suppressor, p190RhoGAP, Differentially Initiates Apoptosis and Confers Docetaxel Sensitivity to Breast Cancer Cells. *Genes and Cancer*.

Luo, L. 2002. Actin cytoskeleton regulation in neuronal morphogenesis and structural plasticity. *Annu Rev Cell Dev Biol*. 18:601-635.

Lutz, R.J. 2000. Role of the BH3 (Bcl-2 homology 3) domain in the regulation of apoptosis and Bcl-2-related proteins. *Biochem Soc Trans*. 28:51-56.

Mabuchi, I., Y. Hamaguchi, H. Fujimoto, N. Morii, M. Mishima, and S. Narumiya. 1993. A rho-like protein is involved in the organisation of the contractile ring in dividing sand dollar eggs. *Zygote*. 1:325-331.

Machesky, L.M., R.D. Mullins, H.N. Higgs, D.A. Kaiser, L. Blanchoin, R.C. May, M.E. Hall, and T.D. Pollard. 1999. Scar, a WASp-related protein, activates nucleation of actin filaments by the Arp2/3 complex. *Proc Natl Acad Sci U S A*. 96:3739-3744.

Madaule, P., and R. Axel. 1985. A novel ras-related gene family. *Cell*. 41:31-40.

Madaule, P., T. Furuyashiki, M. Eda, H. Bito, T. Ishizaki, and S. Narumiya. 2000. Citron, a Rho target that affects contractility during cytokinesis. *Microsc Res Tech*. 49:123-126.

Maddika, S., S.R. Ande, S. Panigrahi, T. Paranjothy, K. Weglarczyk, A. Zuse, M. Eshraghi, K.D. Manda, E. Wiechec, and M. Los. 2007. Cell survival, cell death and cell cycle pathways are interconnected: implications for cancer therapy. *Drug Resist Updat*. 10:13-29.

Maddox, A.S., and K. Burridge. 2003. RhoA is required for cortical retraction and rigidity during mitotic cell rounding. *J Cell Biol*. 160:255-265.

Madesh, M., B. Antonsson, S.M. Srinivasula, E.S. Alnemri, and G. Hajnoczky. 2002. Rapid kinetics of tBid-induced cytochrome c and Smac/DIABLO release and mitochondrial depolarization. *J Biol Chem*. 277:5651-5659.

Mammoto, A., K.M. Connor, T. Mammoto, C.W. Yung, D. Huh, C.M. Aderman, G. Mostoslavsky, L.E. Smith, and D.E. Ingber. 2009. A mechanosensitive transcriptional mechanism that controls angiogenesis. *Nature*. 457:1103-1108.

Mammoto, T., S.M. Parikh, A. Mammoto, D. Gallagher, B. Chan, G. Mostoslavsky, D.E. Ingber, and V.P. Sukhatme. 2007. Angiopoietin-1 requires p190 RhoGAP to protect against vascular leakage in vivo. *J Biol Chem*. 282:23910-23918.

Manchinelly, S.A., J.A. Miller, L. Su, T. Miyake, L. Palmer, M. Mikawa, and S.J. Parsons. 2010. Mitotic down-regulation of p190RhoGAP is required for the successful completion of cytokinesis. *J Biol Chem*. 285:26923-26932.

Mancini, M., D.W. Nicholson, S. Roy, N.A. Thornberry, E.P. Peterson, L.A. Casciola-Rosen, and A. Rosen. 1998. The caspase-3 precursor has a cytosolic and mitochondrial distribution: implications for apoptotic signaling. *J Cell Biol*. 140:1485-1495.

Matarrese, P., L. Falzano, A. Fabbri, L. Gambardella, C. Frank, B. Geny, M.R. Popoff, W. Malorni, and C. Fiorentini. 2007. Clostridium difficile toxin B causes apoptosis in epithelial cells by thrilling mitochondria. Involvement of ATP-sensitive mitochondrial potassium channels. *J Biol Chem*. 282:9029-9041.

Matheson, S.F., K.Q. Hu, M.R. Brouns, R. Sordella, J.D. VanderHeide, and J. Settleman. 2006. Distinct but overlapping functions for the closely related p190 RhoGAPs in neural development. *Dev Neurosci*. 28:538-550.

Matsui, T., and A. Rosenzweig. 2005. Convergent signal transduction pathways controlling cardiomyocyte survival and function: the role of PI 3-kinase and Akt. *J Mol Cell Cardiol*. 38:63-71.

Matsumura, F. 2005. Regulation of myosin II during cytokinesis in higher eukaryotes. *Trends Cell Biol*. 15:371-377.

Matsumura, F., S. Ono, Y. Yamakita, G. Totsukawa, and S. Yamashiro. 1998. Specific localization of serine 19 phosphorylated myosin II during cell locomotion and mitosis of cultured cells. *J Cell Biol*. 140:119-129.

Mayo, L.D., and D.B. Donner. 2001. A phosphatidylinositol 3-kinase/Akt pathway promotes translocation of Mdm2 from the cytoplasm to the nucleus. *Proc Natl Acad Sci U S A*. 98:11598-11603.

Mazumder, S., B. Gong, Q. Chen, J.A. Drazba, J.C. Buchsbaum, and A. Almasan. 2002. Proteolytic cleavage of cyclin E leads to inactivation of associated kinase activity and amplification of apoptosis in hematopoietic cells. *Mol Cell Biol*. 22:2398-2409.

McGee, K., P. Holmfeldt, and M. Fallman. 2003. Microtubule-dependent regulation of Rho GTPases during internalisation of Yersinia pseudotuberculosis. *FEBS Lett*. 533:35-41.

Medema, R.H., A.M. de Vries-Smits, G.C. van der Zon, J.A. Maassen, and J.L. Bos. 1993. Ras activation by insulin and epidermal growth factor through enhanced exchange of guanine nucleotides on p21ras. *Mol Cell Biol*. 13:155-162.

Mikawa, M., L. Su, and S.J. Parsons. 2008. Opposing roles of p190RhoGAP and Ect2 RhoGEF in regulating cytokinesis. *Cell Cycle*. 7:2003-2012.

Miki, H., S. Suetsugu, and T. Takenawa. 1998. WAVE, a novel WASP-family protein involved in actin reorganization induced by Rac. *Embo J*. 17:6932-6941.

Miki, T., K. Okawa, T. Sekimoto, Y. Yoneda, S. Watanabe, T. Ishizaki, and S. Narumiya. 2009. mDia2 shuttles between the nucleus and the cytoplasm through the importin-{alpha}/{beta}- and CRM1-mediated nuclear transport mechanism. *J Biol Chem*. 284:5753-5762.

Miller, K.G., C.M. Field, and B.M. Alberts. 1989. Actin-binding proteins from Drosophila embryos: a complex network of interacting proteins detected by F-actin affinity chromatography. *J Cell Biol*. 109:2963-2975.

Miller, L.D., K.C. Lee, D. Mochly-Rosen, and C.A. Cartwright. 2004. RACK1 regulates Src-mediated Sam68 and p190RhoGAP signaling. *Oncogene*. 23:5682-5686.

Minoshima, Y., T. Kawashima, K. Hirose, Y. Tonozuka, A. Kawajiri, Y.C. Bao, X. Deng, M. Tatsuka, S. Narumiya, W.S. May, Jr., T. Nosaka, K. Semba, T. Inoue, T. Satoh, M. Inagaki, and T. Kitamura. 2003. Phosphorylation by aurora B converts MgcRacGAP to a RhoGAP during cytokinesis. *Dev Cell*. 4:549-560.

Miralles, F., G. Posern, A.I. Zaromytidou, and R. Treisman. 2003. Actin dynamics control SRF activity by regulation of its coactivator MAL. *Cell*. 113:329-342.

Mishima, M., S. Kaitna, and M. Glotzer. 2002. Central spindle assembly and cytokinesis require a kinesin-like protein/RhoGAP complex with microtubule bundling activity. *Dev Cell*. 2:41-54.

Miyamoto, S., A.N. Murphy, and J.H. Brown. 2009. Akt mediated mitochondrial protection in the heart: metabolic and survival pathways to the rescue. *J Bioenerg Biomembr*. 41:169-180.

Miyoshi J., T.Y. 2009. RhoA. *UCSD-Nature Molcule Pages*.

Molina-Ortiz, I., R.A. Bartolome, P. Hernandez-Varas, G.P. Colo, and J. Teixido. 2009. Overexpression of E-cadherin on melanoma cells inhibits chemokine-promoted invasion

involving p190RhoGAP/p120ctn-dependent inactivation of RhoA. *J Biol Chem*. 284:15147-15157.

Montero, A., F. Fossella, G. Hortobagyi, and V. Valero. 2005. Docetaxel for treatment of solid tumours: a systematic review of clinical data. *Lancet Oncol*. 6:229-239.

Monzo, P., N.C. Gauthier, F. Keslair, A. Loubat, C.M. Field, Y. Le Marchand-Brustel, and M. Cormont. 2005. Clues to CD2-associated protein involvement in cytokinesis. *Mol Biol Cell*. 16:2891-2902.

Moon, S.Y., and Y. Zheng. 2003. Rho GTPase-activating proteins in cell regulation. *Trends Cell Biol*. 13:13-22.

Moorman, J.P., D.A. Bobak, and C.S. Hahn. 1996. Inactivation of the small GTP binding protein Rho induces multinucleate cell formation and apoptosis in murine T lymphoma EL4. *J Immunol*. 156:4146-4153.

Moorman, J.P., D. Luu, J. Wickham, D.A. Bobak, and C.S. Hahn. 1999. A balance of signaling by Rho family small GTPases RhoA, Rac1 and Cdc42 coordinates cytoskeletal morphology but not cell survival. *Oncogene*. 18:47-57.

Mori, K., M. Amano, M. Takefuji, K. Kato, Y. Morita, T. Nishioka, Y. Matsuura, T. Murohara, and K. Kaibuchi. 2009. Rho-kinase contributes to sustained RhoA activation through phosphorylation of p190A RhoGAP. *J Biol Chem*. 284:5067-5076.

Morii, N., and S. Narumiya. 1995. Preparation of native and recombinant Clostridium botulinum C3 ADP-ribosyltransferase and identification of Rho proteins by ADP-ribosylation. *Methods Enzymol*. 256:196-206.

Morisco, C., D. Zebrowski, G. Condorelli, P. Tsichlis, S.F. Vatner, and J. Sadoshima. 2000. The Akt-glycogen synthase kinase 3beta pathway regulates transcription of atrial natriuretic factor induced by beta-adrenergic receptor stimulation in cardiac myocytes. *J Biol Chem*. 275:14466-14475.

Morrissey, C., S. Bennett, E. Nitsche, R.S. Guenette, P. Wong, and M. Tenniswood. 1999. Expression of p190A during apoptosis in the regressing rat ventral prostate. *Endocrinology*. 140:3328-3333.

Moyano, J.V., A. Maqueda, B. Casanova, and A. Garcia-Pardo. 2003. Alpha4beta1 integrin/ligand interaction inhibits alpha5beta1-induced stress fibers and focal adhesions via down-regulation of RhoA and induces melanoma cell migration. *Mol Biol Cell*. 14:3699-3715.

Muller, M., E.S. Schleithoff, W. Stremmel, G. Melino, P.H. Krammer, and T. Schilling. 2006. One, two, three--p53, p63, p73 and chemosensitivity. *Drug Resist Updat*. 9:288-306.

Musacchio, A., and E.D. Salmon. 2007. The spindle-assembly checkpoint in space and time. *Nat Rev Mol Cell Biol*. 8:379-393.

Nakagawa, O., K. Fujisawa, T. Ishizaki, Y. Saito, K. Nakao, and S. Narumiya. 1996. ROCK-I and ROCK-II, two isoforms of Rho-associated coiled-coil forming protein serine/threonine kinase in mice. *FEBS Lett*. 392:189-193.

Nakahara, H., S.C. Mueller, M. Nomizu, Y. Yamada, Y. Yeh, and W.T. Chen. 1998. Activation of beta1 integrin signaling stimulates tyrosine phosphorylation of p190RhoGAP and membrane-protrusive activities at invadopodia. *J Biol Chem*. 273:9-12.

Nakayama, K., N. Ishida, M. Shirane, A. Inomata, T. Inoue, N. Shishido, I. Horii, and D.Y. Loh. 1996. Mice lacking p27(Kip1) display increased body size, multiple organ hyperplasia, retinal dysplasia, and pituitary tumors. *Cell*. 85:707-720.

Namba, H., V. Saenko, and S. Yamashita. 2007. Nuclear factor-kB in thyroid carcinogenesis and progression: a novel therapeutic target for advanced thyroid cancer. *Arq Bras Endocrinol Metabol*. 51:843-851.

Naoe, H., K. Araki, O. Nagano, Y. Kobayashi, J. Ishizawa, T. Chiyoda, T. Shimizu, K. Yamamura, Y. Sasaki, H. Saya, and S. Kuninaka. 2010. The anaphase-promoting complex/cyclosome activator Cdh1 modulates Rho GTPase by targeting p190 RhoGAP for degradation. *Mol Cell Biol*. 30:3994-4005.

Narumiya, S., M. Tanji, and T. Ishizaki. 2009. Rho signaling, ROCK and mDia1, in transformation, metastasis and invasion. *Cancer Metastasis Rev*. 28:65-76.

Narumiya, S., and S. Yasuda. 2006. Rho GTPases in animal cell mitosis. *Curr Opin Cell Biol*. 18:199-205.

Nassar, N., G.R. Hoffman, D. Manor, J.C. Clardy, and R.A. Cerione. 1998. Structures of Cdc42 bound to the active and catalytically compromised forms of Cdc42GAP. *Nat Struct Biol*. 5:1047-1052.

Nemeth, T., K. Futosi, C. Hably, M.R. Brouns, S.M. Jakob, M. Kovacs, Z. Kertesz, B. Walzog, J. Settleman, and A. Mocsai. 2010. Neutrophil functions and autoimmune arthritis in the absence of p190RhoGAP: generation and analysis of a novel null mutation in mice. *J Immunol*. 185:3064-3075.

Niederman, R., and T.D. Pollard. 1975. Human platelet myosin. II. In vitro assembly and structure of myosin filaments. *J Cell Biol*. 67:72-92.

Niggli, V. 2003. Microtubule-disruption-induced and chemotactic-peptide-induced migration of human neutrophils: implications for differential sets of signalling pathways. *J Cell Sci*. 116:813-822.

Nimnual, A.S., L.J. Taylor, and D. Bar-Sagi. 2003. Redox-dependent downregulation of Rho by Rac. *Nat Cell Biol*. 5:236-241.

Nishiki, T., S. Narumiya, N. Morii, M. Yamamoto, M. Fujiwara, Y. Kamata, G. Sakaguchi, and S. Kozaki. 1990. ADP-ribosylation of the rho/rac proteins induces growth inhibition, neurite outgrowth and acetylcholine esterase in cultured PC-12 cells. *Biochem Biophys Res Commun*. 167:265-272.

Nishimura, Y., K. Nakano, and I. Mabuchi. 1998. Localization of Rho GTPase in sea urchin eggs. *FEBS Lett*. 441:121-126.

Nishimura, Y., and S. Yonemura. 2006. Centralspindlin regulates ECT2 and RhoA accumulation at the equatorial cortex during cytokinesis. *J Cell Sci*. 119:104-114.

Nobes, C., and A. Hall. 1994. Regulation and function of the Rho subfamily of small GTPases. *Curr Opin Genet Dev*. 4:77-81.

Nogales, E. 2001. Structural insight into microtubule function. *Annu Rev Biophys Biomol Struct*. 30:397-420.

Nogales, E., M. Whittaker, R.A. Milligan, and K.H. Downing. 1999. High-resolution model of the microtubule. *Cell*. 96:79-88.

Noren, N.K., W.T. Arthur, and K. Burridge. 2003. Cadherin engagement inhibits RhoA via p190RhoGAP. *J Biol Chem*. 278:13615-13618.

Nottrott, S., J. Schoentaube, H. Genth, I. Just, and R. Gerhard. 2007. Clostridium difficile toxin A-induced apoptosis is p53-independent but depends on glucosylation of Rho GTPases. *Apoptosis*. 12:1443-1453.

O'Connell, C.B., S.P. Wheatley, S. Ahmed, and Y.L. Wang. 1999. The small GTP-binding protein rho regulates cortical activities in cultured cells during division. *J Cell Biol*. 144:305-313.

O'Connor, L., A. Strasser, L.A. O'Reilly, G. Hausmann, J.M. Adams, S. Cory, and D.C. Huang. 1998. Bim: a novel member of the Bcl-2 family that promotes apoptosis. *Embo J*. 17:384-395.

Oegema, K., M.S. Savoian, T.J. Mitchison, and C.M. Field. 2000. Functional analysis of a human homologue of the Drosophila actin binding protein anillin suggests a role in cytokinesis. *J Cell Biol*. 150:539-552.

Ogata, S., K. Morishige, K. Sawada, K. Hashimoto, S. Mabuchi, C. Kawase, C. Ooyagi, M. Sakata, and T. Kimura. 2009. Fasudil inhibits lysophosphatidic acid-induced invasiveness of human ovarian cancer cells. *Int J Gynecol Cancer*. 19:1473-1480.

Ohashi, K., K. Nagata, M. Maekawa, T. Ishizaki, S. Narumiya, and K. Mizuno. 2000. Rho-associated kinase ROCK activates LIM-kinase 1 by phosphorylation at threonine 508 within the activation loop. *J Biol Chem*. 275:3577-3582.

Oliferenko, S., T.G. Chew, and M.K. Balasubramanian. 2009. Positioning cytokinesis. *Genes Dev*. 23:660-674.

Olson, J.M., and A.R. Hallahan. 2004. p38 MAP kinase: a convergence point in cancer therapy. *Trends Mol Med*. 10:125-129.

Olson, M.F. 2008. Applications for ROCK kinase inhibition. *Curr Opin Cell Biol*. 20:242-248.

Olson, M.F., A. Ashworth, and A. Hall. 1995. An essential role for Rho, Rac, and Cdc42 GTPases in cell cycle progression through G1. *Science*. 269:1270-1272.

Ono, K., and J. Han. 2000. The p38 signal transduction pathway: activation and function. *Cell Signal*. 12:1-13.

Otomo, T., C. Otomo, D.R. Tomchick, M. Machius, and M.K. Rosen. 2005a. Structural basis of Rho GTPase-mediated activation of the formin mDia1. *Mol Cell*. 18:273-281.

Otomo, T., D.R. Tomchick, C. Otomo, S.C. Panchal, M. Machius, and M.K. Rosen. 2005b. Structural basis of actin filament nucleation and processive capping by a formin homology 2 domain. *Nature*. 433:488-494.

Ozdamar, B., R. Bose, M. Barrios-Rodiles, H.R. Wang, Y. Zhang, and J.L. Wrana. 2005. Regulation of the polarity protein Par6 by TGFbeta receptors controls epithelial cell plasticity. *Science*. 307:1603-1609.

Ozes, O.N., L.D. Mayo, J.A. Gustin, S.R. Pfeffer, L.M. Pfeffer, and D.B. Donner. 1999. NF-kappaB activation by tumour necrosis factor requires the Akt serine-threonine kinase. *Nature*. 401:82-85.

Palazzo, A.F., T.A. Cook, A.S. Alberts, and G.G. Gundersen. 2001. mDia mediates Rho-regulated formation and orientation of stable microtubules. *Nat Cell Biol*. 3:723-729.

Palmi, C., G. Fazio, A. Cassetti, A. Aloisi, A. Villa, A. Biondi, and G. Cazzaniga. 2006. TEL/ARG induces cytoskeletal abnormalities in 293T cells. *Cancer Lett*. 241:79-86.

Papakonstanti, E.A., A.J. Ridley, and B. Vanhaesebroeck. 2007. The p110delta isoform of PI 3-kinase negatively controls RhoA and PTEN. *EMBO J*. 26:3050-3061.

Park, Y.J., H.J. Ahn, H.K. Chang, J.Y. Kim, K.H. Huh, M.S. Kim, and Y.S. Kim. 2009. The RhoGDI-alpha/JNK signaling pathway plays a significant role in mycophenolic acid-induced apoptosis in an insulin-secreting cell line. *Cell Signal*. 21:356-364.

Paterson, H.F., A.J. Self, M.D. Garrett, I. Just, K. Aktories, and A. Hall. 1990. Microinjection of recombinant p21rho induces rapid changes in cell morphology. *J Cell Biol*. 111:1001-1007.

Perona, R., P. Esteve, B. Jimenez, R.P. Ballestero, S. Ramon y Cajal, and J.C. Lacal. 1993. Tumorigenic activity of rho genes from Aplysia californica. *Oncogene*. 8:1285-1292.

Pestonjamasp, K.N., C. Forster, C. Sun, E.M. Gardiner, B. Bohl, O. Weiner, G.M. Bokoch, and M. Glogauer. 2006. Rac1 links leading edge and uropod events through Rho and myosin activation during chemotaxis. *Blood*. 108:2814-2820.

Piekny, A., M. Werner, and M. Glotzer. 2005. Cytokinesis: welcome to the Rho zone. *Trends Cell Biol*. 15:651-658.

Piekny, A.J., and M. Glotzer. 2008. Anillin is a scaffold protein that links RhoA, actin, and myosin during cytokinesis. *Curr Biol*. 18:30-36.

Piekny, A.J., and A.S. Maddox. 2010. The myriad roles of Anillin during cytokinesis. *Semin Cell Dev Biol*. 21:881-891.

Pinon, J.D., V. Labi, A. Egle, and A. Villunger. 2008. Bim and Bmf in tissue homeostasis and malignant disease. *Oncogene*. 27 Suppl 1:S41-52.

Plantivaux, A., E. Szegezdi, A. Samali, and L. Egan. 2009. Is there a role for nuclear factor kappaB in tumor necrosis factor-related apoptosis-inducing ligand resistance? *Ann N Y Acad Sci*. 1171:38-49.

Playford, M.P., K. Vadali, X. Cai, K. Burridge, and M.D. Schaller. 2008. Focal adhesion kinase regulates cell-cell contact formation in epithelial cells via modulation of Rho. *Exp Cell Res*. 314:3187-3197.

Pohl, T., R. Gugasyan, R.J. Grumont, A. Strasser, D. Metcalf, D. Tarlinton, W. Sha, D. Baltimore, and S. Gerondakis. 2002. The combined absence of NF-kappa B1 and c-Rel reveals that overlapping roles for these transcription factors in the B cell lineage are restricted to the activation and function of mature cells. *Proc Natl Acad Sci U S A*. 99:4514-4519.

Polyak, K., M.H. Lee, H. Erdjument-Bromage, A. Koff, J.M. Roberts, P. Tempst, and J. Massague. 1994. Cloning of p27Kip1, a cyclin-dependent kinase inhibitor and a potential mediator of extracellular antimitogenic signals. *Cell*. 78:59-66.

Porter, L.A., G. Singh, and J.M. Lee. 2000. Abundance of cyclin B1 regulates gamma-radiation-induced apoptosis. *Blood*. 95:2645-2650.

Poruchynsky, M.S., P. Giannakakou, Y. Ward, J.C. Bulinski, W.G. Telford, R.W. Robey, and T. Fojo. 2001. Accompanying protein alterations in malignant cells with a microtubule-polymerizing drug-resistance phenotype and a primary resistance mechanism. *Biochem Pharmacol*. 62:1469-1480.

Prokopenko, S.N., R. Saint, and H.J. Bellen. 2000. Untying the Gordian knot of cytokinesis. Role of small G proteins and their regulators. *J Cell Biol*. 148:843-848.

Puthalakath, H., D.C. Huang, L.A. O'Reilly, S.M. King, and A. Strasser. 1999. The proapoptotic activity of the Bcl-2 family member Bim is regulated by interaction with the dynein motor complex. *Mol Cell*. 3:287-296.

Puthalakath, H., A. Villunger, L.A. O'Reilly, J.G. Beaumont, L. Coultas, R.E. Cheney, D.C. Huang, and A. Strasser. 2001. Bmf: a proapoptotic BH3-only protein regulated by interaction with the myosin V actin motor complex, activated by anoikis. *Science*. 293:1829-1832.

Qi, Y.X., M.J. Qu, D.K. Long, B. Liu, Q.P. Yao, S. Chien, and Z.L. Jiang. 2008. Rho-GDP dissociation inhibitor alpha downregulated by low shear stress promotes vascular smooth muscle cell migration and apoptosis: a proteomic analysis. *Cardiovasc Res*. 80:114-122.

Qiu, R.G., A. Abo, F. McCormick, and M. Symons. 1997. Cdc42 regulates anchorage-independent growth and is necessary for Ras transformation. *Mol Cell Biol*. 17:3449-3458.

Qiu, R.G., J. Chen, D. Kirn, F. McCormick, and M. Symons. 1995a. An essential role for Rac in Ras transformation. *Nature*. 374:457-459.

Qiu, R.G., J. Chen, F. McCormick, and M. Symons. 1995b. A role for Rho in Ras transformation. *Proc Natl Acad Sci U S A*. 92:11781-11785.

Raman, M., W. Chen, and M.H. Cobb. 2007. Differential regulation and properties of MAPKs. *Oncogene*. 26:3100-3112.

Ramaswamy, M., C. Dumont, A.C. Cruz, J.R. Muppidi, T.S. Gomez, D.D. Billadeau, V.L. Tybulewicz, and R.M. Siegel. 2007. Cutting edge: Rac GTPases sensitize activated T cells to die via Fas. *J Immunol*. 179:6384-6388.

Rao, S., L. He, S. Chakravarty, I. Ojima, G.A. Orr, and S.B. Horwitz. 1999. Characterization of the Taxol binding site on the microtubule. Identification of Arg(282) in beta-tubulin as the site of photoincorporation of a 7-benzophenone analogue of Taxol. *J Biol Chem*. 274:37990-37994.

Rao, S., N.E. Krauss, J.M. Heerding, C.S. Swindell, I. Ringel, G.A. Orr, and S.B. Horwitz. 1994. 3'-(p-azidobenzamido)taxol photolabels the N-terminal 31 amino acids of beta-tubulin. *J Biol Chem*. 269:3132-3134.

Rappaport, R. 1961. Experiments concerning the cleavage stimulus in sand dollar eggs. *J Exp Zool*. 148:81-89.

Rattan, S., R.N. Puri, and Y.P. Fan. 2003. Involvement of rho and rho-associated kinase in sphincteric smooth muscle contraction by angiotensin II. *Exp Biol Med (Maywood)*. 228:972-981.

Rayment, I., H.M. Holden, M. Whittaker, C.B. Yohn, M. Lorenz, K.C. Holmes, and R.A. Milligan. 1993. Structure of the actin-myosin complex and its implications for muscle contraction. *Science*. 261:58-65.

Ren, X.D., W.B. Kiosses, and M.A. Schwartz. 1999. Regulation of the small GTP-binding protein Rho by cell adhesion and the cytoskeleton. *EMBO J*. 18:578-585.

Rennefahrt, U., M. Janakiraman, R. Ollinger, and J. Troppmair. 2005. Stress kinase signaling in cancer: fact or fiction? *Cancer Lett*. 217:1-9.

Reuveny, M., H. Heller, and E. Bengal. 2004. RhoA controls myoblast survival by inducing the phosphatidylinositol 3-kinase-Akt signaling pathway. *FEBS Lett*. 569:129-134.

Ridley, A.J., and A. Hall. 1992. The small GTP-binding protein rho regulates the assembly of focal adhesions and actin stress fibers in response to growth factors. *Cell*. 70:389-399.

Ridley, A.J., A.J. Self, F. Kasmi, H.F. Paterson, A. Hall, C.J. Marshall, and C. Ellis. 1993. rho family GTPase activating proteins p190, bcr and rhoGAP show distinct specificities in vitro and in vivo. *EMBO J*. 12:5151-5160.

Riento, K., and A.J. Ridley. 2003. Rocks: multifunctional kinases in cell behaviour. *Nat Rev Mol Cell Biol*. 4:446-456.

Riento, K., P. Villalonga, R. Garg, and A. Ridley. 2005. Function and regulation of RhoE. *Biochem Soc Trans*. 33:649-651.

Riganti, C., S. Doublier, C. Costamagna, E. Aldieri, G. Pescarmona, D. Ghigo, and A. Bosia. 2008. Activation of nuclear factor-kappa B pathway by simvastatin and RhoA silencing increases doxorubicin cytotoxicity in human colon cancer HT29 cells. *Mol Pharmacol*. 74:476-484.

Riley, T., E. Sontag, P. Chen, and A. Levine. 2008. Transcriptional control of human p53-regulated genes. *Nat Rev Mol Cell Biol*. 9:402-412.

Rohatgi, R., L. Ma, H. Miki, M. Lopez, T. Kirchhausen, T. Takenawa, and M.W. Kirschner. 1999. The interaction between N-WASP and the Arp2/3 complex links Cdc42-dependent signals to actin assembly. *Cell*. 97:221-231.

Rolli-Derkinderen, M., V. Sauzeau, L. Boyer, E. Lemichez, C. Baron, D. Henrion, G. Loirand, and P. Pacaud. 2005. Phosphorylation of serine 188 protects RhoA from ubiquitin/proteasome-mediated degradation in vascular smooth muscle cells. *Circ Res*. 96:1152-1160.

Romashkova, J.A., and S.S. Makarov. 1999. NF-kappaB is a target of AKT in anti-apoptotic PDGF signalling. *Nature*. 401:86-90.

Ron, D., M. Zannini, M. Lewis, R.B. Wickner, L.T. Hunt, G. Graziani, S.R. Tronick, S.A. Aaronson, and A. Eva. 1991. A region of proto-dbl essential for its transforming activity shows sequence similarity to a yeast cell cycle gene, CDC24, and the human breakpoint cluster gene, bcr. *New Biol*. 3:372-379.

Roof, R.W., B.D. Dukes, J.H. Chang, and S.J. Parsons. 2000. Phosphorylation of the p190 RhoGAP N-terminal domain by c-Src results in a loss of GTP binding activity. *FEBS Lett*. 472:117-121.

Roof, R.W., M.D. Haskell, B.D. Dukes, N. Sherman, M. Kinter, and S.J. Parsons. 1998. Phosphotyrosine (p-Tyr)-dependent and -independent mechanisms of p190 RhoGAP-p120 RasGAP interaction: Tyr 1105 of p190, a substrate for c-Src, is the sole p-Tyr mediator of complex formation. *Mol Cell Biol*. 18:7052-7063.

Rose, R., M. Weyand, M. Lammers, T. Ishizaki, M.R. Ahmadian, and A. Wittinghofer. 2005. Structural and mechanistic insights into the interaction between Rho and mammalian Dia. *Nature*. 435:513-518.

Rosenfeldt, H., M.D. Castellone, P.A. Randazzo, and J.S. Gutkind. 2006. Rac inhibits thrombin-induced Rho activation: evidence of a Pak-dependent GTPase crosstalk. *J Mol Signal*. 1:8.

Royal, I., N. Lamarche-Vane, L. Lamorte, K. Kaibuchi, and M. Park. 2000. Activation of cdc42, rac, PAK, and rho-kinase in response to hepatocyte growth factor differentially regulates epithelial cell colony spreading and dissociation. *Mol Biol Cell*. 11:1709-1725.

Ruchaud, S., M. Carmena, and W.C. Earnshaw. 2007. Chromosomal passengers: conducting cell division. *Nat Rev Mol Cell Biol*. 8:798-812.

Sachdev, P., Y.X. Jiang, W. Li, T. Miki, H. Maruta, E.K.M.S. Nur, and L.H. Wang. 2001. Differential requirement for Rho family GTPases in an oncogenic insulin-like growth factor-I receptor-induced cell transformation. *J Biol Chem*. 276:26461-26471.

Saelens, X., N. Festjens, L. Vande Walle, M. van Gurp, G. van Loo, and P. Vandenabeele. 2004. Toxic proteins released from mitochondria in cell death. *Oncogene*. 23:2861-2874.

Sahai, E., and C.J. Marshall. 2002. ROCK and Dia have opposing effects on adherens junctions downstream of Rho. *Nat Cell Biol*. 4:408-415.

Sarbassov, D.D., D.A. Guertin, S.M. Ali, and D.M. Sabatini. 2005. Phosphorylation and regulation of Akt/PKB by the rictor-mTOR complex. *Science*. 307:1098-1101.

Sarner, S., R. Kozma, S. Ahmed, and L. Lim. 2000. Phosphatidylinositol 3-kinase, Cdc42, and Rac1 act downstream of Ras in integrin-dependent neurite outgrowth in N1E-115 neuroblastoma cells. *Mol Cell Biol*. 20:158-172.

Sarrabayrouse, G., C. Synaeve, K. Leveque, G. Favre, and A.F. Tilkin-Mariame. 2007. Statins stimulate in vitro membrane FasL expression and lymphocyte apoptosis through RhoA/ROCK pathway in murine melanoma cells. *Neoplasia*. 9:1078-1090.

Sastry, S.K., Z. Rajfur, B.P. Liu, J.F. Cote, M.L. Tremblay, and K. Burridge. 2006. PTP-PEST couples membrane protrusion and tail retraction via VAV2 and p190RhoGAP. *J Biol Chem*. 281:11627-11636.

Scaffidi, C., S. Fulda, A. Srinivasan, C. Friesen, F. Li, K.J. Tomaselli, K.M. Debatin, P.H. Krammer, and M.E. Peter. 1998. Two CD95 (APO-1/Fas) signaling pathways. *EMBO J*. 17:1675-1687.

Schaeffer, W.I. 1990. Terminology associated with cell, tissue, and organ culture, molecular biology, and molecular genetics. Tissue Culture Association Terminology Committee. *In Vitro Cell Dev Biol*. 26:97-101.

Scheid, M.P., R.W. Lauener, and V. Duronio. 1995. Role of phosphatidylinositol 3-OH-kinase activity in the inhibition of apoptosis in haemopoietic cells: phosphatidylinositol 3-OH-kinase inhibitors reveal a difference in signalling between interleukin-3 and granulocyte-macrophage colony stimulating factor. *Biochem J*. 312 (Pt 1):159-162.

Schieffer, B., W.G. Paxton, Q. Chai, M.B. Marrero, and K.E. Bernstein. 1996. Angiotensin II controls p21ras activity via pp60c-src. *J Biol Chem*. 271:10329-10333.

Schiff, P.B., J. Fant, and S.B. Horwitz. 1979. Promotion of microtubule assembly in vitro by taxol. *Nature*. 277:665-667.

Schmidt, A., and A. Hall. 2002. Guanine nucleotide exchange factors for Rho GTPases: turning on the switch. *Genes Dev*. 16:1587-1609.

Schnelzer, A., D. Prechtel, U. Knaus, K. Dehne, M. Gerhard, H. Graeff, N. Harbeck, M. Schmitt, and E. Lengyel. 2000. Rac1 in human breast cancer: overexpression, mutation analysis, and characterization of a new isoform, Rac1b. *Oncogene*. 19:3013-3020.

Schulz, F., I. Just, and H. Genth. 2009. Prevention of Clostridium sordellii lethal toxin-induced apoptotic cell death by tauroursodeoxycholic acid. *Biochemistry*. 48:9002-9010.

Sekine, A., M. Fujiwara, and S. Narumiya. 1989. Asparagine residue in the rho gene product is the modification site for botulinum ADP-ribosyltransferase. *J Biol Chem*. 264:8602-8605.

Sellers, J.R., E. Eisenberg, and R.S. Adelstein. 1982. The binding of smooth muscle heavy meromyosin to actin in the presence of ATP. Effect of phosphorylation. *J Biol Chem*. 257:13880-13883.

Sessa, F., M. Mapelli, C. Ciferri, C. Tarricone, L.B. Areces, T.R. Schneider, P.T. Stukenberg, and A. Musacchio. 2005. Mechanism of Aurora B activation by INCENP and inhibition by hesperadin. *Mol Cell*. 18:379-391.

Settleman, J., C.F. Albright, L.C. Foster, and R.A. Weinberg. 1992a. Association between GTPase activators for Rho and Ras families. *Nature*. 359:153-154.

Settleman, J., V. Narasimhan, L.C. Foster, and R.A. Weinberg. 1992b. Molecular cloning of cDNAs encoding the GAP-associated protein p190: implications for a signaling pathway from ras to the nucleus. *Cell*. 69:539-549.

Severson, A.F., D.R. Hamill, J.C. Carter, J. Schumacher, and B. Bowerman. 2000. The aurora-related kinase AIR-2 recruits ZEN-4/CeMKLP1 to the mitotic spindle at metaphase and is required for cytokinesis. *Curr Biol*. 10:1162-1171.

Sfakianos, M.K., A. Eisman, S.L. Gourley, W.D. Bradley, A.J. Scheetz, J. Settleman, J.R. Taylor, C.A. Greer, A. Williamson, and A.J. Koleske. 2007. Inhibition of Rho via Arg and p190RhoGAP in the postnatal mouse hippocampus regulates dendritic spine maturation, synapse and dendrite stability, and behavior. *J Neurosci*. 27:10982-10992.

Shandala, T., S.L. Gregory, H.E. Dalton, M. Smallhorn, and R. Saint. 2004. Citron kinase is an essential effector of the Pbl-activated Rho signalling pathway in Drosophila melanogaster. *Development*. 131:5053-5063.

Sharma, S.V. 1998. Rapid recruitment of p120RasGAP and its associated protein, p190RhoGAP, to the cytoskeleton during integrin mediated cell-substrate interaction. *Oncogene*. 17:271-281.

Sheetz, M.P., and J.A. Spudich. 1983a. Movement of myosin-coated fluorescent beads on actin cables in vitro. *Nature*. 303:31-35.

Sheetz, M.P., and J.A. Spudich. 1983b. Movement of myosin-coated structures on actin cables. *Cell Motil*. 3:485-489.

Shen, C.H., H.Y. Chen, M.S. Lin, F.Y. Li, C.C. Chang, M.L. Kuo, J. Settleman, and R.H. Chen. 2008. Breast tumor kinase phosphorylates p190RhoGAP to regulate rho and ras and promote breast carcinoma growth, migration, and invasion. *Cancer Res*. 68:7779-7787.

Shimada, A., M. Nyitrai, I.R. Vetter, D. Kuhlmann, B. Bugyi, S. Narumiya, M.A. Geeves, and A. Wittinghofer. 2004. The core FH2 domain of diaphanous-related formins is an elongated actin binding protein that inhibits polymerization. *Mol Cell*. 13:511-522.

Shimada, H., and L.E. Rajagopalan. 2010. Rho kinase-2 activation in human endothelial cells drives lysophosphatidic acid-mediated expression of cell adhesion molecules via NF-kappaB p65. *J Biol Chem*. 285:12536-12542.

Shimizu, A., A. Mammoto, J.E. Italiano, Jr., E. Pravda, A.C. Dudley, D.E. Ingber, and M. Klagsbrun. 2008. ABL2/ARG tyrosine kinase mediates SEMA3F-induced RhoA inactivation and cytoskeleton collapse in human glioma cells. *J Biol Chem*. 283:27230-27238.

Shinohara, M., W.H. Shang, M. Kubodera, S. Harada, J. Mitsushita, M. Kato, H. Miyazaki, H. Sumimoto, and T. Kamata. 2007. Nox1 redox signaling mediates oncogenic Ras-induced disruption of stress fibers and focal adhesions by down-regulating Rho. *J Biol Chem*. 282:17640-17648.

Shioi, T., J.R. McMullen, P.M. Kang, P.S. Douglas, T. Obata, T.F. Franke, L.C. Cantley, and S. Izumo. 2002. Akt/protein kinase B promotes organ growth in transgenic mice. *Mol Cell Biol*. 22:2799-2809.

Shiota, M., T. Tanihiro, Y. Nakagawa, N. Aoki, N. Ishida, K. Miyazaki, A. Ullrich, and H. Miyazaki. 2003. Protein tyrosine phosphatase PTP20 induces actin cytoskeleton reorganization by dephosphorylating p190 RhoGAP in rat ovarian granulosa cells stimulated with follicle-stimulating hormone. *Mol Endocrinol*. 17:534-549.

Silverman-Gavrila, R.V., K.G. Hales, and A. Wilde. 2008. Anillin-mediated targeting of peanut to pseudocleavage furrows is regulated by the GTPase Ran. *Mol Biol Cell*. 19:3735-3744.

Singleton, P.A., J.G. Garcia, and J. Moss. 2008. Synergistic effects of methylnaltrexone with 5-fluorouracil and bevacizumab on inhibition of vascular endothelial growth factor-induced angiogenesis. *Mol Cancer Ther*. 7:1669-1679.

Sisson, J.C., C. Field, R. Ventura, A. Royou, and W. Sullivan. 2000. Lava lamp, a novel peripheral golgi protein, is required for Drosophila melanogaster cellularization. *J Cell Biol*. 151:905-918.

Skoda, C., B.M. Erovic, V. Wachek, L. Vormittag, F. Wrba, H. Martinek, G. Heiduschka, P. Kloimstein, E. Selzer, and D. Thurnher. 2008. Down-regulation of Mcl-1 with antisense technology alters the effect of various cytotoxic agents used in treatment of squamous cell carcinoma of the head and neck. *Oncol Rep*. 19:1499-1503.

Skommer, J., D. Wlodkowic, and A. Deptala. 2007. Larger than life: Mitochondria and the Bcl-2 family. *Leuk Res*. 31:277-286.

Skurk, C., Y. Izumiya, H. Maatz, P. Razeghi, I. Shiojima, M. Sandri, K. Sato, L. Zeng, S. Schiekofer, D. Pimentel, S. Lecker, H. Taegtmeyer, A.L. Goldberg, and K. Walsh. 2005. The FOXO3a transcription factor regulates cardiac myocyte size downstream of AKT signaling. *J Biol Chem*. 280:20814-20823.

Sofer-Levi, Y., and D. Resnitzky. 1996. Apoptosis induced by ectopic expression of cyclin D1 but not cyclin E. *Oncogene*. 13:2431-2437.

Somers, W.G., and R. Saint. 2003. A RhoGEF and Rho family GTPase-activating protein complex links the contractile ring to cortical microtubules at the onset of cytokinesis. *Dev Cell*. 4:29-39.

Somma, M.P., B. Fasulo, G. Cenci, E. Cundari, and M. Gatti. 2002. Molecular dissection of cytokinesis by RNA interference in Drosophila cultured cells. *Mol Biol Cell*. 13:2448-2460.

Spencer, W., H. Kwon, P. Crepieux, N. Leclerc, R. Lin, and J. Hiscott. 1999. Taxol selectively blocks microtubule dependent NF-kappaB activation by phorbol ester via inhibition of IkappaBalpha phosphorylation and degradation. *Oncogene*. 18:495-505.

Srivastava, R.K., Q.S. Mi, J.M. Hardwick, and D.L. Longo. 1999. Deletion of the loop region of Bcl-2 completely blocks paclitaxel-induced apoptosis. *Proc Natl Acad Sci U S A*. 96:3775-3780.

Stepan, V., S. Ramamoorthy, N. Pausawasdi, C.D. Logsdon, F.K. Askari, and A. Todisco. 2004. Role of small GTP binding proteins in the growth-promoting and antiapoptotic actions of gastrin. *Am J Physiol Gastrointest Liver Physiol*. 287:G715-725.

Straight, A.F., A. Cheung, J. Limouze, I. Chen, N.J. Westwood, J.R. Sellers, and T.J. Mitchison. 2003. Dissecting temporal and spatial control of cytokinesis with a myosin II Inhibitor. *Science*. 299:1743-1747.

Straight, A.F., C.M. Field, and T.J. Mitchison. 2005. Anillin binds nonmuscle myosin II and regulates the contractile ring. *Mol Biol Cell*. 16:193-201.

Strasser, A. 2005. The role of BH3-only proteins in the immune system. *Nat Rev Immunol*. 5:189-200.

Su, L., J.M. Agati, and S.J. Parsons. 2003. p190RhoGAP is cell cycle regulated and affects cytokinesis. *J Cell Biol*. 163:571-582.

Su, L., O. Pertz, M. Mikawa, K. Hahn, and S.J. Parsons. 2009. p190RhoGAP negatively regulates Rho activity at the cleavage furrow of mitotic cells. *Exp Cell Res*. 315:1347-1359.

Suhara, T., H.S. Kim, L.A. Kirshenbaum, and K. Walsh. 2002. Suppression of Akt signaling induces Fas ligand expression: involvement of caspase and Jun kinase activation in Akt-mediated Fas ligand regulation. *Mol Cell Biol*. 22:680-691.

Sumi, T., K. Matsumoto, and T. Nakamura. 2001. Specific activation of LIM kinase 2 via phosphorylation of threonine 505 by ROCK, a Rho-dependent protein kinase. *J Biol Chem*. 276:670-676.

Sunters, A., S. Fernandez de Mattos, M. Stahl, J.J. Brosens, G. Zoumpoulidou, C.A. Saunders, P.J. Coffer, R.H. Medema, R.C. Coombes, and E.W. Lam. 2003. FoxO3a transcriptional regulation of Bim controls apoptosis in paclitaxel-treated breast cancer cell lines. *J Biol Chem*. 278:49795-49805.

Suzuki, C., Y. Daigo, N. Ishikawa, T. Kato, S. Hayama, T. Ito, E. Tsuchiya, and Y. Nakamura. 2005. ANLN plays a critical role in human lung carcinogenesis through the activation of RHOA and by involvement in the phosphoinositide 3-kinase/AKT pathway. *Cancer Res*. 65:11314-11325.

Svoboda, K.K., D.L. Orlow, C.L. Chu, and W.R. Reenstra. 1999. ECM-stimulated actin bundle formation in embryonic corneal epithelia is tyrosine phosphorylation dependent. *Anat Rec*. 254:348-359.

Takai, Y., T. Sasaki, K. Tanaka, and H. Nakanishi. 1995. Rho as a regulator of the cytoskeleton. *Trends Biochem Sci*. 20:227-231.

Takaishi, K., T. Sasaki, T. Kameyama, S. Tsukita, and Y. Takai. 1995. Translocation of activated Rho from the cytoplasm to membrane ruffling area, cell-cell adhesion sites and cleavage furrows. *Oncogene*. 11:39-48.

Takaishi, K., T. Sasaki, M. Kato, W. Yamochi, S. Kuroda, T. Nakamura, M. Takeichi, and Y. Takai. 1994. Involvement of Rho p21 small GTP-binding protein and its regulator in the HGF-induced cell motility. *Oncogene*. 9:273-279.

Takesono, A., S.J. Heasman, B. Wojciak-Stothard, R. Garg, and A.J. Ridley. Microtubules regulate migratory polarity through Rho/ROCK signaling in T cells. *PLoS One*. 5:e8774.

Tal, J., D.J. Fujita, S. Kawai, H.E. Varmus, and J.M. Bishop. 1977. Purification of DNA complementary to the env gene of avian sarcoma virus and analysis of relationships among the env genes of avian leukosis-sarcoma viruses. *J Virol*. 21:497-505.

Tamura, H., M. Fukada, A. Fujikawa, and M. Noda. 2006. Protein tyrosine phosphatase receptor type Z is involved in hippocampus-dependent memory formation through dephosphorylation at Y1105 on p190 RhoGAP. *Neurosci Lett*. 399:33-38.

Tan, T.T., K. Degenhardt, D.A. Nelson, B. Beaudoin, W. Nieves-Neira, P. Bouillet, A. Villunger, J.M. Adams, and E. White. 2005. Key roles of BIM-driven apoptosis in epithelial tumors and rational chemotherapy. *Cancer Cell*. 7:227-238.

Tatsis, N., D.A. Lannigan, and I.G. Macara. 1998. The function of the p190 Rho GTPase-activating protein is controlled by its N-terminal GTP binding domain. *J Biol Chem*. 273:34631-34638.

Thomas, L.W., C. Lam, and S.W. Edwards. 2010. Mcl-1; the molecular regulation of protein function. *FEBS Lett*. 584:2981-2989.

Thornberry, N.A., and Y. Lazebnik. 1998. Caspases: enemies within. *Science*. 281:1312-1316.

Tigyi, G., D.J. Fischer, A. Sebok, F. Marshall, D.L. Dyer, and R. Miledi. 1996. Lysophosphatidic acid-induced neurite retraction in PC12 cells: neurite-protective effects of cyclic AMP signaling. *J Neurochem*. 66:549-558.

Tikoo, A., S. Czekay, C. Viars, S. White, J.K. Heath, K. Arden, and H. Maruta. 2000. p190-A, a human tumor suppressor gene, maps to the chromosomal region 19q13.3 that is reportedly deleted in some gliomas. *Gene*. 257:23-31.

Troller, U., A. Raghunath, and C. Larsson. 2004. A possible role for p190RhoGAP in PKCepsilon-induced morphological effects. *Cell Signal*. 16:245-252.

Trouliaris, S., U. Smola, J.H. Chang, S.J. Parsons, H. Niemann, and T. Tamura. 1995. Tyrosine 807 of the v-Fms oncogene product controls cell morphology and association with p120RasGAP. *J Virol*. 69:6010-6020.

Tsubouchi, A., J. Sakakura, R. Yagi, Y. Mazaki, E. Schaefer, H. Yano, and H. Sabe. 2002. Localized suppression of RhoA activity by Tyr31/118-phosphorylated paxillin in cell adhesion and migration. *J Cell Biol*. 159:673-683.

Tsuji, T., T. Ishizaki, M. Okamoto, C. Higashida, K. Kimura, T. Furuyashiki, Y. Arakawa, R.B. Birge, T. Nakamoto, H. Hirai, and S. Narumiya. 2002. ROCK and mDia1 antagonize in Rho-dependent Rac activation in Swiss 3T3 fibroblasts. *J Cell Biol*. 157:819-830.

Tsuruta, F., J. Sunayama, Y. Mori, S. Hattori, S. Shimizu, Y. Tsujimoto, K. Yoshioka, N. Masuyama, and Y. Gotoh. 2004. JNK promotes Bax translocation to mitochondria through phosphorylation of 14-3-3 proteins. *Embo J*. 23:1889-1899.

U, M., T. Miyashita, Y. Shikama, K. Tadokoro, and M. Yamada. 2001. Molecular cloning and characterization of six novel isoforms of human Bim, a member of the proapoptotic Bcl-2 family. *FEBS Lett*. 509:135-141.

Vader, G., J.J. Kauw, R.H. Medema, and S.M. Lens. 2006. Survivin mediates targeting of the chromosomal passenger complex to the centromere and midbody. *EMBO Rep*. 7:85-92.

Van Aelst, L., and C. D'Souza-Schorey. 1997. Rho GTPases and signaling networks. *Genes Dev*. 11:2295-2322.

van der Geer, P., M. Henkemeyer, T. Jacks, and T. Pawson. 1997. Aberrant Ras regulation and reduced p190 tyrosine phosphorylation in cells lacking p120-Gap. *Mol Cell Biol*. 17:1840-1847.

van Leeuwen, F.N., R.A. van der Kammen, G.G. Habets, and J.G. Collard. 1995. Oncogenic activity of Tiam1 and Rac1 in NIH3T3 cells. *Oncogene*. 11:2215-2221.

Vavylonis, D., J.Q. Wu, S. Hao, B. O'Shaughnessy, and T.D. Pollard. 2008. Assembly mechanism of the contractile ring for cytokinesis by fission yeast. *Science*. 319:97-100.

Vega, F.M., and A.J. Ridley. 2008. Rho GTPases in cancer cell biology. *FEBS Lett*. 582:2093-2101.

Vennstrom, B., and J.M. Bishop. 1982. Isolation and characterization of chicken DNA homologous to the two putative oncogenes of avian erythroblastosis virus. *Cell*. 28:135-143.

Verdier-Pinard, P., F. Wang, B. Burd, R.H. Angeletti, S.B. Horwitz, and G.A. Orr. 2003. Direct analysis of tubulin expression in cancer cell lines by electrospray ionization mass spectrometry. *Biochemistry*. 42:12019-12027.

Verin, A.D., A. Birukova, P. Wang, F. Liu, P. Becker, K. Birukov, and J.G. Garcia. 2001. Microtubule disassembly increases endothelial cell barrier dysfunction: role of MLC phosphorylation. *Am J Physiol Lung Cell Mol Physiol*. 281:L565-574.

Verma, A., M. Mohindru, D.K. Deb, A. Sassano, S. Kambhampati, F. Ravandi, S. Minucci, D.V. Kalvakolanu, and L.C. Platanias. 2002. Activation of Rac1 and the p38 mitogen-activated protein kinase pathway in response to arsenic trioxide. *J Biol Chem*. 277:44988-44995.

Vicente-Manzanares, M., X. Ma, R.S. Adelstein, and A.R. Horwitz. 2009. Non-muscle myosin II takes centre stage in cell adhesion and migration. *Nat Rev Mol Cell Biol*. 10:778-790.

von Dassow, G. 2009. Concurrent cues for cytokinetic furrow induction in animal cells. *Trends Cell Biol*. 19:165-173.

Wagner, E.F., and A.R. Nebreda. 2009. Signal integration by JNK and p38 MAPK pathways in cancer development. *Nat Rev Cancer*. 9:537-549.

Walczak, H., and P.H. Krammer. 2000. The CD95 (APO-1/Fas) and the TRAIL (APO-2L) apoptosis systems. *Exp Cell Res*. 256:58-66.

Wang, D.Z., E.K.M.S. Nur, A. Tikoo, W. Montague, and H. Maruta. 1997. The GTPase and Rho GAP domains of p190, a tumor suppressor protein that binds the M(r) 120,000 Ras GAP, independently function as anti-Ras tumor suppressors. *Cancer Res*. 57:2478-2484.

Wang, H.R., Y. Zhang, B. Ozdamar, A.A. Ogunjimi, E. Alexandrova, G.H. Thomsen, and J.L. Wrana. 2003. Regulation of cell polarity and protrusion formation by targeting RhoA for degradation. *Science*. 302:1775-1779.

Wang, J., and I. Kitajima. 2007. Pitavastatin inactivates NF-kappaB and decreases IL-6 production through Rho kinase pathway in MCF-7 cells. *Oncol Rep*. 17:1149-1154.

Wani, M.C., H.L. Taylor, M.E. Wall, P. Coggon, and A.T. McPhail. 1971. Plant antitumor agents. VI. The isolation and structure of taxol, a novel antileukemic and antitumor agent from Taxus brevifolia. *J Am Chem Soc*. 93:2325-2327.

Watanabe, N., T. Kato, A. Fujita, T. Ishizaki, and S. Narumiya. 1999. Cooperation between mDia1 and ROCK in Rho-induced actin reorganization. *Nat Cell Biol*. 1:136-143.

Watanabe, S., Y. Ando, S. Yasuda, H. Hosoya, N. Watanabe, T. Ishizaki, and S. Narumiya. 2008. mDia2 induces the actin scaffold for the contractile ring and stabilizes its position during cytokinesis in NIH 3T3 cells. *Mol Biol Cell*. 19:2328-2338.

Watanabe, S., K. Okawa, T. Miki, S. Sakamoto, T. Morinaga, K. Segawa, T. Arakawa, M. Kinoshita, T. Ishizaki, and S. Narumiya. 2010. Rho and anillin-dependent control of mDia2 localization and function in cytokinesis. *Mol Biol Cell*. 21:3193-3204.

Weiss, R.H., A. Ramirez, and A. Joo. 1999. Short-term pravastatin mediates growth inhibition and apoptosis, independently of Ras, via the signaling proteins p27Kip1 and P13 kinase. *J Am Soc Nephrol*. 10:1880-1890.

Wen, Y., C.H. Eng, J. Schmoranzer, N. Cabrera-Poch, E.J. Morris, M. Chen, B.J. Wallar, A.S. Alberts, and G.G. Gundersen. 2004. EB1 and APC bind to mDia to stabilize microtubules downstream of Rho and promote cell migration. *Nat Cell Biol*. 6:820-830.

Wendt, T., D. Taylor, K.M. Trybus, and K. Taylor. 2001. Three-dimensional image reconstruction of dephosphorylated smooth muscle heavy meromyosin reveals asymmetry in the interaction between myosin heads and placement of subfragment 2. *Proc Natl Acad Sci U S A*. 98:4361-4366.

Wennerberg, K., M.A. Forget, S.M. Ellerbroek, W.T. Arthur, K. Burridge, J. Settleman, C.J. Der, and S.H. Hansen. 2003. Rnd proteins function as RhoA antagonists by activating p190 RhoGAP. *Curr Biol*. 13:1106-1115.

Wertz, I.E., S. Kusam, C. Lam, T. Okamoto, W. Sandoval, D.J. Anderson, E. Helgason, J.A. Ernst, M. Eby, J. Liu, L.D. Belmont, J.S. Kaminker, K.M. O'Rourke, K. Pujara, P.B. Kohli, A.R. Johnson, M.L. Chiu, J.R. Lill, P.K. Jackson, W.J. Fairbrother, S. Seshagiri, M.J. Ludlam, K.G. Leong, E.C. Dueber, H. Maecker, D.C. Huang, and V.M. Dixit. 2011. Sensitivity to antitubulin chemotherapeutics is regulated by MCL1 and FBW7. *Nature*. 471:110-114.

Weston, C.R., K. Balmanno, C. Chalmers, K. Hadfield, S.A. Molton, R. Ley, E.F. Wagner, and S.J. Cook. 2003. Activation of ERK1/2 by deltaRaf-1:ER* represses Bim expression independently of the JNK or PI3K pathways. *Oncogene*. 22:1281-1293.

Weston, C.R., and R.J. Davis. 2007. The JNK signal transduction pathway. *Curr Opin Cell Biol*. 19:142-149.

Whitehead, I., H. Kirk, C. Tognon, G. Trigo-Gonzalez, and R. Kay. 1995. Expression cloning of lfc, a novel oncogene with structural similarities to guanine nucleotide exchange factors and to the regulatory region of protein kinase C. *J Biol Chem*. 270:18388-18395.

Whitehead, I.P., I.E. Zohn, and C.J. Der. 2001. Rho GTPase-dependent transformation by G protein-coupled receptors. *Oncogene*. 20:1547-1555.

Wickstrom, S.A., K. Alitalo, and J. Keski-Oja. 2003. Endostatin associates with lipid rafts and induces reorganization of the actin cytoskeleton via down-regulation of RhoA activity. *J Biol Chem*. 278:37895-37901.

Wildenberg, G.A., M.R. Dohn, R.H. Carnahan, M.A. Davis, N.A. Lobdell, J. Settleman, and A.B. Reynolds. 2006. p120-catenin and p190RhoGAP regulate cell-cell adhesion by coordinating antagonism between Rac and Rho. *Cell*. 127:1027-1039.

Williams, M.R., J.S. Arthur, A. Balendran, J. van der Kaay, V. Poli, P. Cohen, and D.R. Alessi. 2000. The role of 3-phosphoinositide-dependent protein kinase 1 in activating AGC kinases defined in embryonic stem cells. *Curr Biol*. 10:439-448.

Willis, S.N., and J.M. Adams. 2005. Life in the balance: how BH3-only proteins induce apoptosis. *Curr Opin Cell Biol*. 17:617-625.

Wilson, K.P., M.J. Fitzgibbon, P.R. Caron, J.P. Griffith, W. Chen, P.G. McCaffrey, S.P. Chambers, and M.S. Su. 1996. Crystal structure of p38 mitogen-activated protein kinase. *J Biol Chem*. 271:27696-27700.

Wittinghofer, A., and N. Nassar. 1996. How Ras-related proteins talk to their effectors. *Trends Biochem Sci*. 21:488-491.

Wolf, R.M., N. Draghi, X. Liang, C. Dai, L. Uhrbom, C. Eklof, B. Westermark, E.C. Holland, and M.D. Resh. 2003. p190RhoGAP can act to inhibit PDGF-induced gliomas in mice: a putative tumor suppressor encoded on human chromosome 19q13.3. *Genes Dev*. 17:476-487.

Wolf, R.M., J.J. Wilkes, M.V. Chao, and M.D. Resh. 2001. Tyrosine phosphorylation of p190 RhoGAP by Fyn regulates oligodendrocyte differentiation. *J Neurobiol*. 49:62-78.

Wu, X., T. Sakamoto, F. Zhang, J.R. Sellers, and J.A. Hammer, 3rd. 2006. In vitro reconstitution of a transport complex containing Rab27a, melanophilin and myosin Va. *FEBS Lett*. 580:5863-5868.

Wyllie, A.H., J.F. Kerr, and A.R. Currie. 1980. Cell death: the significance of apoptosis. *Int Rev Cytol*. 68:251-306.

Xia, Z., M. Dickens, J. Raingeaud, R.J. Davis, and M.E. Greenberg. 1995. Opposing effects of ERK and JNK-p38 MAP kinases on apoptosis. *Science*. 270:1326-1331.

Xu, Y., J.B. Moseley, I. Sagot, F. Poy, D. Pellman, B.L. Goode, and M.J. Eck. 2004. Crystal structures of a Formin Homology-2 domain reveal a tethered dimer architecture. *Cell*. 116:711-723.

Yamakita, Y., S. Yamashiro, and F. Matsumura. 1994. In vivo phosphorylation of regulatory light chain of myosin II during mitosis of cultured cells. *J Cell Biol*. 124:129-137.

Yamamoto, K., H. Ichijo, and S.J. Korsmeyer. 1999. BCL-2 is phosphorylated and inactivated by an ASK1/Jun N-terminal protein kinase pathway normally activated at G(2)/M. *Mol Cell Biol*. 19:8469-8478.

Yamamoto, M., N. Marui, T. Sakai, N. Morii, S. Kozaki, K. Ikai, S. Imamura, and S. Narumiya. 1993. ADP-ribosylation of the rhoA gene product by botulinum C3 exoenzyme causes Swiss 3T3 cells to accumulate in the G1 phase of the cell cycle. *Oncogene*. 8:1449-1455.

Yamana, N., Y. Arakawa, T. Nishino, K. Kurokawa, M. Tanji, R.E. Itoh, J. Monypenny, T. Ishizaki, H. Bito, K. Nozaki, N. Hashimoto, M. Matsuda, and S. Narumiya. 2006. The Rho-mDia1 pathway regulates cell polarity and focal adhesion turnover in migrating cells through mobilizing Apc and c-Src. *Mol Cell Biol*. 26:6844-6858.

Yamanaka, K., P. Rocchi, H. Miyake, L. Fazli, A. So, U. Zangemeister-Wittke, and M.E. Gleave. 2006. Induction of apoptosis and enhancement of chemosensitivity in human prostate cancer LNCaP cells using bispecific antisense oligonucleotide targeting Bcl-2 and Bcl-xL genes. *BJU Int*. 97:1300-1308.

Yamashiro, S., G. Totsukawa, Y. Yamakita, Y. Sasaki, P. Madaule, T. Ishizaki, S. Narumiya, and F. Matsumura. 2003. Citron kinase, a Rho-dependent kinase, induces di-phosphorylation of regulatory light chain of myosin II. *Mol Biol Cell*. 14:1745-1756.

Yao, R., and G.M. Cooper. 1995. Requirement for phosphatidylinositol-3 kinase in the prevention of apoptosis by nerve growth factor. *Science*. 267:2003-2006.

Yasuda, S., F. Oceguera-Yanez, T. Kato, M. Okamoto, S. Yonemura, Y. Terada, T. Ishizaki, and S. Narumiya. 2004. Cdc42 and mDia3 regulate microtubule attachment to kinetochores. *Nature*. 428:767-771.

Yin, H., Y. Gui, and X.L. Zheng. 2-methoxyestradiol inhibits atorvastatin-induced rounding of human vascular smooth muscle cells. *J Cell Physiol*. 222:556-564.

Ying, H., S.L. Biroc, W.W. Li, B. Alicke, J.A. Xuan, R. Pagila, Y. Ohashi, T. Okada, Y. Kamata, and H. Dinter. 2006. The Rho kinase inhibitor fasudil inhibits tumor progression in human and rat tumor models. *Mol Cancer Ther*. 5:2158-2164.

Yoshizaki, H., Y. Ohba, M.C. Parrini, N.G. Dulyaninova, A.R. Bresnick, N. Mochizuki, and M. Matsuda. 2004. Cell type-specific regulation of RhoA activity during cytokinesis. *J Biol Chem*. 279:44756-44762.

Yu, C., S. Wang, P. Dent, and S. Grant. 2001. Sequence-dependent potentiation of paclitaxel-mediated apoptosis in human leukemia cells by inhibitors of the mitogen-activated protein kinase kinase/mitogen-activated protein kinase pathway. *Mol Pharmacol*. 60:143-154.

Yuce, O., A. Piekny, and M. Glotzer. 2005. An ECT2-centralspindlin complex regulates the localization and function of RhoA. *J Cell Biol*. 170:571-582.

Yue, Q.X., X. Liu, and D.A. Guo. 2010. Microtubule-binding natural products for cancer therapy. *Planta Med*. 76:1037-1043.

Zandi, E., D.M. Rothwarf, M. Delhase, M. Hayakawa, and M. Karin. 1997. The IkappaB kinase complex (IKK) contains two kinase subunits, IKKalpha and IKKbeta, necessary for IkappaB phosphorylation and NF-kappaB activation. *Cell*. 91:243-252.

Zapata, J.M., K. Pawlowski, E. Haas, C.F. Ware, A. Godzik, and J.C. Reed. 2001. A diverse family of proteins containing tumor necrosis factor receptor-associated factor domains. *J Biol Chem*. 276:24242-24252.

Zeitlin, S.G., and K.F. Sullivan. 2001. Animal cytokinesis: breaking up is hard to do. *Curr Biol*. 11:R514-516.

Zhang, D., L. Qiu, X. Jin, Z. Guo, and C. Guo. 2009. Nuclear factor-kappaB inhibition by parthenolide potentiates the efficacy of Taxol in non-small cell lung cancer in vitro and in vivo. *Mol Cancer Res*. 7:1139-1149.

Zhang, H., and I.G. Macara. 2008. The PAR-6 polarity protein regulates dendritic spine morphogenesis through p190 RhoGAP and the Rho GTPase. *Dev Cell*. 14:216-226.

Zhao, W.M., and G. Fang. 2005a. Anillin is a substrate of anaphase-promoting complex/cyclosome (APC/C) that controls spatial contractility of myosin during late cytokinesis. *J Biol Chem*. 280:33516-33524.

Zhao, W.M., and G. Fang. 2005b. MgcRacGAP controls the assembly of the contractile ring and the initiation of cytokinesis. *Proc Natl Acad Sci U S A*. 102:13158-13163.

Zheng, Y., F. Ouaaz, P. Bruzzo, V. Singh, S. Gerondakis, and A.A. Beg. 2001. NF-kappa B RelA (p65) is essential for TNF-alpha-induced fas expression but dispensable for both TCR-induced expression and activation-induced cell death. *J Immunol*. 166:4949-4957.

Zilfou, J.T., and S.W. Lowe. 2009. Tumor suppressive functions of p53. *Cold Spring Harb Perspect Biol*. 1:a001883.